The host-pathogen interface: Characterising putative secreted proteins of the honeybee pathogen *Nosema ceranae* (Microsporidia).

Submitted by Graham Thomas

to the University of Exeter as a thesis for the degree of

Doctor of Philosophy in Biological Science.

In September 2015

I certify that all material in this thesis which is not my own work has been identified and that no material has previously been submitted and approved for the award of a degree by this or any other University.

Signature: ……..

Abstract

Microsporidia are obligate intracellular eukaryotic parasites related to fungi, possessing greatly reduced genomic and cellular components. The microsporidian *Nosema ceranae* threatens honeybee (*Apis mellifera*) populations. Nosemosis has a complex epidemiology affected by host, pathogen and environmental factors. Although a draft of the *N. ceranae* genome has been published, the molecular basis underpinning pathogenicity is not known. The lack of established culturing techniques and a tractable genetic system necessitates use of model systems for both host and parasite such as *Saccharomyces cerevisiae*. I hypothesise effectors essential to disease progression exist amongst *N. ceranae* secretome genes. In this study I have started characterising these genes using a combination of established and novel techniques for studying microsporidia proteins including bioinformatics, heterologous expression in *S. cerevisiae,* and the genome-wide analysis platform of Synthetic Genetic Arrays. This effort has yielded new insights into *N. ceranae* secreted proteins which lack similarity to known sequences. I identified *N. ceranae* protein NcS77 as a candidate effector implicated in targeting host nuclear pores. NcS50 and NcS85 co-localise with ERG6 a marker for lipid droplets (an organelle known to be targeted by another obligate intracellular pathogen *Chlamydia trachomatis*) when expressed in *S. cerevisiae. N. ceranae* polar tube proteins (PTP) induce filament formation when expressed in *S. cerevisiae* and PTP2 co-localises with the cell wall. Interestingly this phenotype is replicated by another secreted protein which may infer a common function. Together these data contribute to knowledge on *N. ceranae* pathology bringing us closer to understanding the disease and ultimately lead the way to mitigation.

Acknowledgments

I would like to thank my supervisors Ken Haynes and James Cresswell for the opportunity to undertake this PhD, their continuous support and open door policy. You have my sincere appreciation for the learning opportunities I have received.

A special thanks to; Marta Lalik for initial mentoring and training at the commencement of the PhD and for the foundation of *N. ceranae* work she established in the Haynes lab; Jane Usher for SGA screens training and providing critical feedback on the thesis; Hsueh-Lui Ho for demonstrating DNA extractions. Vicky Attah for assistance with my SGA screens and facing the mountain of plates to be pinned; Martin Schuster for microscopy training.

The completion of this thesis would not have been possible without the support and comradery from members of the Haynes lab, thank you team for your input over the past four years.

I would also like to thank Dr. Bryony Williams and members of her group for their willingness to discuss ideas and help troubleshoot practical aspects of microsporidian research.

Thank you Dominic Wiredu-Boakye, David Pascal, Christine Sambles and Sophie Shaw for your patience and assistance with unix and command line queries for bioinformatics and data manipulation for statistical analysis.

Last and most importantly I would like to thank my family for getting me to a point in life where doing a PhD was possible and my wife Hannah for the rock of support she has been and continues to be. Words do my gratitude no justice.

Table of Contents

List of Figures

List of Tables

Abbreviations

3’	Three prime
5’	Five prime
BCE	Before the Common Era
BLAST	Basic Local Alignment Search Tool
bp	Base pair
CCD	Colony Collapse Disorder
CDS	Coding DNA sequence
CFW	Calcofluor White
CSM	Complete synthetic media
DNA	Deoxyribonucleic acid
DM	Double mutant
ER	Endoplasmic reticulum
et al.	and others
EtOH	Ethanol
g	Grams
GFP	Green fluorescent protein
GO	Gene ontology
GPD	Glyceraldehyde phosphate dehydrogenase
g/L	Grams per litre
h	Hour
H_2O	Water

HIV	Human immunodeficiency virus
KanR	Kanamycin resistance
kb	Kilobase
L	Litre
LB	Luria broth media
M	Molar
MAT	Mating type
Mb	Megabases
mg	Milligram
mg/ml	Milligram per milliliter
min	Minutes
ml	Millilitre
ml/L	Millilitre per litre
mM	Millimolar
NcS	*Nosema ceranae* secretome
nm	Nanometres
OD_{600}	Optical density at 600 nm
ORF	Open reading frame
pH	Measure of the acidity or alkalinity of a solution (concentration of protons in a solution)
ppb	Parts per billion
ROS	Reactive oxygen species

SGA	Synthetic genetic array
TAE	Tris-acetate-EDTA
TE	Tris-EDTA
YPD	Yeast extract peptone glucose media
°C	Degrees Celcius
µg	Micrograms
µg/ml	Micrograms per millilitre
µl	Microlitre
µM	Micromolar

Introduction

1.1 Introduction to the present study

Bees are globally important both economically and ecologically and populations of honeybees in North America and Europe have suffered devastating losses in recent years due to a multitude of factors. One major problem is the obligate intracellular pathogen *N. ceranae,* a generalist microsporidian observed infecting a broad range of hosts including different honeybee and bumblebee species. The negative impact of this pathogen on honeybee health is exacerbated by synergistic effects of neurotoxic pesticides. Current knowledge only provides an overview of the *N. ceranae* lifecycle, however there remains a fundamental gap in understanding the molecular mechanisms by which this parasite achieves the many host manipulations necessary for its continued success. Due to their obligate intracellular lifecycle, microsporidia are not amenable to genetic transformation as transgenic material would have to cross the membranes of both host and spore (Williams, 2009). This problem was compounded when the first published microsporidian genome revealed *E. cuniculi* lacks homologues for key RNA interference proteins (DICER, RNA-dependent RNA polymerase and Argonaute) (Katinka et al., 2001). Together, these features have limited the molecular toolbox for studying microsporidia to genome sequencing, comparative gen/transcript/prote - omics, or recombinant protein expression in model organisms such as *S. cerevisiae*. Recent evidence for homologues of DICER and argonaute in *N. ceranae* demonstrate the potential for effective RNAi in this species (Paldi et al., 2010), although the technique has failed to gain ground as an established method and has not been reproduced in five years since its original publication.

Recent efforts have demonstrated the essential utility *S. cerevisiae* serves in elucidating functional biochemistry for effectors from evolutionary distinct pathogens as well as metabolic proteins from microsporidia (Alto et al., 2006; Campodonico et al., 2005; Kramer et al., 2007; Shohdy et al., 2005; Williams et al., 2010). Expression of heterologous proteins in yeast can produce distinct phenotypes by which inferences can be made about those proteins targeted processes or their enzymatic function (Curak et al., 2009). Williams and colleagues demonstrated co-localisation of green fluorescent protein fused to *T. hominis* and *A. locustae* alternative oxidase proteins with the *S. cerevisiae* mitochondrial network (stained with mitotracker red) (Williams et al., 2010). Another method dependent on phenotypic analysis is the high-throughput technique of synthetic genetic array (SGA) where a query strain expressing the heterologous 'bait' protein is crossed with the 'prey' yeast deletion library (~4700 non-essential gene deletions) and systematically pinned onto selective media, selecting for double mutant (DM) strains harbouring both bait and prey traits. The DM library is then screened for either a synthetic sick phenotype where colony size is less than expected or synthetic lethal phenotype where the combination of both traits results in lethality (Alto et al., 2006; Tong & Boone, 2005).

Cornman et al (2009) inferred the putative *N. ceranae* secretome (NcS) of 89 genes and was able to identify peptide domains through bioinformatic analysis for 17 of the predicted translations (Table 1.1) (Cornman et al., 2009). A recent study from the Haynes lab (Lalik, 2015) assessed three of these proteins to determine their functional capacity; NcORF-02039 (NCER_101950), NcORF-01159 (NCER_101108) and NcORF-00654 (NCER_100618) which encode a

Table 1.1 | NcS-ORFs with sequence similarity to known protein domains.

Gene symbol	Homologous domain (pfam)	Signal peptide probability
NCER_100547	UAA transporter family	0.991
NCER_100618	Proteasome A-type and B-type	0.988
NCER_101994	Hsp70 protein	0.986
NCER_100164	Glutaredoxin	0.970
NCER_101626	Preprotein translocase subunit Sec66	0.969
NCER_101673	Ricin-type beta-trefoil lectin domain	0.960
NCER_100557	Ribonuclease 2-5A	0.952
NCER_100987	Short chain dehydrogenase	0.947
NCER_100710	Histidine acid phosphatase	0.923
NCER_101349	SCP-like extracellular protein	0.921
NCER_100505	Dolichyl-phosphate-mannose-protein	0.906
NCER_100163	Acetyltransferase (GNAT) family	0.905
NCER_101950	Thioredoxin	0.897
NCER_101108	Hexokinase	0.838
NCER_100355	TLC ATP/ADP transporter	0.832
NCER_101049	Mechanosensitive ion channel	0.787
NCER_100305	Proteasome A-type and B-type	0.766

Adapted from Cornman et al. (2009).

putative thioredoxin, hexokinase and proteasome subunit respectively. Through heterologous complementation assays the study concluded the *N. ceranae* thioredoxin has catalytic activity when expressed in *S. cerevisiae,* however the functional capacity of *N. ceranae* hexokinase was not determined and the

N. ceranae proteasome subunit was targeted to the nucleus of both *S. cerevisiae* and *D. melanogaster* model systems (Lalik, 2015). These data contribute to the growing body of knowledge on putative microsporidian effectors and suggest *N. ceranae* contributes to host cell oxidative stress resistance by secreting a functionally active thioredoxin which may prolong the host cell longevity allowing the parasite to complete its lifecycle. What role the secreted *N. ceranae* proteasome subunit plays in the infection process remains unclear however studies have shown intracellular pathogens exploit the host ubiquitin-proteasome system to either destroy or prevent destruction of either host or pathogen proteins essential for infection, thereby promoting optimal conditions for replication and avoidance of immune factors (Loureiro & Ploegh, 2006). While functional studies are necessary to confirm protein identities inferred through bioinformatics this approach does not address the majority of microsporidian secretomes which are lineage-specific proteins (78% in the case of *N. ceranae*).

The aim of this study was to functionally characterise a subset of the *N. ceranae* lineage-specific secreted proteins using Gateway® cloning, phenotypic screening and SGA in the model system for eukaryotic genetics *S. cerevisiae*. Furthermore, I have re-assess the *N. ceranae* genome with bioinformatic tools to provide an updated perspective on its secretome. By increasing fundamental knowledge of molecular pathogenesis we move closer to identifying potential drug targets intent on disease mitigation. Advancing this field could have implications for microsporidia in a broader context and may afford insights into the human pathogenic species. This work builds on previous efforts in the Haynes lab (Lalik, 2015) and focusses on a subset of the *N. ceranae* secretome.

Background

1.2 The value of bees

Mankind has an ancient and long standing relationship with honeybees, older than known civilisations and preceding the written word. It is therefore difficult to know exactly when we had our first taste of honey, nature's oldest sweetener. The earliest record of honey consumption is dated ~3500-8000 years before the common era (BCE) (Mancha, 1998) recorded in Mediterranean cave paintings, signifying bees enduring provision throughout our entwined histories. The skill of domestication and bee keeping was passed from the Egyptians to the ancient Greeks (~650 BCE). Centuries later, the Romans were taught by the Greeks (~150 BCE) and are responsible for spreading this knowledge across medieval Europe. Domesticated bees were eventually taken to nearly all habitable corners of the globe (~1600s). The European honeybee, *Apis mellifera L*., is now the most commonly managed bee in the world (VanEngelsdorp & Meixner, 2010).

Today honeybees provide us with many services including direct products such as honey, wax, propolis and royal jelly, they also serve as a biosensor for ecotoxicology studies (D. James & Pham-Delegue, 2002) and are a well-known model for behavioural research (Gravitz, 2015). However, the greatest benefit of bees comes from their significant contribution to ecosystem services. It is known that 35% of the world food crop is dependent on animal pollination for sexual reproduction, including some 87 crops (Klein et al., 2007). Insect pollination provides not only an ecosystem service but also a management tool, where farmers can either rent or purchase commercially sourced honeybees, bumblebees and other bee species to supplement the local pollinator fauna - a

practice observed the world over in crop production (Gallai et al., 2009). The essential pollination service provided by insects has an estimated value of £603 million in the UK alone (Vanbergen et al., 2014), with the total global pollinator-services valuation estimated to be €153 billion in 2005 (certainly more today) (Gallai et al., 2009). Although the honeybee is the dominant contributor to the industry, bumblebees also play a major role. Five bumblebee species currently facilitate crop pollination with the dominant contributors being *Bombus terrestris* from Eurasia and *Bombus impatiens* from North America (Velthuis & Doorn, 2006). It has been reported that *B. terrestris* has become an established species having an impact on local bee fauna in foreign territories as a result of its frequent employment for commercial services. Bumblebees pollinate a range of vegetable, fruit and seed crops, however they are predominantly exploited in pollinating greenhouse tomatoes (Velthuis & Doorn, 2006). There were 40,000 ha of tomato crops pollinated by bumblebees in 2004, with a crop value of € 12 billion. Adopting bees for crop pollination serves the economy by lowering production costs and increasing both fruit yield and quality (Velthuis & Doorn, 2006).

1.3 Population fluctuations and colony collapse disorder

The practice of commercial pollination is indicative of a lack of wild pollinators to adequately meet crop demands. This highlights a fundamental issue with pollinator populations in regard to current agricultural practices. Changing bee populations are a controversial subject and feature prominently in the media. This is due to heterogeneous populations from distinct geographic locales. vanEngelsdorp and Meixner (2010) reported that global honeybee stocks have

risen during the last fifty years, however this is not the case for all regions. Figures reported for the period between 1961 – 2007 show the number of managed hives decreased in Europe (26.5%) and North America (49.5%), yet considerable gains were observed for Asia (426%), Africa (130%), South America (86%), and Oceania (39%) during the same time frame (Food and Agriculture Organisation, 2009). There is also disparity between regional population trends of *A. mellifera* as observed in North America where both the US and Mexico reported losses over the 46-year period, while Canada reported a greater number of colonies. Similar observations on varying population trends have been made for Europe (VanEngelsdorp & Meixner, 2010).

Information on wild pollinator population dynamics is limited but best represented by bumblebees (Goulson et al., 2008). Many European and North American species are observed to have diminishing ranges and four distinct species have become extinct in both regions (Grixti et al., 2009; Kosior et al., 2007; Williams & Osborne, 2009; Williams et al., 2014). Population data for the approximately 22,000 wild bee species is inadequate and this requires attention (Goulson et al., 2015).

All organism populations naturally fluctuate in response to biotic (competition; predation; disease) and abiotic (precipitation; temperature; resource availability) factors, however honeybees have a long history of large-scale colony losses (de Miranda et al., 2010). The apiculture industry has reported many unexplained, widespread and sudden losses of bee colonies from America, Europe and the Middle East (Bacandritsos et al., 2010; Giray et al., 2010; Vanengelsdorp et al., 2007). The phenomenon described as colony collapse disorder (CCD) is

Table 1.2 | Drivers of wild bee declines and honey bee colony losses

Stress	Reference
Parasites and pathogens	
Viruses	
Acute Bee Paralysis Virus	(Genersch et al. 2010)
Deformed Wing Virus	(Genersch et al. 2010)
Israeli Acute Paralysis Virus	(Cox-Foster et al. 2007)
Bacteria	
Melissococcus plutonius	(Roetschi et al 2008; Wilkins et al. 2007)
Fungi	
Nosema ceranae	(Higes et al. 2008)
Metazoan parasites	
Varroa destructor	(Genersch et al. 2010)
Habitat loss	(Goulson et al. 2008; Brown & Paxton 2009; Potts et al. 2010; Vanbergen et al. 2013)
Pesticides	(Goulson et al. 2010; Pisa et al. 2014)
Monotonous diets	(Goulson et al. 2015)
Shipping fever	(Bakonyi et al. 2002; Goulson et al. 2015)
Competition	(Goulson 2003; Forup & Memmott 2005; Walther-Hellwig et al. 2006)
Climate change	(Willmer 2012)
Interactions between stressors	(Sih et al. 2004; Coors & Meester 2008)

Adapted from Goulson et al 2015 & Genersch 2010

defined as a pathological condition affecting a large number of honeybee colonies, in which various stresses may lead to the abrupt disappearance of worker bees from the hive. No dead bees are found in affected hives, and although there are often many disease organisms present, no overt signs of disease, pests, or parasites exist. If any individuals remain they will only include the queen and recently emerged bees (distinguishing CCD from a swarming event), resulting in a 'collapsed' colony (Oldroyd, 2007). CCD has a high prevalence in both Europe and North America where it has been identified to cause up to 90% colony loss (Cox-Foster et al., 2007). The exact cause of CCD remains cryptic, however many factors are known to affect honeybee populations (discussed below), some of which have been causatively associated with CCD.

1.4 Factors affecting bee populations

Table 1.2 describes the dominant factors that affect honeybee populations. The biotic stresses include but are not limited to pathogens (bacterial, fungal, viral, microsporidial); parasites (mites); predators (bears, birds, humans); and pests (beetles, moths) (Manley et al., 2015; Ritter & Akratanakul, 2006). The abiotic stresses include climate change, bee keeping practices, trade, economics, toxicity from pesticides and herbicides, prolonged antibiotic treatments affecting natural gut microbiota composition, development of antibiotic resistance in pathogenic species and nutritional stress due to the loss of native wild flower diversity and habitat, which has in turn resulted from a century of intense agricultural industrialisation (Bennett et al., 2015; Cresswell, 2011; Herbert et al., 2014; Higes et al., 2008; Jones et al., 2005; Klein et al., 2007; Lee et al., 2015; Naug, 2009; Rundlöf et al.,

2015; Sharpe & Heyden, 2009; Tian et al., 2012; VanEngelsdorp et al., 2010). It is generally accepted that not one particular stress is responsible for CCD. Many of these different stresses occur simultaneously and many also demonstrate adverse synergistic effects outlined below.

1.4.1 Primary abiotic factors affecting bee populations

1.4.1.1 Pesticides

The human population has more than doubled in the last 50 years and global agricultural production has increased to meet this growing demand. However, land use for arable crops has only increased by 10%. Pesticide use has grown as a consequence of the necessity to maximise yields from finite land resources (Bennett et al., 2015; Köhler & Triebskorn, 2013). Pesticides provide a clear economic benefit when used appropriately but cause controversy for their impact on non-target species including bees that are exposed to treated crops or contaminated water and soil (Schaafsma et al., 2015). As many as 161 different pesticides and their metabolites have been found in honeybee colonies (Chauzat et al., 2006; Frazier et al., 2008; Mullin et al., 2010; Sanchez-Bayo & Goka, 2014), which represents a considerable toxin burden. A recent risk assessment of pesticide residues affecting honeybees highlighted three neonicotinoids; imidacloprid, thiamethoxam and clothianidin, and the organophosphates phosmet and chlorpyrifos as presenting the largest risk to *A. mellifera* populations where these chemicals are prevalent (Sanchez-Bayo & Goka, 2014). In 2013, the European Union introduced a two-year moratorium on these three neonicotinoids

due to increasing reports of their deleterious effects on bees (EFSA, 2013). Neonicotinoids are neurotoxins affecting the central nervous system of insects and can have both lethal and sub-lethal effects through their action of binding to postsynaptic nicotinic acetylcholine receptors (Tomizawa & Casida, 2005). Pollinator exposure occurs as a result of these systemic insecticides spreading throughout plant tissues into the pollen and nectar of flowering crops after initially being applied as seed-treatments. They are a relatively new class of insecticides, and have been strongly implicated in causing the decline of bee populations (Goulson, 2013; Pisa et al., 2014). Lethality is observed in overwintering honeybee hives following long-term chronic exposure to relatively low neonicotinoid doses (imidacloprid 0.25 ppb) (Rondeau et al., 2014). Various pesticides including neonicotinoids can also have sub-lethal effects on bees and other pollinators. Sub-lethal effects are much more difficult to demonstrate, however neonicotinoids have been shown to impact honey, bumble and solitary bees learning, foraging and homing ability, possibly as a result of both over-stimulation and reduced motor activity. Colony level effects of neonicotinoids include reduced number of eggs hatching, reduced number of developing larvae, impaired communication (decreased waggle dancing) and lethargy in adult bees with a propensity to abandon the colony (Desneux et al., 2007; Eiri & Nieh, 2012; Feltham et al., 2014; Henry et al., 2012; Mommaerts et al., 2010; van Tomé et al., 2012; Yang et al., 2008; Zaluski et al., 2015). Disparate observations have been made regarding the effects of neonicotinoids at both the individual and colony level between different bee genera. Bumblebees exposed to field realistic doses of imidacloprid progressively developed a dose-dependent reduction (10-30%) in feeding rate

overtime (Cresswell et al., 2012) which may cause observed reductions in fecundity (Laycock et al., 2012) and colonies suffer poor growth with only 15% optimum queen production (Whitehorn et al., 2012). In contrast, honeybees showed no response to either dietary imidacloprid or clothianidin at the individual level, and a recent study also demonstrated honeybee colonies lacked a significant response to the seed coating Elado, an insecticide containing a combination of the neonicotinoid clothianidin and the non-systemic pyrethroid b-cyfluthrin, when wild bee densities were reduced along with solitary bee nesting, and bumblebee colony growth and reproduction under field conditions (Cresswell et al., 2012; Rundlöf et al., 2015; Schneider et al., 2012). Cresswell et al (2012) hypothesise that the differential sensitivity of honeybees and bumblebees to imidacloprid is a result of honeybees being more pre-adapted to feed on nectars containing synthetic alkaloids, such as imidacloprid, than bumblebees by virtue of their ancestral adaptation to tropical nectars in which natural alkaloids are prevalent (Cresswell et al., 2012). There is not only disparity between the responses of different bee genera to neonicotinoids, but also variation in the responses of different genotypes of the same species as demonstrated for *A. mellifera L* (Laurino et al., 2010; Sandrock et al., 2014).

1.4.1.1.1 Toxic synergy observed with pesticide combinations

Pesticide toxicity can be compounded by synergistic effects of multiple toxicants. Impaired foraging behaviour of bumblebees and increased worker mortality has been observed following chronic exposure to two pesticides (neonicotinoid and pyrethroid) at field realistic concentrations (Gill et al., 2012).

This led to significant reductions in brood development and colony success. Another example is that of ergosterol-biosynthesis-inhibitor (EBI) fungicides which can increase the toxicity of some neonicotinoids and pyrethroids by as much as 1,000 times. These agrochemicals are however relatively non-toxic by themselves (Pilling & Jepson, 1993; Schmuck et al., 2003). One recent study has interestingly reported a contradictory result that a sub-lethal dose of imidacloprid and coumaphos actually enhanced olfactory learning and memory in *A. mellifera* (Williamson et al., 2013). As previously discussed, bees are exposed to multiple pesticide residues and so more attention needs to be paid to the dynamic effects of residue combinations.

1.4.1.1.2 Parasite-pesticide interactions

As well as synergy with other pesticides, there have been numerous reports of the deleterious synergy between other stresses in combination with pesticide exposure. This comes as a consequence of the effect pesticides have on bee physiology, i.e. some pesticides impair aspects of the bee immune response which increases their susceptibility to pathogens. Both clothianidin and imidacloprid have been shown to negatively modulate NF-κB immune signalling in insects and adversely affect honeybee antiviral defences controlled by this transcription factor (Di Prisco et al., 2013). This induced immunosuppression occurred below field realistic concentrations and yet was shown to escalate replication of the deformed wing virus (DWV) in hosts with covert infections. Fauser-Misslin et al (2014) reported that chronic exposure of the bumblebee *B. terrestris* to thiamethoxam and clothianidin, and the prevalent trypanosome gut parasite *Crithidia bombi* resulted in

truncated worker production, reduced worker longevity and decreased overall colony reproductive success. The authors also demonstrated a significant interaction between neonicotinoid exposure and parasite infection negatively affecting survival of mother queens (Fauser-Misslin et al., 2014).

1.4.1.1.3 Pesticide interactions with the microsporidian *Nosema ceranae*

The microsporidian species *N. ceranae* and *Nosema apis* are the causative agents of Nosemosis and will be comprehensively described in subsequent sections, however there are many recorded instances of *N. ceranae* synergistically interacting with pesticides, where their combined effect on bee fitness is significantly greater than the effect of either stress by itself. This is the case with the pesticide fipronil, where the most significant impact on honeybee survival is observed when the two stresses are in combination (Aufauvre et al., 2012). The case of *N. ceranae* and fipronil remains unclear as, Aufauvre et al (2014) reported combinations of *N. ceranae*-insecticide (fipronil and imidacloprid) induced a significant increase in honeybee mortality rates however, did not lead to a synergistic effect in this instance. It was suggested that synergy may have been masked by the unusually high mortality rates observed for the singular stresses in the study. The authors also report that chronic insecticide exposure repressed the expression of immunity-related genes including genes encoding the serine proteases SP22 and SP40, glucose dehydrogenase 2, lysozyme 1, hymenoptaecin and GMC oxidoreductase 3 (Aufauvre et al., 2014). Similar observations of potential synergy between the pesticide imidacloprid and *N. ceranae* have been reported by Pettis and colleagues (2012), who demonstrated an indirect effect of

pesticides on pathogen growth in honeybees, increasing susceptibility to the pathogen and reducing rates of host survival (Pettis et al., 2012). There have been multiple reports of sub-lethal field-realistic concentrations of the neonicotinoid thiacloprid acting in synergy with *N. ceranae,* albeit in a dose dependent manner, as well as additively with the pathogen black queen cell virus (BQCV), where the pesticide increased viral loads (Doublet et al., 2014; Retschnig et al., 2014).

It has been suggested that bees could avoid or dilute exposure to pesticides by choosing to forage on other available flowers (DEFRA, 2013; Godfray et al., 2014). However, these assertions were invalidated when Kessler et al (2015) demonstrated that honey and bumblebees (*A. mellifera* & *B. terrestris*) not only fail to avoid nectar-relevant concentrations of neonicotinoids (imidacloprid, thiamethoxam and clothianidin), but actually prefer to eat pesticide contaminated sucrose solutions than sucrose alone (Kessler et al., 2015).

1.4.1.1.4 Broader implications of pesticides

Pesticides can affect food webs and the natural environment beyond the primary invertebrate consumers. A recent report highlights the declines in insectivorous birds as a result of high neonicotinoid concentrations. Many bird species rely heavily on invertebrates for dietary requirements during the breeding season (Snow & Perrins, 1997) and bird population trends in the Netherlands are considerably more negative in areas with higher surface-water concentrations of imidacloprid. This observation was determined to coincide with the timescale of imidacloprids introduction to the region, in the mid-1990s (Hallmann et al., 2014).

1.4.1.2 Herbicides

In line with maximising crop yields, herbicides are regularly employed to reduce the occurrence of weeds, which frequently results in farmland consisting of near-pure monocultures representing a barren wasteland in regards to biodiversity (Goulson et al., 2015). Herbicide toxicity has also been shown to have a direct effect on honeybee consumption rates and learning when chronically exposed to field-realistic concentrations of glyphosate, suggesting glyphosate can reduce the sensitivity of honeybees to nectar reward and impair associative learning (Herbert et al., 2014).

1.4.1.3 Weather and climate

Changeable weather can directly affect honeybee colony productivity. Honeybees are most productive when ambient temperatures are high, due to a lower metabolic demand on foragers (Harrison & Fewell, 2002). However, when ambient temperatures are cool and during extended rain fall, productivity is negatively affected as bees stay in the hive. The most prominent effects of climate on colony productivity are indirect. Optimum colony productivity is dependent on optimum temperature and rainfall, necessary for plants to maximise nectar production (Shuel, 1992; Voorhies et al., 1933). Poor overwintering in the north-eastern US has been attributed to harsh seasonal weather patterns such as prolonged summer drought or heavy autumn showers as they inhibit autumn plants from generating optimal pollen and nectar. A lack of pollen in autumn means brood-rearing ends too early in the season resulting in long-lived winter bees (Mattila & Otis, 2007). Survival rates are poor for colonies with long-lived winter

bees. Different pathogens have also been shown to be affected by the weather, e.g. varroa mite populations are affected by temperature and humidity (Harris et al., 2003; VanEngelsdorp & Meixner, 2010). Climate change may also drive range shifts which can result in spatial mismatches of plants and their pollinators as has been seen for some butterfly species (Forister et al., 2010) and is predicted to be the case for bees (Williams & Osborne, 2009). Climate change has the potential to be a growing cause of stress in the future which could exasperate other stressors (Goulson et al., 2015).

1.4.1.4 Socio-economic factors

There are many anthropogenic impacts on bees, such as illegal smuggling which leads to the spread of bee diseases and parasites (Matheson, 1995). Changes in the market for bee products are also believed to affect populations. For example, the rising demand for honey followed by the rising price for honey during World War I is considered as the principle driver for the growth of managed colony numbers at that time (Phillips, 1928). Economic factors affecting bee keeping are clearly demonstrated by the political upheaval in eastern Europe during the 1990's, which resulted in the number of bee hives in the former German Democratic Republic being reduced to approximately 25% within the course of a year (VanEngelsdorp & Meixner, 2010).

1.4.2 Primary biotic factors affecting bee populations

1.4.2.1 *Varroa destructor* – a parasite and viral vector

The most devastating biotic factor to which bees are subject is the ectoparasitic mite *V. destructor* which switched host to *A. mellifera* from its original host the Asian honeybee *Apis ceranae* almost 60 years ago in 1957 (Oldroyd, 1999). *V. destructor* has subsequently spread to nearly all continents harbouring *A. mellifera*, although not Australia. Disease symptoms are non-uniform and described as varroosis or parasitic mite syndrome (Martin et al., 2012; Rosenkranz et al., 2010; Shimanuki et al., 1994). Dramatic colony losses have been consistently attributed to mite infestation in affected countries (Finley et al., 1996; Guzmán-Novoa et al., 2010; Lee et al., 2015; Martin et al., 1998; Vanengelsdorp et al., 2007). *V. destructor* depends on bee brood for reproduction. The primary effect of pathogenicity on individual bees is reduced fitness through nutritional deficits, resulting from mites feeding on the haemolymph of both larvae and adult host's (Figure 1.1) (Duay et al., 2003; Garedew et al., 2004). However it is the secondary effect of pathogen vectoring that makes *V. destructor* worthy of its name. *V. destructor* has been shown to transmit honeybee viruses (Chen & Siede, 2007; Genersch & Aubert, 2010) and debilitate the host immune system, which in turn increases susceptibility to infection by the transmitted viruses (Yang & Cox-Foster, 2005).

The first honeybee virus was discovered in 1963 and there are nearly 20 known to date, many of which appear to have a distribution pattern matching that of *V. destructor* (Bailey et al., 1963; Chen & Siede, 2007; Ellis & Munn, 2005).

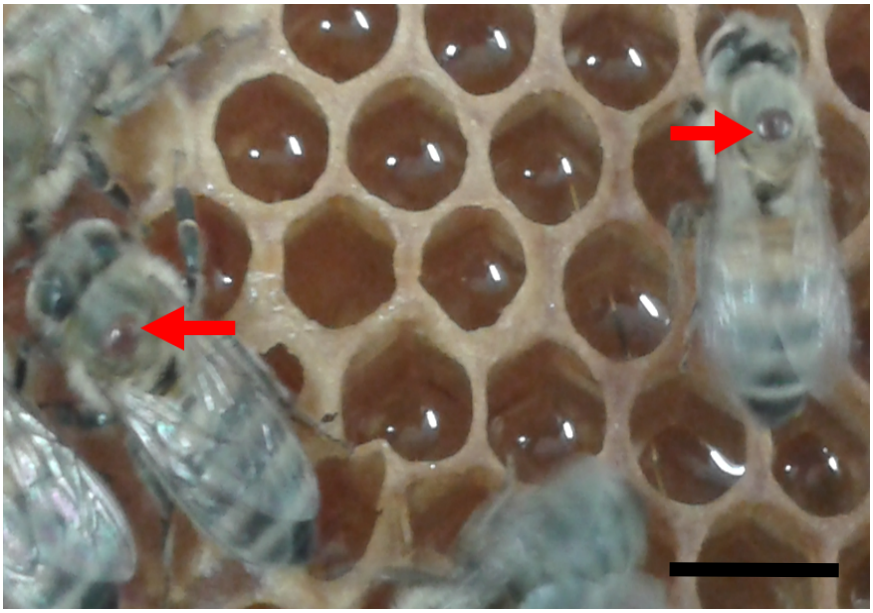

Figure 1.1 | *V. destructor* parasitising juvenile *A. mellifera.* Single mature female mites are indicated by red arrows. Many mites can parasitise a single bee. Infected individuals do not always present disease symptoms. Scale bar is 1 cm.

It is believed that many honeybee viruses exist and even co-exist within their hosts without causing symptomatic infections, however Deformed Wing Virus (DWV) (*Iflaviridae*) and Acute Bee Paralysis Virus (ABPV) (*Dicistroviridae*) have become of increasing concern since the *V. destructor* pandemic (Gauthier et al., 2007; Genersch & Aubert, 2010; Tentcheva et al., 2004). DWV is rather benign when transmitted vertically through drones and queens or horizontally through larval food. However, clinical symptoms such as deformed wings, a shortened and bloated abdomen and miscolouring, usually only occur when virion transmission is from mite to pupae. It has been shown repeatedly that DWV is not only transmitted efficiently by the mite, but it also replicates within mite tissues which significantly increases viral titres in parasitized hosts. Bees showing clinical symptoms of DWV are not viable and only survive for 3 days post-emergence at most. DWV in

association with *V. destructor* causes severe detrimental effects on individual bees and the entire colony (Allen, 1988; Bowen-Walker et al., 1999; de Miranda & Fries, 2008; Highfield et al., 2009; Tentcheva et al., 2006; Yang & Cox-Foster, 2007; Yue & Genersch, 2005; Yue et al., 2006, 2007).

Historically, ABPV was also known to benignly co-exist in honeybees without causing clinical symptoms or leading to colony death before *V. destructor* was present, but the prevalence of ABPV in Europe increased with the arrival of *V. destructor*. However, a recent study demonstrated a significant relationship between ABPV infection in autumn and colony collapse in the following winter season independent of varroa infestation. ABPV has not been observed to replicate within *V. destructor* tissue but it has been confirmed that infections with this virus are more deadly in combination with varroa infestation, however the exact role *V. destructor* plays in affecting ABPV virulence is still unclear (Allen & Ball, 1996; Bailey & Gibbs, 1964; Genersch et al., 2010).

Israeli Acute Paralysis Virus (IAPV) is a closely related species to ABPV initially purified in 2002 from a hive near Alon Hagalil in Israel, but subsequently demonstrated to be a long time persistent virus of honeybees (Chen & Evans, 2007; Maori et al., 2007; Palacios et al., 2008). Originally isolated from the Middle East, IAPV has also been shown to be prevalent in Australia and the US, but is less frequently observed in Europe and can present varying pathology in different geographic regions (Chen et al., 2014; de Miranda et al., 2010). This virus has a strong correlation with CCD in the US but not Europe, which may be explained by its pervasiveness in that region and high levels of standing genetic variation between isolates (Chen et al., 2014; Cox-Foster et al., 2007; Genersch, 2010b).

IAPV has not yet been shown to interact with varroa and so the mites only act as a physical vector in this case, however considering IAPV virulence is increased when injected (Maori et al., 2007), it has been suggested that virus titre is increased within hives suffering mite infestation due to the method of delivery i.e. injection via the mites feeding apparatus (Di Prisco et al., 2011; Genersch, 2010b). This virus attacks every stage and caste of honeybees and causes systemic infection of the host. IAPV affects host mitochondrial function which suggests infection causes significant disturbance in energy-related processes. Infection also triggers an active immune response by inducing expression of immune-pathway genes in adult bees (Chen et al., 2014).

Significant hive losses would occur if appropriate pest management of varroa was not implemented, because the combined impact of *V. destructor* infestation and infection with the viruses it vectors, namely DWV, contributes to approximately 70% of colony losses (Kielmanowicz et al., 2015). It has been suggested that a western honeybee colony suffering *V. destructor* infestation without receiving treatment to kill the parasite, has a high probability of collapse within one to three years (Fries et al., 2006; Korpela et al., 1993). When surveyed on the extreme winter losses of 2006-2007, US beekeepers considered *V. destructor* to be the third most important contributor to mortality after queen failure and starvation (van Engelsdorp et al., 2008).

1.4.2.2 Foulbrood - Bacteria

There are two known bacterial pathogens of honeybees and both are pathogens for honeybee brood only. *Paenibacillus larvae* is the causative agent of

American Foulbrood (AFB) (Genersch, 2010a; Genersch et al., 2006) and *Melissococcus plutonius* is the causative agent of European Foulbrood (EFB) (Bailey & Bailey, 1983; Bailey, 1956; Forsgren, 2010). Both AFB & EFB are notifiable diseases in many countries making it a legal requirement to report observed instances of the disease to government authorities, facilitating monitoring and warning of possible outbreaks. Due to the relative ease of diagnosis, which leads to early mitigation, neither of the foulbrood diseases are implicated in CCD. AFB is more virulent than EFB and considered the most serious bacterial disease of *A. mellifera*. The global apiculture industry experiences significant economic losses due to the high frequency of AFB occurrence and so it is considered a major threat to honeybee health. EFB was not as problematic historically as it has become today, especially in areas of Europe, such as Switzerland and the UK, where it has become a major problem for apiculture in recent years (Bailey & Ball, 1991; Belloy et al., 2007; Budge et al., 2010; Forsgren et al., 2005; Roetschi et al., 2008; Tomkies et al., 2009; Wilkins et al., 2007). Current mitigation practices involve destroying infected hives by incineration to prevent the spread of disease. Several countries including the US permit the prophylactic use of antibiotics to control AFB however this method is controversial and not permitted in many other countries. Antibiotics are not effective in killing spores and their over use can lead to increased occurrence of resistant AFB strains as well as antibiotic residues accumulating in the honey (Kochansky et al., 2001; Lodesani et al., 2006; Miyagi et al., 2000; Mussen, 2000).

1.4.2.3 Poor Queens

In a survey of honeybee colony losses in the US from autumn 2007 to spring 2008, beekeepers ranked poor queens (increased rates of queen failure, supersedure, and drone laying) as the number one cause of winter mortality (van Engelsdorp et al., 2008). The cause of poor quality queens is not apparent but is likely attributable to multiple factors. Infections of queens by the microsporidian *N. apis* and other potential parasites may increase supersedure frequency (Camazine et al., 1998). There are reports that poor queens may also be a consequence of pesticides residues contaminating the wax comb. Increasing concentrations of lipophilic miticides can build up in the wax over time (Bogdanov, 2006). The highly prevalent coumaphos has been shown to have a negative impact on queen rearing (Pettis et al., 2004).

1.4.2.4 Insufficient foraging pastures

As previously mentioned in section 1.1.3.2, the agricultural industry has evolved to be ever more efficient in maximising crop yields from a finite area of farmed land, and in so doing has reduced the biodiversity of wild flowering plants and with them, bee pasture. For example the extensive use of herbicides has not only reduced weeds from among crops, but also from the crop edges in the field margins (Bohan et al., 2005). Limited pasture affects bee health which in turn affects beekeepers bottom line. Increased colony losses in the US have been associated with changing land use and the ratios of open land to developed land. Trends in good colony productivity have been associated with regions harbouring considerable open space, which is associated with them having a greater forage

availability (Naug, 2009). If productivity is excessively low, total colony numbers will be corresponding less than optimal for many reasons such as, failing to acquire sufficient resources can lead to starvation through the winter. Starvation alone was identified as the second major factor that leads to collapsing colonies in the US (van Engelsdorp et al., 2008). Nutritional stress has been associated with increased susceptibility to disease and reduced tolerance to pesticides (Gilliam, 2000; Wahl & Ulm, 1983). Along with developed agriculture, land designated for urban development has further reduced the available locations which could support apiaries, however it is difficult to gauge what impact this has on total colony numbers (VanEngelsdorp & Meixner, 2010).

1.4.2.5 Nosemosis and the emergent pathogen *N. ceranae*

I have previously discussed the combined effects of pesticides and infection with the microsporidian *N. ceranae* on bee health and populations (section 1.4.1.1.3), however nosemosis is a major biotic factor affecting bee populations in itself. The obligate-intracellular microsporidium *N. apis* was discovered just over a century ago as being the causative agent of nosemosis (Zander, 1909) and is now widely regarded as one of the honeybees most ubiquitous and economically harmful pathogens. For this reason, it has received much attention from the research community and advances have been made regarding knowledge of *N. apis* biology, site of infection and the consequences of infection on both individual bees and whole colonies (Fries, 1993; Fries et al., 1984). *N. apis* is a parasite of the adult honeybee ventricular epithelial cells and is commonly transmitted horizontally by ingesting spores from the environment (Fries, 1997).

Infected colonies may not present symptoms of disease and rarely suffer fatality. Although *N. apis* is considered to be pandemic, it is not considered to be highly virulent. Acute symptoms may present as; trembling of honeybee workers; dilated abdomens; brown faecal marks on combs and hive entrance; dead or dying bees outside of the hive; decreased brood production and colony size, particularly in spring; and potentially colony collapse when overwintering (only observed in heavily infected colonies) (Anderson & Giacon, 1992; Bailey, 1955; Fries et al., 1984; Office International des Epizooties (OIE), 2008).

N. apis was identified as the only causative agent of nosemosis in honeybees until 1994, when *N. ceranae* was observed infecting the Asian honeybee (*A. ceranae*) (Fries et al., 1996). The 'new' species *N. ceranae* was subsequently found infecting colonies of the western honeybee in Taiwan and Spain in 2005. However its presence in Europe has since been determined to date back to at least 1998 and in North America since the mid-1990's (Chen et al., 2008; Higes et al., 2006; Huang et al., 2007; Klee et al., 2007). *N. ceranae* is now found in *A. mellifera* colonies from five continents, presenting a different epidemiological pattern and pathology compared to *N. apis*. It is considered a greater health risk, inducing significantly higher rates of mortality and has been causally linked to CCD (Antúnez et al., 2009; Bromenshenk et al., 2010; Cox-Foster et al., 2007; Giersch et al., 2009; Higes et al., 2008, 2013; Martín-Hernández et al., 2007; Paxton et al., 2007). The two species can be distinguished by differences in their ultrastructure (determined by transmission electron microscopy) and sequence variation in their small subunit (16S) rRNA gene (Fries et al., 2006). Co-infection with both species has been observed in Europe and

North America (Copley et al., 2012; Gisder et al., 2010) and it has been suggested that *N. ceranae* may be replacing *N. apis* in *A. mellifera* globally, although there is conflicting data regarding increased virulence of *N. ceranae* (Forsgren & Fries, 2010; Paxton et al., 2007). Milbrath et al (2015) demonstrated that *N. ceranae* does not appear to have a strong within-host advantage over *N. apis* and so differences in virulence between the two species remain cryptic (Milbrath et al., 2015; Paxton et al., 2007). Climate exhibits a role in *N. ceranae* virulence where variation in intraspecific *N. ceranae* pathology has been reported between colonies residing at different latitudes. Virulence appears greater in the Mediterranean region between latitudes of 30° and 45° compared to Northern climates, between latitudes of 45° and 55° (Gisder et al., 2010; Higes et al., 2009; Van der Zee et al., 2014).

N. ceranae can reduce the adult bee population of a colony and so to compensate for the loss of available foragers, younger bees will start foraging sooner than intended, which modifies the whole colony work profile (Amdam & Omholt, 2003; Huang & Robinson, 1996; Wang & Moeller, 1970). This effect can have many implications for colony health such as; reduced bee lifespan (Schmidhempel & Wolf, 1988; Wolf & Schmid-Hempel, 1989); impaired foraging efficiency and resilience (Oskay, 2007); reduced colony growth and brood production; reduced nurse bee activities (hygiene and brood caring); and increased risk of developing brood diseases such as chalkbrood (Hedtke et al., 2011). Advancing behavioural development of worker bees caused by *Nosema* infection, correlates with increased titres of juvenile hormone (Ares et al., 2012; Higes et al., 2010; Lin et al., 2009), downregulation of vitellogenin gene expression (Antúnez et

al., 2009) and increased pheromone production (Dussaubat et al., 2010). Each of these factors plays a role in bee development such as, maturation, nurse-forager transition and the division of labour among worker bees. Microsporidia have previously been shown to manipulate endocrine function of the infected host insect, a phenomena described as an adaptive mechanism to maximise spore yield by prolonging the host larval state (Down et al., 2008; Higes et al., 2013).

N. ceranae is a generalist parasite considering its ability to infect not only *A. mellifera, A. ceranae* and other *Apis* species (Chaimanee et al., 2010, 2011, 2013), but also bees of the genus *Bombus.* In this regard *N. ceranae* appears to be one of the many pathogens that have spilt over from managed honeybees to wild pollinators i.e. bumblebees (Fürst et al., 2014; Plischuk et al., 2009). Under controlled conditions, *N. ceranae* exhibits greater virulence in bumblebees than it does in honeybees (Graystock et al., 2013). While the effects on wild bumblebee populations are currently unknown, they could be potentially disastrous for wild, unmanaged pollinator populations that are not subject to the same intervention practices as managed honeybee colonies. There are currently no vaccines against nosemosis (OIE, 2008) and the only widely used treatment against *N. apis* infection since the 1950's, is the antibiotic dicyclohexylammonium fumagillin (hereafter, fumagillin), isolated from the fungus *Aspergillus fumigatus* (Bailey, 1953; Higes et al., 2011). This antibiotic inhibits the enzyme methionine aminopeptidase-2 (MetAP2) (Sin et al., 1997) and can effectively block MetAP2 in *Encephalitozoon cuniculi*, a microsporidian pathogen of humans (Katinka et al., 2001). However, fumagillin does not have the same efficacy in the treatment of *N. ceranae,* where it only temporarily supresses pathogen load (Williams et al.,

2008, 2011). Moreover, a recent study by Huang et al (2013) reported *N. ceranae* not only escapes fumagillin control, but spore production within individuals from treated colonies increased up to 100% more than individuals from untreated colonies, as fumagillin concentration declined throughout the season (Webster, 1994), demonstrating the potential of this antibiotic to exacerbate infection levels, rather than supress them (Huang et al., 2013). Fumagillin treatment has also been shown to be ineffective against the closely related *Nosema bombi* which infects bumblebees (Whittington & Winston, 2003).

With *N. ceranae* being recognised as one of the major biotic factors affecting the global apiculture industry, considerable efforts have been made to elucidate its epidemiology and while advances have been made, the molecular mechanisms of pathology remain unknown. Details such as life cycle and evolutionary adaptations will now be discussed in the broader context of the microsporidia phylum.

1.5 Microsporidia

Microsporidia are eukaryotic single celled, obligate intracellular parasites. They were discovered in the 1850's and described by Louis Pasteur as the causative agent of pébrine (*Nosema bombycis*), a disease of silk worms which seriously threatened Europe's silk industry (Nageli, 1857; Pasteur, 1870). There are currently 187 genera exceeding 1400 described species, parasitizing all animal phyla, including hosts of medical, veterinary, agricultural and aquacultural importance (Table 1.3) (Ghosh & Weiss, 2012; Keeling & Fast, 2002; Stentiford et al., 2013; Wittner & Weiss, 1999). Microsporidia are delineated as a monophyletic

taxon by the presence of the autapomorphic, pre-formed infection mechanism (polar tube) within the spore (Vávra & Lukeš, 2013).

An observed lack of typical eukaryotic organelles such as mitochondria, centrioles, peroxisomes, and microtubules (Vávra & Larsson, 1999), led to microsporidia historically being considered primitive amitochondriate protozoa (Cavalier-Smith, 1983; Weiss, 2001). However, as our understanding of microsporidian natural history has changed with time (discussed below) so too has our reasoning for this highly specialised cellular architecture. Instead of being viewed as primitive simplicity, it is now suggested to be a result of the evolutionary mechanism, reduction (Katinka et al., 2001; Keeling & Fast, 2002; Méténier & Vivarès, 2001; Peyretaillade et al., 1998; Vivarès & Méténier, 2000).

Originally, phylogenetic analysis placed microsporidia as ancient eukaryotes (Vossbrinck et al., 1987), however it has since been established this placement was an artefact of long-branch attraction. The first phylogeny connecting microsporidia to fungi was based on single genes (alpha and beta tubulin) and only included a limited diversity of both fungi and microsporidia (Edlind et al., 1996; Keeling & Doolittle, 1996). This made it difficult to determine whether they were related to fungi or were actually fungi, however the answer to this question has developed with advances in phylogenetic techniques; concatenated multi-gene trees; distribution of insertions/deletions from elongation factor; assessing gene order conservation and increasing availability of biologically diverse sequences from equally diverse environments (Capella-Gutiérrez et al., 2012; Jones et al., 2011; Koestler & Ebersberger, 2011; Lee et al., 2010; Tanabe et al., 2002).

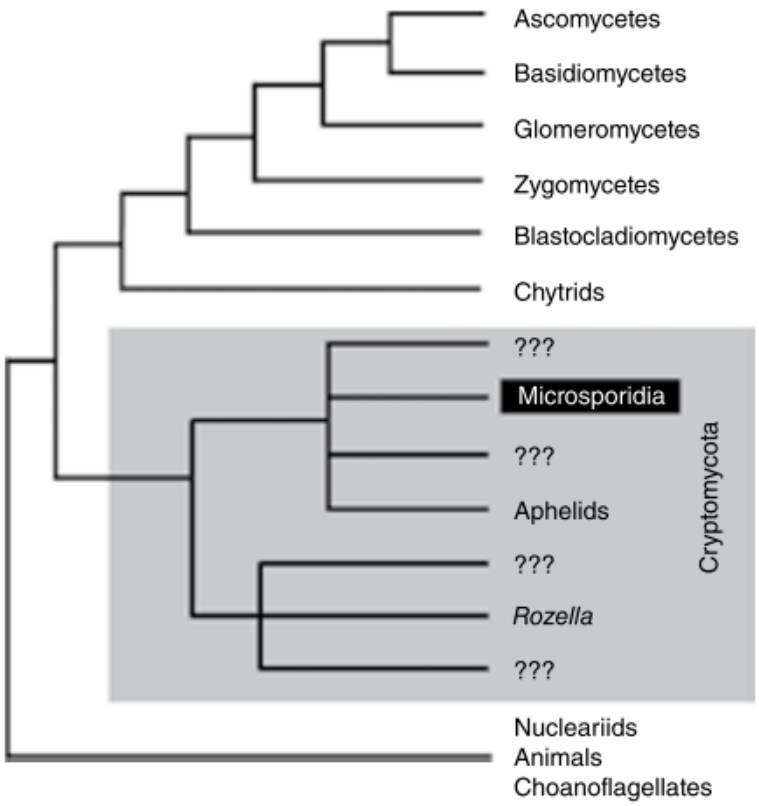

Figure 1.2 | Schematic phylogenetic tree showing the currently best supported position of microsporidia based on analysis of multiple protein-coding genes. This tree is synthesized from a number of recent studies (Capella-Gutierrez et al. 2012; Jones et al. 2011; Karpov et al. 2013; Letcher et al. 2013; Lutzoni et al. 2004). The greater part of Cryptomycota diversity remains restricted to environmental SSU rRNA sequences, and the uncertainty of how these related to the known organisms, *Rozella*, aphelids, and microsporidia, is indicated by their being interspersed by lineages marked with "???". Reprinted from Keeling, 2014 in Weiss & Becnel 2014.

Two recent discoveries have impacted our view of microsporidia's relationship with fungi (Figure1.2), 1; discovery of the Cryptomycota the putative earliest branching clade of the fungal kingdom (Jones et al., 2011) and includes the fungus *Rozella,* which also forms a clade with microsporidia (James et al., 2013).

Observed members of the Cryptomycota are as numerous and diverse as known fungal species. 2; the first molecular data showing strong support for connecting the aphelid, *Amoeboaphelidium protococcarum*, with the Cryptomycota (Karpov et al., 2013). Multigene phylogenies have shown that *A. protococcarum*, and *Rozella allomycis* form a clade with microsporidia, with *A. protococcarum* as sister to the microsporidia (Karpov et al. 2013). These recent discoveries and continuous reclassification through time highlight how our view of microsporidian evolutionary history is subject to change and improve as we discover new species, and develop new techniques to assess them with.

1.5.1 Human infections

There have been 17 species of microsporidia identified from eight genera infecting humans since their first clinical detection in 1959 (Table 1.3) (Didier & Weiss, 2011; Matsubayashi et al., 1959). Infection predominantly occurs via the fecal-oral route as a consequence of ingesting contaminated food or water (Izquierdo et al., 2011), although other transmission routes have been identified (vertical, horizontal, zoonotic) (Dunn & Smith, 2001; Mathis et al., 2005). *Enterocytozoon bieneusi, Encephalitozoon intestinalis, Encephalitozoon hellem*, and *E. cuniculi* are the most common species causing human infections. Pathology is described as microsporidiosis and symptoms vary depending on the infecting species and range from diarrhoea, hepatitis, encephalitis and nephritis, though the disease most commonly presents as a gastrointestinal tract infection. Microsporidiosis is usually associated with immunocompromised patients, predominantly those with HIV/AIDS, but also individuals on immunosuppressive

drugs for either organ transplants or chemotherapy in the treatment of cancer (Chandramathi et al., 2012; Didier & Weiss, 2006; Didier & Weiss, 2011; Kicia et al., 2014; Lono et al., 2008). However, cases of microsporidian infection have also been reported in immune-competent individuals (Weber & Bryan, 1994). Microsporidia are frequently overlooked and under-diagnosed due to their small size and a lack of standardised diagnostics (Moretto et al., 2015). Initially diagnosis was achieved through analysing faeces or other body fluids using the laborious method of electron-microscopy. Improvements in staining/light-microscopy has facilitated identification of microsporidia spores to the genus level (Weber et al., 1992). Distinguishing spores at the species level can be accomplished using antibodies (polyclonal or monoclonal) or by the molecular method, polymerase chain reaction (PCR) (Franzen & Müller, 1999; Visvesvara et al., 1994). Moreover, further analysis of PCR products by either restriction fragment length polymorphism or sequencing can resolve subspecies identities distinguishing individual genotypes (Didier et al., 1995). Existing treatments include various drug therapies such as albendazole and fumagillin, which also vary in their efficacy depending on the species being treated and site of infection (Costa & Weiss, 2000).

Table 1.3 | Microsporidia of socioeconomic importance.

Species	Natural host(s)	References
Encephalitozoon (syn. Nosema) cuniculi	Human, fox, goat, horse, rabbit, rodents, ticks	Deplazes et al. (1996)
Enterocytozoon bieneusi	Human, cat, chicken, cow, dog, goat, pig, rabbit, ticks	Desportes et al. (1985)
Enterocytozoon hellem	Human, chicken, finch, ostrich, parrot, ticks	Didier et al. (1991); Cali et al. (1993)
Enterocytozoon (syn. Septata) intestinalis	Human, cow, dog, donkey, goat, gorilla, pig, ticks	Hartskeerl et al. (1995)
Microsporidium africanum (syn. Nosema sp.)	Human	Pinnolis et al. (1981)
Microsporidium ceylonensis (syn. Nosema sp.)	Human	Ashton and Wirasinha (1973); Canning et al. (1998)
Microsporidium sp.	Human	Suankratay et al. (2012)
Pleistophora ronneafiei (syn. Pleistophora sp.)	Human, fish	Ledford et al. (1985); Cali and Takvorian (2003)
Trachipleistophora hominis	Human	Field et al. (1996); Hollister et al. (1996); Rauz et al. (2004)
Trachipleistophora anthropopthera	Human	Yachnis et al. (1996); Vávra et al. (1998); Juarez et al. (2003)
Tubulinosema sp.	Human	Choudhary et al. (2011)
Anncaliia (syn. Nosema, Brachiola) algerae	Human, mosquito	Coyle et al. (2004); Visvesvara et al. (1999)
Anncaliia (syn. Nosema, Brachiola) connori	Human	Margileth et al. (1973), Sprague (1974)
Anncaliia (Brachiola) vesicularum	Human	Cali et al. (1998)
Vittaforma corneae (syn. Nosema corneum)	Human	Davis et al. (1990); Shadduck et al. (1990)
Nosema ocularum	Human	Cali et al. (1991)
Nosema sp.	Human	Curry et al. (2007)
Nosema bombycis	Silkworm	Pasteur (1870)
Nosema antheraeae	Silkworm	Ding et al. (1998)
Nosema ceranae	Honey bee, bumblebee	Fries et al. (1996)
Nosema apis	Honey bee	Zander (1909)
Loma salmonae	Salmon, trout	Morrison and Sprague (1983)
Spraguea lophii	Monkfish	Sprague and Vavra (1976)
Myosporidium merluccius	Hake	Baquero et al. (2005)
Tetramicra brevifilum	Turbot	Matthews and Matthews (1980)
Enterospora canceri	Edible crab	Stentiford et al. (2007)
*Edhazardia aedis**	Mosquito	Becnel et al (1989)
*Vavraia culicis**	Mosquito	Andreadis (2007)
*Paranosema locustae**	Rangeland grasshoppers	Johnson (1997)
*Nosema pyrausta**	European corn borer	Steinhaus (1952)
*Nosema lymantriae**	Gypsy moth	Weiser (1957); Vavra et al. (2006)
*Vairimorpha disparis **	Gypsy moth	Vavra et al. (2006)
*Amblyospora connecticus**	Mosquito	Andreadis (1988)
*Kneallhazia solenopsae**	Red imported fire ant	Sokolova and Fuxa (2008)
*Vairimorpha invictae **	Red imported fire ant	Jouvenaz and Ellis (1986)

*Microsporidia used for biocontrol of pest insect species.
Adapted from Weiss & Becnel, 2014

1.5.2 Key animal infections

Microsporidia are principally associated with insect hosts. As previously discussed*, N. ceranae* is a major pathogen of bees and *N. bombycis* was the first microsporidian species to be discovered in diseased silk worms. Pébrine disease infects all stages and breeds of the silkworm and determines the success or failure of sericulture industry in any country (Bhat et al., 2009; Pasteur, 1870). Spores are transmitted both vertically and horizontally, with chronic infections causing extensive somatic injury (intestines, silk glands, muscles, and malpighian tubules), resulting in reduced silk production and fertility (Pan et al., 2013). Symptoms in the larvae include inactivity, slow development and later, formation of the black spots which delineate pébrine disease and which lead to eventual death. *N. bombycis* can, and is, recorded through history as causing devastating economic losses which can be attributed in part to a lack of effective methods of treatment. A recent study demonstrated the size of the *N. bombycis* genome has expanded through multiple mechanisms (discussed below) in contrast to the microsporidian trait of genome reduction (Pan et al., 2013).

Microsporidia have not only been shown to be pathogens of beneficial insects, but they have also been adopted as biological control agents of pest species e.g. the control of; rangeland grasshoppers; the European corn borer (*Ostrinia nubilalis*); gypsy moth (*Lymantria dispar dispar*); and numerous mosquito species (Table 1.3) (for review see Bjornson & Oi, 2014).

Beyond insect hosts there has been an increasing incidence of microsporidiosis reported from the aquaculture industry. Many economically important crustaceans are affected, e.g. white shrimp (*Litopenaeus setiferus*), giant

tiger shrimp (*Penaeus monodon*), blue crab (*Callinectes sapidus*) and edible crab (*Cancer pagurus*), along with many commercial fish species e.g. Atlantic salmon (*Salmo salar*), South African hake (*Merluccius capensis*), monkfish (*Lophius piscatorius*) and turbot (*Scophthalmus maximus*) (Table 1.3) (for review see Stentiford et al., 2013).

In summary, microsporidia can infect a broad range of hosts, including humans and commercially important animals. A fundamental lack of knowledge regarding diagnosis and treatment has meant incidences remain high, although this has changed for human infecting species as a result of improved methodologies. The impact of microsporidian infections on farmed and cultured animals warrants further study of epidemiology and pathology if we hope to mitigate these diseases by developing effective treatments.

1.5.3 Reduced eukaryotic genomes

Utilisation of host resources over evolutionary time scales has allowed microsporidia to loose components in several biochemical pathways and complexes, including the tricarboxylic acid cycle, oxidative phosphorylation, electron transport, and de novo biosynthesis of nucleotides and amino acids resulting in reduced genomes (Corradi & Slamovits, 2011; Katinka et al., 2001; Weidner et al., 1999). This loss of function, together with a reduction of intergenic regions, introns and mobile genetic elements, has resulted in genome compaction to the lowest level seen for eukaryotes, making microsporidia a model for studying minimal eukaryotic systems and host-pathogen interactions (Corradi et al., 2010). Indeed, *E. cuniculi* was one of the first eukaryotic genomes to be sequenced and

not only revealed all of these traits, but also that amongst its approximate 2000 genes within its 2.9 Mbp genome, genes with orthologues in the genetic-model-eukaryote *Saccharomyces cerevisiae,* were truncated and on average 15% smaller (Katinka et al., 2001). A consequence of the short intergenic regions observed in microsporidian genomes (e.g. *Encephalitozoon* spp average 135 base pairs between genes), is a high density of coding sequences (see below). Corradi et al (2010) have shown that the non-coding regions of *Encephalitozoon* spp. are under strong selective pressure, evolving relatively slowly, indicating they have reached the functionally-essential limit of reduction (Corradi et al., 2010). Another consequence of extreme genome reduction is multigene transcripts which contain sequence from more than one ORF (Corradi et al., 2008). Although this feature is extremely uncommon in eukaryotes, the multigene transcripts of microsporidia are distinct and not the functional operons observed in bacteria, but rather, fragments of adjacent ORFs either up or downstream, or even from the opposing coding strand (Corradi et al., 2008).

Although the general trend for microsporidian genomes is to be streamlined and reduced, there is considerable variation between species ranging from the smallest genome of *E. intestinalis* at 2.3 Mbp, to the largest known microsporidian genome of *Edhazardia aedis* (a pathogen of the disease vectoring mosquito *Aedes aegypti* that transmits dengue haemorrhagic fever, yellow fever and chikungunya), which is 51.3 Mbp (Corradi et al., 2009; Desjardins et al., 2015). Despite the broad range in size, all microsporidian genomes maintain comparable gene content with a near identical complement of essential gene families and the observed > 20 fold size difference across the phylum appears to be due to variation in lineage-specific

genes of unknown function as well as gene density e.g. 0.86 genes per kbp compared to 0.21 genes per kb for *E. intestinalis* and *Hamiltosporidium tvaerminnensis* respectively. *H. tvaerminnensis* is a pathogen of the arthropod *Daphnia magna* and has the second largest known microsporidian genome at 24 Mbp (Corradi et al., 2009, 2010; Haag et al., 2011). The large genome size of *E. aedis* is accounted for by expanded AT-rich intergenic regions, with 78% of the genome being AT and only 9% gene coding (Desjardins et al., 2015). Some species may have near identical gene content as well as gene density and in these cases data suggests the difference in genome size is the result of partial genome duplication events (Brugere et al., 2001). This observation is true for the genus *Nosema* where *N. ceranae* and *N. apis* have intermediate genome sizes of 7.9 & 8.5 Mbp respectively, which is comparable to that of *N. antheraeae* (a pathogen of undomesticated silkworms *Antheraea pernyi*) (6.6 Mbp), yet its sister species *N. bombycis* has a large sized genome at 15.7 Mbp (Chen et al., 2013; Cornman et al., 2009; Pan et al., 2013). Although the genome size differential between the two silk worm pathogens could be accounted for by a whole genome duplication event when considering size alone, Pan and colleagues (2013) demonstrate this not to be the case. The *N. bombycis* genome assembly revealed multiple tandem and segmental duplications that occurred recently over a short evolutionary period on separate occasions, increasing the repertoire of *N. bombycis*-specific uncharacterised genes. The genome expansion observed in *N. bombycis* is also due to horizontal gene transfer from bacteria and an expanded cohort of transposable elements (Pan et al., 2013). This is the only case to date

demonstrating genome expansion as an evolutionary outcome in microsporidia compared to their renowned genome reduction.

Microsporidia exhibit dynamic genome evolution, with an initial event of gene loss resulting in a highly reduced ancestral proteome consisting of a core set of genes (Nakjang et al., 2013). The initial reduction was followed by expansion of some gene families such as transporter proteins predicted to locate at the cell surface, as well as gene families enriched for secretion (72% being microsporidian specific), many of which have unknown functions and no similarity to known sequences in public databases. Horizontal gene transfer (HGT) has been shown to be one mechanism of expansion in transporter proteins and has served in the acquisition of genes from bacterial and animal origins (Cuomo et al., 2012; Pombert et al., 2012; Richards et al., 2003). These acquired genes and the proteins they encode facilitate import of essential substrates from the host that the parasites can no-longer synthesis *de novo.* The fact that these expanded gene families are conserved throughout microsporidia against a strong selective pressure of reductive evolution, is indicative that these genes participate in conserved features of host–parasite interactions and warrant further study if we are to fully understand these dynamic processes (Nakjang et al., 2013).

1.5.4 The microsporidian life cycle and biology

Microsporidia endure environmental stress and are disseminated as a resilient spore, while during the developmental stages of their lifecycle they are bound within and dependant on the host cell (Cali & Takvorian, 1999). Previously considered metabolically dormant, the extracellular spores of *Antonospora*

locustae and *Trachipleistophora hominis* have exhibited activity, engaging in glycolysis (Dolgikh et al., 2011; Heinz et al., 2012). 'Dormant' spores can survive in the environment for many years and can range in diameter length from 1 to 40 μm (Vávra & Larsson, 1999). Various organelles specific to microsporidia can be found within the spore such as a large posterior vacuole (approximately half the spore volume); membranous polaroplast located at the anterior end of the cell; coiled polar tube ('harpoon like' mechanism of infection); and the anchoring disc, which joins the cell to the polar tube. As previously discussed, the microsporidian polar tube is already present within the spore ready for germination and in this regard is distinct from the infection apparatus of other fungi e.g. the appressorium of the ascomycete *Magnaporthe oryzae* which is formed upon infection (de Jong et al., 1997; Williams, 2009). Three polar tube proteins were identified from *E. cuniculi* and accordingly named polar tube protein (PTP) 1, PTP2 and PTP3 (Delbac et al., 1997; 2001; Peuvel et al., 2002). How these proteins interact to form the functional polar tube is not known, but they do form a complex and exhibit direct interaction with each other, as determined by yeast two-hybrid studies (Bouzahzah et al., 2010). Li and colleagues (2012) have also demonstrated that PTP2 & PTP3 interact with spore wall protein 5 (SWP5) in *N. bombycis* (Li et al., 2012). Bioinformatic analysis revealed orthologues for all three polar tube proteins in the *N. ceranae* genome (Cornman et al., 2009). Other spore wall proteins are involved in host cell recognition and along with environmental factors (upon entering the gut) such as changes in pH or cation/anion concentration, are essential for infection (Keohane & Weiss, 1999). Studies in *E. cuniculi* have revealed that a protein of the endospore (endospore protein 1, EnP1) is necessary for host cell

adhesion, recognising and binding to host-cell-surface glycosaminoglycans. EnP1 contains multiple heparin-binding motifs, which are known to interact with extracellular matrices and this binding may serve to 'aim' the 'firing' end of the spore towards the host membrane, optimising successful host penetration (Southern et al., 2007; Williams, 2009). Germination occurs when the polaroplast and posterior vacuole rapidly swell, leading to a sharp rise in pressure inside the spore, resulting in the explosive discharge of the polar tube (Kudo, 1918; Lom & Vavra, 1963; Xu & Weiss, 2005). This process is not fully understood, however some evidence suggests that swelling is induced by calcium/calmodulin binding at the spore surface, triggering a signalling cascade that results in a rapid influx of water across the plasma membrane, via aquaporin channels (Frixione et al., 1997; Weidner & Byrd, 1982). One hypothesis for drawing water into these organelles to achieve the required turgor pressure, is that osmotic potential rises in response to the rapid breakdown of the disaccharide trehalose into monomers of glucose, via activity of trehalase enzymes (Dolgikh & Semenov, 2003; Undeen & Vander Meer, 1999). While a decrease in trehalose and an increase in glucose levels during germination has been demonstrated for some species e.g. *Anncaliia algerae,* the same is not true of all microsporidia. Findley et al (2005) proposed an alternative hypothesis for increasing pressure within the spore, that the posterior vacuole is an atypical peroxisome containing catalase and so hydrogen peroxide is reduced to its constituent parts, water and oxygen, resulting in the spore swelling (Findley et al., 2005). However, the case against this theory has been made in light of genes for peroxisome catalase being absent from all of the microsporidian genomes sequences so far.

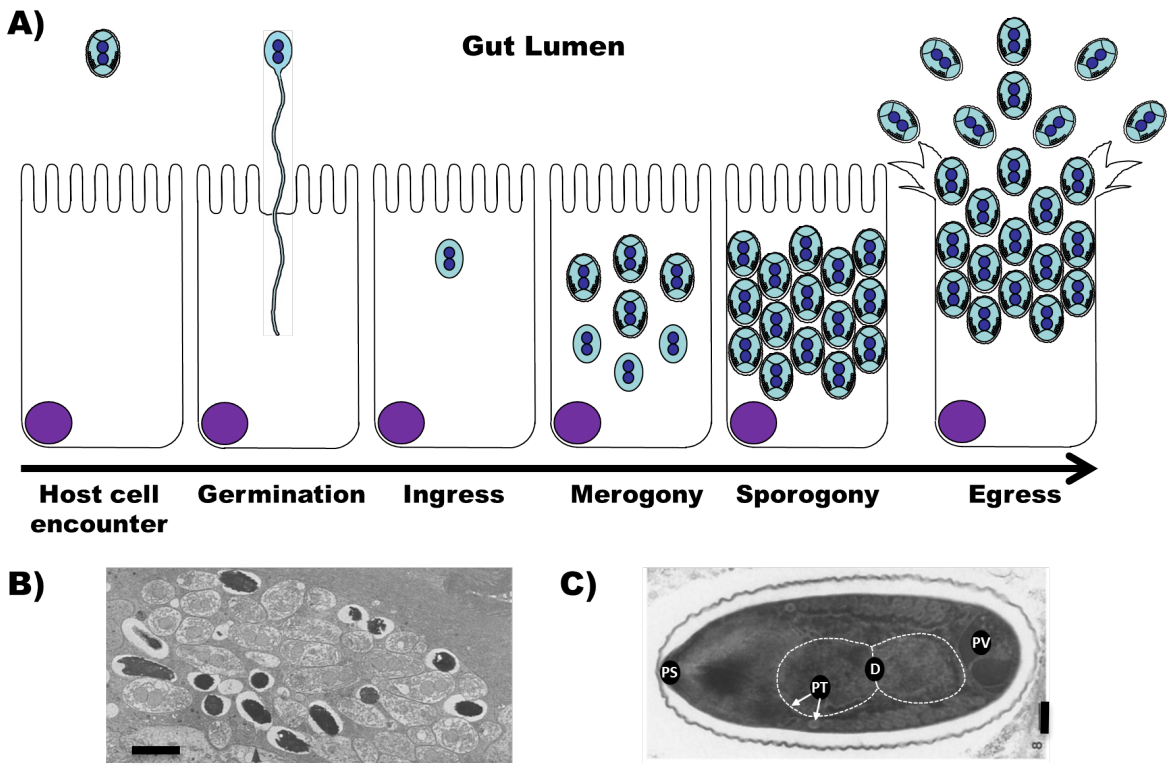

Figure 1.3 | A) Lifecycle of *N. ceranae*. Environmental cues and contact with an epithelial cell of the host ventriculus causes the mature spore to germinate, extruding the polar tube which penetrates the host cell and becomes a conduit for the sporoplasm to pass inside. Initial replication takes place (merogony), followed by maturation of meronts and spore wall development (sporogony). The last stage is spore egress. B) Micrograph showing an infected bee cell full of spores at different developmental stages. Scale bar = 10 μm. C) Longitudinally sectioned mature spore showing internal structures, PS = polar sac, PV = posterior vacuole, PT = polar tube (arrows), D = diplokaryon highlighted with white dashed outline. Scale bar = 0.25 μm. Micrograph images from Fries et al., 1996.

Under sufficient pressure, the narrowest part of the spore wall at the anterior pole is ruptured and the anchoring disc is everted to form a collar-like structure. The polar tube is expelled and its length extended by protein polymerisation (Weidner & Byrd, 1982), followed swiftly by passage of the sporoplasm into the host cytoplasm. As the spore contents is inverted through the polar tube upon germination it undergoes membrane polarity reversal, resulting in cytoplasmic proteins (e.g. tubulin and dynactin) appearing on the outer surface of the plasma membrane (Weidner, 2000). The developing stages either take place directly in the host cytoplasm or nucleus, or encapsulated by a parasitophorous vacuole that is rapidly formed from host lipids upon entry (e.g. *E. cuniculi*) (Franzen, 2004; Lom & Vavra, 1963; Williams, 2009; Xu & Weiss, 2005). However, in the case of *N. ceranae*, the organism is genuinely an intracytoplasmic parasite, with the plasma membrane of the sporoplasm exposed to the host cytoplasm (Chen et al., 2009).

Four developmental stages follow host-cell entry; growth of a meront from the sporoplasm; replication of meronts, filling the host cell (merogony); synthesis of spore-wall proteins (chitin, SWPs & PTPs) in developing sporonts; and sporont maturation into a complex infective spore (sporogony) (Figure 1.3). The mechanisms triggering each developmental stage are not currently known (Brosson et al., 2005; Hayman et al., 2001; Peuvel-Fanget et al., 2006; Southern et al., 2007; Wu et al., 2008; Xu et al., 2006). Owing to the evolutionary adaptation of remaining hidden within host cells while completing their development cycle, microsporidia are able to avoid recognition by many host immune factors (Vávra & Lukeš, 2013). The sporoplasm is described as being a minimal eukaryotic cell

packed with ribosomes and an indistinct nucleus (or two in diplokaryon species such as *N. ceranae* (Chen et al., 2009)). While cell membranes and organelles do progressively appear throughout development, many features are initially lacking, such as, cellular compartments, Golgi, or cristae associated organelles (mitochondria). Some organelles are lost altogether within microsporidia, including peroxisomes, while many exhibit severe reduction, as is the case for mitochondria (reduced to mitosomes with the primary function of iron-sulphur cluster assembly) and the Golgi apparatus (unstacked) (Dacks & Field, 2007; Dolgikh et al., 2010; Mironov et al., 2007; Takvorian et al., 2005; Vávra & Larsson, 1999; Weidner, 1972).

1.5.5 Host cell manipulations

Of course there are many nuances between how different microsporidian species interact with their hosts and the effects they can have, ranging from the formation of xenomas (grossly distended host cell) to feminisation. Xenomas present as extreme host-cell hypertrophy, with the malformed cell containing a vast number of spores. *Spraguea lophii* is a microsporidian species that infects monkfish (*Lophius piscatorius* and *L. budegassa*) and forms large cysts (cm's in diameter) full of xenomas, which are themselves visible to the naked eye (Campbell et al., 2013). An explanation for what causes this unique phenotype remains unknown. Neither is it clear whether the resulting structure is formed from a host defence response surrounding the infection to prevent its dissemination, or the microsporidian manipulating host resources to serve its own purpose by optimising its environment for replication, or acting as a defence against the host

immune system (Williams, 2009). These questions are difficult to address as there is currently no established continuous culture method for xenoma-forming microsporidian species.

One intriguing example of microsporidia manipulating host biology is observed where some species have the capacity to distort host sex ratios. This phenomenon occurs in species that are transmitted vertically from host mothers to daughters, and infection promotes development of daughters over sons. In the regard of sex determination, microsporidia are the only eukaryotic parasites known to have this capability (Bulnheim and Vávra, 1968). To affect the sex ratios in host populations, microsporidia will either induce feminisation or have an increased virulence in males. *Nosema granulosis* (a parasite of the amphipod *Gammarus duebeni*) suppresses development of the androgenic gland, inhibiting hormone production which results in impaired suppression of female characteristics i.e. leads to more females being produces (Ironside & Alexander, 2015). For the strategy of male-killing, there are several microsporidian parasites of mosquitos that kill males before maturity, at the fourth instar of development. While infection is observed to be virulent in males, no symptoms are observed in females even though infection and indeed transmission (transovarial) does occur (Andreadis, 2005). The molecular mechanisms that bring about this process are not currently known.

As previously mentioned, microsporidia have reduced metabolism and can only obtain ATP through the glycolytic pathway or by importing it from the host cytoplasm. Indeed I have discussed their expanded import-protein gene families and the *E. cuniculi* genome encodes membrane bound proteins common to

intracellular bacteria e.g. *Chlamydia* and *Rickettsia* that transport ATP from the host to the parasite (Katinka et al., 2001; Tsaousis et al., 2008). Supplementing ATP produced through glycolysis with ATP sourced from the host may have contributed to microsporidian-mitochondria being reduced to mitosomes that have lost the capacity to produce ATP (Katinka et al., 2001; Williams et al., 2002). Not only do these pathogens take this essential energy currency from their host, but they optimise the process by manipulating the host mitochondrial network, surrounding themselves with host mitochondria, closing the gap between the parasite and host resources (Scanlon et al., 2004).

Other effects of microsporidian infections observed in insects include; reducing host lipids, sugars and glycogen; gigantism in larvae caused by extending the development period; and *N. ceranae* can reduce honeybee hypopharyngeal gland protein production and lifespan (Blaser & Schmid-Hempel, 2005; Down et al., 2008; Henn & Solter, 2000; Rivero et al., 2007; Suwannapong et al., 2011). Although there is a great diversity in host-parasite interactions, there is very little known about how any of these manipulations are achieved by the parasites, however some progress has been made in recent years to identify potential host manipulating systems and will be discussed in the next section.

1.5.6 Secreted proteins – the hunt for microsporidian effectors

A broad range of cell types offer niche intracellular environments exploited by a multitude of phylogenetically distinct organisms including, viruses, symbionts and pathogens (prokaryotic and eukaryotic) (Casadevall, 2008). Life inside a host cell presents inherent challenges that all intracellular organisms have to overcome,

including microsporidia, which has resulted in convergent adaptation for many survival strategies (Haldar et al., 2006). They have to deal with numerous host immune responses such as; production of reactive oxygen species (ROS), apoptosis, autophagy, lysosomes and interferon-inducible GTPases (Carmen & Sinai, 2007; Martens & Howard, 2006; Nathan & Shiloh, 2000). There is evidence that microsporidia have the capacity to inhibit apoptotic pathways, but the mechanisms remain unknown (Carmen & Sinai, 2007; del Aguila et al., 2006). Beyond avoiding host defences, it has already been discussed microsporidia are dependent on host resources for replication and survival, so they must possess mechanisms for manipulating the host to accommodate this need. As many microsporidia, including *N. ceranae* are in direct contact with the host cytoplasm, two intuitive means of host-pathogen interactions would be 1) proteins bound to the sporoplasm membrane that project into the host environment and 2) secreted proteins that can translocate from the developing parasite to the host and be trafficked to specific host compartments where they are able to interact with target molecules (Senderskiy et al., 2014). Targeted trafficking is a complex process and in most cases depends on the presence of a N-terminal signal peptide (SP), but the degree of complexity can vary depending on where these soluble proteins are destined to function and may require additional targeting domains (Cooke et al., 2004). All SPs demonstrate the conserved feature of a length of 10-30 amino acids with three defined regions; N (basic/positively charged NH_2 terminal), H (hydrophobic amino acids) and C (negatively charged amino acids upstream of the signal peptidase cleavage site) (Figure 1.4) (Martoglio & Dobberstein, 1998; Nothwehr & Gordon, 1989, 1990). Bioinformatic tools have been developed which

exploit these conserved features to predict the presence of a SP from sequence or structural data alone i.e. without experimental assessment, e.g. SignalP, TargetP (Emanuelsson et al., 2007; Petersen et al., 2011). These tools can identify putative secretomes and have already revealed SP presence in numerous microsporidian proteins, including hexokinase and trehalase which could drive host production of basic metabolites to be exploited by the parasite (Campbell et al., 2013; Cuomo et al., 2012; Desjardins et al., 2015; Senderskiy et al., 2014). Indeed the draft genome of *N. ceranae* revealed 89 gene models with predicted SP, 78% of which are lineage-specific and lack similarity to known sequences (Cornman et al., 2009).

The secretome of many eukaryotic protozoan parasites is fundamentally important for host cell manipulation and virulence. Members of the apicomplexan parasitic genera *Plasmodium* and *Toxoplasma* have even evolved specific secretory organelles e.g. rhoptries and micronemes (Kessler et al., 2008; Sam-Yellowe, 1996). The *Plasmodium falciparum* genome encodes approximately 60 var genes, which encode a family of adhesins called the *P. falciparum* erythrocyte membrane protein 1 (PfEMP1) that are trafficked to and exposed on the surface of infected erythrocytes. Successful trafficking is dependent on eight *P. falciparum* genes. PfEMP1 proteins facilitate adhesion of erythrocytes to the vascular linings of the brain and placenta and are linked to both cerebral and placental malaria, which cause millions of child deaths annually (Maier et al., 2008; Miller et al., 2002).

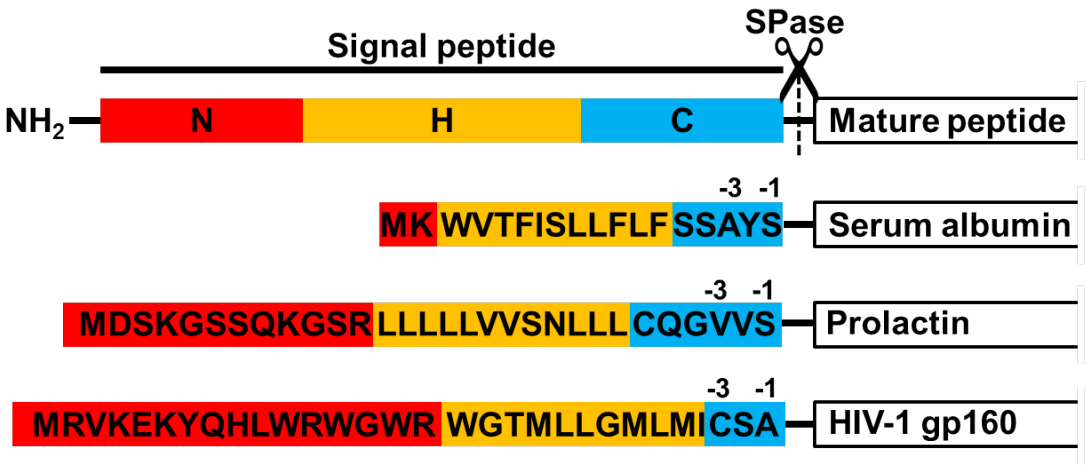

Figure 1.4 | Eukaryotic signal peptides have a tripartite structure recognised by the secretory machinery: a central hydrophobic h-region (yellow) and hydrophilic N- (red) and C-terminal (blue) flanking regions. Three examples of signal sequences with n-regions of different length are shown. Scissors: cleavage site for signal peptidase (SPase). Amino acids at the -3 and - 1 position of the signal peptidase cleavage site are negatively charged. Adapted from Martoglio and Dobberstein (1998).

There have been considerable advances in the field of filamentous plant-pathogen effectors (both fungi and oomycetes) revealing different effector categories (e.g. apoplastic and cytoplasmic) (Giraldo & Valent, 2013) and while the 'form' of these organisms may be quite different, their cytoplasmic effector 'functions' are likely to share conserved features with cytoplasmic effectors from single celled, intracellular parasites. Cytoplasmic effectors from these plant-pathogens have been shown to target the host ubiquitylation system and defence signalling. The ubiquitylation system is important to positively and negatively regulate plant immunity (Giraldo & Valent, 2013; Park et al., 2012).

Molecular tools for studying microsporidia are limited (see below), however some studies have addressed questions on early pathogenesis in different species

by assessing gene expression profiles, whether as a time course of early infection or by comparing un-germinated versus germinated spores (Campbell et al., 2013; Cuomo et al., 2012). Cuomo et al (2012) performed a transcriptomic time course assessment on early pathogenesis of two *Caenorhabditis* infecting microsporidian species (*Nematocida parisii* and *Nematocida sp1*) and identified hexokinase as the only glycolytic enzyme highly expressed at 8 h post infection. The authors showed that hexokinase was the only glycolytic pathway enzyme to have a SP and that it was functional, capable of directing proteins through the secretory pathway of another fungus (*S. cerevisiae*). Included in the analysis and confirmed as functional SPs were the hexokinase secretion signal sequences from *E. cuniculi, A. locustae*, and *N. ceranae*. It appears that secreted hexokinase enzymes are specific to microsporidia which may reflect conserved adaptation of these organisms to the intracellular host environment (Cuomo et al., 2012). These findings could explain previous observations that microsporidia infection can cause both a decrease in host glycogen and an increased rate of glucose uptake (Méténier & Vivarès, 2001).

Campbell et al (2013) published the *S. lophii* genome identifying expansion of a Leucine-Rich-Repeat (LRR) protein family, > 70% of which have predicted SPs. LRR proteins play a role in protein-protein interactions and have been established as pathogenicity factors in other fungi (Butler et al., 2009; Campbell et al., 2013). Interestingly, the authors performed a proteomic analysis on germinated versus un-germinated spores and observed no consistent variation in protein content between the two lifecycle stages, suggesting that germination occurs too quickly for translation and that microsporidia are likely to pre-package proteins essential for early infection. Perhaps the most interesting result was observed from

analysing the culture media which showed the presence of 37 different proteins from the germinated spores compared to 0 for un-germinated spores, suggesting these proteins were secreted upon germination. Only 46 % of these proteins were predicted to have SP by bioinformatic tools inferring 54% have a non-canonical secretion mechanism. Many of the proteins found in the culture medium and believed to have been secreted from the germinated spores do not share sequence similarity with known pathogenicity factors or any non-microsporidian sequences, highlighting the importance of uncharacterised, hypothetical proteins in the early infection processes of microsporidia. Very few of the secreted proteins shared similarity with other microsporidian sequences, one was a homolog of *N. bombycis* SWP7, and two others were members of the RICIN B-lectin-like (carbohydrate binding) protein family, which are broadly conserved across the phylum, including *N. ceranae*. Evasion of host immunity is one of a diverse range of functions that lectins perform in parasites. They can engage different parasite developmental pathways through binding to host proteins (Loukas & Maizels, 2000; Petri et al., 2002). Genes from this protein family present conserved synteny in the genomes of *E. cuniculi* and *N. ceranae*, comparable to effector gene clusters observed in fungal pathogens e.g. *Ustilago maydis* (Kämper et al., 2006) and the RXLR and crinkler effector families in oomycetes e.g. *Phytophthora* spp. (Schornack et al., 2009). Campbell et al (2013) observed there is no conserved effector-protein associated motif comparable to oomycete RXLR or crinkler, which could help to define the microsporidian secretome, limiting microsporidian secretome identification to be inferred by SP predictions. Approximately 40% of *S. lophii* secreted proteins are uncharacterised and fast evolving, demonstrating

the important role these lineage-specific proteins play in microsporidia pathogenesis (Campbell et al., 2013).

A recent transcriptomic study of two mosquito pathogen microsporidian species, the generalist *Vavraia culicis* and the specialist *E. aedis* revealed contrasting host-pathogen interactions where *E. aedis* retains the capacity for enhanced cell surface modifications and signalling, while also upregulating protein trafficking and secretion during infection compared to *V. culicis*. Secreted protein complexes are so abundant during the later stages of *E. aedis* infection they are clearly visible in micrographs, yet the function of these structures and their contents remain unknown. The putative secreted hexokinase and trehalase of *E. aedis* were both significantly up-regulated following a blood meal in *Ae. aegypti*, suggesting an increased control of host metabolism. Desjardins and colleagues (2015) hypothesis the possibility that increased secretion of these enzymes by *E. aedis* mitigates a typical reduction in glycolytic activity in *Ae. aegypti* following a bloodmeal. The authors determined that *E. aedis* retains abundant surface decorations and secreted proteins that could interact with the host and this may reflect the adaptation of *E. aedis* to a specific host, whereas *V. culicis* has maintained a simpler lifecycle, allowing it to grow in a wider range of hosts (Desjardins et al., 2015).

Functional experiments have shown microsporidia possess a range of enzymes and regulatory proteins capable of being secreted into infected cells and likely function to control host metabolic processes and molecular programs (Senderskiy et al., 2014). As a convergent evolutionary strategy for interacting with host cells, secreted proteins function as essential effectors of pathogenicity from a

broad range of organisms demonstrating their central role in nutrient acquisition, proliferation and subduing host defences. Although many secretome factors have been identified with some putative functions inferred through bioinformatic analysis, these proteins constitute the ‘arms race’ of host-pathogen interactions and are therefore frequently fast evolving proteins with limited homologous features to existing sequences. This leaves the majority of key pathogenicity factors beyond the purview of bioinformatic assessment and is most likely the reason why the molecular mechanisms responsible for the vast range of host cell manipulation described in previous sections remain elusive. Identifying secreted proteins and determining their molecular functions is crucial for gaining insight to pathogenesis of these socioeconomically important organisms.

Chapter 2 | General Methods

All chemicals were purchased from Sigma or Fisher unless otherwise stated. All solutions were either autoclaved or filter sterilised using appropriate sized Nalgene filters. All standard molecular biology protocols were performed as set out in Sambrook et al., (1989).

2.1 Microorganisms and growth conditions

Yeast strains used in this study are listed in Appendix I. The *MAT***a** deletion mutant array was purchased from OpenBiosystems (Catalog no. YSC1053). Strains expressing the empty advanced gateway vectors and vectors housing NcS-ORFs were produced by transformation of the parental yeast strain *S. cerevisiae*-BY4741 with the respective gateway vectors made in this study. *S. cerevisiae* strains were grown in either YPD (1% (w/v) yeast extract, 2% (w/v) bactopeptone, 2% (w/v) D-glucose) or synthetic drop-out media (0.67% (w/v) yeast nitrogen base without amino acids, 2% (w/v) D-glucose, drop-out amino acid mixture (Fisher)) at 30ºC in a shaking incubator at 180 rpm (Sherman, 1998). For growth on plates, 2% (w/v) agar was added. Stock cultures (500 µl cell aliquots containing 20% (v/v) glycerol) were stored at -80ºC.

2.2 Nosema Spore purification

Honey bees were collected from hives located on Streatham campus, University of Exeter, UK and stored at -80ºC. Whole bees were crushed in sterile water and spores purified as described by Cornman et al (2009).

2.3 Genomic DNA extraction from *Nosema* spores

Genomic DNA was extracted based on a modified version of the method described by Hoffman and Winston (1987). Approximately 10^6 purified spores were centrifuged at 3500 x g for 5 min, supernatant discarded and 200 µl genomic extraction buffer added (GE buffer – 100 µM NaCl, 10 mM Tris-HCl pH 8, 1 mM EDTA pH 8, 2% (v/v) Triton-x-100, 1% (v/v) SDS). Approximately 350 µl of 425-600 µm diameter acid washed glass beads (Sigma) were added before disrupting the spores at 4 m^{-s} for 45 seconds using a FastPrep®-24 Cell Disrupter (MP Biomedical). Genomic DNA was extracted in an equal volume of phenol/chloroform/isoamyl alcohol (25:24:1) and precipitated with 100% ethanol, before being re-suspended in 50 µl of TE (10 mM Tris-HCl pH 8, 1 mM EDTA). DNA concentration and purity was determined using a Nanodrop 1000 spectrophotometer (Thermo Scientific), measuring absorption at 230 nm, and ratios of absorption at 260/280 nm and 260/230 nm. Genomic DNA was assessed for *Nosema* species by PCR using species-specific primers (Appendix III) (Chen et al., 2008; Martín-Hernández et al., 2007).

2.4 Bacterial transformation and plasmid propagation

For plasmid construction, selection, and propagation, competent *Escherichia coli* DH5α™ and One Shot® *ccd*B Survival™ (Invitrogen) were heat shock transformed and cultured in luria broth (LB - 0.5% (w/v) NaCl, 0.5% (w/v) yeast extract and 1% (w/v) bactotryptone) at 37ºC, 180 rpm as described (Sambrook et al., 1989). Antibiotics (100 mg/ml kanamycin or 200 mg/ml ampicilin) were added, relative to the selection markers of the different gateway vectors used

in this study. For growth on plates, 2% agar was added. The gateway entry vector pDONR221 (Invitrogen) was used to produce pENTRY clones and advanced gateway destination vectors (Table 2.1) were used to produce expression vectors for each NcS-ORF.

2.5 Standard cloning

Standard recombinant DNA manipulations were performed as described previously (Sambrook et al., 1989). Oligonucleotides were designed to amplify each NcS-ORF from genomic DNA excluding the SP (Prof. Rosalia Diez-Orejas, Madrid, Spain). The primers included the *att*P flanking sequences required for gateway cloning. Oligonucleotides are listed in Appendix III and were synthesized by Sigma. Phusion® high fidelity DNA polymerse (New England Biolabs) and GoTaq® DNA polymerase (Promega) were used for polymerase chain reaction (PCR) following the manufacturer's directions. PCR reactions annealing temperatures were initially trialed at the melting temperature (Tm) - 10°C and optimised when necessary. PCR products were resolved by DNA gel electrophoresis (1% (w/v) agarose in TAE (40 mM Tris, 20 mM acetic acid, 1 mM EDTA (pH 8)) containing 0.5 mg/ml ethidium bromide (Sigma Aldrich) and visualised using the G:BOX and GeneSys software (Syngene). PCR products were identified under UV light and manually excised for purification using the QIAquick PCR purification kit (Qiagen). DNA was quantified using a nanodrop spectrophotometer (Thermo scientific).

2.6 Gateway® cloning and plasmid purification

Gateway® cloning was achieved using the Invitrogen multisite gateway recombinational cloning technology, carried out following the manufacturer's guidelines using half the recommended reagent volumes (see page 77) (Alberti et al., 2007). One Shot® *ccd*B Survival™ *E. coli* strain was used to propagate the gateway donor vector pDONR221 and the destination vectors (Table 2.1) (Invitrogen; Alberti et al., 2007). Both entry and expression vectors were propagated using competent *E. coli* strain DH5α™. All plasmids were purified using the GenElute™ HP Plasmid Miniprep Kit following the manufacturers protocol (Sigma) and confirmed by DNA sequencing (Oxford Zoology Sequencing Department).

2.7 Yeast Transformation

Transformation of *S. cerevisiae* cells was performed using the method described by Ito et al (Ito et al., 1983) with adaptations. Overnight cell cultures were diluted to approximately 6 x 10^6 cells/ml, and harvested during log phase at approximately 2.4 x 10^7 cells/ml. Cells were washed in 0.1 M lithium acetate (LiAc), incubated at 30ºC for 10 minutes and washed again in 1 ml 0.1 M LiAc. Plasmid DNA (1 µg) mixed with salmon sperm carrier DNA (5 µg) was added to 50 µl of the cell suspension and 500 µl of 50% PEG3500, 0.1 M LiAc solution was added drop wise, before incubating at 30ºC for 1 hour. Cells were heat shocked at 42ºC for 15 minutes before plating on selective media (complete synthetic media (CSM) without histidine).

2.8 Dot assays and growth curves

Cells were grown in standard YPD or CSM supplemented with glucose to a final concentration of 2%, unless otherwise described. Cells were grown to mid-log phase and then either growth curve or dot assays were performed. Semi-aerobic growth curve analysis was performed in triplicate on VersaMax Microplate Reader (Molecular Devices) in sealed plates, at 30°C with shaking at 180 rpm prior to the OD_{600} measurements that were taken every 5 min over a 24 h period. Dot assays were performed by spotting 5 µl of 10-fold serial dilutions (OD_{600} = 0.1, 0.01, 0.001, 0.0001) onto specified media, and sealed plates were incubated at 30°C. All growth curve and dot assay experiments were repeated using three different isolates of each strain.

2.9 Microscopy

S. cerevisiae strains were grown overnight in YPD, washed 3 times in non-fluorescent phosphate buffered saline (PBS) and visualised using the Olympus IX-81 inverted fluorescence microscope, micrographs were processed using ImageJ (Abràmoff et al., 2004).

2.10 Synthetic genetic array

Synthetic genetic interaction screens of NcS-ORFs. The deletion mutant array was robotically manipulated using a Singer RoToR HDA (Singer Instruments, U.K.). For the genome-wide SGA screens the *MAT***α** query strain Y7092 (Tong et al., 2001) was transformed with pAG426GPD::NcS-ORF (Appendix II). The resulting query strains were mated to the *MAT***a** deletion mutant array and SGA

methodology (Tong & Boone, 2005; Tong et al., 2001) was used with the modifications previously described to maintain selection of the plasmid. All genome-wide screens were performed in triplicate at 30°C and colony size and SGA scores were determined using SGAtools (Baryshnikova et al., 2010; Wagih et al., 2013) after 1 day of growth. Putative genetic interactions were accepted to be valid when observed in a minimum of two out of three replicates for both screens.

Table 2.1 | Gateway® plasmids used during this study.

Plasmid	Description	Source
pDONR221	Gateway entry vector	Invitrogen
pAG423GPD-*ccd*B-EGFP	High copy, yeast destination vector. Promoter: constitutive GPD; selection: *his3,* ampR; tag: C-terminal EGFP	Addgene
pAG426GPD-*ccd*B-EGFP	High copy, yeast destination vector. Promoter: constitutive GPD; selection: *ura3,* ampR; tag: C-terminal EGFP	Addgene
pAG423GPD-*ccd*B-DsRed	High copy, yeast destination vector. Promoter: constitutive GPD; selection: *his3,* ampR; tag: C-terminal DsRed	Addgene
pAG426GPD-*ccd*B-DsRed	High copy, yeast destination vector. Promoter: constitutive GPD; selection: *ura3,* ampR; tag: C-terminal DsRed	Addgene
pAG426GPD-*ccd*B	High copy, yeast destination vector. Promoter: constitutive GPD; selection: ura3, ampR; tag: None	Addgene

(Vector maps can be accessed at http://www.addgene.org/)

Chapter 3 | Comparative analysis of microsporidian secretomes and functional assessment of *N. ceranae* species-specific secretome ORFs.

3.1 Introduction

Secreted effector proteins are the tools employed by pathogenic microbes to manipulate host biological processes, hijacking host resources and bypassing immune defences (De Wit et al., 2009). Eukaryotes secrete proteins through either a classical or non-classical route (Nickel, 2003) and while non-classical mechanisms remain unclear, classical secretion has been well characterised, requiring an N-terminal SP to direct proteins through the endoplasmic reticulum (ER) and golgi secretory system. As previously discussed microsporidia have undergone genomic reduction limiting pathway and complex components to the bare essential requirements and this observation is true for their protein export machinery, highlighted when considering the 16 components of standard eukaryotic vesicular transport has been reduced to only 3 broadly retained components (Sec22, Ykt6 and Stx1) (Campbell, 2013) suggesting these are the essential minimum requirements for microsporidian export machinery. Although microsporidian genomes are characteristically streamlined, some gene families are expanded and include species-specific secreted proteins (Campbell et al., 2013; Cuomo et al., 2012; Desjardins et al., 2015; Nakjang et al., 2013). *Nematocida parisii* and *Nematocida sp*1 are both natural pathogens of *Caenorhabditis* nematodes and analysis of their genomes identified the presence of an N terminal SP encoded within the hexokinase gene (Cuomo et al., 2012). This is a conserved feature across much of the phylum including *N. ceranae.* Hexokinase is a

component of the glycolytic pathway, catalysing the conversion of glucose to glucose-6-phosphate, but is not known to be secreted in other eukaryotes. Cuomo and colleagues (2012) determined the putative SP's were capable of directing the hexokinase gene products through the *S. cerevisiae* secretion system experimentally and suggested they may be targeted into the host cell to reprogram it towards biosynthesis. The functional capacity of predicted SP's from a broad range of proteins and domain families in the microsporidian *A. locustae* has also been recently demonstrated and includes; chaperone Hsp70, trehalase, LRR proteins (one family A, one family B), hexokinase, α/β-hydrolase and ricin B-like lectin (Senderskiy et al., 2014). Finally, the genomes of both *E. aedis* and *V. culicis* encode putatively secreted hexokinase and trehalase enzymes, but also a ubiquitin hydrolase (Desjardins et al., 2015) which could function to disrupt host immunity as the ubiquitin system was recently implicated in the immune defence of *C. elegans* against microsporidian infection (Bakowski et al., 2014). Desjardins et al. (2015) also identified 335 and 169 secreted proteins in the *E. aedis* and *V. culicis* genomes, respectively, that are expressed during infection which appear to be species-specific and lack predicted domains. Microsporidian secretomes have been shown to be dominated by microsporidian-specific proteins (72%) compared to proteins they share with other eukaryotes (Nakjang et al., 2013). Taken together these data suggests that microsporidia possess a broad set of enzymes and regulatory proteins including many lineage specific families, capable of being secreted into infected cells and directing host metabolic processes and molecular programs. Due to their over-representation, characterising the lineage-specific

proteins is essential if we want to understand the mechanisms of pathology in *N. ceranae* and indeed all microsporidia.

There are situations where proteins that possess an SP are not secreted extracellularly; when they contain a hydrophobic signal in the C terminus which anchors the protein in the ER; when they possess transmembrane (TM) domains; or in the case of glycosylphosphatidylinositol (GPI) anchors which stay inserted in the membrane due to C terminal linked glycolipids (Petersen et al., 2011)

To assess the *N. ceranae* secretome (NcS) in the context of the microsporidian phylum and especially its closest relative *N. apis*, predicted proteomes for every available sequenced species were downloaded from NCBI and subjected to bioinformatic assessment using SignalP-4.1, TMHMM, BIG-PI, Pfam and BLASTP to predict the presence of SP's, transmembrane helices (TM), GPI anchors, known domains, and orthologues. The most broadly retained domains were also identified as well as species-specific proteins.

Original bioinformatic assessment of the *N. ceranae* genome identified 89 genes which putatively encode SP's (using SignalP-3.0) comprising the known NcS (Cornman et al., 2009). Half of these genes have previously been cloned to produce an ORFeome tool by which NcS proteins can be interrogated experimentally and determine their function (Lalik, 2015). I set out to clone the outstanding NcS genes from the originally predicted 89 and characterise their encoded proteins when heterologously expressed in the model-host *S. cerevisiae.* To achieve this, primers were designed to amplify the processed peptide only, i.e. excluding the SP sequence, ensuring the expressed proteins are not secreted out

of the model-host. The NcS subset in this study is entirely comprised of microsporidian-specific proteins which lack known homologs.

Here I show the expansion of the NcS in conjunction with improved SP prediction algorithms, namely the release of SignalP-4.1 (Petersen et al., 2011). *N. ceranae* possesses a larger arsenal of secreted proteins compared to *N. apis,* yet having a smaller genome. The larger secretome may account for its greater pathogenicity and broader host range amongst different bee species compared to *N. apis*. I also present the first functional characterisation of lineage-specific hypothetical proteins from the microsporidia, which present distinct phenotypes when expressed in *S. cerevisiae* and may point towards the processes they target in native host bee cells.

3.2 Methods

3.2.1 Bioinformatics

The sequences of available microsporidian proteomes were downloaded from the National Centre for Biotechnology Information (NCBI) (http://www.ncbi.nlm.nih.gov/) including; *E. cuniculi* (GB-M1), *E. romaleae, E. hellem, E. intestinalis, E. bieneusi, Ne. parisii* (ERTm1_V3), *Nematocida sp.* (ERTm6_V2), *A. algerae, S. lophii, T. hominis, N. bombycis, N. antheraeae, N. ceranae, N. apis, E. aedis* and *V. culicis.* All proteomes were searched for predicted secreted proteins using default SignalP-4.1 score criteria for eukaryotes: D-cut-off for SignalP-noTM networks; 0.45, D-cut-off for SignalP-TM networks; 0.5) (Petersen et al., 2011). The predicted secretomes were assessed for TM's using TMHMM Server v. 2.0 (Krogh et al., 2001) and mature peptides determined as having a TM were excluded from further analysis. Conserved domains were determined using Pfam 28.0 (Finn et al., 2014). The predicted NcS was searched against the NCBI non-redundant protein database using BLASTP (protein-protein BLAST) to identify orthologous sequences with a predefined cut-off of $1e^{-05}$ (Altschul et al., 1990). Species-specific sequences were identified using BLASTP ($1e^{-05}$) against a custom built microsporidian database (Camacho et al., 2009).

3.2.2 Cloning *N. ceranae* secreted proteins and their heterologous expression in *S. cerevisiae*

N. ceranae spores were purified and DNA extracted as described in Chapter 2. NcS-ORFs were amplified from genomic DNA using ORF specific primers (which added the *att*P adapters required for gateway cloning, Appendix III) and

Phusion high fidelity DNA polymerase (New England Biolabs). The majority of ORFs were amplified with an annealing temperature of 68°C, and optimised where necessary. PCR amplicons were assessed by gel electrophoresis and cloned into the entry vector pDONR221 by BP Clonase reaction following the manufacturer's directions (Life Technologies) to complete the NcS entry clone ORFeome (Lalik, 2015). NcS entry clones were shuttled to destination vectors to produce expression clone libraries by LR Clonase reaction following the manufacturer's directions (Life Technologies). Destination vectors; pAG423GPD-*ccd*B-EGFP and pAG423GPD-*ccd*B-DsRed contain the *HIS1* gene for auxotrophic selection on media lacking histidine and are under the glycerol-3-phosphate dehydrogenase (GPD) constitutive promoter with either an EGFP C-terminal tag or a DsRed C-terminal tag respectively; pAG426GPD-*ccd*B-EGFP and pAG426GPD-*ccd*B-DsRed contain the *URA3* gene for auxotrophic selection on media lacking uracil and are also under the GPD constitutive promoter with either an EGFP C-terminal tag or a DsRed C-terminal tag respectively (Table 2.1). Sequence confirmed plasmids were used to transform the parental strain *S. cerevisiae* BY4741 as described in Chapter 2 and plated onto complete synthetic media (CSM) without histidine for pAG423 plasmids or without uracil for pAG426 plasmids. Created strains are listed in Appendix II.

3.2.3 Fluorescent microscopy of heterologously expressed GFP tagged *N. ceranae* ORFs

S. cerevisiae BY4741 strain containing the empty pAG423GPD-*ccd*B-EGFP plasmid and strains containing the pAG423GPD-NcS-ORF-EGFP plasmids

(Appendix II) were inoculated into 5 ml CSM-His broth and cultured for 16 h at 30°C, 180 rpm. Cells were harvested by centrifugation at 1,500 x g, washed 3 times and re-suspended in sterile PBS. Cells were then mounted and observed with a 100 x objective lens using the Olympus IX-81 inverted fluorescence microscope under DIC and fluorescence at an excitation/emission wavelength of 488/510 nm. Images were processed with ImageJ software (Abràmoff et al., 2004).

3.2.4 Co-localisation assay for DsRed-fused *N. ceranae* proteins with *S. cerevisiae* GFP-fused compartment marker proteins

S. cerevisiae strains expressing GFP-fused compartment marker proteins are listed in Appendix IV (Thermo Fisher Scientific) (Huh et al., 2003). The Yeast GFP collection strain Erg6-GFP (Delta (24)-sterol C-methyltransferase; converts zymosterol to fecosterol and is the sixth enzyme in the ergosterol biosynthetic pathway, co-localises with lipid droplets) was transformed with the empty pAG426GPD-*ccd*B-DsRed plasmid control; pAG426GPD-NcS-50-DsRed and pAG426GPD-NcS-85-DsRed as described in Chapter 2 and plated onto CSM-His-Ura. The resulting strains were prepared for fluorescent microscopy as described above, excitation/emission wavelengths for DsRed are 554/586 nm.

3.2.5 Over expression screen of *N. ceranae* secreted proteins in *S. cerevisiae*

To determine the effect of NcS protein expression on the cellular fitness of *S. cerevisiae,* ORFs were cloned into the destination plasmid pAG423GPD-*ccd*B-EGFP which is constitutively expressed under the GPD promoter and contains a C-terminal GFP fusion. Strains were grown overnight, cell concentration was

measured using a neubauer haemocytometer and diluted to 1 x 10^8 cells/ml. Standardised cultures were spotted (5 µl) onto solid CSM-HIS media in a serial dilution. Plates were incubated at 30°C for 72 h and the resulting colonies were imaged using a G:BOX (Syngene).

3.3 Results

3.3.1 Comparative analysis of microsporidian secretomes

The size of predicted secretomes from the broad diversity of microsporidia included in the present study range from 67-431 proteins (*E. romaleae* and *N. bombycis* respectively) (Figure 3.1), which constitutes 3-13% of their genome encoded proteins (Table 3.1). *N. ceranae* has a smaller genome compared to *N. apis* (7.9 Mb and 8.5 Mb respectively), yet has a greater proportion of its proteome committed to secreted proteins (6.7% and 4.8% respectively). The *N. ceranae* secretome includes 175 proteins (*N. apis* = 132) predicted to encode an N-terminal SP (Figure 3.1), double the number previously predicted (Cornman et al., 2009). With the current version of SignalP (4.1), 13 proteins from the original list no longer meet the software's criteria and are not predicted to be secreted (Appendix I). Sixty-nine of the inferred NcS-ORFs have orthologues in *N. apis,* 38 of which have no similarity to known sequences and 31 are suggested as having conserved domains (Appendix V). Interestingly there appears to be a correlation between secretome size and species relatedness (see Desjardins et al., 2015 Figure 2a) as indicated by the grouped colour blocks identifying host organism in Figure 3.1, with the only exception being *T. hominis* a pathogen of humans, which has a secretome size within the range of the two nematode pathogens *Ne. parisii* and *Nematocida sp*. Another interesting observation is the disparity between the *Nosema* genus where the two bee pathogens *N. ceranae* and *N. apis* have comparable secretome size in the context of the phylum, as do the silk worm pathogens *N. bombycis* and *N. antheraeae,* however the silk worm pathogens both have considerably larger secretomes than the bee pathogens (Figure 3.1).

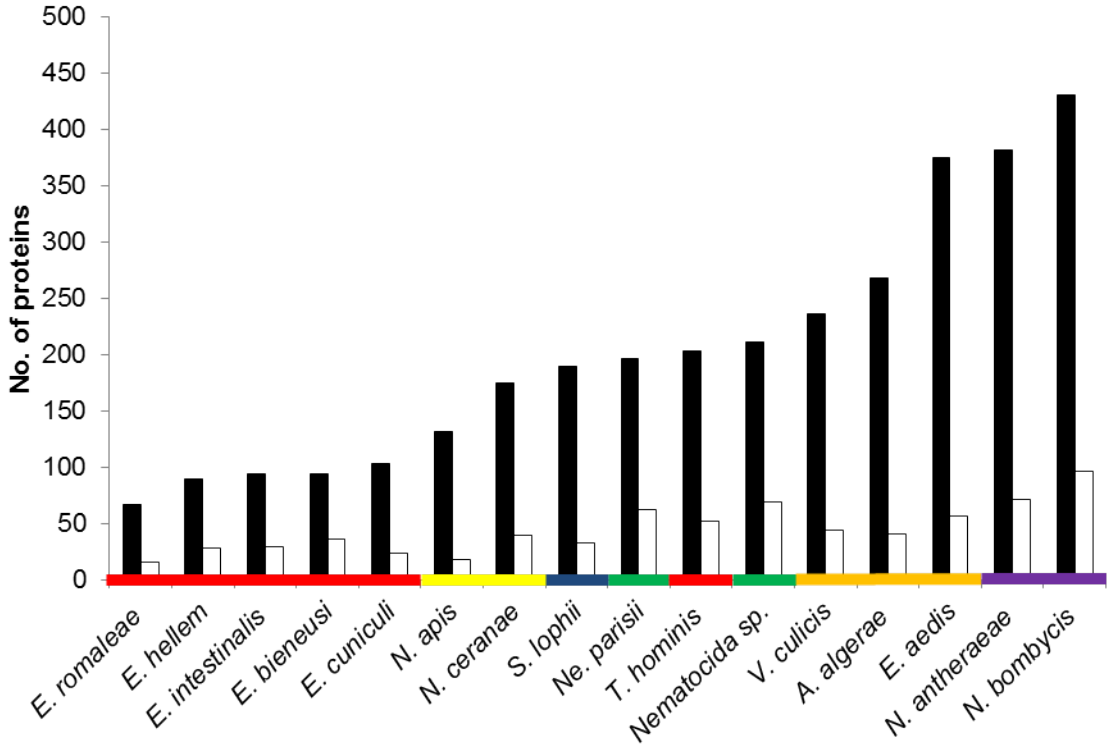

Figure 3.1 | Comparison of the predicted secretome size in microsporidia with completed or draft genomes.

Proteome sequences for each species were downloaded from NCBI (Tatusova et al., 2014) and secretomes determined using SignalP-4.1 default criteria (organism group; eukaryotes, D-cut-off for SignalP-noTM networks; 0.45, D-cut-off for SignalP-TM networks; 0.5) (Petersen et al., 2011). Secretomes were subsequently assessed for transmembrane domains using TMHMM Server v. 2.0 (Krogh et al., 2001). Black bars show all proteins predicted to have a signal peptide. White bars show number of proteins predicted to have a transmembrane domain. Secretome comparison shows > 6 fold variation in protein number ranging from 67 predicted secreted proteins in *E. romaleae* to 431 in *N. bombycis*. The *N. ceranae* secretome is predicted to include 175 proteins. Colours indicate host organism: red = human; yellow = bee; blue = fish; green = nematode; orange = mosquito; purple = silk worm.

Table 3.1 | Features of microsporidian secretomes.

Species	Proteome	Secretome	Secretome as a proportion of proteome (%)	Secretome with protein/domain homologues (%)	Species-specific secretome proteins (%)
E. bieneusi	3804	94	2.5	30	81.2
E. romaleae	1629	67	4.1	36	0.0
N. apis	2764	132	4.8	15	64.0
E. hellem	1848	90	4.9	33	1.6
E. intestinalis	1848	94	5.1	33	9.4
E. cuniculi	1997	104	5.2	28	40.0
T. hominis	3266	204	6.2	17	34.2
N. ceranae	2614	175	6.7	19	45.9
Ne. parisii	2661	197	7.4	17	18.7
S. lophii	2573	190	7.4	33	47.1
Nematocida sp.	2770	211	7.6	16	11.3
V. culicis	2773	237	8.5	17	31.6
E. aedis	4190	375	8.9	9	90.3
N. bombycis	4458	431	9.7	16	18.0
N. antheraeae	3413	382	11.2	12	14.5
A. algerae	2075	268	12.9	8	85.9

N. ceranae has 33 secreted proteins with conserved domains (Appendix VI) meaning 81% of its secretome has undetermined function compared to only 20 proteins with conserved domains in *N. apis*, however this is proportionally similar (85%) (Table 3.1). A large percentage of the inferred secretomes have undetermined function/domains ranging from 64% in *E. romaleae* to 92% in *A. algerae*.

When considering the proportion of secretomes that are predicted to encode TM's, species that are closely related are once again grouped together (Figure 3.1). The exception to this observation is *N. apis* which differs from the rest of the *Nosema* genus and only has 14% of its predicted secretome as TM's followed by; the mosquito pathogens (*V. culicis, A. algerae* and *Ed. Aedis*) (19-15%), *N. ceranae, N. bombycis* and *N. antheraeae* (19-23%), *Encephalitozoon* species (24-32%), *Nematocida* species (32%) and *E. bieneusi* having the greatest proportion of TM's at 38%.

The number of species-specific secreted proteins ranges from 0-287 (0-90% of secretome) in *E. romaleae* and *E. aedis* respectively. Having no species-specific proteins and the smallest microsporidian secretome, the human pathogen *E. romaleae* exhibits the lowest currently known limit for a potential effector repertoire, so identifying orthologues of the *E. romaleae* secretome in *N. ceranae* could potentially identify essential virulence factors. There are 55 *E. romaleae* homologs in the NcS, of these, 28 have known domains (22 without TM's) and 27 are without conserved domains (Appendix VII). *N. ceranae* has 62 (46%) species-specific secreted proteins that do not have TM's, only one of which has a

conserved domain and is predicted to be a nucleoporin FG-repeat (Appendix VI). FG repeats act as transport receptors and have been shown to participate in pathogenicity and nuclear import of viruses (Matreyek et al., 2013), as well as bearing transcriptional activation activity, suggested to be a shared pathogenic function of nucleoporins implicated in human acute myeloid leukaemia (Kasper et al., 1999).

Microsporidia have broadly conserved secretome proteins including components of stress resistance, protein degradation, basic metabolite transporters and chaperones (Table 3.2). Thioredoxin is the most broadly conserved protein across the phylum and is found in 15/16 of the species analysed. Furthermore, the *N. ceranae* genome encodes 3 putatively secreted thioredoxin genes (Appendix VI). Other prominent enzymes include polysaccharide deacetylases, mannosyltransferase, hexokinase, subtilase, trehalase, phospholipase, glutaredoxin and components of the ubiquitin system. Although only two species have conserved DnaJ domains and two separate species have conserved serpin, these proteins were found in numerous copy numbers, while *N. ceranae* has one DnaJ domain protein, *E. bieneusi* has 6. *N. bombycis* has 7 serpin proteins (serine protease inhibitor) and *N. antheraeae* has 5. The most frequently occurring domain in microsporidia secretomes when taken as the total sum of proteins is LRR, the majority (28) being found in the genome of *S. lophii* alone, with *N, apis* having 7 and *E. hellem* having 2. *N. ceranae* possesses multiple copies of conserved domain proteins; 3 x thioredoxin; 3 x ring finger domain; 2 x glutaredoxin; 2 x proteasome subunit; 2 x T-complex protein 1 (chaperone).

Table 3.2 | Common proteins/domains observed throughout microsporidian secretomes.

Protein/domain	*E. cuniculi*	*E. romaleae*	*E. hellem*	*E. intestinalis*	*E. bieneusi*	*Ne. parisii* ERTm1_V3	*Nematocida sp.* ERTm6_V2	*A. algerae*	*S. lophii*	*T. hominis*	*N. bombycis*	*N. antheraeae*	*N. ceranae*	*N. apis*	*A. aedis*	*V. culicis*
Thioredoxin	●	●	●	●	○	●	●	●	●	●	●	●	●	●	●	●
Hsp70 protein	●	●	●	●	○	●	○	●	●	●	●	●	●	●	○	●
Polysaccharide deacetylase	●	●	●	●	○	●	●	○	●	●	●	●	●	○	●	●
Sel1 repeat	●	●	●	●	○	●	●	○	○	●	●	●	●	●	●	●
Spore wall protein	●	●	●	●	○	●	●	○	●	●	●	●	●	○	○	●
Cyclophilin type cis-trans isomerase/CLD	●	○	●	●	○	●	●	○	●	●	○	○	●	●	●	●
Mannosyltransferase	●	●	●	●	○	●	●	○	●	●	●	●	●	○	○	○
Endoplasmic Reticulum Oxidoreductin 1 (ERO1)	●	●	●	●	○	●	○	○	●	○	●	●	○	○	●	●
Polar tube protein 2	○	●	●	●	●	○	○	○	●	●	●	○	●	○	●	●
emp24/gp25L/p24 family/GOLD	○	○	○	●	●	●	●	●	●	●	●	○	○	○	○	●
Hexokinase	●	○	○	●	○	●	●	○	○	●	○	●	●	○	●	●
Peptidase C13 family	○	●	●	○	○	●	●	○	●	●	○	○	●	○	●	●
Subtilase family	○	●	●	●	○	●	●	○	○	○	●	●	○	●	●	○
Gamma-glutamyltranspeptidase	○	○	●	●	●	●	○	●	●	○	○	○	○	●	○	●
GDA1/CD39 (nucleoside phosphatase) family	●	●	●	●	●	○	○	○	○	○	○	●	○	●	●	○
Ring finger domain	○	○	○	○	○	●	●	○	●	●	●	●	●	○	○	●
Cysteine-rich secretory protein family	○	●	●	●	○	●	●	○	○	○	●	○	○	○	●	○
Leucine Rich Repeat	●	○	●	●	○	●	●	○	●	○	○	○	○	●	○	○

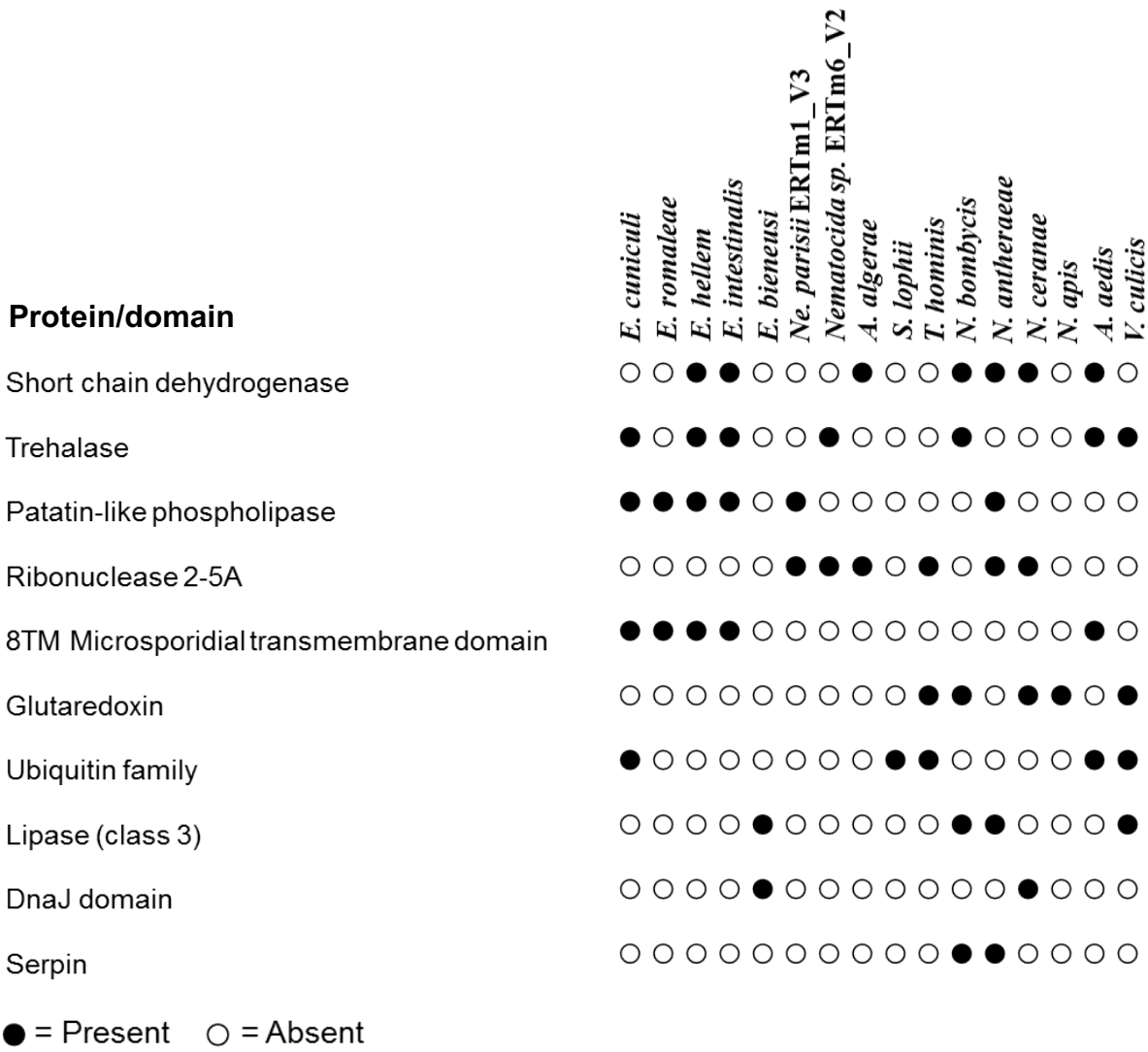

3.3.2 *N. ceranae* secreted protein expression and sub-cellular distribution in *S. cerevisiae* cells

To confirm *N. ceranae* protein expression NcS-ORFs were C-terminally tagged with GFP in plasmid pAG423GPD-EGFP and observed by fluorescence microscopy in *S. cerevisiae.* Of the 40 strains bearing NcS-ORF-GFP plasmids, 13 were confirmed to express *N. ceranae* proteins with distinctive patterns of fluorescence (Figure 3.2). From these 13 strains, 4 separate phenotype categories

were observed for *N. ceranae* proteins; 1) conferring a morphological defect; 2) cytosolic fluorescence; 3) punctate fluorescence and; 4) association with the cell periphery (Figure 3.2, Table 3.3). Three of these categories were consistent with previous data (Lalik, 2015), however the morphological defect is a new phenotype observed in *S. cerevisiae* expressing *N. ceranae* secreted proteins. Examples representing each phenotype category are displayed in Figure 3.2. The wild type bearing empty vector displays minimal fluorescence. While most strains display a single phenotype category some ORFs can present a combination of phenotypes e.g. NcS-51 displays a morphological defect and punctate fluorescence. The range of phenotypes observed suggests these proteins have separate, independent functions.

The bioinformatic data presented above identified NcS-77 as the only species-specific secreted protein with no TM's and predicted to have a conserved domain. This protein is said to encode a nucleoporin FG repeat domain. Figure 3.2 shows NcS-77 presents cytosolic distribution with the signal intensity accumulating in a specific area of the cell (red dashed line). Based on the bioinformatic identification I speculate the area of interest may be protein aggregation at the nuclear envelope, however this hypothesis needs to be confirmed. Interestingly this strain exhibited retarded fluorescence compared to all other strains even though under the same constitutive promoter. The reason for the reduced fluorescence signal remains unknown.

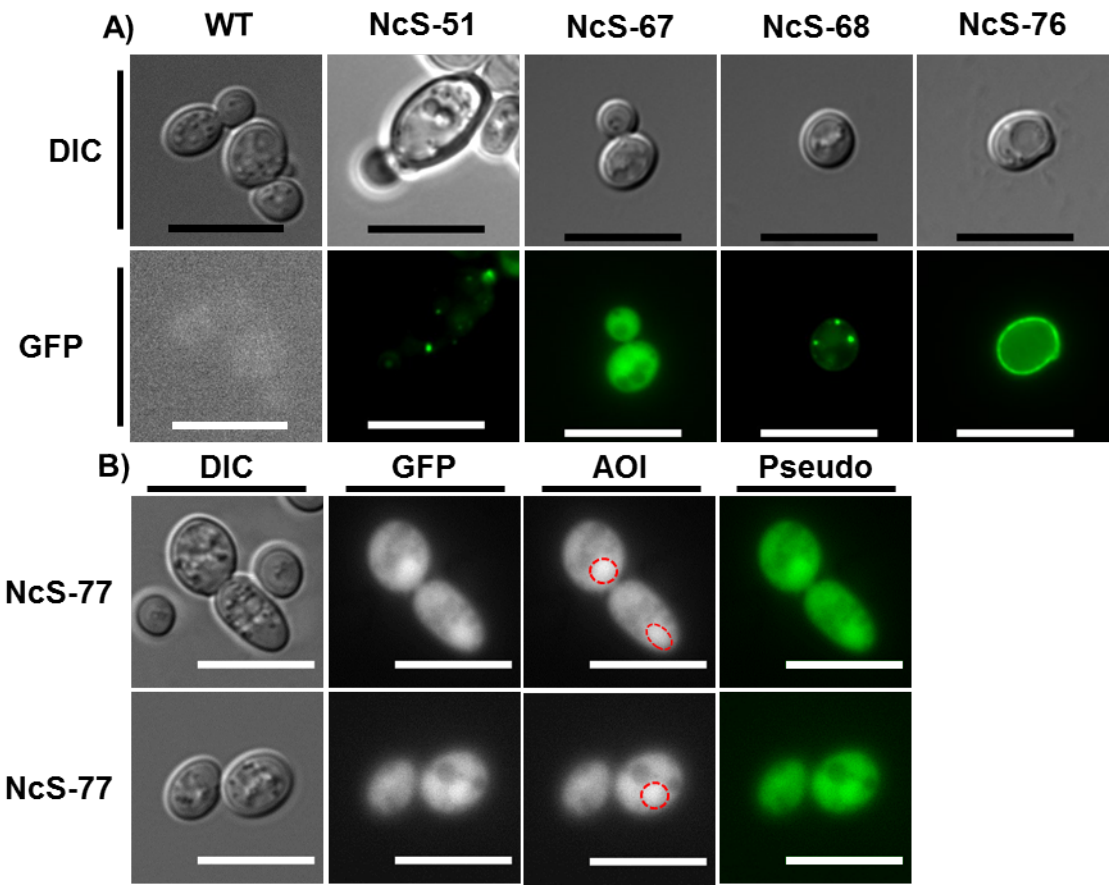

Figure 3.2 | Fluorescent phenotypes of GFP-fused *N. ceranae* secreted proteins expressed in the model-host *S. cerevisiae.*

Cells were grown overnight in CSM-His and washed 3 x in PBS before imaging. **A)** Putative *N. ceranae* secreted proteins exhibit 1 of 4 distinct phenotypes when heterologously expressed in *S. cerevisiae*. NcS-51 displays an example of defected morphology. NcS-67 displays an example of cytosolic localisation. NcS-68 displays an example of punctate fluorescence and NcS-76 displays protein association with the cell periphery. WT = wild type yeast transformed with the empty pAG423GFP-*ccd*B-EGFP plasmid and displays minimal fluorescence. **B)** NcS-77 is the only species-specific secreted protein with a predicted conserved domain - Nucleoporin FG repeat. This strain only expresses a weak GFP signal even though under the same promoter as the other strains. It presents a cytosolic localisation with signal intensity concentrated in one area of each cell highlighted in the area-of-interest (AOI) panel with a dashed red line (scale bar = 10 μm).

Table 3.3 | Fluorescent phenotypes of *N. ceranae* secreted proteins with C-terminal GFP tag expressed in *S. cerevisiae.*

NcS-ORF	Phenotype
NcS-49	Cytosol
NcS-50	Punctate
NcS-51 (PTP*1)	Morphological defect/cytosol
NcS-65	Punctate
NcS-67	Cytosol
NcS-68	Punctate
NcS-75 (PTP*2)	Morphological defect/cell periphery
NcS-76	Morphological defect/cell periphery
NcS-77	Cytosol
NcS-79	Punctate
NcS-83	Cytosol
NcS-85	Punctate
NcS-86	Cytosol

*Polar tube protein.

3.3.3 Co-localisation of *N. ceranae* proteins with *S. cerevisiae* lipid droplets

Order is maintained in the extremely dynamic and complex environment that is the eukaryotic cell through an elaborate network of membranes and compartments, which have varied and specific biological functions. Knowing where proteins localise can inform on the biological processes they participate in and contribute to (Huh et al., 2003). Thus, I sought to identify the subcellular targets of the NcS-ORFs that were identified as exhibiting a punctate fluorescence phenotype. Yeast GFP collection strain Erg6-GFP, bearing NcS-ORFs C-terminally tagged with DsRed in plasmid pAG426GPD-DsRed, were grown overnight in CSM-His-Ura broth and observed by fluorescence microscopy (Figure 3.3). Two

N. ceranae secreted proteins NcS-50 and NcS-85 were observed co-localising with *S. cerevisiae* Erg6 which is a marker for lipid droplets (LD). Two examples are shown for each strain. The observation of co-localisation is supported by fluorescence intensity plot profiles of each sample where the peaks for Erg6-GFP perfectly align with the peaks for NcS-ORF-DsRed (Figure 3.3, E-H) suggesting that NcS-50 and NcS-85 target and bind to lipid droplets.

Lipid droplets are primarily considered for their role in neutral lipid storage but have also been shown to function in co-ordinating immune responses, contributing to the generation of prostaglandins, participating in interferon responses and antigen cross presentation (Saka & Valdivia, 2012). Many diverse mammalian pathogens including hepatitis C, Dengue viruses, *Chlamydia*, and *Mycobacterium* are seen targeting LDs during infection, with the perceived purpose of nutrition acquisition or disrupting LD innate immune functions. The observation of *N. ceranae* secreted proteins localising to LDs may be an example of a convergent evolutionary strategy for obligate intracellular pathogens.

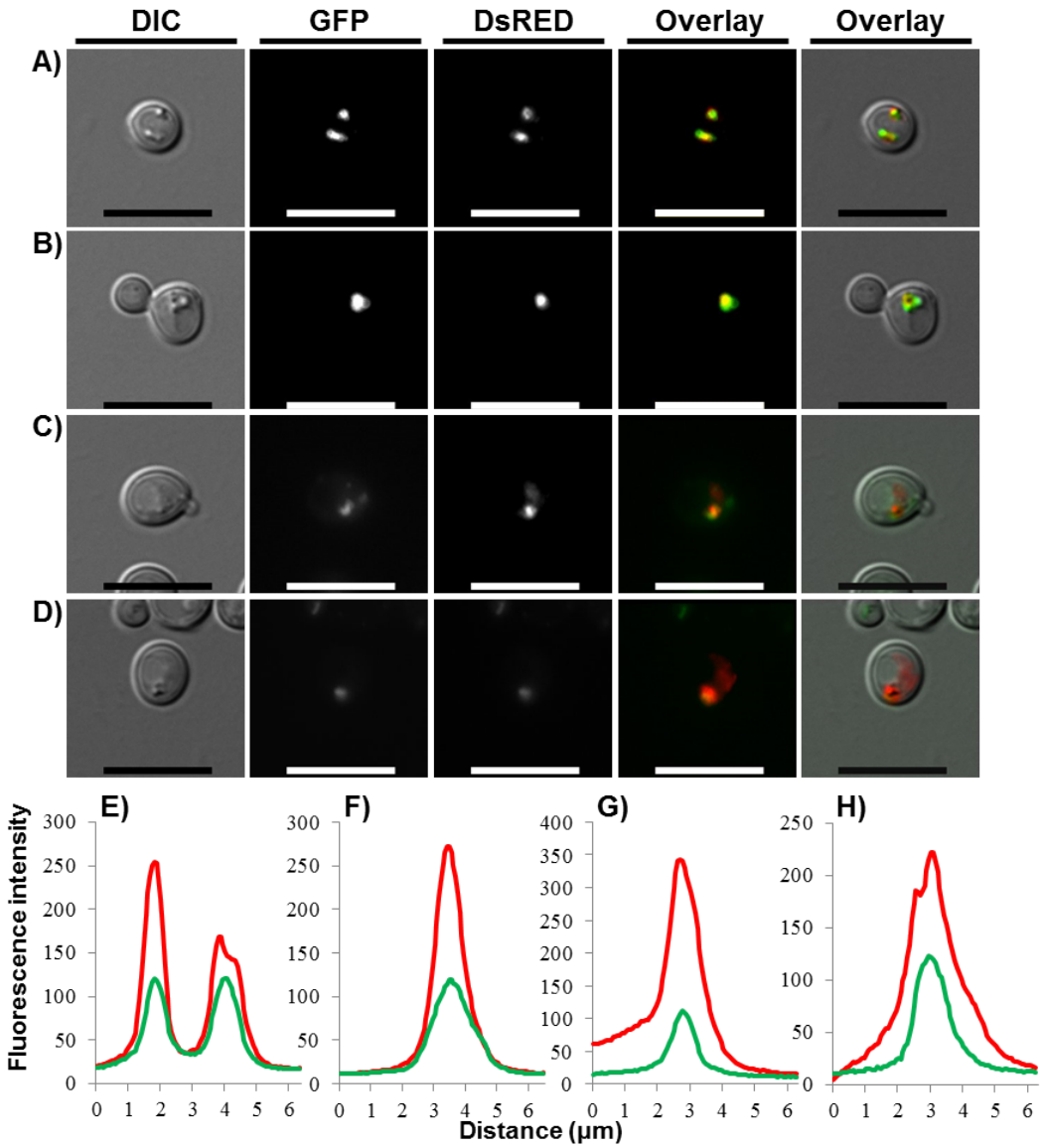

Figure 3.3 | Co-localisation of NcS proteins with *S. cerevisiae* lipid droplets. *S. cerevisiae* ergosterol-6 (Erg6) is a marker for lipid droplets. Cells were grown overnight in CSM-His-Ura and washed 3x in PBS before imaging. **A-B)** *N. ceranae* protein NcS-50 tagged with DsRed was over-expressed in *S. cerevisiae::*Erg6-GFP. **C-D)** *N. ceranae* protein NcS-85 tagged with DsRed over-expressed in *S. cerevisiae::*Erg6-GFP. **E-H)** Fluorescent profile plots of GFP (green line) and DsRed (red line) images from panels A-D (E = panel A, F = panel B, G = panel C and H = panel D). GFP and DsRed patterns are comparable in each sample indicating co-localisation of *N. ceranae* proteins with lipid droplets, confirmed by aligning peaks of fluorescent profile plots (scale bar = 10 µm).

3.3.4 Impact of *N. ceranae* secretome ORFs on cellular fitness of *S. cerevisiae* as a model-host system

Following transformation of *S. cerevisiae* BY4741 with pAG423GPD-NcS-ORF-EGFP plasmids, 13 strains were confirmed to express *N. ceranae* proteins by fluorescent microscopy. To determine the effect of NcS-ORF expression on *S. cerevisiae* cellular fitness, these 13 strains and *S. cerevisiae* bearing pAG423GPD-*ccd*B-EGFP were grown on selective agar media from standardised cell concentrations for 72 h at 30°C (Figure 3.4). As expected all starting concentrations of the serially diluted wild type strain bearing empty vector grew without issue, inferring little effect of the plasmid itself. A varied degree of growth inhibition is observed for the different NcS proteins. Expression of; NcS-49, NcS-50, NcS-67, NcS-68, NcS-77 and NcS-79 did not confer an identifiable growth defect to *S. cerevisiae* compared to the wild type control, but a moderate growth defect was observed for; NcS-65, NcS-75, NcS-76, NcS-83, NcS-85, NcS-86 and is most pronounced in strain expressing NcS-51. These results were supported by growth curve analysis in liquid media under the same conditions (data not shown) suggesting that different *N. ceranae* secreted proteins have distinct physiological effects on *S. cerevisiae* cells. This may relate to their different targeted processes and biochemical functions.

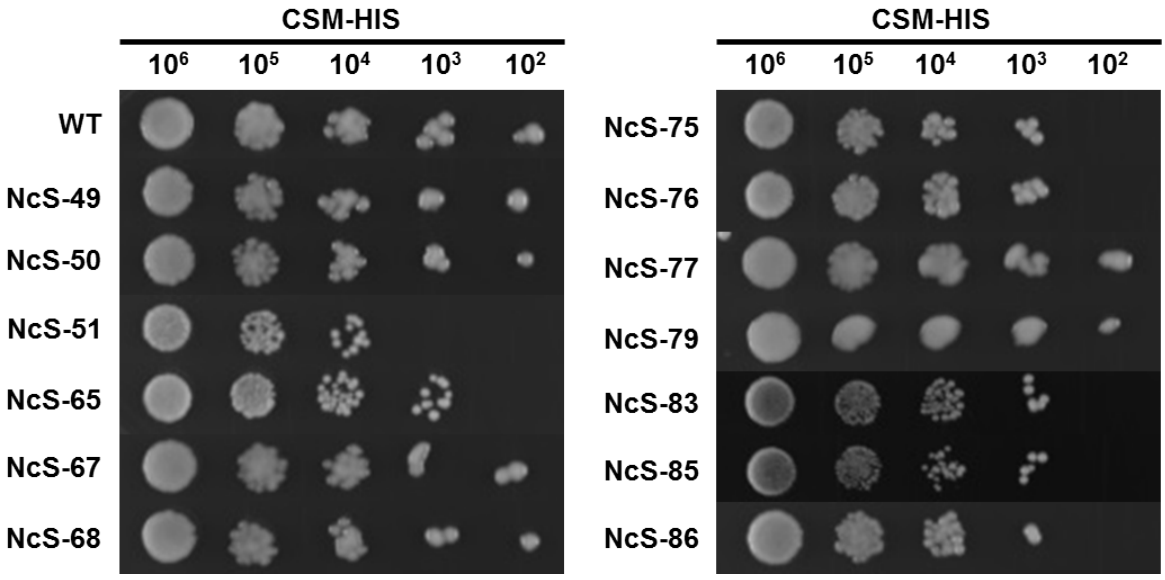

Figure 3.4 | Over expression screen of *N. ceranae* secretome (NcS) ORFs in *S. cerevisiae* on solid growth medium.

S. cerevisiae BY4741 expressing empty plasmid control pAG426GPD-*ccd*B-EGFP (WT) and NcS-ORFs C-terminally tagged with EGFP were spotted onto solid CSM – HIS from a serial dilution. Cells were grown at 30°C for 72 hours. A moderate growth defect is observed for NcS-65, NcS-75, NcS-76, NcS-83, NcS-85, NcS-86 and is most pronounced in strain NcS-51 suggesting this ORF confers the greatest stress to the yeast cells. Normal growth is observed for strains NcS-49, NcS-50, NcS-67, NcS-68, NcS-77 and NcS-79.

3.4 Discussion

Microsporidia can drastically affect host cell physiology with examples including; re-organisation of the mitochondrial network; re-positioning the host nucleus; host cell lysis leading to the formation of syncytia and much more (see section 1). These organisms also create a significant energetic deficit to the host during sporogony while the developing spores sequester metabolic resources (Mayack & Naug, 2009). The diverse range of effects from these host-pathogen interactions have been characterised morphologically, yet the molecular processes driving them remain unknown, not least because of microsporidian intractability to genetic manipulation. Knowledge has been growing over the past few decades on the essential role secreted effector proteins play as virulence factors of bacterial, fungal and oomycete pathogens of many different host organisms (Deslandes & Rivas, 2012; J. G. Ellis et al., 2009; Giraldo & Valent, 2013; Giraldo et al., 2013; Hunter & Sibley, 2012; Morgan & Kamoun, 2007; Schornack et al., 2009; Valdivia, 2008). The microsporidian species assessed in this study show varied secretome sizes with *E. romaleae* having only 67 secreted proteins, compared to *N. bombycis* having 431 representing 2.5-12.9% of the proteome (Figure 3.1).

Interestingly *N. ceranae* which is widely reported as being more pathogenic to honeybees compared to *N. apis,* has the smaller genome of the two species and yet retains many more secreted proteins (175 compared to *N. apis* 132). I hypothesise that having a larger arsenal of effectors could be a contributing factor to *N. ceranae* having greater pathogenicity. *N. ceranae* shares 69 orthologous proteins with *N. apis* in their secretomes (40%). This provides a cohort of 106

proteins that could confer a competitive advantage to *N. ceranae* over *N. apis* that warrant prioritising for future study (Appendix V).

While *N. ceranae* is reported to be pathogenic in a broad range of hosts including different honeybee and bumblebee species, there is limited information on the capacity of *N. apis* to infect a comparable host range. *N. apis* is known to infect different honeybee species however I have not found any study reporting its ability to infect bumblebees. This may not reflect a limitation in the pathogen but may rather reflect the long history of apiculture research focusing on honeybees. As it stands, available information suggests *N. ceranae* has a broader host range compared to *N. apis* and so the observation of *N. ceranae* having the larger secretome contradicts a recent report on mosquito pathogens comparing secretome sizes of a generalist with a specialist (*E. aedis* and *V. culicis* respectively). Desjardins et al. (2015) show that *E. aedis* which is only found infecting *Aedes aegypti* (disease vector of dengue haemorrhagic fever, yellow fever and chikungunya) upregulates the expression of twice the number of secreted proteins during infection, compared to *V. culicis* which infects multiple mosquito genera including species of *Culex* (vector of West Nile virus) and species of *Anopheles* (vector of malaria). The authors suggest the larger secretome and upregulation of the majority of secreted proteins in *E. aedis* reflects its adaptation to a specific host and that the strategy of a generalist is to maintain a simpler lifecycle which allows it to grow in a wider range of hosts (Desjardins et al., 2015).
The observation that related microsporidian species have comparable secretome sizes reflects that they retain similar infection strategies, this is especially noticeable for *E. romaleae* which has no species-specific proteins and orthologs

are found for every one of its secreted proteins in the secretomes of the other *Encephalitozoon* species (Figure 3.1, Table 3.1).

There is considerable over-representation of lineage or even species-specific proteins in microsporidian secretomes which has been suggested to be a reflection of adaptation to different host cell environments (Nakjang et al., 2013). Intriguingly, the only species-specific secreted protein in the *N. ceranae* secretome with a conserved domain and not encoding a TM is predicted to be a nucleoporin-FG-repeat (NcS-77, Appendix VI). Furthermore, when fused to GFP and expressed in *S. cerevisiae* this protein presents a cytosolic localisation phenotype with maximum fluorescence in one specific sub-cellular location (Figure 3.2), which may be indicative of the protein aggregating at the nuclear envelope, however this hypothesis remains to be confirmed. It has previously been shown that viral capsid protein mediates the dependency on cellular nucleoporin (NUP) 153 during HIV-1 infection, through interactions between its N-terminal domain and the FG-repeat enriched NUP153 C-terminal domain to affect viral nuclear import (Matreyek et al., 2013). It is believed that FG-repeats on nuclear pore complex proteins interact with FG-repeats on receptors to facilitate transport of soluble proteins and one hypothesis suggests FG-repeats enable these proteins to function as their own transport receptors (Kerr & Schirmer, 2011). A focus for future studies would be to assess any potential role NcS-77 plays in interactions with the host cell nuclear envelope.

Pathogen secretomes possess functional redundancy which makes studying individual gene products difficult (Tan et al., 2015). When considering the proportion of the NcS with inferred domains, identifying protein enrichment for

biological processes could identify complex pathogen-effector systems. I have shown *N. ceranae* has redundancy for thioredoxin proteins and proteins involved with the ubiquitylation/proteasome system (3 proteins each, Appendix VI). Ubiquitination regulates many cellular processes, including protein degradation by the proteasome and endocytosis from the plasma membrane (Torto-Alalibo et al., 2010). Many pathogens exploit the host ubiquitin pathway to supress immune responses which might suggest a possible role for these three *N. ceranae* proteins. Varied phenotypes of *N. ceranae* protein distribution expressed in *S. cerevisiae* cells is indicative of a range of functions for the separate NcS proteins (Figure 3.2), which is supported by the varying impact these proteins have on *S. cerevisiae* cellular fitness (Figure 3.4). Of particular interest are the two proteins seen associating with *S. cerevisiae* LDs. LDs are ubiquitous in eukaryotic cells serving as storage organelles for neutral lipids. They also interact with other organelles of the cell, including the endoplasmic reticulum, mitochondria and peroxisomes. But potentially their most significant function regarding the present study is in coordinating immune responses to intracellular pathogens (Saka & Valdivia, 2012). The obligate intracellular human pathogen *Chlamydia trachomatis* has been shown to secrete effector proteins that interact with and cause LDs to aggregate at the membrane of the bacteria-containing vacuole. Furthermore, inhibition of LD formation negatively impacts pathogen replication suggesting a dependence on host LDs for survival and replication (Kumar et al., 2006). Although I did not find homologs of these LD targeting proteins in the *N. ceranae* genome, NcS-50 and NcS-85 may present components of a convergent evolutionary strategy of obligate intracellular pathogens to co-opt host organelles.

Chapter 4 | Unique phenotypes of *N. ceranae* polar tube proteins and a new component of the *N. ceranae* invasion apparatus.

4.1 Introduction

Microsporidia are defined by distinct ultrastructural features including the unique invasion apparatus of the polar filament, also known as, and referred to in the present study as the polar tube. In most species the polar tube is threadlike and considerably longer than the spore itself. Common features include; a straight anterior section approximately one-third of the spore length called the manubrium, this section ends in a sharp bend toward and extends to the spore wall, and the last section includes the majority of the polar tube length which exists as multiple filament coils (Figure 4.1, A) (Franzen & Müller, 1999; Franzen, 2004; Vávra & Larsson, 1999). The polar tube grows throughout sporogony with new coils being added until spore maturity, where immature coils are more narrow than mature ones and with a less complex internal organisation. When fully mature the polar tube appears multi-layered comprised of a number of concentric rings of different thickness and electron density, with the entire structure being surrounded by a membrane sheath (Figure 4.1, B) (Cali et al., 2002; Larsson, 1986; Takvorian & Cali, 1981, 1986; Vavra, 1976). The number of coils depends on the species and does not significantly vary within a species. The 4.4 x 2.2 µm diameter spore of *N. ceranae* is observed to have 18-21 coils of the polar tube arranged in a single layer anteriorly and a double layer of coils posteriorly (Chen et al., 2009). The polar tube terminates with the polar sac-anchoring disk complex which contains mannose-rich glycoproteins, located at the internal apex of the spore (Figure 4.1,

A) (Taupin et al., 2007). This is the site of spore rupture through which the polar tube germinates as a result of it being the thinnest part of the spore wall. Following polar tube eversion the lamellar polaroplast becomes distended and fills more than half of the spore volume, the polar tube cross sections are rearranged within the spore and the nucleus and cytoplasm initially remain where they are. Studies of *A. algerae* have shown the everted polar tube may have a dense fibrous coating in contrast to its pre-extrusion appearance (Cali et al., 2002). Following ejection of the spore contents through the everted polar tube, a process that takes < 2 seconds (Frixione et al., 1992), the sporoplasm and empty spore shell can remain attached to the polar tube for several minutes (Cali et al., 2002; Scarborough-Bull & Weidner, 1985).

The secretory machinery of microsporidia functions to sort three main protein groups involved with pathogenesis; effectors (secreted extracellularly), transmembrane proteins, and key components of the invasion apparatus (polar tube and spore wall) (Williams et al., 2014). A portion of the large mature Golgi observed in the sporoblast serves to contain PTPs. The polar tube originates in most microsporidia as an oval body of membranes, the formation of a Golgi-like structure including cisternae, small vesicles, sacs, and finally, vacuole-like structures are formed into tubules producing hollow rings that are pinched off resulting in the polar tube (Sprague & Vernick, 1968; Takvorian & Cali, 1996; Williams et al., 2014).

Identifying PTPs has been the focus of considerable research due to the essential role the polar tube plays during infection. PTPs were first observed in *Ameson michaelis* (Weidner, 1976) and the full amino-acid sequences of PTP1,

PTP2 and PTP3 were first determined for *E. cuniculi* (Delbac et al., 1998, 2001; Peuvel et al., 2002). Each of these proteins are encoded by single copy genes in the *E. cuniculi* genome with *ptp1* and *ptp2* being tandemly arranged on chromosome VI. PTP1 is an acidic proline-rich protein, with a deduced molecular mass of 37 kDa, containing four tandemly arranged 26-amino-acid repeats (Delbac et al., 1998). In comparison PTP2 has a basic lysine-rich core with an acidic tail and has a molecular mass of 30 kDa (Delbac et al., 2001). PTP2 differs from PTP1 in that it lacks large tandem repeats. Delbac et al. (2001) identified the interspecies conservation of cysteine residues in these proteins which supports a major role of disulphide bridges in polar tube assembly, possibly contributing to the high tensile strength of the polar tube (Delbac 2001). The *E. cuninculi ptp3* gene is on chromosome XI and is predicted to encode a 1256-amino acid protein with a cleavable signal peptide and has a molecular mass of 136.2 kDa. This much larger PTP not only differs from PTP1 and PTP2 in size but also lacks cysteine residues. The large acidic core of PTP3 is flanked by highly basic N- and C-terminal regions. PTP3 has been shown to be involved in the sporoblast-to-spore polar tube biogenesis (Peuvel et al., 2002). All three PTPs have been identified forming a large multimeric complex with a few other unidentified proteins. *Ecptp2* and *Ecptp3* have orthologues in the *N. ceranae* genome and while there is not significant sequence similarity between *Nc*PTP1 and *Ec*PTP1 as determined by BLASTP, the identity of *Ncptp1* was inferred by its synteny with *Ncptp2* and encoded protein features such as a predicted SP, inferred protein size and amino acid composition (Cornman et al., 2009).

I sought to characterise *N. ceranae* PTPs when overexpressed in *S. cerevisiae* to identify any defining phenotypes which may facilitate identification of undiscovered PTPs from the multimeric complex reported by Peuvel et al. (2002) in *E. cuniculi*. Here I describe a conserved effect of induced morphological deformity when overexpressing *Nc*PTP*s* in yeast and furthermore *Nc*PTP2 associates with the *S. cerevisiae* cell wall. Based on pheno-mimicry I propose the identity of a novel putative PTP.

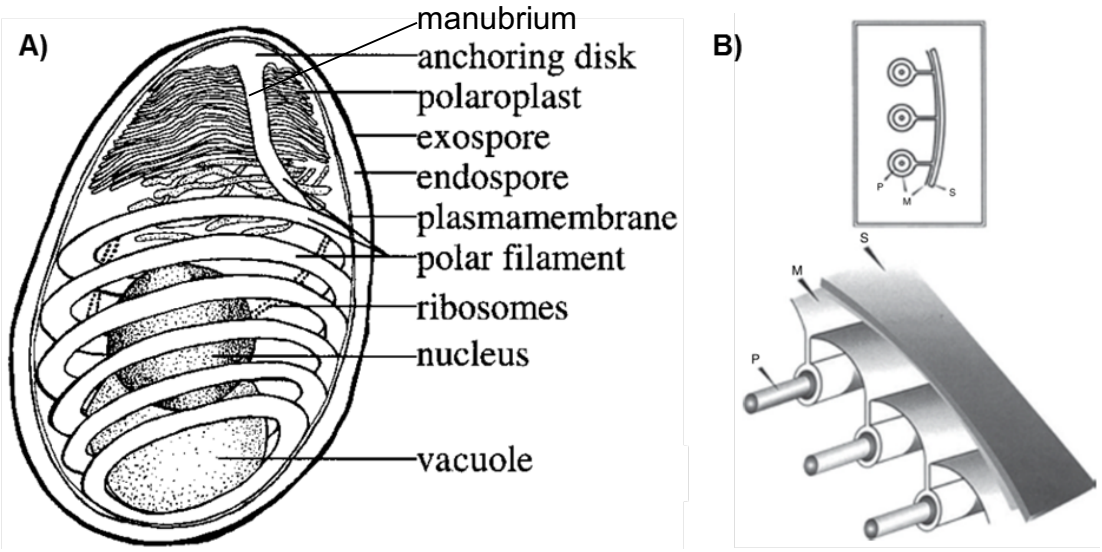

Figure 4.1 | The microsporidian polar tube within the mature spore.
A) Diagram of a generalised microsporidian spore. Polar filament = polar tube. **B)** Two simplified diagrammatic representations of a portion of the spore, illustrating the isolation of the polar filament (P) by the spore plasma membrane (M) system. The polar filament coils are surrounded by a membrane system which forms from a series of infolding's of the membrane that underlies the spore coat (S), thus resulting in the extra-cytoplasmic location of the polar filament in relationship to the sporoplasm (Adapted from Cali et al., 2002 and Franzen & Müller, 1999).

4.2 Methods

4.2.1 Heterologous expression and fluorescent microscopy of PTPs

S. cerevisiae BY4741 parental strain was transformed with the empty overexpression vector pAG423GPD-*ccd*B-EGFP as control, and gateway expression vectors; pAG423GPD::*Ncptp1EGFP,* pAG423GPD::*Ncptp2EGFP,* and pAG423GPD::*NcS76* which contain the *HIS1* gene for auxotrophic selection on media lacking histidine, controlled by the constitutive GPD high copy number promoter and fuses EGFP to the C-terminal of the inserted gene. Transformants were plated onto CSM-His agar plates. Resulting strains were inoculated into 5 ml CSM-His broth and grown overnight at 30ºC, 180 rpm. Cells were harvested, washed 3 x in sterile PBS, mounted on cover slips and assessed for GFP fluorescence using the Olympus IX-81 inverted fluorescence microscope. Micrographs were processed using ImageJ (Abràmoff et al., 2004).

The same method was used to confirm co-localisation of *N. ceranae* proteins with the *S. cerevisiae* cell wall with the addition of 0.01% (w/v) Calcofluor White (CFW, Sigma Aldrich) after the first cell wash, and incubated for 15 min in the dark at room temperature. Samples were once again washed 3x in sterile PBS to remove excess CFW and reduce non-specific background staining and assessed for fluorescence. CFW excitation and emission wavelengths were 365/435 nm respectively.

To confirm co-localisation of PTP2 with NcS76 in *S. cerevisiae* the expression clone previously transformed with pAG423GPD::*ptp2EGFP* was subsequently transformed with the expression vector pAG426GPD::*NcS76DsRed* which contains the *URA3* gene for auxotrophic selection on media lacking uracil

again under the control of the constitutive GPD high copy number promoter and fuses DsRed to the C-terminal of *NcS76.* Transformants were plated onto CSM-His-Ura agar plates. This strain was inoculated into 5 ml CSM-His-Ura broth and grown overnight. Cells were harvested, washed 3x in PBS, mounted onto coverslips and assessed for GFP and DsRed fluorescence as previously described. DsRed excitation and emission wavelengths were 557/592 nm respectively.

4.2.2 Bioinformatics

Amino acid sequence similarity of proteins was assessed by BLASTP using the predefined cut off of 1 x e^{-05}. Molecular weights for processed proteins i.e. excluding SP were calculated using ExPASy compute pI/Mw tool (http://web.expasy.org/compute_pi/). Multiple sequence alignments were performed using the online web service MUSCLE (Edgar, 2004). Protein structures were inferred using the Phyre2 web portal for protein modelling, prediction and analysis (Kelley et al., 2015).

4.3 Results

4.3.1 *N. ceranae* PTP expression in *S. cerevisiae* produces morphological deformities.

The *N. ceranae* genes encoding PTPs consist of 1311, 756 and 4194 bp for *ptp1*, *ptp2* and *ptp3* respectively. I successfully cloned *ptp1* and *ptp2* from *N. ceranae* genomic DNA but could not successfully clone *ptp3*. The effects of PTP1 and PTP2 on *S. cerevisiae* cells were assessed by fluorescent microscopy and compared to a wild type empty vector control. Expression of *ptp*1, *ptp*2 and *NcS*-76 in *S. cerevisiae* BY4741 resulted in development of hyphal like structures. This was not seen in *S. cerevisiae* BY4741 transformed with the empty vector control (Figure 4.2). PTP1 exhibits a cytosolic localisation inferred by GFP fluorescence. This strain also exhibits a cell separation defect with many cells aggregating together. Furthermore, amorphous cells can have multiple buds that remain attached with both the unseparated mother and daughter cells swelling to a size much larger than wild type (Figure 4.2). The separation defect is supported by growth data (Figure 3.4) and that liquid culture of this strain exhibits flocculating cells and sedimentation (data not shown).

Expression of PTP2 in *S. cerevisiae* results in a very similar morphological defect to that of PTP1 expression, but PTP2 localises to the cell periphery as inferred by GFP fluorescence (Figure 4.2). Interestingly, one more NcS protein; NcS76 had the same capacity to induce the filament forming phenotype as both of the PTPs and this protein also exhibits association with the cell periphery and presents the same phenotype as PTP2 as inferred by GFP fluorescence.

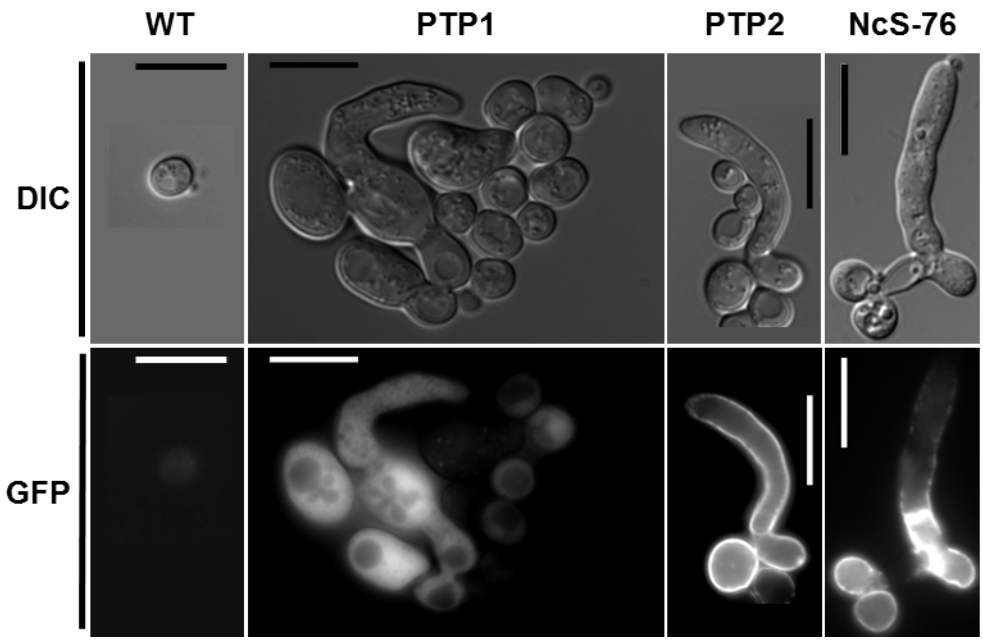

Figure 4.2 | *N. ceranae* polar tube proteins (PTP) affect *S. cerevisiae* cell shape.

Cells were grown overnight in CSM-His and washed 3x in PBS before imaging. Wild type (WT) BY4741 was transformed with the empty pAG423GPD-*ccd*B-EGFP vector as control and minimal fluorescence is observed. PTPs confer morphological deformity to *S. cerevisiae* cells appearing swollen and elongated to a length many times greater than wild type. PTP1 (NcS51) presents cytosolic localisation inferred by GFP fluorescence. PTP2 (NcS75) and NcS76 present cell periphery localisation inferred by GFP fluorescence. Average WT cell diameter measured 5 µm. The longest cell length for each sample following the cell midline measured; 41, 27 and 36 µm for PTP1, PTP2 and NcS76 respectively (scale bar = 10 µm).

4.3.2 NcPTP2 and NcS76 co-localise with the *S. cerevisiae* cell wall.

To investigate the observation of *N. ceranae* proteins associating with the *S. cerevisiae* cell periphery these strains were assessed for co-localisation of GFP fluorescence with CFW, a fluorescent stain that strongly binds chitin, a component of the fungal cell wall (Herth & Schnepf, 1980). While PTP1 is observed localising to the cytoplasm, the GFP signal clearly shows this protein does not enter the vacuole as indicated by the fluorescence signal void. PTP1 once again presents an amorphous phenotype with multiple swollen cells joined together with shared cytoplasm inferred by GFP fluorescence (Figure 4.3). Furthermore, the PTP1 CFW panel (Figure 4.3, A, CFW) shows continuous fluorescence on the cell periphery that does not cross the bud neck. In agreement with the clearly distinct fluorescent patterns, the PTP1 overlay image shows bright green cytoplasm and a bright blue cell wall, the two colours do not bleed, indicating they are separate from one another. This data is supported by the fluorescence intensity profile plot (Figure 4.3, D) where the two peaks for CFW signal are at 1 and 10 µm which indicate the cell wall boundary (diameter of the cell) and the GFP intensity is less at these measurements but much greater between these two points indicating GFP signal is greatest inside the cell boundary. PTP2 and NcS76 exhibit clear association with the cell wall where both present very similar micrographs for both the GFP fused *N. ceranae* proteins and CFW stained cell wall (Figure 4.3, B-C). In contrast to the PTP1 overlay image, the overlays for both PTP2 and NcS76 show aqua-marine blue/green due to colour bleed inferring the fluorescence signals occupy the same space and PTP2 and NcS76 associate with the cell wall. This observation is supported by the fluorescence intensity plots (Figure 4.3, E-F) where GFP and

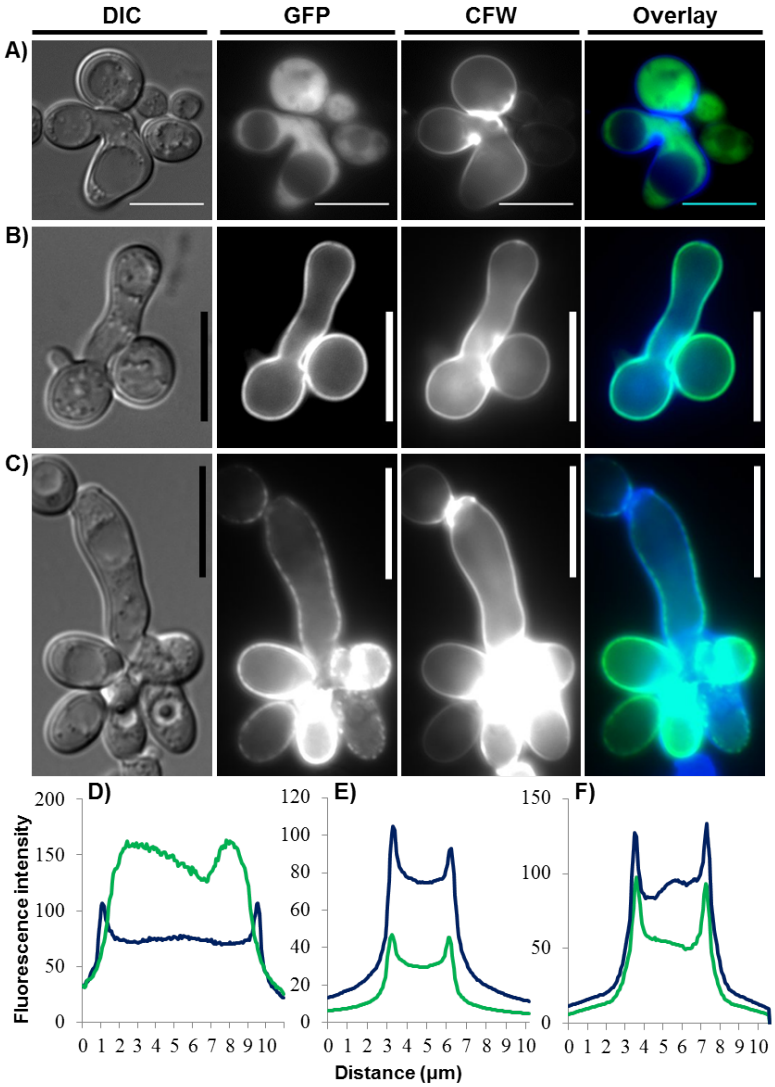

Figure 4.3 | Co-localisation of PTP2 and NcS76 with *S. cerevisiae* cell wall.
To confirm co-localisation of C-terminal GFP tagged *N. ceranae* proteins with the *S. cerevisiae* cell wall, strains were grown overnight in selective media, washed in PBS and incubated with 0.01% calcofluor white (CFW). **A)** PTP1 (NcS51) presents different patterns of fluorescence for GFP and CFW highlighting this protein does not localise at the cell wall. **B)** PTP2 (NcS75) and **C)** NcS76 present the same patterns of fluorescence for GFP and CFW indicating these proteins associate closely with the chitinous cell wall. **D-F)** Fluorescence intensity plots for CFW (blue line) and GFP (green line) corresponding to panels A-C respectively. **D)** Dissimilar profiles for PTP1-GFP and CFW supports micrograph image. **E-F)** Comparable profiles with aligning peaks suggests co-localisation of PTP2 and NcS76 with the *S. cerevisiae* cell wall (scale bar = 10 µm).

CFW maximum signal peaks perfectly align.

4.3.3 PTP2 co-localises with NcS76 when co-expressed in *S. cerevisiae*.

To investigate a potential interaction between PTP2 and NcS76 I co-expressed both proteins with different C-terminal fluorophores (see methods above) simultaneously in *S. cerevisiae*. PTP2 and NcS76 are seen co-localising with each other (Figure 4.4) and producing the same amorphous structures as when they are expressed independently i.e. we do not see an increase or decrease in their capacity to confer the morphological defect when expressed together. Overexpressing these two proteins simultaneously does not have a lethal effect on *S. cerevisiae* however there is an observed increase in energetic burden demonstrated by slower growth rates compared to the single mutant strains (data not shown). All three examples show elongated cells with both *N. ceranae* proteins localising to the cell wall and associating with each other as inferred by the yellow overlay images and supported by the fluorescence intensity plots which show very similar profiles between the GFP and DsRed signal.

4.3.4 Comparative analysis of known and novel *N. ceranae* PTPs.

Because of the pheno-mimicry displayed between PTP2 and NcS76 I wanted to compare whether they retain any common features that may account for their shared function as well as comparing features with other known and inferred PTPs to establish whether there are features common amongst these protein families. Two new PTPs (PTP4 and PTP5) have recently been identified in *E. cuniculi* through proteomic experiments and immunofluorescence assays and

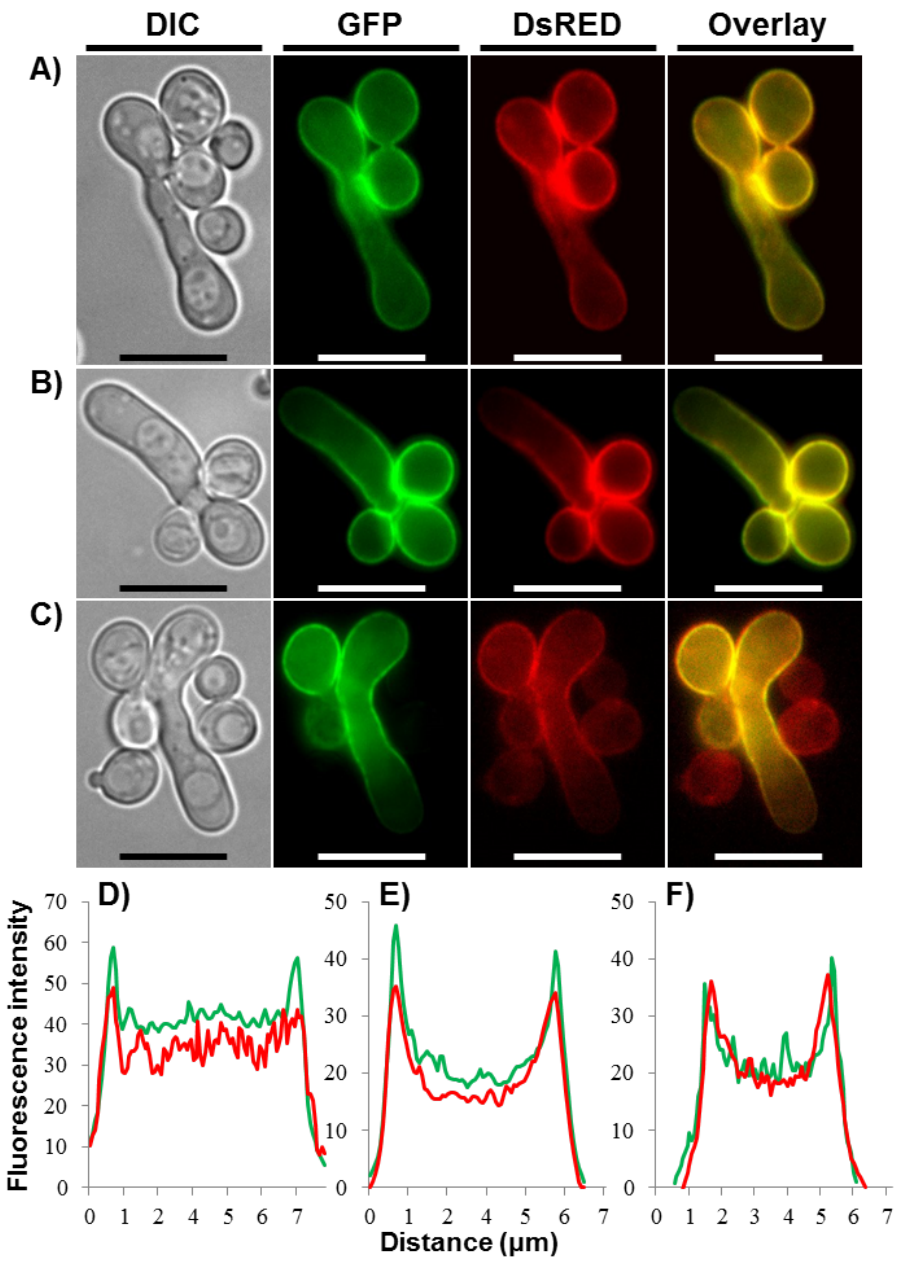

Figure 4.4 | Co-localisation of PTP2 with NcS76 in *S. cerevisiae.*

S. cerevisiae BY4741 strain constitutively expressing PTP2-GFP under histidine selection and NcS76-DsRed under uracil selection was grown overnight in CSM-His-Ura. **A-C)** Three separate examples of the same double mutant strain showing *N. ceranae* proteins co-localising with each other. **D-F)** Fluorescence intensity plots for PTP2-GFP (green line) and NcS76-DsRed (red line) corresponding to panels A-C respectively. Comparable profiles with aligning peaks suggests co-localisation of PTP2 with NcS76 (scale bar = 10 µm).

orthologues for these proteins were identified in the *N. ceranae* genome (Weiss *et al., In preparation;* cited in Weiss & Becnel, 2014). It should be noted that *Nc*PTP5 is not predicted to be a secreted protein, the only PTP where this is the case (Table 4.1). PTP4 is predicted to be secreted and identified in the present study as NcS108 and shall be referred to as PTP4 going forward. While NcS76 does not share significant sequence similarity with *Nc*PTP2 ($e > 1e^{-05}$) it is identified as sharing sequence similarity with three other NcS proteins; NcS1, NcS150 and NcS172, therefore these three proteins were also included in the analysis to complete the list of known and novel *N. ceranae* PTPs (Table 4.1).

*Nc*PTP2 and NcS76 share many common features including size of mature peptide both in terms of amino acid number (252 and 272 respectively) and molecular weight (27.68 and 31.23 kDa respectively), they are both basic lysine rich molecules and retain the same proportion of cysteine residues, which is indicative of a comparable role for disulphide bridges in their secondary structures. Due to these proteins lacking similarity with many known protein sequences their secondary structures could not be predicted with confidence (data not shown). The only proteins with a portion of confidently inferred secondary structure were *Nc*PTP3 and *Nc*PTP4 where 6 % of the *Nc*PTP3 C-terminal amino acid sequence is predicted to be a cell adhesion structure (89.9 % confidence), and 29% of the *Nc*PTP4 central amino acid sequence is predicted to be a polypeptide- N-acetylgalactosaminyltransferase structure (90.6% confidence) (Appendix VIII). *Nc*PTP2 is more similar to NcS76 than compared to *Nc*PTP1 or *Nc*PTP3 when considering the features described in Table 4.1.

Table 4.1 | Features of known and novel *N. ceranae* polar tube proteins (PTP).

Protein ID	SP AA	TM	Mature peptide AA	Mw kDa	pI	Dominant residue %	Cys %	Pro %	N gly sites	O gly sites	Predicted structure
PTP1[a] (NcS51)	19	0	437	44.81	4.54	P, 20	3.2	20	3	59	N
PTP2[a] (NcS76)	23	0	252	27.68	9.41	K, 11	3.2	7.1	4	4	N
PTP3[a] (NcS72)	15	0	1399	155.84	6.37	N, 9	0.1	5.5	9	81	Y
PTP4[a] (NcS108)	16	0	192	22.10	6.84	K, 12	2.6	2.1	0	2	Y
PTP5[a]* (NCER_100527)	0	0	268	31.80	9.05	K, 17	3.7	3.0	1	0	N
NcS76[b]	15	0	272	31.23	8.41	K, 16	3.3	1.5	3	5	N
NcS1[b]	17	0	251	28.90	5.7	K, 12	2.8	1.2	4	12	N
NcS150[b]	16	0	301	34.50	8.08	K, 16	1.7	1.7	2	19	N
NcS172[b]	16	0	187	22.00	8.94	K, 15	2.7	0.0	0	3	N

[a]known polar tube protein
[b]novel polar tube protein
*no signal peptide predicted
Mw; molecular weight
pI; isoelectric point
N gly; N-glycosylation sites
O gly; O-glycosylation sites

The distinction of *Nc*PTP2 from *Nc*PTP1 and *Nc*PTP3 is perhaps most evident from the predicted number of post-translational O-glycosylation sites which is high in *Nc*PTP1 and *Nc*PTP3 (59 and 81 respectively) and low in *Nc*PTP2 (4) which is comparable to NcS76 (5). The only feature where *Nc*PTP2 and NcS76 are dissimilar, with *Nc*PTP2 being more comparable to *Nc*PTP1 and *Nc*PTP3, is the proportion of proline residues. *Nc*PTP1-3 have a large proportion of proline (20, 7.1 and 5.5 % respectively) compared to NcS76 (1.5 %) (Table 4.1).

In an effort to identify residues conserved between PTPs of different species (the most likely residues of undiscovered domains) I searched for orthologous sequences with significant sequence similarity ($e < 1e^{-05}$, BLASTP). Orthologues of *Nc*PTP1-5 were identified mostly from within the *Nosema* genus (Table 4.2), however *Nc*PTP3 and *Nc*PTP4 also share significant sequence similarity with members of the *Encephalitozoon* genus (data not shown). Interestingly *N. apis* does not share the most significant sequence similarity for all PTPs with *N. ceranae*, only PTP2. The most highly conserved residues between *Nc*PTP2 and *Na*PTP2 are lysine (15), asparagine (10) and cysteine (8). Lysine and cysteine also feature as prominently conserved residues between *Nc*PTP4 and *Nan*PTP4 (15 and 5 residues respectively), and *Nc*PTP5 and *Nb*PTP5 (25 and 10 residues respectively).

Table 4.2 | Orthologues of *N. ceranae* polar tube proteins and their conserved amino acids.

***N. ceranae* protein**	**Orthologue**	**E-value**	**Identity %**	***1° #**	***2° #**	***3° #**	**Protein description**
PTP1	*N. antheraeae* NOANT_034027.p01	2.00E-10	31.48	P, 31	C, 8	G, 8	unknown secreted protein
PTP1	*N. apis* EQB60694.1	4.00E-08	30.96	-	-	-	hypothetical protein
PTP2	*N. apis* EQB61988.1	3.00E-38	38.15	K, 15	N, 10	C, 8	polar tube protein 2
PTP2	*N. bombycis* EOB15197.1	9.00E-28	30.65	-	-	-	polar tube protein 2
PTP2	*N. antheraeae* NOANT_034026.p01	5.00E-27	30.57	-	-	-	hypothetical protein
PTP3	*N. bombycis* EOB15062.1	0	39.92	A, 50	E, 50	P, 49	polar tube protein 3
PTP3	*N. antheraeae* NOANT_012086.p01	0	42.99	-	-	-	polar tube protein 3
PTP3	*N. apis* EQB60507.1	1.00E-86	36.60	-	-	-	hypothetical protein
PTP4	*N. antheraeae* NOANT_024051.p01	6.00E-46	41.58	K, 15	I, 9	C, 5	hypothetical protein
PTP5^	*N. bombycis* EOB12332.1	7.00E-74	45.25	K, 25	D, 12	L, 11	hypothetical protein
PTP5	*N. antheraeae* NOANT_024050.p01	3.00E-73	45.25	-	-	-	hypothetical protein
PTP5	*N. apis* EQB59823.1	9.00E-29	46.80	-	-	-	hypothetical protein

***** conserved amino acid residues from sequence alignments of *N. ceranae* PTPs and their listed orthologues.
^ The 4th conserved amino acid for *Nc*PTP5 and *Nb*PTP5 is cysteine.

4.4 Discussion

The microsporidian polar tube is the defining structure for this phylum of obligate intracellular eukaryotic pathogens. The unique preformed invasion apparatus acts like a harpoon, penetrating the host cell, facilitating spore ingress and in turn, allowing the active stage of the microsporidian life cycle to take place within a host cell. PTPs are directed through the Golgi/ER secretory pathway by an N-terminal SP and so these proteins are encompassed within the microsporidian secretome. When PTP1, PTP2 and PTP3 were first characterised in *E. cuniculi* using cross-linker and immunoprecipitation experiments, they were observed forming a complex with each other and unidentified proteins (Bouzahzah et al., 2010; Peuvel et al., 2002). In an effort to increase knowledge on the *N. ceranae* infection process I sought to functionally assess known PTPs and identify common traits e.g. induced phenotypes, that may be shared with previously unidentified PTPs.

N. ceranae PTP expression has an intriguing effect on *S. cerevisiae* development where cells can grow very large or even form filament structures (Figures 4.2-4.4). PTP1 localises in the cytoplasm which infers the observed structural effect is unlikely to result from PTP1 incorporation with the *S. cerevisiae* cell wall. I hypothesise there are two possibilities by which PTP1 can cause the observed effect; 1) this protein forms large polymers within the cytoplasm disrupting the cytoskeleton causing the cell to grow elongated and swollen around the perturbed cytoskeleton or; 2) PTP1 interferes with the *S. cerevisiae* cell wall biogenesis pathway. Both of these hypotheses require experimental investigation.

In contrast PTP2 is observed associating with the *S. cerevisiae* cell wall which suggests the observed pseudo-hyphal phenotype is caused by a close association of PTP2 with *S. cerevisiae* cell wall proteins. PTP2 from *N. bombycis* has previously been shown to interact with a spore wall protein (SWP5) (Li et al., 2012). This interaction has not yet been demonstrated for *N. ceranae* however the authors did identify an *N. ceranae* SWP5 homologue through sequence features even though it lacked significant sequence similarity. *Nc*SWP5 does not homologous with any *S. cerevisiae* proteins nor other known sequences and so it is unlikely *Nc*PTP2 is interacting with a *Sc*SWP5 homologue, but there remains a possibility *Nc*SWP5 shares as yet undetermined structural similarity with an *S. cerevisiae* protein. Immunoprecipitation, mass spectrometry, and immunofluorescence analyses revealed that *Nb*SWP5 interacts with both *Nb*PTP2 and *Nb*PTP3 (Li et al., 2012). The authors suggested this feature of cell wall association may contribute to the close association of the pre-extruded coiled polar tube with the spore wall.

Because both of the known PTPs assessed in the present study produce the same effect of cell swelling and elongation when expressed in *S. cerevisiae*, this may be indicative of a conserved trait for other PTPs. Based on this hypothesis and the observation that NcS76 replicates a very similar phenotype to *Nc*PTP2 and co-localises with it when co-expressed in *S. cerevisiae,* I propose NcS76 is a novel PTP. Due to the nature of heterologous expression experiments this hypothesis needs to be validated in the native system of the *N. ceranae* spore, which can be achieved by immunolocalisation experiments using antibodies raised against NcS76 in conjunction with an *in vitro* germination assay (Gisder et al., 2010). I

identified NcS76 has significant sequence similarity (BLASTP e < $1e^{-05}$) with other NcS proteins (NcS1, NcS150 and NcS172) suggesting that these three proteins could be functionally related to NcS76. NcS1, NcS150 and NcS172 share many peptide features with NcS76 including size of predicted SP, Mw of the mature peptides, being lysine rich and having numerous cysteine residues, however a functional relationship is yet to be determined.

Previous studies have shown that *Ec*PTP1 is O-glycosylated suggesting a role in adherence of the polar tube to a host cell mannose receptor (Bouzahzah et al., 2010; Polonais et al., 2005). The pathogenic fungus *Candida albicans* has been shown to possess O-mannosylated spore wall proteins that directly interact with host cell fibrinogen leading to host cell adhesion (Casanova et al., 1992; Timpel et al., 2000). Furthermore, interaction between mannosylated *Eh*PTP1 and some unknown host cell mannose-binding molecule is important for the *E. hellem* infection process (Xu et al., 2004). Bioinformatic analysis suggests the feature of glycosylation is conserved amongst *Nc*PTP1 and *Nc*PTP3 which are predicted to have many O-glycosylation sites (59 and 81 respectively) in contrast to *Nc*PTP2 which is predicted to have very few (4). This allows us to hypothesis the functional role of host cell adhesion in PTP1 and PTP3 is conserved throughout the phylum and that PTP2 has a reduced role in host cell adhesion but is primarily involved with polar tube - spore wall interactions which may also involve NcS76.

In summary, I have shown that *Nc*PTPs produce a distinct phenotype in *S. cerevisiae* which may facilitate identification of novel PTPs. The characterisation of new PTPs creates new perspectives to understand the mechanism of the microsporidian infection apparatus. This protein and those proteins identified with

similar sequences warrant further study to elucidate the complex structure of the polar tube and due to their low sequence similarity with other eukaryotes may serve as potential drug targets for future therapeutics.

Chapter 5 | A novel approach to investigate microsporidian gene function using Synthetic Genetic Array (SGA)

5.1 Introduction

Identifying molecular mechanisms responsible for morphologically characterised host-cell manipulations is a difficult process in microsporidia, due to their intracellular lifecycle hindering genetic manipulation. We and others have shown the powerful utility *S. cerevisiae* serves as a heterologous system to characterise microsporidian proteins (Campbell, 2013; Lalik, 2015; Usher et al., 2015). The high-throughput platform of SGA has proved useful for inferring the function of gene products for which no experimental or bioinformatic data was previously available (Tong et al., 2001) and so may serve as a powerful approach in microsporidian research.

S. cerevisiae demonstrates genetic redundancy where approximately 85% of the ~5800 known or suspected genes can be individually deleted without lethal effects. This has allowed the creation of ~5000 viable haploid gene-deletion mutants, where approximately 70% of the deleted genes have known roles in biological processes (Cherry et al., 2012; Giaever et al., 2002; Winzeler et al., 1999). This deletion library forms a key resource for screening genetic interactions which occur when a genetic perturbation leads to an extreme phenotype e.g. reduced cell growth inferred by reduced colony size (Baryshnikova et al., 2010; Costanzo et al., 2010; Wagih et al., 2013). Two types of synthetic genetic interactions can reveal functional redundancy of genes; 1) a “synthetic lethal” interaction when the combination of two mutations causes cell death compared to non-lethal single mutations or; 2) a “synthetic sick” interaction when the combined

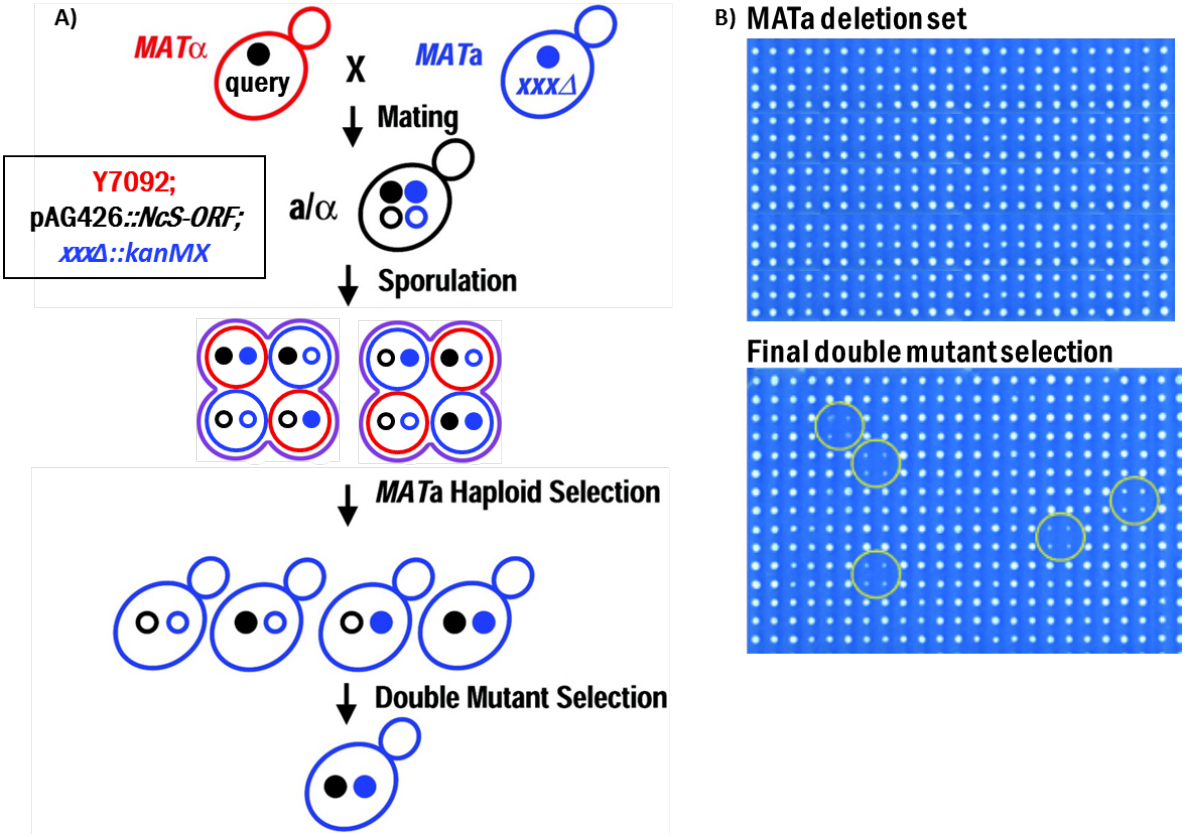

Figure 5.1 | Diagrammatic overview of the Synthetic Genetic Array (SGA) method.

A) *S. cerevisiae MAT***α** query strain Y7092 (Tong et al., 2001) was transformed with pAG426GPD bearing a single query *N. ceranae* gene (either *NcS-50, NcS-65, NcS-68, NcS-79* or *NcS-85* each in a separate SGA experiment). The resulting query strain was crossed with the *MAT***a** deletion mutant array through a series of pinning steps. Sporulation of resultant diploid cells led to the formation of double-mutant meiotic progeny. Both the query mutation and the gene-deletion mutations were linked to dominant selectable markers to allow for selection of double mutants. **B)** Final pinning results in an ordered array of double-mutant haploid strains whose growth rate is monitored by visual inspection or image analysis of colony size. An example set of array plates including control single mutants (top) which are compared to the respective double mutants (bottom). The control plate presents relatively uniform colony sizes, whereas the double mutant plate shows five instances of a synthetic sick phenotype (circles, where each strain is grown in quadruplicate) (adapted from Tong et al., 2001).

mutations result in significantly retarded colony growth compared to either single mutation alone (see Figure 5.1 for overview of the SGA method used in the present study) (Guarente, 1993; Novick et al., 1989; Tong et al., 2001).

Synthetic genetic interactions can identify genes acting in the same biochemical pathway or separate pathways with functionally related processes and this approach has identified genes participating in cell morphogenesis, protein trafficking, DNA damage and repair, and many others (Bender & Pringle, 1991; Chen & Graham, 1998; Hartman et al., 2001; Mullen et al., 2001; Tong et al., 2001). Furthermore, this methodology has facilitated elucidation of function for non *S. cerevisiae* genes either through assessing *S. cerevisiae* orthologues of target genes e.g. key genes of human diseases (Louie et al., 2012; van Pel et al., 2013) or exogenous query gene expression. Indeed heterologous overexpression of non *S. cerevisiae* genes in the *S. cerevisiae* SGA query strain have aided studies in the pathogenic yeast species *Candida glabrata* and *Cryptococcus neoformans* yielding cross-species genetic interaction networks to expand fundamental knowledge on disease processes (Ames, 2013; Brown & Madhani, 2012; Usher et al., 2015).

The capability of SGA was increased further when Costanzo et al. (2010) constructed a genome-scale genetic interaction map by examining ~5.4 million gene-gene pairs for synthetic genetic interactions. The authors generated a network based on quantitative genetic interaction profiles for ~75% of all *S. cerevisiae* genes revealing a functional map of the cell, where genes of similar biological processes cluster together in coherent subsets (Costanzo et al., 2010). This data is a tool for the research community which can be statistically compared to the genetic interaction profile of a query gene to determine where the gene of

interest resides within the functional map and whether it nests with a specific biological process cluster, from which inferences of function can be made and tested.

Due to the limited toolkit for studying microsporidia and the proven track record of SGA in determining function for uncharacterised genes in both model and non-model organisms, our aim was to apply this methodology to assess the *N. ceranae* ORFs studied in Chapter 3. Due to the logistics associated with the method (time consuming and expensive ~ 3 months wet lab per screen and labor intensive data analysis), only a subset of *N. ceranae* ORFs were selected for SGA analysis consisting of those ORFs identified presenting punctate protein localisation as inferred by their fluorescent phenotypes (NcS-50, NcS-65, NcS-68, NcS-79 and NcS-85). This subset was selected on the hypothesis that their interaction profiles may correlate with genes involved in biological processes specific to certain cellular compartments which may provide insight into the observed protein localisations and lead to the identification of their functions.

5.2 | Method

5.2.1 Yeast strains

The yeast strains used in this study are listed in Appendix II and also included the *MAT***a** deletion mutant array purchased from OpenBiosystems (Catalogue no. YSC1053). NcS-ORFs 50, 65, 68, 79 and 85 were shuttled from pENTRY clones to destination vector pAG426GPD containing the *URA3* gene for auxotrophic selection on media lacking uracil under the GPD constitutive high copy number promoter excluding either N- or C-terminal tags. SGA query strains were made for the genome-wide SGA screens by transforming the *MAT***α** query strain Y7092 (Tong et al., 2001) with the resulting plasmids (Appendix II) using standard LiAc protocol described in Chapter 2. Positive transformants were confirmed by colony PCR using ORF specific forward primers and plasmid specific reverse primers as detailed in Chapter 2 (Appendix III).

5.2.2 Robotic manipulations generating deletion mutant arrays

The deletion mutant library was robotically manipulated using a Singer RoToR HDA (Singer Instruments, UK) transferring the library from glycerol stocks in 96-well microtiter plate format, to YPD G418 agar PlusPlate© 96 spot format. The solid media deletion library was incubated for 24 h at 30°C before being condensed into 1536 spot format on fresh YPD G418 PlusPlates© with two technical replicates of each strain per plate. Condensed deletion arrays were incubated at 30°C for 24 h.

5.2.3 SGA screens and scores

The SGA method is described in Chapter 2 and Figure 5.1 (Tong & Boone, 2005; Tong et al., 2001, 2004). Resulting double mutant array plates and single mutant control plates were imaged using a Syngene G:BOX. Raw digital images from the screen were processed with the web service SGAtools (http://sgatools.ccbr.utoronto.ca/) (Baryshnikova et al., 2010; Wagih et al., 2013) to produce colony size measurements. Colony sizes are normalised to account for common biases that affect growth including; plate effect; row/column effect and; the spatial effect (see Wagih et al., 2013), before calculating SGA scores which are used as a measure of genetic interaction strength for each double mutant strain. This is achieved using the standard multiplicative score (W_{ij}-W_iW_j), where W_{ij} represents the fitness of the observed value in the experiment, W_i represents the median fitness of all strains in the experiment (estimated from the control plate) and W_j represents the median fitness of the array strain (estimated as the median value of all its replicates) (Wagih et al., 2013). Through visual interrogation I found that multiplicative scores below -0.5 indicate a synthetic sick effect. Synthetic genetic interaction networks were rendered using Osprey version 1.2.0 (Breitkreutz et al., 2003). Functional enrichment of synthetically interacting genes was determined using the web service FunSpec (http://funspec.med.utoronto.ca/) (Robinson et al., 2002).

5.2.4 Determining *N. ceranae* ORF position in the 'functional map of a cell'

S. cerevisiae synthetic genetic interaction profiles were downloaded from http://drygin.ccbr.utoronto.ca/~costanzo2009/. Pearsons correlation coefficients

(PCC) were calculated comparing the array of SGA scores (i.e. the interaction-profile) for each of our NcS SGA double mutant strains against the array of SGA scores for every SGA double mutant strain from Costanzo et al (2010), using the statistical analysis package R (http://www.R-project.org/) (R Core Team, 2013). Only *S. cerevisiae* gene pairs with $r > 0.2$ were included in the network (Costanzo et al., 2010). The ten largest PCC scores for the NcS SGA strains were used to root the NcS nodes in the network. Edges within the network are weighted by r values and a spring embedded layout algorithm was applied using Cytoscape (Shannon et al., 2003).

5.3 Results

5.3.1 Interrogating a subset of the *N. ceranae* secretome with SGA

To investigate the functional role of putative *N. ceranae* virulence factors I selected NcS-ORFs previously identified as producing punctate fluorescence phenotypes when expressed in *S. cerevisiae* (NcS-50, NcS-65, NcS-68, NcS-79 and NcS-85, see Chapter 3) for SGA analysis to determine whether these ORFs share synthetic genetic interactions with any *S. cerevisiae* genes. I hypothesise the function of NcS gene products will be inferred by association with *S. cerevisiae* genes they have a synthetic genetic interaction with.

5.3.2 Genetic interactors of *N. ceranae* ORFs

Through genome-wide SGA screens I have identified *NcS50, NcS65, NcS68, NcS79* and *NcS85* have cross-species genetic interactions with 102, 149, 55, 119 and 138 *S. cerevisiae* genes respectively (Figure 5.2). I performed enrichment analysis for the genetic interactors of each *N. ceranae* ORF with the intention of identifying the biological processes these five individual *N. ceranae* putative virulence factors may target. *N. ceranae* secretome ORFs *NcS50* and *NcS85* have genetic interactions with genes from a broader spectrum of biological processes compared to *NcS65, NcS68* and *NcS79* (Tables 5.1-5.5). The genetic interactors of *NcS50* are enriched for genes involved in mRNA localisation, DNA damage and repair, vacuolar protein metabolism, ascospore wall assembly and more (Table 5.1). Of the 149 genes synthetically interacting with *NcS65* we see enrichment for biological processes including; endosome transport, DNA repair and eisosome assembly/endocytosis (Table 5.2).

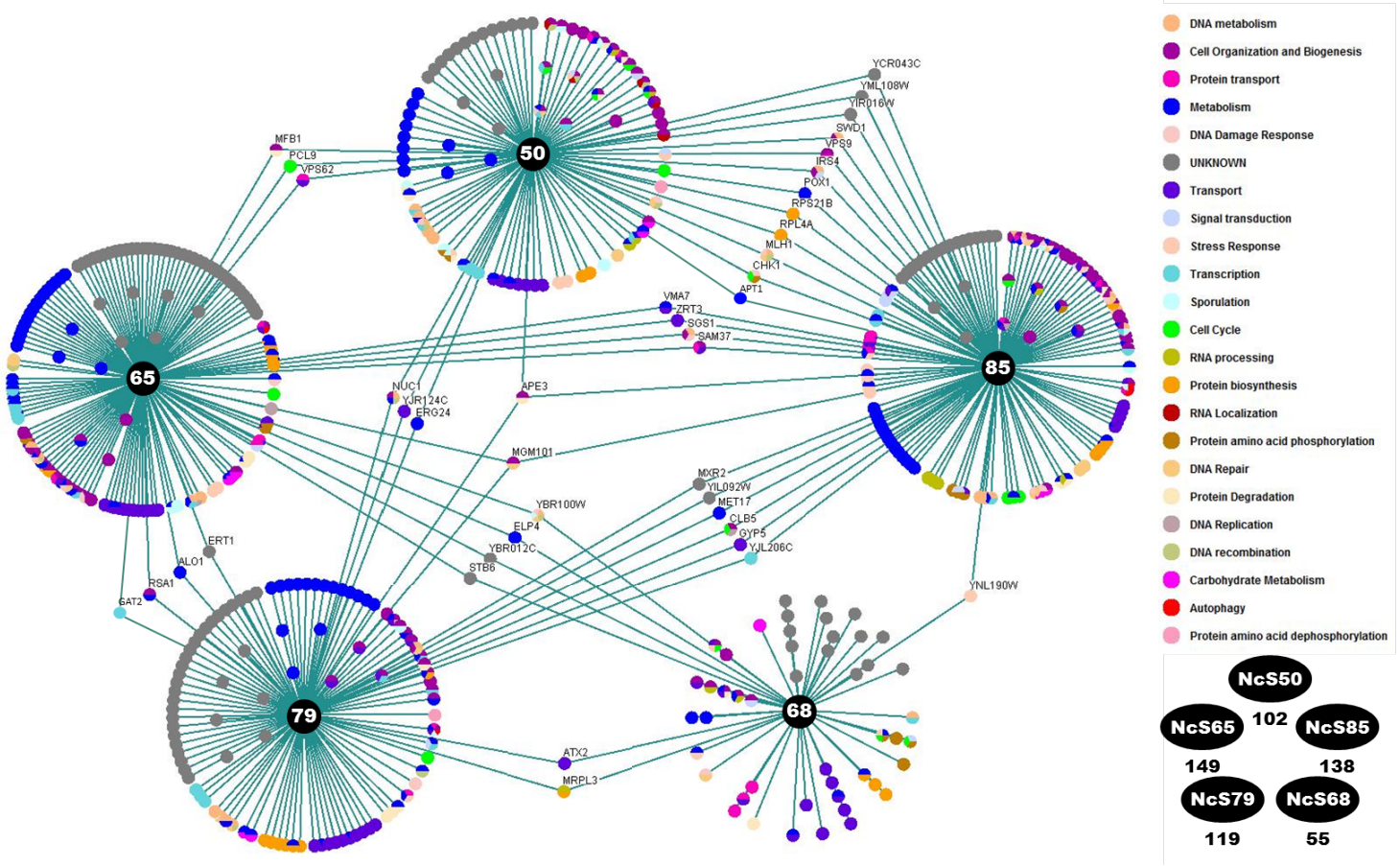

Figure 5.2 | Genetic interaction network map for SGA query strains *S. cerevisiae* Y7092 overexpressing *NcS50*, *NcS65, NcS68, NcS79* or *NcS85* respectively. Query strains are represented by large black nodes with white labels. Edges connecting nodes represent genetic interactions between genes. Nodes are coloured according to associated GO terms listed in the colour key on the right. Total number of interactions for each query gene is shown below the key. See Appendix IX-XIII for complete genetic interaction lists.

Table 5.1 | GO term enrichment of *S. cerevisiae* genes that have synthetic genetic interactions with *N. ceranae* secretome ORF-50.

Biological Process Category	p-value	In Category from Cluster	k	f
intracellular mRNA localization [GO:0008298]	0.0001	*MYO4 LOC1 TPM2 SHE4*	4	14
maintenance of meiotic sister chromatid cohesion [GO:0034090]	0.0011	*IML3 SGO1*	2	3
meiotic joint molecule formation [GO:0000709]	0.0011	*RAD51 RAD52*	2	3
vacuolar protein catabolic process [GO:0007039]	0.0013	*APE3 REG1 PRB1*	3	12
ascospore wall assembly [GO:0030476]	0.0017	*AMA1 SPS100 PFS1 CDA2 GAS4*	5	46
endonucleolytic cleavage to generate mature 3'-end of SSU-rRNA from (SSU-rRNA, 5.8S rRNA, LSU-rRNA) [GO:0000461]	0.0021	*RPS21B RPS21A*	2	4
DNA damage checkpoint [GO:0000077]	0.0037	*CHK1 RAD9 RAD17*	3	17
intra-S DNA damage checkpoint [GO:0031573]	0.0051	*RAD9 ESC2*	2	6
double-strand break repair via single-strand annealing [GO:0045002]	0.0070	*RAD51 RAD52*	2	7
meiotic sister chromatid segregation [GO:0045144]	0.0070	*IML3 SGO1*	2	7
cellular response to starvation [GO:0009267]	0.0070	*PRB1 IRS4*	2	7
mating type switching [GO:0007533]	0.0070	*MYO4 SHE4*	2	7
mitotic cell cycle spindle assembly checkpoint [GO:0007094]	0.0078	*MAD2 HHT2 SGO1*	3	22
calcium-mediated signalling [GO:0019722]	0.0092	*RSF1 BXI1*	2	8

k = number of genes from input in a given category.

f = total number of genes in a given category.

Table 5.2 | GO term enrichment of *S. cerevisiae* genes that have synthetic genetic interactions with *N. ceranae* secretome ORF-65.

Biological Process Category	p-value	In Category from Cluster	k	f
endosome transport [GO:0016197]	0.0014	*SLM1 SLM2*	2	3
tRNA wobble position uridine thiolation [GO:0002143]	0.0045	*NCS6 TUM1*	2	5
DNA repair [GO:0006281]	0.0062	*HHT1 POL4 RAD57 MGM101 RTT109 RAD5 MLH2 SGS1 RAD14 DDC1*	10	183
intra-S DNA damage checkpoint [GO:0031573]	0.0066	*SGS1 DDC1*	2	6
eisosome assembly [GO:0070941]	0.0091	*SLM1 SLM2*	2	7

Table 5.3 | GO term enrichment of *S. cerevisiae* genes that have synthetic genetic interactions with *N. ceranae* secretome ORF-68.

Biological Process Category	p-value	In Category from Cluster	k	f
transmembrane transport [GO:0055085]	0.0007	*FLR1 VPS73 CCH1 GEX2 YNL095C ESBP6 SIL1 ATX2 FSF1*	9	303
protein phosphorylation [GO:0006468]	0.0007	*KIN3 FUS3 YPK3 ELM1 NPR1 HRK1*	6	133
positive regulation of mitochondrial translation [GO:0070131]	0.0041	*CBS1 MSS51*	2	12
actin filament organisation [GO:0007015]	0.0051	*SLA1 RHO2 WHI2*	3	43
phosphorylation [GO:0016310]	0.0064	*KIN3 FUS3 YPK3 ELM1 NPR1 HRK1*	6	206

Table 5.4 | GO term enrichment of *S. cerevisiae* genes that have synthetic genetic interactions with *N. ceranae* secretome ORF-79.

Biological Process Category	p-value	In Category from Cluster	k	f
tryptophan transport [GO:0015827]	0.0003	*TAT1 TAT2*	2	2
premeiotic DNA replication [GO:0006279]	0.0044	*LGE1 CLB5*	2	6
histone methylation [GO:0016571]	0.0061	*RTF1 LGE1*	2	7
pyruvate metabolic process [GO:0006090]	0.0080	*MAE1 PDC1*	2	8
amino acid transmembrane transport [GO:0003333]	0.0082	*TAT1 AGP2 TAT2*	3	24

Table 5.5 | GO term enrichment of *S. cerevisiae* genes that have synthetic genetic interactions with *N. ceranae* secretome ORF-85.

Biological Process Category	p-value	In Category from Cluster	k	f
intralumenal vesicle formation [GO:0070676]	0.0002	*DID4 VPS24 VPS4*	3	5
response to DNA damage stimulus [GO:0006974]	0.0005	*NTG1 CHK1 RAD28 RAD51 RAD6 MGM101 APN1 PSY3 UNG1 NPL6 YIM1 MLH1 SGS1 RAD50*	14	197
base-excision repair [GO:0006284]	0.0006	*NTG1 APN1 UNG1 RAD50*	4	16
AMP biosynthetic process [GO:0006167]	0.0007	*ADO1 APT1*	2	2
endonucleolytic cleavage to generate mature 3'-end of SSU-rRNA from (SSU-rRNA, 5.8S rRNA, LSU-rRNA) [GO:0000461]	0.0038	*RPS0A RPS21B*	2	4
purine ribonucleoside salvage [GO:0006166]	0.0038	*ADO1 APT1*	2	4
cellular response to water deprivation [GO:0042631]	0.0038	*SIP18 YNL190W*	2	4
carbon utilization [GO:0015976]	0.0038	*ACN9 PKP1*	2	4
transcription elongation from RNA polymerase I promoter [GO:0006362]	0.0062	*RPA34 RPA49*	2	5
glucose mediated signalling pathway [GO:0010255]	0.0062	*GPB2 GPB1*	2	5
cellular response to oxidative stress [GO:0034599]	0.0071	*NTG1 GPX2 MXR2 TRX2 GRE3 TSA1*	6	67
DNA repair [GO:0006281]	0.0071	*NTG1 RAD28 RAD51 RAD6 MGM101 APN1 PSY3 UNG1 MLH1 SGS1 RAD50*	11	183
chromatin silencing [GO:0006342]	0.0086	*ESC8 HST1 HST3*	3	17
meiotic DNA double-strand break processing [GO:0000706]	0.0091	*SGS1 RAD50*	2	6
protein deacetylation [GO:0006476]	0.0091	*HST1 HST3*	2	6
negative regulation of Ras protein signal transduction [GO:0046580]	0.0091	*GPB2 GPB1*	2	6

Table 5.6 | GO term enrichment of *S. cerevisiae* genes with the greatest synthetic genetic interactions with *N. ceranae* secretome ORFs determined by SGA score.

Biological Process Category	p-value	In Category from Cluster	k	f
Strongest interactors with *NcS50*				
transcription from RNA polymerase II promoter [GO:0006366]	0.0002	*SRB5 MET18 CSE2*	3	74
transcription, DNA-dependent [GO:0006351]	0.0062	*SRB5 MET18 CSE2 SFL1*	4	540
regulation of transcription from RNA polymerase II promoter [GO:0006357]	0.0082	*SRB5 CSE2*	2	93
Strongest interactors with *NcS68*				
transmembrane transport [GO:0055085]	0.0065	*FLR1 GEX2 FSF1*	3	303
Strongest interactors with *NcS79*				
cellular response to oxidative stress [GO:0034599]	0.0043	*SRX1 ALO1*	2	67
Strongest interactors with *NcS85*				
response to DNA damage stimulus [GO:0006974]	0.0027	*CHK1 PSY3 MLH1*	3	197

Enrichment based on 10 highest SGA scores for each ORF. Note there was no enrichment for the 10 highest ranked SGA scores of *NcS65.*

Table 5.7 | GO term enrichment of *S. cerevisiae* genes that have synthetic genetic interactions with multiple *N. ceranae* secretome ORFs.

Biological Process Category	p-value	In Category from Cluster	k	f
Interacting with *NcS50* and *NcS85*				
lipid metabolic process [GO:0006629]	0.0056	*POX1 IRS4*	2	58
Molecular Function Category				
Interacting with *NcS65* and *NcS79*				
DNA binding [GO:0003677]	0.0028	*ERT1 MGM101 GAT2*	3	449
sequence-specific DNA binding transcription factor activity [GO:0003700]	0.0042	*ERT1 GAT2*	2	138
sequence-specific DNA binding [GO:0043565]	0.0059	*ERT1 GAT2*	2	165
Biological Process Category				
Interacting with *NcS65* and *NcS85*				
ion transport [GO:0006811]	0.0025	*VMA7 ZRT3*	2	107
DNA repair [GO:0006281]	0.0072	*MGM101 SGS1*	2	183
response to DNA damage stimulus [GO:0006974]	0.0083	*MGM101 SGS1*	2	197

Table 5.8 | Matrix showing number of genetic interactions *N. ceranae* ORFs have in common.

ORF	NcS65	NcS68	NcS79	NcS85
NcS50	3	0	4	13
NcS65	-	4	4	5
NcS68	-	-	2	1
NcS79	-	-	-	8

NcS68 has the least number of synthetic genetic interactions and the products of these genes are enriched for processes such as transmembrane transport, protein phosphorylation, regulation of mitochondrial translation and actin filament organisation (Table 5.3). *NcS79* had significant enrichment of interacting genes involved with amino acid transmembrane transport, DNA replication and pyruvate metabolism (Table 5.4). The *N. ceranae* secretome ORF with the broadest spectrum of biological process enriched interacting genes was *NcS85* with 16 separate GO terms including; vesicle formation, DNA repair, nucleotide metabolism, stress response (water deprivation and oxidative stress) and signal transduction (Table 5.5).

Because the high-throughput image analysis and processing methods employed for SGA produce quantitative data, we are able to interrogate those genes which present the strongest synthetic sick phenotypes, indicating the strongest synthetic genetic interactions and therefore may provide the best insights into NcS-ORF functions. The top 10 SGA score genes from the *NcS50, NcS68,*

NcS79 and *NcS85* screens are enriched for transcription, transmembrane transport, oxidative stress response and DNA repair respectively (Table 5.6).

The majority of genetic interactions identified in the five SGA screens were unique to each *N. ceranae* ORF however; interestingly some synthetic genetic interactions are common to multiple *N. ceranae* ORFs (Figure 5.2, Table 5.8). The two *N. ceranae* ORFs with the greatest number of shared interactions are *NcS50* and *NcS85* with 13 synthetic genetic interactions in common including; *APE3, APT1, CHK1, MLH1, RPL4A, RPS21B, POX1, IRS4, VPS9, SWD1, YIR016W, YML108W* and *YCR043C*. Interestingly, these genes show significant GO term enrichment for lipid metabolic processes (*POX1* and *IRS4,* $p < 0.01$) and both NcS50 and NcS85 were both observed associating with lipid droplets in *S. cerevisiae* through GFP-fused recombinant expression and fluorescence microscopy (Chapter 3). In an effort to elucidate a mechanism or purpose for the co-localisation of NcS50 and NcS85 with ERG6 a marker for lipid droplets, I searched their synthetic genetic interactors for genes with cellular component GO terms that matched ERG6 (lipid particle [GO:0005811] and endoplasmic reticulum [GO:0005783]) as well as the biological process GO term of lipid metabolic process [GO:0006629]. Both *NcS50* and *NcS85* have synthetic genetic interactions with 11 *S. cerevisiae* genes either associated with the endoplasmic reticulum or lipid metabolic processes supporting previous observations (Table 5.9).

NcS65 and *NcS79* have five genetic interactors in common including; *ALO1, ERT1, GAT2, MGM101* and *RSA1,* with significant enrichment for the molecular function of DNA binding (*ERT1, MGM101* and *GAT2*, $p < 0.01$). There is enrichment for ion transport (*VMA7* and *ZRT3,* $p < 0.01$) and DNA repair (*MGM101*

Table 5.9 | *NcS50* and *NcS85* genetic interactors with GO terms in common with *ERG6*.

ORF	Interactor	SGA score	GO Biological Process	GO Cellular Component
NcS50	*POX1*	-0.59	peroxisomal matrix	lipid metabolic process
NcS50	*GEP4*	-0.52	mitochondrial matrix	lipid metabolic process
NcS50	*IRS4*	-0.52	pre-autophagosomal structure	lipid metabolic process
NcS50	*YLR118C*	-0.58	cytoplasm/nucleus	lipid metabolic process
NcS50	*NTE1*	-0.70	endoplasmic reticulum	lipid metabolic process
NcS50	*ERG24*	-0.65	endoplasmic reticulum	lipid metabolic process
NcS50	*AVT2*	-0.64	endoplasmic reticulum	unknown
NcS50	*ORM1*	-0.74	endoplasmic reticulum	cellular sphingolipid homeostasis
NcS50	*BXI1*	-0.50	endoplasmic reticulum	apoptotic process
NcS50	*SEY1*	-0.66	endoplasmic reticulum	endoplasmic reticulum organization
NcS50	*YPR071W*	-0.89	endoplasmic reticulum	unknown
NcS85	*POX1*	-0.67	peroxisomal matrix	lipid metabolic process
NcS85	*IRS4*	-0.62	pre-autophagosomal structure	lipid metabolic process
NcS85	*SUR4*	-0.66	endoplasmic reticulum	lipid metabolic process
NcS85	*ROT2*	-0.87	endoplasmic reticulum	fungal-type cell wall beta-glucan biosynthetic process
NcS85	*PMT5*	-0.87	endoplasmic reticulum	protein O-linked mannosylation
NcS85	*HVG1*	-0.94	endoplasmic reticulum	unknown
NcS85	*USA1*	-0.81	endoplasmic reticulum	ER-associated ubiquitin-dependent protein catabolic process
NcS85	*INP54*	-0.52	endoplasmic reticulum	phosphatidylinositol dephosphorylation
NcS85	*VPS4*	-0.62	endoplasmic reticulum	intralumenal vesicle formation/sterol metabolic process
NcS85	*IES5*	-0.88	Ino80 complex	telomere maintenance via recombination
NcS85	*OSH6*	-0.88	cortical endoplasmic reticulum	sterol metabolic process

and *SGS1*, $p < 0.01$) for the five genetic interactors common to *NcS65* and *NcS85* which include; *MGM101, SAM37, SGS1, VMA7* and *ZRT3.* The second largest set of shared genetic interactors is between *NcS85* and *NcS79* which includes*; APE3, CLB5, GYP5, MET17, MGM101, MXR2, YIL092W* and *YJL206C,* however these genes do not show enrichment for common biological processes (Figure 5.2). Other shared genetic interactions are summarised in Figure 5.2.

I identified two hubs in the genetic interaction map; *APE3* is a vacuolar aminopeptidase and a synthetic genetic interactor common to three *N. ceranae* ORFs; *NcS50, NcS79* and *NcS85*; and *MGM101*, which is required for the repair of oxidative mitochondrial DNA damage and mitochondrial genome maintenance is a genetic interactor also common to three *N. ceranae* ORFs; *NcS65, NcS79* and *NcS85* (Figure 5.2).

5.3.3 *N. ceranae* secretome ORFs in the context of a cell's genetic landscape

Costanzo et al. (2010) demonstrated the utility of comparing entire interaction profiles for query genes rather than only considering synthetic genetic interactors i.e. comparing the SGA score for every double mutant from one screen with the SGA score for every double mutant of another screen regardless of the double mutants presenting an interaction phenotype. The authors completed this approach for ~5.4 million gene pairs to build a functional map of the eukaryotic cell and this resource is available to the community (Costanzo et al., 2010). I applied this approach to capitalise on my SGA data.

To yield a network with highly correlated functional process clusters only *S. cerevisiae* interaction profiles with correlation values of $r > 0.2$ were included.

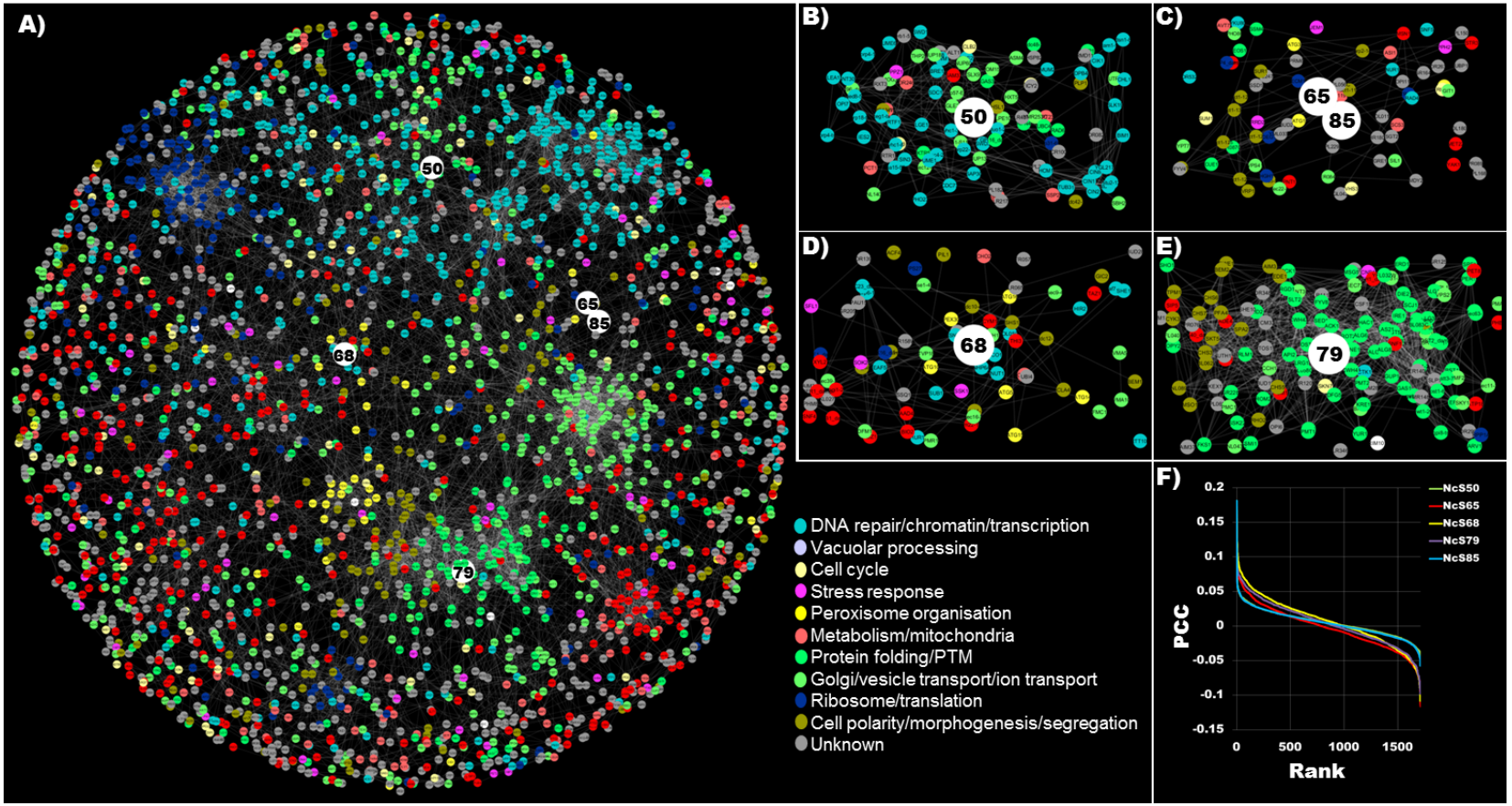

Figure 5.3 | *N. ceranae* ORFs clustering within the genetic landscape of a cell.

The network is based on genetic interaction-profile correlation values. Nodes within the network represent genes and different colours represent GO biological processes for the associated gene **A)**. Following genome-wide SGA analysis of *N. ceranae* ORFs and determining SGA scores for double mutants from each screen to yield an interaction profile for each query gene, the interaction profiles of *NcS50, NcS65, NcS68, NcS79* and *NcS85* were added to the Costanzo et al., (2010) genetic

interaction matrix and genetic profile similarities were measured for all gene pairs by computing Pearson Correlation Coefficients (PCC) **F)**. *S. cerevisiae* gene pairs with an interaction profile PCC > 0.2 were used to build the network. The 10 highest PCC scores for each NcS query were used to integrate the *N. ceranae* ORFs. The network was rendered using an edge-weighted spring-embedded layout algorithm in Cytoscape with edges weighted by their PCC values. Distinct clustering of genes involved in defined GO biological processes indicated by node colours is observed and the relative distance between distinct clusters appears to reflect shared functionality (Costanzo et al., 2010). **B)** Magnified view shows *NcS50* clusters with blue and green nodes (processes of transcription and nuclear to cytoplasmic transport. **C)** Magnified view of *NcS65* and *NcS85* clustering together. **D)** Magnified view of *NcS68.* **E)** Magnified view *NcS79* clustering with dark green nodes (processes linked to transmembrane transport.

As discussed in previous chapter's *N. ceranae* secretome ORFs show no homology to known sequences and so we can expect their correlation values with *S. cerevisiae* interaction profiles to be lower than this threshold (Figure 5.3-F). The top 10 correlating interaction profiles for each of the five SGA screens was used to integrate the *N. ceranae* ORFs with the network. The functional map shows *NcS50* clusters with *S. cerevisiae* genes involved with DNA repair/chromatin/transcription represented by light blue nodes (Figure 5.3-B). *NcS65* and *NcS85* cluster together but do not reside within a cluster of genes with highly similar biological function (Figure 5.3-C). *NcS68* does not associate with a biological process cluster, or with the other NcS-ORFs (Figure 5.3-D)**.** *NcS79* clusters with *S. cerevisiae* genes involved in protein folding/post-translational modification (PTM) e.g. glycosylation/ cell wall biogenesis and integrity indicated by green nodes (Figure 5.3-E).

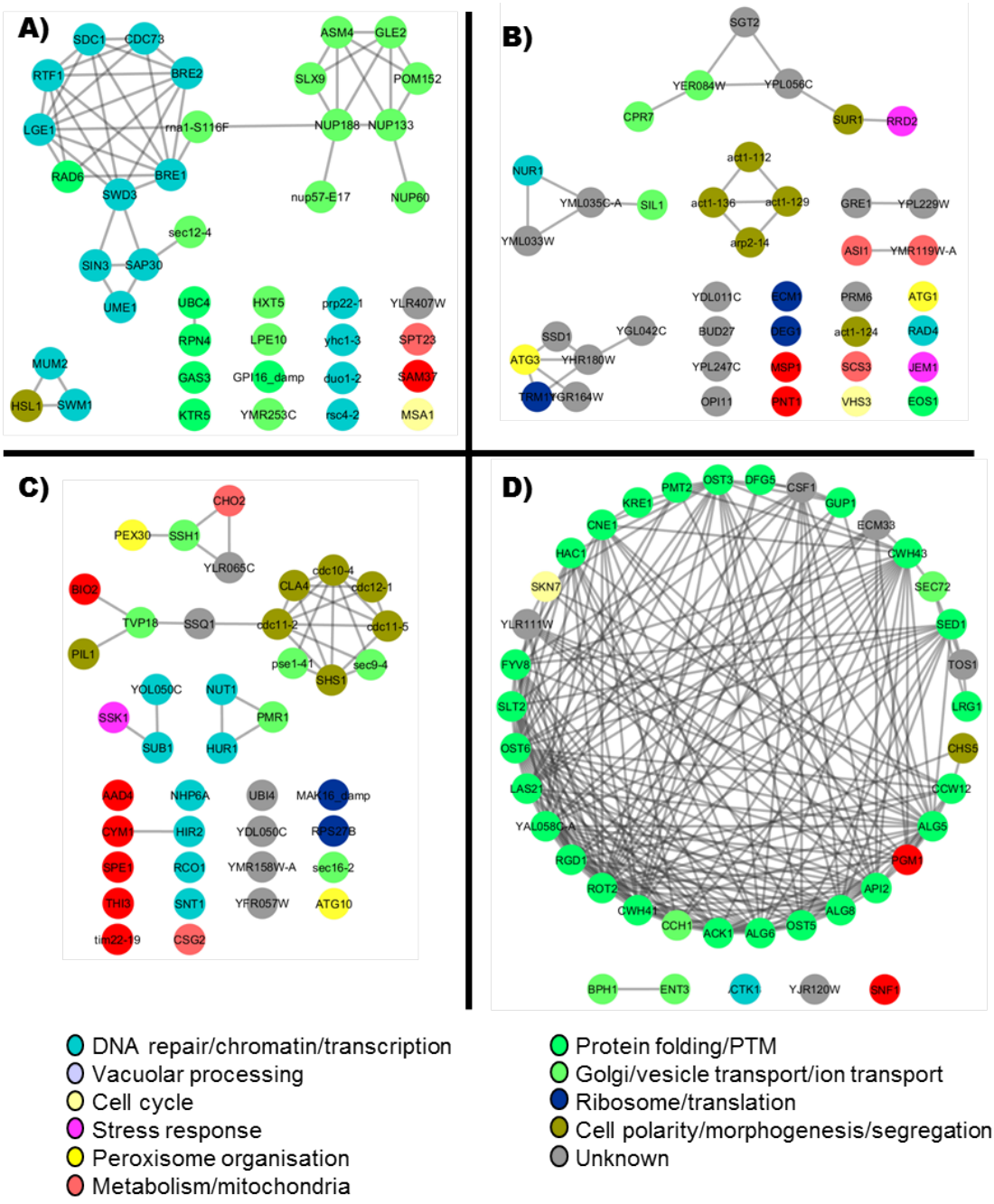

Figure 5.4 | Proximal node interconnectivity from interaction profile network. Networks were re-rendered from the magnified proximity clusters in Figure 5.3. **A)** Relationship of nodes in proximity to *NcS50.* **B)** Relationship of nodes in proximity to *NcS65* and *NcS85*. **C)** and **D)** Relationship of nodes in proximity to *NcS68* and *NcS79* respectively.

Utilising the functional map of a cell to interrogate SGA data increases output three fold i.e. as well as having a list of genetic interactors which can be used to interrogate genes of interest, a data set of closest correlating interaction profiles and a data set of proximally clustering genes are also yielded. Figure 5.4-A highlights that nodes within functional clusters of the network may not all be identified by correlating interaction profiles alone e.g. all light blue nodes of the sub-network are involved in transcription/chromatin however, there are other blue nodes also involved in transcription/chromatin which are not connected. This observation is repeated for the light green nodes, genes associated with nuclear-cytoplasmic transport, many of which are connected in the sub-network however many are also observed in proximity but not connected. Conversely a high degree of proximal node interconnectivity can also be observed e.g. Figure 5.3-D shows a high degree of interconnectivity for the genes *NcS79* clusters with that are involved in processes of protein folding/glycosylation/cell wall biogenesis and ER traffic.

Functional enrichment of nodes *NcS50* clusters with in the genetic landscape of the cell (Table 5.10) supports observations of functional enrichment of *NcS50* synthetic genetic interactors (Table 5.1) where we observe highly related processes such as mRNA processes, DNA damage checkpoint and chromatin related functions. Enrichment of function for nodes proximal to *NcS65, NcS68* and *NcS85* do not correlate with enriched functions of their respective genetic interactors (Tables 5.11-5.12 and Tables 5.2-5.3 and 5.5 respectively). Nodes clustering with *NcS79* show functional enrichment for endoplasmic reticulum and membrane processes (Table 5.13) which supports enrichment of *NcS79* genetic interactors with amino acid transmembrane transport (Table 5.4).

Table 5.10 | GO term enrichment of *S. cerevisiae* genes that cluster with *N. ceranae* secretome ORF-50 in the genetic landscape of the cell.

Biological Process Category	p-value	In Category from Cluster	k	f
histone monoubiquitination [GO:0010390]	<0.0001	*BRE1 RAD6 RTF1*	3	3
nucleocytoplasmic transport [GO:0006913]	<0.0001	*NUP60 ASM4 GLE2 NUP188 POM152*	5	37
negative regulation of transcription from RNA polymerase I promoter [GO:0016479]	<0.0001	*SAP30 SIN3 UME1*	3	6
histone methylation [GO:0016571]	<0.0001	*RTF1 CDC73 LGE1*	3	7
mRNA transport [GO:0051028]	<0.0001	*NUP60 ASM4 GLE2 NUP188 POM152*	5	58
chromatin silencing at telomere [GO:0006348]	<0.0001	*SWD3 BRE1 SDC1 RAD6 BRE2*	5	58
histone H3-K4 methylation [GO:0051568]	<0.0001	*SWD3 SDC1 BRE2*	3	9
chromatin modification [GO:0016568]	<0.0001	*BRE1 RAD6 SAP30 SIN3 LGE1 UME1*	6	114
mRNA export from nucleus in response to heat stress [GO:0031990]	<0.0001	*NUP60 ASM4 NUP188*	3	10
negative regulation of chromatin silencing at telomere [GO:0031939]	<0.0001	*SAP30 SIN3 UME1*	3	11
regulation of transcription, DNA-dependent [GO:0006355]	<0.0001	*RPN4 SDC1 RAD6 RTF1 CDC73 SAP30 SIN3 MSA1 LGE1 UME1*	10	507
mitotic cell cycle G1/S transition DNA damage checkpoint [GO:0031571]	<0.0001	*BRE1 RAD6*	2	3
negative regulation of chromatin silencing at rDNA [GO:0061188]	<0.0001	*SAP30 SIN3*	2	3
negative regulation of chromatin silencing at silent mating-type cassette [GO:0061186]	<0.0001	*SAP30 SIN3*	2	3
protein monoubiquitination [GO:0006513]	<0.0001	*UBC4 RAD6 LGE1*	3	18
transcription, DNA-dependent [GO:0006351]	<0.0001	*RPN4 RAD6 RTF1 BRE2 CDC73 SAP30 SIN3 MSA1 LGE1 UME1*	10	540
nuclear pore organization [GO:0006999]	<0.0001	*ASM4 NUP188 POM152*	3	21
histone deacetylation [GO:0016575]	0.0002	*SAP30 SIN3 UME1*	3	27
premeiotic DNA replication [GO:0006279]	0.0003	*MUM2 LGE1*	2	6

transcription-dependent tethering of RNA polymerase II gene DNA at nuclear periphery [GO:0000972]	0.0005	*NUP60 GLE2*	2	8
meiotic DNA double-strand break formation [GO:0042138]	0.0009	*BRE1 RAD6*	2	10
positive regulation of transcription from RNA polymerase II promoter [GO:0045944]	0.0010	*SPT23 SAP30 SIN3 UME1*	4	100
double-strand break repair via homologous recombination [GO:0000724]	0.0013	*BRE1 RAD6*	2	12
posttranscriptional tethering of RNA polymerase II gene DNA at nuclear periphery [GO:0000973]	0.0015	*NUP60 GLE2*	2	13
protein ubiquitination [GO:0016567]	0.0018	*UBC4 SWM1 RAD6*	3	54
post-translational protein modification [GO:0043687]	0.0020	*UBC4 RAD6*	2	15
transmembrane transport [GO:0055085]	0.0021	*NUP60 ASM4 GLE2 HXT5 NUP188 POM152*	6	303
NLS-bearing substrate import into nucleus [GO:0006607]	0.0033	*NUP60 NUP188*	2	19
protein export from nucleus [GO:0006611]	0.0040	*NUP60 NUP188*	2	21
poly(A)+ mRNA export from nucleus [GO:0016973]	0.0044	*NUP60 GLE2*	2	22
transcription from RNA polymerase II promoter [GO:0006366]	0.0044	*BRE1 RAD6 RTF1*	3	74
protein polyubiquitination [GO:0000209]	0.0048	*UBC4 RAD6*	2	23
protein transport [GO:0015031]	0.0063	*NUP60 ASM4 GLE2 NUP188 SAM37 POM152*	6	379
G2/M transition of mitotic cell cycle [GO:0000086]	0.0070	*RPN4 HSL1*	2	28
regulation of cell size [GO:0008361]	0.0080	*MSA1 LGE1*	2	30
protein import into nucleus [GO:0006606]	0.0091	*NUP188 POM152*	2	32
telomere maintenance [GO:0000723]	0.0091	*SWD3 BRE2*	2	32

Table 5.11 | GO term enrichment of *S. cerevisiae* genes that cluster with *N. ceranae* secretome ORFs-65 and 85 in the genetic landscape of the cell.

Biological Process Category	p-value	In Category from Cluster	k	f
autophagic vacuole assembly [GO:0000045]	0.0015	*ATG1 ATG3*	2	12
protein peptidyl-prolyl isomerization [GO:0000413]	0.0031	*CPR7 RRD2*	2	17
mitochondrion degradation [GO:0000422]	0.0090	*ATG1 ATG3*	2	29

Table 5.12 | GO term enrichment of *S. cerevisiae* genes that cluster with *N. ceranae* secretome ORF-68 in the genetic landscape of the cell.

Biological Process Category	p-value	In Category from Cluster	k	f
RNA polymerase III transcriptional preinitiation complex assembly [GO:0070898]	0.0003	*SUB1 NHP6A*	2	6
regulation of transcription, DNA-dependent [GO:0006355]	0.0065	*SNT1 NUT1 SSK1 SUB1 RCO1 HIR2 NHP6A*	7	507
histone deacetylation [GO:0016575]	0.0065	*SNT1 RCO1*	2	27

Table 5.13 | GO term enrichment of *S. cerevisiae* genes that cluster with *N. ceranae* secretome ORF-79 in the genetic landscape of the cell.

Biological Process Category	p-value	In Category from Cluster	k	f
endoplasmic reticulum membrane [GO:0005789]	<0.0001	*PMT2 CNE1 CWH43 CWH41 LAS21 SEC72 OST6 ALG6 ALG8 OST3 ALG5*	11	318
endoplasmic reticulum [GO:0005783]	<0.0001	*PMT2 CNE1 ROT2 CWH43 CWH41 GUP1 LAS21 OST6 ALG6 ALG8 OST3 ALG5*	12	416
membrane [GO:0016020]	<0.0001	*PMT2 CNE1 ECM33 CWH43 BPH1 SED1 SNF1 CWH41 GUP1 OST5 CCH1 LAS21 CSF1 CCW12 CHS5 OST6 DFG5 KRE1 ALG6 ALG8 OST3 ALG5*	22	1671
oligosaccharyltransferase complex [GO:0008250]	<0.0001	*OST5 OST6 OST3*	3	9
anchored to membrane [GO:0031225]	<0.0001	*ECM33 SED1 CCW12 DFG5 KRE1*	5	61
fungal-type cell wall [GO:0009277]	0.0001	*ECM33 TOS1 SED1 CCW12 KRE1*	5	85
extracellular region [GO:0005576]	0.0001	*ECM33 TOS1 SED1 CCW12 KRE1*	5	95
cell wall [GO:0005618]	0.0005	*ECM33 SED1 CCW12 KRE1*	4	68
integral to membrane [GO:0016021]	0.0021	*PMT2 CNE1 CWH43 CWH41 GUP1 OST5 CCH1 LAS21 CSF1 OST6 KRE1 ALG6 ALG8 OST3 ALG5*	15	1303
integral to plasma membrane [GO:0005887]	0.0074	*CWH43 LAS21*	2	24

5.4 Discussion

I have previously identified five *N. ceranae* secretome ORFs that present a punctate fluorescence phenotype when expressed in *S. cerevisiae* (NcS50, NcS65, NcS68, NcS79 and NcS85), suggesting these proteins target specific subcellular compartments. To try and gain insight into possible functions for these putative *N. ceranae* virulence factors I tried to identify what structures or complexes they were associating with in a previous chapter. Initial results suggested that NcS50 and NcS85 co-localise with ERG6 which is a marker for lipid droplets. I have not yet identified what structures NcS65, NcS68 and NcS79 associate with when expressed in *S. cerevisiae.* As previously discussed there is very little information available for these *N. ceranae* proteins and very limited tools for studying molecular processes in microsporidia. The high throughput genome-wide analysis of SGA has a proven track record of yielding functional information for proteins for which no previous information was available, both in model and non-model systems (Brown & Madhani, 2012; Costanzo et al., 2010; Tong & Boone, 2005; Tong et al., 2001, 2004; Usher et al., 2015). I have adopted this approach to further characterise the five *N. ceranae* ORFs with punctate phenotypes in an attempt to expand current knowledge and identify their functional roles.

N. ceranae ORFs have many synthetic genetic interactions with *S. cerevisiae* genes (102, 149, 55, 119 and 138 for *NcS50, NcS65, NcS68, NcS79* and *NcS85* respectively). Furthermore, many interactions are common between different NcS-ORFs, an observation that is most prominent for *NcS50* and *NcS85* which share 13 synthetic genetic interactions in common. Having the highest number of common genetic interactors may be indicative of a common function for

these two proteins which may explain the observation of both proteins co-localising with ERG6, a lipid droplet marker. This hypothesis is supported by the synthetic genetic interactors common to both *NcS50* and *NcS85* being significantly enriched for genes whose products are implicated in lipid metabolic processes [GO:0006629] (*POX1* and *IRS4*, $p < 0.01$). POX1 is a fatty-acyl coenzyme A oxidase involved in the fatty acid beta-oxidation pathway and localises with the peroxisomal matrix (Hiltunen et al., 2003). Peroxisomes along with lipid droplets are established as central players in cellular lipid homeostasis (Kohlwein et al., 2013). IRS4 is an EH domain-containing protein involved in regulating phosphatidylinositol 4,5-bisphosphate levels and autophagy (Morales-Johansson et al., 2004). Beyond these two genetic interactors both *NcS50* and *NcS85* each has nine different synthetic genetic interactors related to ERG6 either through a common cellular component (lipid droplet or endoplasmic reticulum) or biological process (lipid metabolism, Table 5.9). Identifying a total of 11 genes each with either a shared cellular component or biological process with ERG6 serves as a key cohort of candidate genes to interrogate as potential mechanisms by which *NcS50* and *NcS85* co-localise with ERG6 and should be prioritised in future studies.

While some genetic interactors were identified as common to multiple *N. ceranae* ORFs, the majority were unique and so the patterns of genetic-interactor functional enrichment were different for each *N. ceranae* ORF. The genetic interactors of *NcS50* show greatest enrichment for genes implicated in transcription/chromatin/DNA damage and repair, as well as vacuolar protein metabolism and ascospore wall assembly, however when considering only the 10

strongest genetic interactions, the functional enrichment is reduced to only include transcription. It has previously been established that genetic interactions frequently occur between genes that participate in the same biological process (Dixon et al., 2009) and so I propose a role for NcS50 in targeting host transcription to affect pathogenesis (to be confirmed). Microsporidia are obligately intracellular pathogens depending on essential host resources for survival and so if NcS50 does target host transcription, it may be a key candidate as a mechanism for host cell reprogramming.

N. ceranae secretome ORF-65 has genetic interactions enriched for genes implicated in endosome transport/DNA damage and repair and endocytosis. Furthermore, three of the five most highly correlated interaction profiles include endonucleases (*SLX1, SLX4* and *RAD27*). SLX1 and SLX4 are involved in DNA recombination and repair while RAD27 is involved in long-patch base-excision repair and large loop repair of Okazaki fragments (Fricke & Brill, 2003; Sparks et al., 2012). I therefore propose NcS65 may be involved in host DNA recombination and repair. Many microbial pathogens are known to manipulate host cellular environments to create optimal conditions for their own replication; they alter cellular structures, divert signaling pathways, modify host epigenetic programs, and influence metabolism (Weitzman & Weitzman, 2014). The host DNA damage and repair cascades activated by pathogens operate to combat infection and can therefore be considered as another aspect of cellular defense. Infecting microbes implement counter measures which can have devastating consequences for host cells and the infected organism (Weitzman & Weitzman, 2014). In this light, NcS65

may function to overcome an aspect of a host cell defense mechanism, but this hypothesis is yet to be confirmed.

The list of genes that present a synthetic genetic interaction with *NcS68* show enrichment of encoded proteins involved in transmembrane transport, three of which are included in the 10 strongest genetic interactions (*FLR1, GEX2 and FSF1*). FLR1 is a plasma membrane transporter of the major facilitator superfamily involved in drug efflux and relocalises from the nucleus to the plasma membrane upon DNA replication stress (Tkach et al., 2012). GEX2 is a proton:glutathione antiporter which localises at the vacuolar and plasma membranes and has a potential role in resistance to oxidative stress (Dhaoui et al., 2011). Taken together these data suggest NcS68 is involved in transmembrane transport. This putative secreted protein may therefore be a peripheral protein that associates with and modifies the function of an undetermined transport protein, contributing to processes of recruitment which plug conserved gaps in microsporidian biosynthesis and metabolism (Nakjang et al., 2013).

Genes that synthetically interact with *NcS79* show enrichment for amino acid transmembrane transport, chromatin/DNA replication and pyruvate metabolism however, this ORF also localises within the Golgi/vesicle/transport and protein processing cluster of the functional map of a cell (light and dark green nodes Figure 5.3 and 5.4), which supports the observed enrichment of interactors with amino acid transport. I propose these data suggest a possible role for NcS79 in amino acid transport.

Of all the genetic interactions identified in the present study *NcS85* shows the greatest enrichment for a specific biological process with 14 genes associated

with response to DNA damage stimulus and three of these are also amongst the 10 greatest genetic interactions with *NcS85* (*CHK1, PSY3* and *MLH1*). CHK1 is a serine/threonine kinase and DNA damage checkpoint effector which mediates cell cycle arrest via phosphorylation of Pds1p (Liu et al., 2000). PSY3 is a component of the Shu complex involved in error-free DNA post-replication repair (L. G. Ball et al., 2009). These data provide the strongest inference of function for all of the *N. ceranae* ORFs assessed by SGA and imply NcS85 is involved in processes relating to DNA damage stimulus, and therefore also potentially targeting host intracellular defense systems (see above).

Historically, SGA provided insight to a query genes function by identifying genes with which it had a synthetic genetic interaction. Costanzo *et al.* increased the robustness of SGA analysis by statistically comparing every *S. cerevisiae* double mutant (~5.4 million gene pairs) to generate quantitative genetic interaction profiles for approximately 75% of the genes in the *S. cerevisiae* genome and by determining the correlation between interaction profiles, were able to reveal the functional map of a cell (Costanzo et al., 2010). I have exploited this community resource by statistically comparing the entire interaction profile of each double mutant overexpressing an *N. ceranae* ORF and with a specific *S. cerevisiae* gene deletion to the interaction profiles from the functional map of a cell which revealed where the *N. ceranae* ORFs cluster in the genetic landscape. The output from this analysis supports observations made regarding functional enrichment of the genes with which *N. ceranae* ORFs have genetic interactions with. Specifically, *NcS50* clusters with genes involved in transcription, *NcS79* clusters with genes involved with protein transport and *NcS65* and *NcS85* cluster together which is in

agreement with them both having genetic interactors enriched for DNA repair. It should be noted that these data need to be considered carefully with the synthetic interaction dataset as the correlation values are low which is to be expected from exogenous genes with no homologs in public databases or even any sequence similarities. I present here the first genome-scale functional analysis of putative virulence factors from microsporidia and demonstrate the effective employment of SGA to investigate microsporidian proteins. The three datasets presented here; genetic interactors, interaction profiles and proximate nodes within the functional map of a cell provide direction for functional characterisation of these putative *N. ceranae* effectors in future studies.

Chapter 6 | General Discussion

Bees are vitally important to the global economy and ecology but have faced increasing abiotic and biotic stresses in recent years e.g. viruses, bacteria, fungi, metazoan parasites as well as toxic pesticides and habitat loss, which have negatively affected their populations in both Europe and the US. The microsporidian *N. ceranae* is rated as one of the major contributors to declining honeybee populations behind the ectoparasitic mite *V. destructor* and has also been identified as a pathogen of wild unmanaged bumblebee populations, which may have significant implications in light of these key pollinators not receiving disease mitigating interventions that are applied to honeybee hives by bee keepers (Fürst et al., 2014). Microsporidia have been the focus of scientific research since their discovery in the 1950's when *N. bombycis* was discovered as the causative agent of pébrine, a disease of silk worms that devastated the European silk industry. Since that time aspects of microsporidian biology including; ultrastructure, phylogeny, genetics, biochemistry, physiology and epidemiology have been elucidated however there has remained a distinct lack of knowledge in the area of molecular mechanisms of pathology, reasons for which are attributed to their very nature of an obligate intracellular active lifecycle, rendering them intractable for forward and reverse genetic analysis. This has limited the molecular tools for microsporidian research to genome sequencing, comparative genomics, transcriptomics, proteomics and heterologous expression for proteins of interest in model organisms such as *S. cerevisiae*.

It stands to reason that the means by which an intracellular pathogen can manipulate a host cell to facilitate development, growth and replication consists of the proteins on the surface of its cell which are in direct contact with host material, and soluble proteins which are secreted out of the pathogen cell into the host cell and interact with host pathways and complexes directly, known as effector proteins or virulence factors. Research into bacterial, fungal and oomycete effector proteins has been growing over the past few decades, revealing the essential roles they play in pathogenesis (Deslandes & Rivas, 2012; J. G. Ellis et al., 2009; Giraldo & Valent, 2013; Giraldo et al., 2013; Hunter & Sibley, 2012; Morgan & Kamoun, 2007; Schornack et al., 2009; Valdivia, 2008). This rationale formed the basis of the present study and in an effort to advance current understanding of the molecular mechanisms of *N. ceranae* pathology I have investigated the organisms secretome.

Although microsporidian secreted proteins are currently poorly characterised, this area of research has been building momentum in the last few years. The first microsporidian secreted proteins were identified in *N. parisii* and *Nematocida sp1* which infect nematode worms (Cuomo et al., 2012) and were actually discovered because of the interesting observation that the genomes of these organisms encode a hexokinase with an N-terminal SP. The authors showed the secretion signal is functional in a yeast cell. This discovery was shortly followed by Senderskiy and colleagues revealing microsporidia secrete proteins with a broad range of biological functions; chaperone Hsp70, trehalase, LRR, hexokinase, a/b hydrolase and ricin b-like lectin (Senderskiy et al., 2014), and the diversity of functions grew with the growing availability of sequenced genomes. The mosquito

pathogens *E. aedis* and *V. culicis* were also revealed to encode a ubiquitin hydrolase predicted to be secreted in their genomes (Desjardins et al., 2015). The functions of identified microsporidian secreted proteins span the processes of nutrient acquisition and immune system subversion the two main roles of virulence factors. Desjardins et al. also showed vast numbers of putatively secreted proteins are expressed during *E. aedis* and *V. culicis* infection. Secretion in *E. aedis* is drastic with huge vesicles fusing with the spore membrane for exocytosis (Desjardins et al., 2015).

This investigation aims to increase understanding of *N. ceranae* pathology by characterising putative virulence factors i.e. secreted proteins using a combination of established tools for assessing microsporidian proteins e.g. bioinformatics and heterologous recombinant expression in the model system for eukaryotic genetics *S. cerevisiae,* as well as novel technologies such as SGA.

Through comparative bioinformatic analysis I have assessed the *N. ceranae* secretome in the context of the available microsporidian secretome sequences to determine key features, paying special attention to the similarities and differences between the secretomes of *N. ceranae* and *N. apis*. Even though *N. ceranae* has the smaller genome of these closely related bee pathogens, it possesses many more secreted proteins. I speculate this could be a contributing factor to *N. ceranae* being more pathogenic than *N. apis*. As well as having many more total secreted proteins, *N. ceranae* possesses 106 proteins in its secretome without orthologues in the *N. apis* secretome which could confer a competitive advantage to *N. ceranae* over *N. apis*. This hypothesis warrants further study and these proteins unique to *N. ceranae* should be prioritised in future investigations.

Bioinformatic analysis identified microsporidian secretomes are considerably over-represented by lineage or even species-specific proteins, in agreement with previous observations, and this has been said to be a reflection of microsporidian adaptation to different host cell environments (Nakjang et al., 2013). There is only one species-specific secreted protein (NcS77) in the *N. ceranae* secretome with a conserved domain predicted to be a nucleoporin-FG-repeat. In consideration of nucleoporin-FG-repeats being implicated as pathogen factors of viruses and cancer (Matreyek et al., 2013), this protein warrants focus for future studies to determine whether it has a role interacting with the host cell nuclear envelope.

Pathogen secretomes possess functional redundancy i.e. components that target the same processes or perform a very similar function which makes studying individual gene products difficult (Tan et al., 2015). When considering the proportion of the NcS with inferred domains, identifying protein enrichment for biological processes could identify complex pathogen-effector systems. I have shown *N. ceranae* has redundancy for thioredoxin proteins and proteins involved with the ubiquitylation/proteasome system (3 proteins each, Appendix VI). Ubiquitination regulates many cellular processes, including protein degradation by the proteasome and endocytosis from the plasma membrane (Torto-Alalibo et al., 2010). Many pathogens exploit the host ubiquitin pathway to supress immune responses which might suggest a possible role for these three *N. ceranae* proteins. Beyond bioinformatic analysis I have completed the NcS ORFeome, for what was previously believed to be the full set of secreted proteins. This is a resource available to the community to interrogate *N. ceranae* virulence factors. However, in this study I have shown that the *N. ceranae* secretome is twice as large as

originally thought. This discovery is attributable to improvements in SP prediction algorithms, and means the new NcS ORFs will need to be cloned to complete the resource.

Through assessing DsRed tagged NcS proteins by fluorescent microscopy I have identified two putative *N. ceranae* virulence factors co-localising with *S. cerevisiae* ERG6 fused to GFP which is a marker for lipid droplet's. Owing to lipid droplets role in coordinating immune responses to intracellular pathogens (Saka & Valdivia, 2012) and in light of the obligate intracellular human pathogen *C. trachomatis* being known to secrete effector proteins that interact with lipid droplets, a process essential to pathogenicity, NcS50 and NcS85 are good candidates as effectors which may serve as a mechanism for a convergent evolutionary strategy of obligate intracellular pathogens.

In the focussed effort of characterising *N. ceranae* secreted proteins I have also assessed components of the unique invasion apparatus of the polar tube and discovered that expression of PTPs in *S. cerevisiae* results in a distinct phenotype of filament induction. Furthermore, PTP2 localises at the cell wall, a trait also observed for NcS76. Based on the observed pheno-mimicry and comparable peptide features, NcS76 may be a novel PTP, however this is yet to be confirmed.

Finally, genetic approaches to understanding mechanisms of virulence have a track record for efficiently identifying genes necessary for pathogens to cause disease (Saitoh et al., 2012). However, a major impediment for this process is the lack of tools that can aid revealing the function of a gene product when it has no similarity to known sequences and therefore its biochemical function is unknown. The SGA platform has proven successful for yielding data on genes for which no

previous information was available. Furthermore, this method has successfully been applied in a cross-species analysis of a non-model organism to provide information on fungal pathogenicity factors that lack *S. cerevisiae* orthologues (Brown & Madhani, 2012). I present here the first application of SGA to quantitatively interrogate genetic interactions of microsporidian genes, coupled with comparison to the recently available data on the functional map of a cell, establishing the *N. ceranae* genes in the context of global cellular genetic interactions (Costanzo et al., 2010).

I have subjected five *N. ceranae* secreted proteins to SGA analysis based on the distinct punctate fluorescent phenotypes they present when expressed in *S. cerevisiae*. This cohort also included *NcS50* and *NcS85* which I have previously identified as co-localising with ERG6 with the hope of uncovering a functional role for this co-localisation. Indeed the output from SGA provides some insight into potential mechanisms by which these two proteins localise with ERG6, specifically they both share genetic interactions in common with two lipid metabolic process genes; *POX1* and *IRS4.* Beyond the genetic interaction *NcS50* and *NcS85* have in common, they each also have nine separate genetic interactions with genes related to *ERG6* either through a common cellular component of the lipid droplet or endoplasmic reticulum, or common biological process of lipid metabolism. Future experiments should interrogate potentially relationship of *NcS50* and *NcS85* with these genes.

Even though *NcS50* and *NcS85* have some genetic interactions with genes implicating in lipid droplets, this was not the biological process predicted for these two genes based on enrichment analysis of their respective genetic interactors. In

fact *NcS50* is implicated in roles related to transcription while *NcS85* is implicated in roles related to DNA repair. Interestingly *NcS85* was highlighted has being similar to *NcS65* in regards to their clustering within the functional map of the cell and supported by both having interactors enriched for DNA repair. The remaining two *N. ceranae* genes *NcS68* and *NcS79* were implicated in transmembrane transport based on enrichment of their genetic interactors.

This study provides valuable insight to the function of putative secreted proteins of *N. ceranae*. I have shown that 81% of the *N. ceranae* secretome has no homology to known sequences. The only way we will gain a comprehensive knowledge of molecular mechanisms of *N. ceranae* pathogenesis is to functionally characterise all of these unknown proteins. The present study has made the first attempt at this task and grown the knowledge base for putative *N. ceranae* virulence factors.

References

Abràmoff, M. D., P. J. Magalhães, and S. J. Ram. 2004. Image processing with imageJ. Biophotonics International 11:36–41.

del Aguila, C., F. Izquierdo, A. G. Granja, C. Hurtado, S. Fenoy, M. Fresno, and Y. Revilla. 2006. *Encephalitozoon* microsporidia modulates p53-mediated apoptosis in infected cells. International Journal for Parasitology 36:869–876.

Alberti, S., A. D. Gitler, and S. Lindquist. 2007. A suite of Gateway® cloning vectors for high-throughput genetic analysis in *Saccharomyces cerevisiae*. Yeast (Chichester, England).

Allen, M., and B. Ball. 1996. The incidence and world distribution of honey bee viruses. Bee World 77:141–162.

Alto, N. M., F. Shao, C. S. Lazar, R. L. Brost, G. Chua, S. Mattoo, S. A. McMahon, P. Ghosh, T. R. Hughes, C. Boone, and J. E. Dixon. 2006. Identification of a bacterial type III effector family with G protein mimicry functions. Cell 124:133–145.

Altschul, S. F., W. Gish, W. Miller, E. W. Myers, and D. J. Lipman. 1990. Basic local alignment search tool. Journal of Molecular Biology 215:403–10.

Amdam, G. V., and S. W. Omholt. 2003. The hive bee to forager transition in honeybee colonies: The double repressor hypothesis. Journal of Theoretical Biology 223:451–464.

Ames, L. C. 2013. Functional characterisation of *Candida glabrata* open reading frames with no orthologue in *Saccharomyces cerevisiae*. Unpublished PhD thesis. University of Exeter.

Anderson, D. L., and H. Giacon. 1992. Reduced Pollen Collection by Honey Bee (Hymenoptera: Apidae) Colonies Infected with *Nosema apis* and Sacbrood Virus. Journal of Economic Entomology 85:47–51.

Andreadis, T. G. 2005. Evolutionary strategies and adaptations for survival between mosquito-parasitic microsporidia and their intermediate copepod hosts: a comparative examination of *Amblyospora connecticus* and *Hyalinocysta chapmani* (Microsporidia: Amblyosporidae). Folia Parasitologica 52:23–35.

Antúnez, K., R. Martín-Hernández, L. Prieto, A. Meana, P. Zunino, and M. Higes. 2009. Immune suppression in the honey bee (*Apis mellifera*) following infection by *Nosema ceranae* (Microsporidia). Environmental Microbiology 11:2284–2290.

Ares, A. M., M. J. Nozal, J. L. Bernal, R. Martín-Hernández, M.Higes, and J. Bernal. 2012. Liquid chromatography coupled to ion trap-tandem mass spectrometry to evaluate juvenile hormone III levels in bee hemolymph from *Nosema* spp. infected colonies. Journal of Chromatography B: Analytical

Technologies in the Biomedical and Life Sciences 899:146–153.

Aufauvre, J., D. G. Biron, C. Vidau, R. Fontbonne, M. Roudel, M. Diogon, B. Viguès, L. P. Belzunces, F. Delbac, and N. Blot. 2012. Parasite-insecticide interactions: a case study of *Nosema ceranae* and fipronil synergy on honeybee. Scientific Reports 2:1–7.

Aufauvre, J., B. Misme-Aucouturier, B. Viguès, C. Texier, F. Delbac, and N. Blot. 2014. Transcriptome analyses of the honeybee response to *Nosema ceranae* and insecticides. PloS ONE 9:e91686.

Bacandritsos, N., A. Granato, G. Budge, I. Papanastasiou, E. Roinioti, M. Caldon, C. Falcaro, A. Gallina, and F. Mutinelli. 2010. Sudden deaths and colony population decline in Greek honey bee colonies. Journal of Invertebrate Pathology 105:335–340.

Bailey, L. 1953. Effect of Fumagillin upon *Nosema apis* (Zander). Nature 171:212–213.

Bailey, L. 1955. The Epidemiology and Control of *Nosema* Disease of the Honey-Bee. Annals of Applied Biology 43:379–389.

Bailey, L. 1956. Ætiology of European Foul Brood; a Disease of the Larval Honey-bee.

Bailey, L., and L. Bailey. 1983. *Melissococcus pluton*, the cause of European foulbrood of honey bees (*Apis* spp.). Journal of Applied Bacteriology 55:65–69.

Bailey, L., and B. V. Ball. 1991. Honey Bee Pathology. Second Edition. Elsevier.

Bailey, L., and A. J. Gibbs. 1964. Acute infection of bees with Paralysis Virus. Journal of Insect Pathology 6:395–407.

Bailey, L., A. J. Gibbs, and R. D. Woods. 1963. Two Viruses From Adult Honey Bees (*Apis mellifera* Linnaeus). Virology 21:390–5.

Bakowski, M. A., C. A. Desjardins, M. G. Smelkinson, T. A. Dunbar, I. F. Lopez-Moyado, S. A. Rifkin, C. A. Cuomo, and E. R. Troemel. 2014. Ubiquitin-Mediated Response to Microsporidia and Virus Infection in *C. elegans*. PLoS Pathogens 10.

Ball, B. V., and M. F. Allen. 1988. The prevalence of pathogens in honey bee (*Apis mellifera*) colonies infested with the parasitic mite *Varroa jacobsoni*. Annals of Applied Biology 113:237–244.

Ball, L. G., K. Zhang, J. A. Cobb, C. Boone, and W. Xiao. 2009. The yeast Shu complex couples error-free post-replication repair to homologous recombination. Molecular microbiology 73:89–102.

Baryshnikova, A., M. Costanzo, Y. Kim, H. Ding, J. Koh, K. Toufighi, J.-Y. Youn, J. Ou, B.-J. San Luis, S. Bandyopadhyay, M. Hibbs, D. Hess, A.-C. Gingras, G.

D. Bader, O. G. Troyanskaya, G. W. Brown, B. Andrews, C. Boone, and C. L. Myers. 2010. Quantitative analysis of fitness and genetic interactions in yeast on a genome scale. Nature Methods 7:1017–1024.

Belloy, L., A. Imdorf, I. Fries, E. Forsgren, H. Berthoud, R. Kuhn, and J.-D. Charrière. 2007. Spatial distribution of *Melissococcus plutonius* in adult honey bees collected from apiaries and colonies with and without symptoms of European foulbrood. Apidologie 38:136–140.

Bender, A., and J. R. Pringle. 1991. Use of a screen for synthetic lethal and multicopy suppressee mutants to identify two new genes involved in morphogenesis in *Saccharomyces cerevisiae*. Molecular and Cellular Biology 11:1295–305.

Bennett, D. J., A. Choimes, B. Collen, J. Day, A. De Palma, S. Dı, M. J. Edgar, A. Feldman, M. Garon, M. L. K. Harrison, T. Alhusseini, S. Echeverria-london, D. J. Ingram, Y. Itescu, J. Kattge, V. Kemp, L. Kirkpatrick, M. Kleyer, D. Laginha, P. Correia, C. D. Martin, S. Meiri, M. Novosolov, Y. Pan, H. R. P. Phillips, D. W. Purves, A. Robinson, J. Simpson, S. L. Tuck, E. Weiher, H. J. White, R. M. Ewers, and G. M. Mace. 2015. Global effects of land use on local terrestrial biodiversity. Nature 520:45–50.

Bhat, S. A., I. Bashir, and A. S. Kamili. 2009. Microsporidiosis of silkworm, *Bombyx mori* L. (Lepidoptera- bombycidae): A review. African Journal of Agricultural Research 4:1519–1523.

Bjornson, S., and D. Oi. 2014. Microsporidia Biological Control Agents and Pathogens of Beneficial Insects. Pages 635–670 *in* L. M. Weiss and J. J. Becnel, editors. Microsporidia: Pathogens of Opportunity. 1st edition.

Blaser, M., and P. Schmid-Hempel. 2005. Determinants of virulence for the parasite *Nosema whitei* in its host *Tribolium castaneum*. Journal of Invertebrate Pathology 89:251–257.

Bogdanov, S. 2006. Contaminants of bee products. Apidologie 37:1–18.

Bohan, D. A, C. W. H. Boffey, D. R. Brooks, S. J. Clark, A. M. Dewar, L. G. Firbank, A. J. Haughton, C. Hawes, M. S. Heard, M. J. May, J. L. Osborne, J. N. Perry, P. Rothery, D. B. Roy, R. J. Scott, G. R. Squire, I. P. Woiwod, and G. T. Champion. 2005. Effects on weed and invertebrate abundance and diversity of herbicide management in genetically modified herbicide-tolerant winter-sown oilseed rape. Proceedings of The Royal Society B 272:463–474.

Bouzahzah, B., F. Nagajyothi, K. Ghosh, P. M. Takvorian, A. Cali, H. B. Tanowitz, and L. M. Weiss. 2010. Interactions of *Encephalitozoon cuniculi* polar tube proteins. Infection and Immunity 78:2745–2753.

Bowen-Walker, P., S. Martin, and a Gunn. 1999. The transmission of deformed wing virus between honeybees (*Apis mellifera* L.) by the ectoparasitic mite *Varroa jacobsoni* Oud. Journal of Invertebrate Pathology 73:101–6.

Breitkreutz, B.-J., C. Stark, and M. Tyers. 2003. Osprey: a network visualization system. Genome Biology 4:R22.

Bromenshenk, J. J., C. B. Henderson, C. H. Wick, M. F. Stanford, A. W. Zulich, R. E. Jabbour, S. V. Deshpande, P. E. McCubbin, R. A. Seccomb, P. M. Welch, T. Williams, D. R. Firth, E. Skowronski, M. M. Lehmann, S. L. Bilimoria, J. Gress, K. W. Wanner, and R. A. Cramer. 2010. Iridovirus and microsporidian linked to honey bee colony decline. PLoS ONE 5.

Brosson, D., L. Kuhn, G. Prensier, C. P. Vivarès, and C. Texier. 2005. The putative chitin deacetylase of *Encephalitozoon cuniculi*: A surface protein implicated in microsporidian spore-wall formation. FEMS Microbiology Letters 247:81–90.

Brown, J. C. S., and H. D. Madhani. 2012. Approaching the Functional Annotation of Fungal Virulence Factors Using Cross-Species Genetic Interaction Profiling. PLoS Genetics 8.

Brugere, J. F., E. Cornillot, T. Bourbon, G. Metenier, and C. P. Vivarès. 2001. Inter-strain variability of insertion/deletion events in the *Encephalitozoon cuniculi* genome: a comparative KARD-PFGE analysis. The Journal of Eukaryotic Microbiology Suppl:50S–55S.

Budge, G. E., B. Barrett, B. Jones, S. Pietravalle, G. Marris, P. Chantawannakul, R. Thwaites, J. Hall, A. G. S. Cuthbertson, and M. A. Brown. 2010. The occurrence of *Melissococcus plutonius* in healthy colonies of *Apis mellifera* and the efficacy of European foulbrood control measures. Journal of Invertebrate Pathology 105:164–170.

Butler, G., M. D. Rasmussen, M. F. Lin, M. A. S. Santos, S. Sakthikumar, C. A. Munro, E. Rheinbay, M. Grabherr, A. Forche, J. L. Reedy, I. Agrafioti, M. B. Arnaud, S. Bates, A. J. P. Brown, S. Brunke, M. C. Costanzo, D. a Fitzpatrick, P. W. J. de Groot, D. Harris, L. L. Hoyer, B. Hube, F. M. Klis, C. Kodira, N. Lennard, M. E. Logue, R. Martin, A. M. Neiman, E. Nikolaou, M. A. Quail, J. Quinn, M. C. Santos, F. F. Schmitzberger, G. Sherlock, P. Shah, K. A. T. Silverstein, M. S. Skrzypek, D. Soll, R. Staggs, I. Stansfield, M. P. H. Stumpf, P. E. Sudbery, T. Srikantha, Q. Zeng, J. Berman, M. Berriman, J. Heitman, N. A. R. Gow, M. C. Lorenz, B. W. Birren, M. Kellis, and C. A. Cuomo. 2009. Evolution of pathogenicity and sexual reproduction in eight *Candida genomes*. Nature 459:657–662.

Cali, A., and P. M. Takvorian. 1999. The Microsporidia and Microsporidiosis. (L. M. Weiss and M. Wittner, Eds.). American Society of Microbiology.

Cali, A., L. M. Weiss, and P. M. Takvorian. 2002. *Brachiola algerae* spore membrane systems, their activity during extrusion, and a new structural entity, the multilayered interlaced network, associated with the polar tube and the sporoplasm. The Journal of Eukaryotic Microbiology 49:164–74.

Camacho, C., G. Coulouris, V. Avagyan, N. Ma, J. Papadopoulos, K. Bealer, and T. L. Madden. 2009. BLAST+: architecture and applications. BMC

Bioinformatics 10:421.

Camazine, S., I. Çakmak, K. Cramp, J. Finley, J. Fisher, M. Frazier, and A. Rozo. 1998. How Healthy are Commercially-produced U.S. Honey Bee Queens? American Bee Journal 138:677–680.

Campbell, S. E. 2013. Secreted proteins in microsporidian parasites : a functional and evolutionary perspective on host-parasite interactions. Unpublished PhD theisis. University of Exeter.

Campbell, S. E., T. A. Williams, A. Yousuf, D. M. Soanes, K. H. Paszkiewicz, and B. A. P. Williams. 2013. The Genome of *Spraguea lophii* and the Basis of Host-Microsporidian Interactions. PLoS Genetics 9:1–15.

Campodonico, E. M., L. Chesnel, and C. R. Roy. 2005. A yeast genetic system for the identification and characterization of substrate proteins transferred into host cells by the *Legionella pneumophila* Dot/Icm system. Molecular Microbiology 56:918–933.

Capella-Gutiérrez, S., M. Marcet-Houben, and T. Gabaldón. 2012. Phylogenomics supports microsporidia as the earliest diverging clade of sequenced fungi. BMC Biology 10:47.

Carmen, J. C., and A. P. Sinai. 2007. Suicide prevention: Disruption of apoptotic pathways by protozoan parasites. Molecular Microbiology 64:904–916.

Casadevall, A. 2008. Evolution of intracellular pathogens. Annual Review of Microbiology 62:19–33.

Casanova, M., J. L. Lopez-Ribot, C. Monteagudo, A. Llombart-Bosch, R. Sentandreu, and J. P. Martinez. 1992. Identification of a 58-kilodalton cell surface fibrinogen-binding mannoprotein from *Candida albicans*. Infection and Immunity 60:4221–9.

Cavalier-Smith, T. 1983. A 6-Kingdom Classification and a Unified Phylogeny. Endocytobiology 2:1027–1034.

Chaimanee, V., Y. Chen, J. S. Pettis, S. R. Cornman, and P. Chantawannakul. 2011. Phylogenetic analysis of *Nosema ceranae* isolated from European and Asian honeybees in Northern Thailand. Journal of Invertebrate Pathology 107:229–233.

Chaimanee, V., J. S. Pettis, Y. Chen, J. D. Evans, K. Khongphinitbunjong, and P. Chantawannakul. 2013. Susceptibility of four different honey bee species to *Nosema ceranae*. Veterinary Parasitology 193:260–265.

Chaimanee, V., N. Warrit, and P. Chantawannakul. 2010. Infections of *Nosema ceranae* in four different honeybee species. Journal of Invertebrate Pathology 105:207–210.

Chandramathi, S., K. Suresh, Z. B. Anita, and U. R. Kuppusamy. 2012. Infections

of *Blastocystis hominis* and microsporidia in cancer patients: Are they opportunistic? Transactions of the Royal Society of Tropical Medicine and Hygiene 106:267–269.

Chauzat, M.-P., J.-P. Faucon, A.-C. Martel, J. Lachaize, N. Cougoule, and M. Aubert. 2006. A survey of pesticide residues in pollen loads collected by honey bees in France. Journal of Economic Entomology 99:253–62.

Chen, C. Y., and T. R. Graham. 1998. An arf1Delta synthetic lethal screen identifies a new clathrin heavy chain conditional allele that perturbs vacuolar protein transport in *Saccharomyces cerevisiae*. Genetics 150:577–89.

Chen, Y., and J. D. Evans. 2007. Historical presence of Israeli Acute Paralysis Virus in the United States. American Bee Journal:29–31.

Chen, Y., J. D. Evans, I. B. Smith, and J. S. Pettis. 2008. *Nosema ceranae* is a long-present and wide-spread microsporidian infection of the European honey bee (*Apis mellifera*) in the United States. Journal of Invertebrate Pathology 97:186–188.

Chen, Y. P., J. D. Evans, C. Murphy, R. Gutell, M. Zuker, D. Gundensen-Rindal, and J. S. Pettis. 2009. Morphological, molecular, and phylogenetic characterization of *Nosema ceranae*, a microsporidian parasite isolated from the European honey bee, *Apis mellifera*. Journal of Eukaryotic Microbiology 56:142–147.

Chen, Y. P., J. S. Pettis, M. Corona, W. P. Chen, C. J. Li, M. Spivak, P. K. Visscher, G. DeGrandi-Hoffman, H. Boncristiani, Y. Zhao, D. VanEngelsdorp, K. Delaplane, L. Solter, F. Drummond, M. Kramer, W. I. Lipkin, G. Palacios, M. C. Hamilton, B. Smith, S. K. Huang, H. Q. Zheng, J. L. Li, X. Zhang, A. F. Zhou, L. Y. Wu, J. Z. Zhou, M. L. Lee, E. W. Teixeira, Z. G. Li, and J. D. Evans. 2014. Israeli Acute Paralysis Virus: Epidemiology, Pathogenesis and Implications for Honey Bee Health. PLoS Pathogens 10.

Chen, Y. P., J. S. Pettis, Y. Zhao, X. Liu, L. J. Tallon, L. D. Sadzewicz, R. Li, H. Zheng, S. Huang, X. Zhang, M. C. Hamilton, S. F. Pernal, A. P. Melathopoulos, X. Yan, and J. D. Evans. 2013. Genome sequencing and comparative genomics of honey bee microsporidia, *Nosema apis* reveal novel insights into host-parasite interactions. BMC Genomics 14:451.

Chen, Y. P., and R. Siede. 2007. Honey bee viruses. Advances in Virus Research 70:33–80.

Cherry, J. M., E. L. Hong, C. Amundsen, R. Balakrishnan, G. Binkley, E. T. Chan, K. R. Christie, M. C. Costanzo, S. S. Dwight, S. R. Engel, D. G. Fisk, J. E. Hirschman, B. C. Hitz, K. Karra, C. J. Krieger, S. R. Miyasato, R. S. Nash, J. Park, M. S. Skrzypek, M. Simison, S. Weng, and E. D. Wong. 2012. *Saccharomyces* Genome Database: the genomics resource of budding yeast. Nucleic Acids Research 40:D700–5.

Cooke, B. M., K. Lingelbach, L. H. Bannister, and L. Tilley. 2004. Protein trafficking in *Plasmodium falciparum*-infected red blood cells. Trends in Parasitology 20:581–589.

Copley, T. R., H. Chen, P. Giovenazzo, E. Houle, and S. H. Jabaji. 2012. Prevalence and seasonality of *Nosema* species in Québec honey bees. The Canadian Entomologist 144:577–588.

Cornman, R. S., Y. P. Chen, M. C. Schatz, C. Street, Y. Zhao, B. Desany, M. Egholm, S. Hutchison, J. S. Pettis, W. I. Lipkin, and J. D. Evans. 2009. Genomic analyses of the microsporidian *Nosema ceranae*, an emergent pathogen of honey bees. PLoS Pathogens 5.

Corradi, N., L. Burri, and P. J. Keeling. 2008. mRNA processing in *Antonospora locustae* spores. Molecular Genetics and Genomics 280:565–574.

Corradi, N., K. L. Haag, J.-F. Pombert, D. Ebert, and P. J. Keeling. 2009. Draft genome sequence of the *Daphnia* pathogen *Octosporea bayeri*: insights into the gene content of a large microsporidian genome and a model for host-parasite interactions. Genome Biology 10:R106.

Corradi, N., J.-F. Pombert, L. Farinelli, E. S. Didier, and P. J. Keeling. 2010. The complete sequence of the smallest known nuclear genome from the microsporidian *Encephalitozoon intestinalis*. Nature Communications 1:77.

Corradi, N., and C. H. Slamovits. 2011. The intriguing nature of microsporidian genomes. Briefings in Functional Genomics 10:115–124.

Costa, S. F., and L. M. Weiss. 2000. Drug treatment of microsporidiosis. Drug Resistance Updates 3:384–399.

Costanzo, M., A. Baryshnikova, J. Bellay, Y. Kim, E. D. Spear, C. S. Sevier, H. Ding, J. L. Y. Koh, K. Toufighi, S. Mostafavi, J. Prinz, R. P. St Onge, B. VanderSluis, T. Makhnevych, F. J. Vizeacoumar, S. Alizadeh, S. Bahr, R. L. Brost, Y. Chen, M. Cokol, R. Deshpande, Z. Li, Z.-Y. Lin, W. Liang, M. Marback, J. Paw, B.-J. San Luis, E. Shuteriqi, A. H. Y. Tong, N. van Dyk, I. M. Wallace, J. A. Whitney, M. T. Weirauch, G. Zhong, H. Zhu, W. a Houry, M. Brudno, S. Ragibizadeh, B. Papp, C. Pál, F. P. Roth, G. Giaever, C. Nislow, O. G. Troyanskaya, H. Bussey, G. D. Bader, A.-C. Gingras, Q. D. Morris, P. M. Kim, C. A. Kaiser, C. L. Myers, B. J. Andrews, and C. Boone. 2010. The genetic landscape of a cell. Science (New York, N.Y.) 327:425–431.

Cox-Foster, D. L., S. Conlan, E. C. Holmes, G. Palacios, J. D. Evans, N. A. Moran, P.-L. Quan, T. Briese, M. Hornig, D. M. Geiser, V. Martinson, D. vanEngelsdorp, A. L. Kalkstein, A. Drysdale, J. Hui, J. Zhai, L. Cui, S. K. Hutchison, J. F. Simons, M. Egholm, J. S. Pettis, and W. I. Lipkin. 2007. A metagenomic survey of microbes in honey bee colony collapse disorder. Science (New York, N.Y.) 318:283–287.

Cresswell, J. E. 2011. A meta-analysis of experiments testing the effects of a

neonicotinoid insecticide (imidacloprid) on honey bees. Ecotoxicology 20:149–157.

Cresswell, J. E., C. J. Page, M. B. Uygun, M. Holmbergh, Y. Li, J. G. Wheeler, I. Laycock, C. J. Pook, N. H. de Ibarra, N. Smirnoff, and C. R. Tyler. 2012. Differential sensitivity of honey bees and bumble bees to a dietary insecticide (imidacloprid). Zoology 115:365–371.

Cuomo, C. A., C. A. Desjardins, M. A. Bakowski, J. Goldberg, A. T. Ma, J. J. Becnel, E. S. Didier, L. Fan, D. I. Heiman, J. Z. Levin, S. Young, Q. Zeng, and E. R. Troemel. 2012. Microsporidian genome analysis reveals evolutionary strategies for obligate intracellular growth. Genome Research 22:2478–2488.

Curak, J., J. Rohde, and I. Stagljar. 2009. Yeast as a tool to study bacterial effectors. Current Opinion in Microbiology 12:18–23.

Dacks, J. B., and M. C. Field. 2007. Evolution of the eukaryotic membrane-trafficking system: origin, tempo and mode. Journal of Cell Science 120:2977–2985.

DEFRA. 2013. An assessment of key evidence about Neonicotinoids and bees.

Delbac, F., I. Peuvel, G. Metenier, E. Peyretaillade, and C. P. Vivares. 2001. Microsporidian invasion apparatus: Identification of a novel polar tube protein and evidence for clustering of ptp1 and ptp2 genes in three *Encephalitozoon* species. Infection and Immunity 69:1016–1024.

Delbac, F., P. Peyret, G. Méténier, D. David, A. Danchin, and C. P. Vivarès. 1998. On proteins of the microsporidian invasive apparatus: Complete sequence of a polar tube protein of *Encephalitozoon cuniculi*. Molecular Microbiology 29:825–834.

Desjardins, C. A., N. D. Sanscrainte, J. M. Goldberg, D. Heiman, S. Young, Q. Zeng, H. D. Madhani, J. J. Becnel, and C. A. Cuomo. 2015. Contrasting host–pathogen interactions and genome evolution in two generalist and specialist microsporidian pathogens of mosquitoes. Nature Communications 6:7121.

Deslandes, L., and S. Rivas. 2012. Catch me if you can: Bacterial effectors and plant targets. Trends in Plant Science 17:644–655.

Desneux, N., A. Decourtye, and J.-M. Delpuech. 2007. The sublethal effects of pesticides on beneficial arthropods. Annual review of entomology 52:81–106.

Dhaoui, M., F. Auchère, P.-L. Blaiseau, E. Lesuisse, A. Landoulsi, J.-M. Camadro, R. Haguenauer-Tsapis, and N. Belgareh-Touzé. 2011. Gex1 is a yeast glutathione exchanger that interferes with pH and redox homeostasis. Molecular biology of the cell 22:2054–67.

Didier, E. S., C. R. Vossbrinck, M. D. Baker, L. B. Rogers, D. C. Bertucci, and J. A. Shadduck. 1995. Identification and characterization of three *Encephalitozoon cuniculi* strains. Parasitology 111:411–421.

Didier, E. S., and L. M. Weiss. 2006. Microsporidiosis: current status. Current Opinion in Infectious Diseases 19:485–492.

Didier, E. S., and L. M. Weiss. 2011. Microsporidiosis. Current Opinion in Infectious Diseases 24:490–495.

Dixon, S. J., M. Costanzo, A. Baryshnikova, B. Andrews, and C. Boone. 2009. Systematic mapping of genetic interaction networks. Annual Review of Genetics 43:601–625.

Dolgikh, V. V, and P. B. Semenov. 2003. Trehalose catabolism in microsporidia *Nosema grylli* spores. Parazitologiia 37:333–42.

Dolgikh, V. V, I. V Senderskiĭ, O. A. Pavlova, and G. V Beznusenko. 2010. Analysis of expression of vesicular transport genes in avesicular cells of the microsporidium *Paranosema (Antonospora) locustae*. Tsitologiia 52:5–11.

Dolgikh, V. V, I. V. Senderskiy, O. a. Pavlova, A. M. Naumov, and G. V. Beznoussenko. 2011. Immunolocalization of an alternative respiratory chain in *Antonospora (Paranosema) locustae* spores: Mitosomes retain their role in microsporidial energy metabolism. Eukaryotic Cell 10:588–593.

Doublet, V., M. Labarussias, J. R. de Miranda, R. F. A. Moritz, and R. J. Paxton. 2014. Bees under stress: Sublethal doses of a neonicotinoid pesticide and pathogens interact to elevate honey bee mortality across the life cycle. Environmental Microbiology.

Down, R. E., H. A. Bell, G. Bryning, A. E. Kirkbride-Smith, J. P. Edwards, and R. J. Weaver. 2008. Infection by the microsporidium *Vairimorpha necatrix* (Microspora: Microsporidia) elevates juvenile hormone titres in larvae of the tomato moth, *Lacanobia oleracea* (Lepidoptera: Noctuidae). Journal of Invertebrate Pathology 97:223–229.

Duay, P., D. De Jong, and W. Engels. 2003. Weight loss in drone pupae (*Apis mellifera*) multiply infested by *Varroa destructor* mites. Apidologie 34:61–65.

Dunn, A. M., and J. E. Smith. 2001. Microsporidian life cycles and diversity: The relationship between virulence and transmission. Microbes and Infection 3:381–388.

Dussaubat, C., A. Maisonnasse, C. Alaux, S. Tchamitchan, J. L. Brunet, E. Plettner, L. P. Belzunces, and Y. Le Conte. 2010. *Nosema* spp. Infection Alters pheromone production in honey bees (*Apis mellifera*). Journal of Chemical Ecology 36:522–525.

Edgar, R. C. 2004. MUSCLE: Multiple sequence alignment with high accuracy and high throughput. Nucleic Acids Research 32:1792–1797.

Edlind, T. D., J. Li, G. S. Visvesvara, M. H. Vodkin, G. L. McLaughlin, and S. K. Katiyar. 1996. Phylogenetic Analysis of β-Tubulin Sequences from Amitochondrial Protozoa. Molecular Phylogenetics and Evolution Elsevier

5:359–367.

Eiri, D. M., and J. C. Nieh. 2012. A nicotinic acetylcholine receptor agonist affects honey bee sucrose responsiveness and decreases waggle dancing. Journal of Experimental Biology 215:2022–2029.

Ellis, J. G., M. Rafiqi, P. Gan, A. Chakrabarti, and P. N. Dodds. 2009. Recent progress in discovery and functional analysis of effector proteins of fungal and oomycete plant pathogens. Current Opinion in Plant Biology 12:399–405.

Ellis, J., and P. Munn. 2005. The worldwide health status of honey bees. Bee World 86:88–101.

Emanuelsson, O., S. Brunak, G. von Heijne, and H. Nielsen. 2007. Locating proteins in the cell using TargetP, SignalP and related tools. Nature protocols 2:953–71.

European Food Security Authority. 2013. Conclusion on the peer review of the pesticide risk assessment for bees for the active substance clothianidin. EFSA Journal 11:3066.

van Engelsdorp, D., J. Hayes, R. M. Underwood, and J. Pettis. 2008. A survey of honey bee colony losses in the U.S., Fall 2007 to Spring 2008. PLoS ONE 3:8–13.

Feltham, H., K. Park, and D. Goulson. 2014. Field realistic doses of pesticide imidacloprid reduce bumblebee pollen foraging efficiency. Ecotoxicology 23:317–323.

Findley, A. M., E. H. Weidner, K. R. Carman, Z. Xu, and J. S. Godbar. 2005. Role of the posterior vacuole in *Spraguea lophii* (Microsporidia) spore hatching. Folia Parasitologica 52:111–7.

Finley, J., S. Camazine, and M. Frazier. 1996. The epidemic of honey bee colony losses during the 1995-1996 season. American Bee Journal 136:805–808.

Finn, R. D., A. Bateman, J. Clements, P. Coggill, R. Y. Eberhardt, S. R. Eddy, A. Heger, K. Hetherington, L. Holm, J. Mistry, E. L. L. Sonnhammer, J. Tate, and M. Punta. 2014. Pfam: The protein families database. Nucleic Acids Research 42:222–230.

Forister, M. L., A. C. McCall, N. J. Sanders, J. a Fordyce, J. H. Thorne, J. O'Brien, D. P. Waetjen, and A. M. Shapiro. 2010. Compounded effects of climate change and habitat alteration shift patterns of butterfly diversity. Proceedings of the National Academy of Sciences of the United States of America 107:2088–2092.

Forsgren, E. 2010. European foulbrood in honey bees. Journal of Invertebrate Pathology 103:S5–S9.

Forsgren, E., and I. Fries. 2010. Comparative virulence of *Nosema ceranae* and

Nosema apis in individual European honey bees. Veterinary Parasitology 170:212–217.

Forsgren, E., A. C. Lundhagen, A. Imdorf, and I. Fries. 2005. Distribution of *Melissococcus plutonius* in honeybee colonies with and without symptoms of European foulbrood. Microbial Ecology 50:369–374.

Franzen, C. 2004. Microsporidia: How can they invade other cells? Trends in Parasitology 20:275–279.

Franzen, C., and A. Müller. 1999. Molecular Techniques for Detection, Species Differentiation, and Phylogenetic Analysis of Microsporidia. Clinical Microbiology Reviews 12:243–285.

Frazier, M., C. Mullin, J. Frazier, and S. Ashcraft. 2008. What Have Pesticides Got to Do with It? American Bee Journal 148:521–523.

Fricke, W. M., and S. J. Brill. 2003. Slx1-Slx4 is a second structure-specific endonuclease functionally redundant with Sgs1-Top3. Genes & Development 17:1768–78.

Fries, I. 1993. *Nosema-Apis* - A Parasite In The Honey-Bee Colony. Bee World 74:5–19.

Fries, I. 1997. Protozoa. Pages 59–76 *in* R. A. Morse and K. Flottum, editors. Honey Bee Pests, Predators and Diseases. Third Edition. A. I. Root Company, Medina, Ohio, US.

Fries, I., G. Ekbohm, and E. Villumstad. 1984. *Nosema Apis*, Sampling Techniques and Honey Yield. Journal of Apicultural Research 23:102–105.

Fries, I., F. Feng, A. da Silva, S. B. Slemenda, and N. J. Pieniazek. 1996. *Nosema ceranae* n. sp. (Microspora, Nosematidae), morphological and molecular characterization of a microsporidian parasite of the Asian honey bee *Apis cerana* (Hymenoptera, Apidae). European Journal of Protistology 32:356–365.

Fries, I., A. Imdorf, and P. Rosenkranz. 2006a. Survival of mite infested (*Varroa destructor*) honey bee (*Apis mellifera*) colonies in a Nordic climate. Apidologie 37:564–570.

Fries, I., R. Martin, A. Meana, P. Garcia-Palencia, and M. Higes. 2006b. Natural infections of *Nosema ceranae* in European honey bees. Journal of Apicultural Research 45:230–233.

Frixione, E., L. Ruiz, J. Cerbón, and A. H. Undeen. 1997. Germination of *Nosema algerae* (Microspora) spores: conditional inhibition by D2O, ethanol and Hg2+ suggests dependence of water influxupon membrane hydration and specific transmembrane pathways. The Journal of Eukaryotic Microbiology 44:109–16.

Frixione, E., L., L. Ruiz, M. Santillan, L. V. de Vargas, J. M. Tejero, and A. H. Undeen. 1992. Dynamics of polar filament discharge and sporoplasm

expulsion by microsporidian spores. Cell Motility and the Cytoskeleton 22:38–50.

Fürst, M. A, D. P. McMahon, J. L. Osborne, R. J. Paxton, and M. J. F. Brown. 2014. Disease associations between honeybees and bumblebees as a threat to wild pollinators. Nature 506:364–6.

Gallai, N., J. M. Salles, J. Settele, and B. E. Vaissière. 2009. Economic valuation of the vulnerability of world agriculture confronted with pollinator decline. Ecological Economics 68:810–821.

Garedew, A., E. Schmolz, and I. Lamprecht. 2004. The energy and nutritional demand of the parasitic life of the mite *Varroa destructor*. Apidologie 35:419–430.

Gauthier, L., D. Tentcheva, M. Tournaire, G. Laurent, T. Diana, T. Magali, D. Benjamin, C. François, M. E. C, and B. Max. 2007. Viral load estimation in asymptomatic honey bee colonies using the quantitative RT-PCR technique. Apidologie 38:426–435.

Genersch, E. 2010a. Honey bee pathology: Current threats to honey bees and beekeeping. Applied Microbiology and Biotechnology 87:87–97.

Genersch, E. 2010b. American Foulbrood in honeybees and its causative agent, *Paenibacillus larvae*. Journal of Invertebrate Pathology 103:S10–S19.

Genersch, E., and M. Aubert. 2010. Emerging and re-emerging viruses of the honey bee (*Apis mellifera* L.). Veterinary Research 41.

Genersch, E., E. Forsgren, J. Pentikäinen, A. Ashiralieva, S. Rauch, J. Kilwinski, and I. Fries. 2006. Reclassification of *Paenibacillus larvae* subsp. *pulvifaciens* and *Paenibacillus larvae* subsp. *larvae* as *Paenibacillus larvae* without subspecies differentiation. International Journal of Systematic and Evolutionary Microbiology 56:501–511.

Genersch, E., W. Von Der Ohe, H. Kaatz, a Schroeder, C. Otten, R. Buchler, S. Berg, W. Ritter, W. Muhlen, S. Gisder, M. Meixner, G. Liebig, and P. Rosenkranz. 2010. The German bee monitoring project: A long term study to understand periodically high winter losses of honey bee colonies. Apidologie 41:332–352.

Ghosh, K., and L. M. Weiss. 2012. T cell response and persistence of the microsporidia. FEMS Microbiology Reviews 36:748–760.

Giaever, G., A. M. Chu, L. Ni, C. Connelly, L. Riles, S. Véronneau, S. Dow, A. Lucau-Danila, K. Anderson, B. André, A. P. Arkin, A. Astromoff, M. El-Bakkoury, R. Bangham, R. Benito, S. Brachat, S. Campanaro, M. Curtiss, K. Davis, A. Deutschbauer, K.-D. Entian, P. Flaherty, F. Foury, D. J. Garfinkel, M. Gerstein, D. Gotte, U. Güldener, J. H. Hegemann, S. Hempel, Z. Herman, D. F. Jaramillo, D. E. Kelly, S. L. Kelly, P. Kötter, D. LaBonte, D. C. Lamb, N.

Lan, H. Liang, H. Liao, L. Liu, C. Luo, M. Lussier, R. Mao, P. Menard, S. L. Ooi, J. L. Revuelta, C. J. Roberts, M. Rose, P. Ross-Macdonald, B. Scherens, G. Schimmack, B. Shafer, D. D. Shoemaker, S. Sookhai-Mahadeo, R. K. Storms, J. N. Strathern, G. Valle, M. Voet, G. Volckaert, C. Wang, T. R. Ward, J. Wilhelmy, E. A. Winzeler, Y. Yang, G. Yen, E. Youngman, K. Yu, H. Bussey, J. D. Boeke, M. Snyder, P. Philippsen, R. W. Davis, and M. Johnston. 2002. Functional profiling of the *Saccharomyces cerevisiae* genome. Nature 418:387–91.

Giersch, T., T. Berg, F. Galea, and M. Hornitzky. 2009. *Nosema ceranae* infects honey bees (*Apis mellifera*) and contaminates honey in Australia. Apidologie 40:117–123.

Gill, R. J., O. Ramos-Rodriguez, and N. E. Raine. 2012. Combined pesticide exposure severely affects individual- and colony-level traits in bees. Nature 490:105–108.

Gilliam, M. 2000. Infectivity and Survival of the Chalkbrood Pathogen, *Ascosphaera apis*. Apidologie 17:93–100.

Giraldo, M. C., Y. F. Dagdas, Y. K. Gupta, T. A. Mentlak, M. Yi, A. L. Martinez-Rocha, H. Saitoh, R. Terauchi, N. J. Talbot, and B. Valent. 2013. Two distinct secretion systems facilitate tissue invasion by the rice blast fungus *Magnaporthe oryzae*. Nature communications 4:1996.

Giraldo, M. C., and B. Valent. 2013. Filamentous plant pathogen effectors in action. Nature Reviews. Microbiology 11:800–14.

Giray, T., M. Kence, D. Oskay, M. Döke, and A. Kence. 2010. Scientific note: colony losses survey in Turkey and causes of bee deaths. Apidologie 41:451–453.

Gisder, S., K. Hedtke, N. Möckel, M. C. Frielitz, A. Linde, and E. Genersch. 2010. Five-year cohort study of *Nosema* spp. in Germany: Does climate shape virulence and assertiveness of *Nosema ceranae*? Applied and Environmental Microbiology 76:3032–3038.

Godfray, H. C. J., T. Blacquière, L. M. Field, R. S. Hails, G. Petrokofsky, S. G. Potts, N. E. Raine, A. J. Vanbergen, and A. R. McLean. 2014. A restatement of the natural science evidence base concerning neonicotinoid insecticides and insect pollinators. Proceedings of the Royal Society B: Biological Sciences 281:20140558.

Goulson, D. 2013. An overview of the environmental risks posed by neonicotinoid insecticides. Journal of Applied Ecology 50:977–987.

Goulson, D., G. C. Lye, and B. Darvill. 2008. Decline and conservation of bumble bees. Annual Review of Entomology 53:191–208.

Goulson, D., E. Nicholls, C. Botias, and E. L. Rotheray. 2015. Bee declines driven by combined stress from parasites, pesticides, and lack of flowers. Science.

Gravitz, L. 2015. Nested instincts. Nature 521:60–61.

Graystock, P., K. Yates, B. Darvill, D. Goulson, and W. O. H. Hughes. 2013. Emerging dangers: Deadly effects of an emergent parasite in a new pollinator host. Journal of Invertebrate Pathology 114:114–119.

Grixti, J. C., L. T. Wong, S. A. Cameron, and C. Favret. 2009. Decline of bumble bees (*Bombus*) in the North American Midwest. Biological Conservation 142:75–84.

Guarente, L. 1993. Synthetic enhancement in gene interaction: a genetic tool come of age. Trends in Genetics 9:362–6.

Guzmán-Novoa, E., L. Eccles, Y. Calvete, J. Mcgowan, P. G. Kelly, and A. Correa-Benítez. 2010. *Varroa destructor* is the main culprit for the death and reduced populations of overwintered honey bee (*Apis mellifera*) colonies in Ontario, Canada. Apidologie 41:443–450.

Haag, K. L., J. I. R. Larsson, D. Refardt, and D. Ebert. 2011. Cytological and molecular description of *Hamiltosporidium tvaerminnensis* gen. et sp. nov., a microsporidian parasite of *Daphnia magna*, and establishment of *Hamiltosporidium magnivora* comb. nov. Parasitology 138:447–462.

Haldar, K., S. Kamoun, N. L. Hiller, S. Bhattacharje, and C. van Ooij. 2006. Common infection strategies of pathogenic eukaryotes. Nature Reviews. Microbiology 4:922–931.

Hallmann, C. A., R. P. B. Foppen, C. A. M. Van Turnhout, H. De Kroon, and E. Jongejans. 2014. Declines in insectivorous birds are associated with high neonicotinoid concentrations. Nature 511:341–343.

Harris, J. W., J. R. Harbo, J. D. Villa, and R. G. Danka. 2003. Variable population growth of *varroa destructor* (mesostigmata: varroidae) in colonies of honey bees (hymenoptera: apidae) during a 10-year period. Environmental Entomology 32(6):1305–1312.

Harrison, J. F., and J. H. Fewell. 2002. Environmental and genetic influences on flight metabolic rate in the honey bee, *Apis mellifera*. Comparative Biochemistry and Physiology Part A 133:323–333.

Hartman, J. L., B. Garvik, and L. Hartwell. 2001. Principles for the buffering of genetic variation. Science (New York, N.Y.) 291:1001–4.

Hayman, J. R., S. F. Hayes, J. Amon, and T. E. Nash. 2001. Developmental expression of two spore wall proteins during maturation of the microsporidian *Encephalitozoon intestinalis*. Infection and Immunity 69:7057–7066.

Hedtke, K., P. M. Jensen, A. B. Jensen, and E. Genersch. 2011. Evidence for emerging parasites and pathogens influencing outbreaks of stress-related diseases like chalkbrood. Journal of Invertebrate Pathology 108:167–173.

Heinz, E., T. A. Williams, S. Nakjang, C. J. Noël, D. C. Swan, A. V. Goldberg, S. R. Harris, T. Weinmaier, S. Markert, D. Becher, J. Bernhardt, T. Dagan, C. Hacker, J. M. Lucocq, T. Schweder, T. Rattei, N. Hall, R. P. Hirt, and T. M. Embley. 2012. The Genome of the Obligate Intracellular Parasite *Trachipleistophora hominis*: New Insights into Microsporidian Genome Dynamics and Reductive Evolution. PLoS Pathogens 8.

Henn, M. W., and L. F. Solter. 2000. Food utilization values of gypsy moth *Lymantria dispar* (Lepidoptera: Lymantriidae) larvae infected with the microsporidium *Vairimorpha* sp. (Microsporidia: Burenellidae). Journal of Invertebrate Pathology 76:263–269.

Henry, M., M. Béguin, F. Requier, O. Rollin, J.-F. Odoux, P. Aupinel, J. Aptel, S. Tchamitchian, and A. Decourtye. 2012. A common pesticide decreases foraging success and survival in honey bees. Science (New York, N.Y.) 336:348–50.

Herbert, L. H., D. E. Vazquez, A. Arenas, and W. M. Farina. 2014. Effects of field-realistic doses of glyphosate on honeybee appetitive behaviour. The Journal of Experimental Biology:3457–3464.

Herth, W., and E. Schnepf. 1980. The fluorochrome, calcofluor white, binds oriented to structural polysaccharide fibrils. Protoplasma 105:129–133.

Higes, M., R. Martín, and A. Meana. 2006. *Nosema ceranae*, a new microsporidian parasite in honeybees in Europe. Journal of Invertebrate Pathology 92:93–95.

Higes, M., R. Martín-Hernández, C. Botías, E. G. Bailón, A. V. González-Porto, L. Barrios, M. J. Del Nozal, J. L. Bernal, J. J. Jiménez, P. G. Palencia, and A. Meana. 2008. How natural infection by *Nosema ceranae* causes honeybee colony collapse. Environmental Microbiology 10:2659–2669.

Higes, M., R. Martín-Hernández, E. Garrido-Bailón, A. V. González-Porto, P. García-Palencia, A. Meana, M. J. del Nozal, R. Mayo, and J. L. Bernal. 2009. Honeybee colony collapse due to *Nosema ceranae* in professional apiaries. Environmental Microbiology Reports 1:110–113.

Higes, M., R. Martín-Hernández, and A. Meana. 2010. *Nosema ceranae* in Europe: an emergent type C nosemosis. Apidologie 41:375–392.

Higes, M., A. Meana, C. Bartolomé, C. Botías, and R. Martín-Hernández. 2013. *Nosema ceranae* (Microsporidia), a controversial 21st century honey bee pathogen. Environmental Microbiology Reports 5:17–29.

Higes, M., M. J. Nozal, A. Alvaro, L. Barrios, A. Meana, R. Martín-Hernández, J. L. Bernal, and J. Bernal. 2011. The stability and effectiveness of fumagillin in controlling *Nosema ceranae* (Microsporidia) infection in honey bees (*Apis mellifera*) under laboratory and field conditions. Apidologie 42:364–377.

Highfield, A. C., A. El Nagar, L. C. M. Mackinder, L. M. L. J. Noël, M. J. Hall, S. J. Martin, and D. C. Schroeder. 2009. Deformed wing virus implicated in

overwintering honeybee colony losses. Applied and Environmental Microbiology 75:7212–7220.

Hiltunen, J. K., A. M. Mursula, H. Rottensteiner, R. K. Wierenga, A. J. Kastaniotis, and A. Gurvitz. 2003. The biochemistry of peroxisomal beta-oxidation in the yeast *Saccharomyces cerevisiae*. FEMS microbiology reviews 27:35–64.

Hoffman, C. S., and F. Winston. 1987. A ten-minute DNA preparation from yeast efficiently releases autonomous plasmids for transformation of *Escherichia coli*. Gene 57:267–272.

Huang, W. F., J. H. Jiang, Y. W. Chen, and C. H. Wang. 2007. A *Nosema ceranae* isolate from the honeybee *Apis mellifera*. Apidologie 38:30–37.

Huang, W. F., L. F. Solter, P. M. Yau, and B. S. Imai. 2013. *Nosema ceranae* Escapes Fumagillin Control in Honey Bees. PLoS Pathogens 9.

Huang, Z. Y., and G. E. Robinson. 1996. Regulation of honey bee division of labor by colony age demography. Behavioral Ecology and Sociobiology 39:147–158.

Huh, W-K., J. V. Falvo, L. C. Gerke, A. S. Carroll, R. W. Howson, J. S. Weissman and E. K. O'Shea. 2003. Global analysis of protein localization in budding yeast. Nature 425:686–91.

Hunter, C. A., and L. D. Sibley. 2012. Modulation of innate immunity by *Toxoplasma gondii* virulence effectors. Nature Reviews Microbiology 10:766–778.

Ironside, J. E., and J. Alexander. 2015. Microsporidian parasites feminise hosts without paramyxean co-infection: support for convergent evolution of parasitic feminisation. International Journal for Parasitology 45:427–433.

Ito, H., Y. Fukuda, and K. Murata. 1983. Transformation of intact yeast cells treated with alkali Cations. Journal of Bacteriology 153:166–168.

Izquierdo, F., J. A. Castro Hermida, S. Fenoy, M. Mezo, M. González-Warleta, and C. Del Aguila. 2011. Detection of microsporidia in drinking water, wastewater and recreational rivers. Water Research 45:4837–4843.

James, D., and M.-H. Pham-Delegue. 2002. Honey Bees: Estimating the Environmental Impact of Chemicals. Taylor & Francis, London.

James, T. Y., A. Pelin, L. Bonen, S. Ahrendt, D. Sain, N. Corradi, and J. E. Stajich. 2013. Shared Signatures of Parasitism and Phylogenomics Unite Cryptomycota and Microsporidia. Current Biology 23:1548–1553.

Jones, J. C., P. Helliwell, M. Beekman, R. Maleszka, and B. P. Oldroyd. 2005. The effects of rearing temperature on developmental stability and learning and memory in the honey bee, *Apis mellifera*. Journal of Comparative Physiology A 191:1121–1129.

Jones, M. D. M., I. Forn, C. Gadelha, M. J. Egan, D. Bass, R. Massana, and T. A. Richards. 2011. Discovery of novel intermediate forms redefines the fungal tree of life. Nature 474:200–203.

de Jong, J., B. McCormack, N. Smirnoff, and N. Talbot. 1997. Glycerol generates turgor in rice blast. Nature 389:244.

Kämper, J., R. Kahmann, M. Bölker, L.-J. Ma, T. Brefort, B. J. Saville, F. Banuett, J. W. Kronstad, S. E. Gold, O. Müller, M. H. Perlin, H. A. B. Wösten, R. de Vries, J. Ruiz-Herrera, C. G. Reynaga-Peña, K. Snetselaar, M. McCann, J. Pérez-Martín, M. Feldbrügge, C. W. Basse, G. Steinberg, J. I. Ibeas, W. Holloman, P. Guzman, M. Farman, J. E. Stajich, R. Sentandreu, J. M. González-Prieto, J. C. Kennell, L. Molina, J. Schirawski, A. Mendoza-Mendoza, D. Greilinger, K. Münch, N. Rössel, M. Scherer, M. Vranes, O. Ladendorf, V. Vincon, U. Fuchs, B. Sandrock, S. Meng, E. C. H. Ho, M. J. Cahill, K. J. Boyce, J. Klose, S. J. Klosterman, H. J. Deelstra, L. Ortiz-Castellanos, W. Li, P. Sanchez-Alonso, P. H. Schreier, I. Häuser-Hahn, M. Vaupel, E. Koopmann, G. Friedrich, H. Voss, T. Schlüter, J. Margolis, D. Platt, C. Swimmer, A. Gnirke, F. Chen, V. Vysotskaia, G. Mannhaupt, U. Güldener, M. Münsterkötter, D. Haase, M. Oesterheld, H.-W. Mewes, E. W. Mauceli, D. DeCaprio, C. M. Wade, J. Butler, S. Young, D. B. Jaffe, S. Calvo, C. Nusbaum, J. Galagan, and B. W. Birren. 2006. Insights from the genome of the biotrophic fungal plant pathogen *Ustilago maydis*. Nature 444:97–101.

Karpov, S. A., K. V. Mikhailov, G. S. Mirzaeva, I. M. Mirabdullaev, K. A. Mamkaeva, N. N. Titova, and V. V. Aleoshin. 2013. Obligately phagotrophic aphelids turned out to branch with the earliest-diverging fungi. Protist 164:195–205.

Kasper, L. H., P. K. Brindle, C. A. Schnabel, C. E. Pritchard, M. L. Cleary, and J. M. van Deursen. 1999. CREB binding protein interacts with nucleoporin-specific FG repeats that activate transcription and mediate NUP98-HOXA9 oncogenicity. Molecular and cellular biology 19:764–776.

Katinka, M. D., S. Duprat, E. Cornillot, G. Méténier, F. Thomarat, G. Prensier, V. Barbe, E. Peyretaillade, P. Brottier, P. Wincker, F. Delbac, H. El Alaoui, P. Peyret, W. Saurin, M. Gouy, J. Weissenbach, and C. P. Vivarès. 2001. Genome sequence and gene compaction of the eukaryote parasite *Encephalitozoon cuniculi*. Nature 414:450–453.

Keeling, P. J., and W. F. Doolittle. 1996. Alpha-tubulin from early-diverging eukaryotic lineages and the evolution of the tubulin family. Molecular Biology and Evolution 13:1297–305.

Keeling, P. J., and N. M. Fast. 2002. Microsporidia: biology and evolution of highly reduced intracellular parasites. Annual Review of Microbiology 56:93–116.

Kelley, L. A., S. Mezulis, C. M. Yates, M. N. Wass, and M. J. E. Sternberg. 2015. The Phyre2 web portal for protein modeling , prediction and analysis. Nature Protocols 10:845–858.

Keohane, E. M., and L. M. Weiss. 1999. The Microsporidia and Microsporidiosis. (L. M. Weiss and M. Wittner, Eds.). American Society of Microbiology.

Kerr, A. R., and E. C. Schirmer. 2011. FG repeats facilitate integral protein trafficking to the inner nuclear membrane. Communicative & Integrative biology 4:557–9.

Kessler, H., A. Herm-Götz, S. Hegge, M. Rauch, D. Soldati-Favre, F. Frischknecht, and M. Meissner. 2008. Microneme protein 8--a new essential invasion factor in *Toxoplasma gondii*. Journal of Cell Science 121:947–956.

Kessler, S. C., E. J. Tiedeken, K. L. Simcock, S. Derveau, J. Mitchell, S. Softley, J. C. Stout, and G. A. Wright. 2015. Bees prefer foods containing neonicotinoid pesticides. Nature 521, 74–76.

Kicia, M., M. Wesolowska, K. Jakuszko, Z. Kopacz, B. Sak, D. Kvetonova, M. Krajewska, and M. Kva . 2014. Concurrent Infection of the Urinary Tract with *Encephalitozoon cuniculi* and *Enterocytozoon bieneusi* in a Renal Transplant Recipient. Journal of Clinical Microbiology 52:1780–1782.

Kielmanowicz, M. G., A. Inberg, I. M. Lerner, Y. Golani, N. Brown, C. L. Turner, G. J. R. Hayes, and J. M. Ballam. 2015. Prospective Large-Scale Field Study Generates Predictive Model Identifying Major Contributors to Colony Losses. PLOS Pathogens 11:e1004816.

Klee, J., A. M. Besana, E. Genersch, S. Gisder, A. Nanetti, D. Q. Tam, T. X. Chinh, F. Puerta, J. M. Ruz, P. Kryger, D. Message, F. Hatjina, S. Korpela, I. Fries, and R. J. Paxton. 2007. Widespread dispersal of the microsporidian *Nosema ceranae*, an emergent pathogen of the western honey bee, *Apis mellifera*. Journal of Invertebrate Pathology 96:1–10.

Klein, A.-M., B. E. Vaissière, J. H. Cane, I. Steffan-Dewenter, S. A. Cunningham, C. Kremen, and T. Tscharntke. 2007. Importance of pollinators in changing landscapes for world crops. Proceedings of The Royal Society B 274:303–313.

Kochansky, J., D. a Knox, M. F. Feldlaufer, and J. S. Pettis. 2001. Screening alternative antibiotics against and -resistant *Paenibacillus larvae*. Apidologie 32:215–222.

Koestler, T., and I. Ebersberger. 2011. Zygomycetes, microsporidia, and the evolutionary ancestry of sex determination. Genome Biology and Evolution 3:186–94.

Köhler, H.-R., and R. Triebskorn. 2013. Wildlife ecotoxicology of pesticides: can we track effects to the population level and beyond? Science (New York, N.Y.) 341:759–65.

Kohlwein, S. D., M. Veenhuis, and I. J. van der Klei. 2013. Lipid droplets and peroxisomes: key players in cellular lipid homeostasis or a matter of fat-store ’em up or burn 'em down. Genetics 193:1–50.

Korpela, S., A. Aarhus, I. Fries, and H. Hansen. 1993. *Varroa jacobsoni* Oud. in cold climates: population growth, winter mortality and influence on the survival of honey bee colonies. Journal of Apicultural Research 31:157–164.

Kosior, A., W. Celary, P. Olejniczak, J. Fijal, W. Król, W. Solarz, and P. Plonka. 2007. The decline of the bumble bees and cuckoo bees (Hymenoptera: Apidae: Bombini) of Western and Central Europe. Oryx 41:79.

Kramer, R. W., N. L. Slagowski, N. a. Eze, K. S. Giddings, M. F. Morrison, K. A. Siggers, M. N. Starnbach, and C. F. Lesser. 2007. Yeast functional genomic screens lead to identification of a role for a bacterial effector in innate immunity regulation. PLoS Pathogens 3:0179–0190.

Krogh, A., B. Larsson, G. von Heijne, and E. L. Sonnhammer. 2001. Predicting transmembrane protein topology with a hidden Markov model: application to complete genomes. Journal of Molecular Biology 305:567–580.

Kudo, R. 1918. Experiments on the Extrusion of Polar Filaments of Cnidosporidian Spores. The Journal of Parasitology 4:141–147.

Kumar, Y., J. Cocchiaro, and R. H. Valdivia. 2006. The Obligate Intracellular Pathogen *Chlamydia trachomatis* Targets Host Lipid Droplets. Current Biology 16:1646–1651.

Lalik, M. 2015. Characterisation of the partners of secreted *Nosema ceranae* proteins. Unpublished PhD Thesis. University of Exeter.

Larsson, R. 1986. Ultrastructure, funtion and classification of microsporidia. Progress in Protistology 1:325–390.

Laurino, D., a Manino, a Patetta, M. Ansaldi, and M. Porporato. 2010. Acute Oral Toxicity of Neonicotinoids on Different Honey Bee Strains. RediaGiornale Di Zoologia 93:99–102.

Laycock, I., K. M. Lenthall, A. T. Barratt, and J. E. Cresswell. 2012. Effects of imidacloprid, a neonicotinoid pesticide, on reproduction in worker bumble bees (*Bombus terrestris*). Ecotoxicology 21:1937–1945.

Lee, K. V., N. Steinhauer, K. Rennich, M. E. Wilson, D. R. Tarpy, D. M. Caron, R. Rose, K. S. Delaplane, K. Baylis, E. J. Lengerich, J. Pettis, J. a. Skinner, J. T. Wilkes, R. Sagili, and D. vanEngelsdorp. 2015. A national survey of managed honey bee 2013–2014 annual colony losses in the USA. Apidologie:292–305.

Lee, S. C., N. Corradi, S. Doan, F. S. Dietrich, P. J. Keeling, and J. Heitman. 2010. Evolution of the sex-related locus and genomic features shared in microsporidia and fungi. PloS ONE 5:e10539.

Li, Z., G. Pan, T. Li, W. Huang, J. Chen, L. Geng, D. Yang, L. Wang, and Z. Zhou. 2012. SWP5, a spore wall protein, interacts with polar tube proteins in the parasitic microsporidian *Nosema bombycis*. Eukaryotic Cell 11:229–237.

Lin, H., J. Sullivan, and Z. Huang. 2009. Mechanisms through which *Nosema apis* affects onset of foraging in worker honeybees (*Apis mellifera* L.). Proc. Workshop “Nosema disease: lack of knowledge and work standardization".

Liu, Y., G. Vidanes, Y. C. Lin, S. Mori, and W. Siede. 2000. Characterization of a *Saccharomyces cerevisiae* homologue of *Schizosaccharomyces pombe* Chk1 involved in DNA-damage-induced M-phase arrest. Molecular & general genetics 262:1132–46.

Lodesani, M., C. Costa, and M. Man. 2006. Limits of Chemotherapy In Beekeeping: Development Of Resistance And The Problem Of Residues. Bulletin of University of Agricultural Sciences and Veterinary Medicine Cluj-Napoca 6:1–7.

Lom, J., and J. Vavra. 1963. The mode of sporoplasm extrusion in microsporidian spores. Acta Protozoologica 1:81–92.

Lono, A. R., S. Kumar, and T. T. Chye. 2008. Incidence of microsporidia in cancer patients. Journal of Gastrointestinal Cancer 39:124–129.

Louie, R. J., J. Guo, J. W. Rodgers, R. White, N. Shah, S. Pagant, P. Kim, M. Livstone, K. Dolinski, B. A. McKinney, J. Hong, E. J. Sorscher, J. Bryan, E. A. Miller, and J. L. Hartman. 2012. A yeast phenomic model for the gene interaction network modulating CFTR-ΔF508 protein biogenesis. Genome Medicine 4:103.

Loukas, A., and R. M. Maizels. 2000. Helminth C-type lectins and host-parasite interactions. Parasitology Today 16:333–339.

Loureiro, J., and H. L. Ploegh. 2006. Antigen Presentation and the Ubiquitin-Proteasome System in Host-Pathogen Interactions. Advances in Immunology 92:225–305.

Maier, A. G., M. Rug, M. T. O’Neill, M. Brown, S. Chakravorty, T. Szestak, J. Chesson, Y. Wu, K. Hughes, R. L. Coppel, C. Newbold, J. G. Beeson, A. Craig, B. S. Crabb, and A. F. Cowman. 2008. Exported Proteins Required for Virulence and Rigidity of *Plasmodium falciparum*-Infected Human Erythrocytes. Cell 134:48–61.

Mancha, C. 1998. Mediterranean rock art (Spain). UNESCO No 874. Article 40.

Manley, R., M. Boots, and L. Wilfert. 2015. Emerging viral disease risk to pollinating insects: ecological, evolutionary and anthropogenic factors. Journal of Applied Ecology 52:331–340.

Maori, E., S. Lavi, R. Mozes-Koch, Y. Gantman, Y. Peretz, O. Edelbaum, E. Tanne, and I. Sela. 2007. Isolation and characterization of Israeli acute paralysis virus, a dicistrovirus affecting honeybees in Israel: Evidence for diversity due to intra- and inter-species recombination. Journal of General Virology 88:3428–3438.

Martens, S., and J. Howard. 2006. The interferon-inducible GTPases. Annual review of cell and developmental biology 22:559–589.

Martin, S., A. Hogarth, J. van Breda, and J. Perrett. 1998. A scientific note on *Varroa jacobsoni* Oudemans and the collapse of *Apis mellifera* L. colonies in the United Kingdom. Apidologie 29:369–370.

Martin, S. J., A. C. Highfield, L. Brettell, E. M. Villalobos, G. E. Budge, M. Powell, S. Nikaido, and D. C. Schroeder. 2012. Global Honey Bee Viral Landscape Altered by a Parasitic Mite. Science 336:1304–1306.

Martín-Hernández, R., A. Meana, L. Prieto, A. M. Salvador, E. Garrido-Bailón, and M. Higes. 2007. Outcome of colonization of *Apis mellifera* by *Nosema ceranae*. Applied and Environmental Microbiology 73:6331–6338.

Martoglio, B., and B. Dobberstein. 1998. Signal sequences: More than just greasy peptides. Trends in Cell Biology 8:410–415.

Matheson, A. 1995. World Bee Health Update. Bee World 76:31–39.

Mathis, A., R. Weber, and P. Deplazes. 2005. Zoonotic potential of the microsporidia. Clinical Microbiology Reviews 18:423–445.

Matreyek, K. A., S. S. Yücel, X. Li, and A. Engelman. 2013. Nucleoporin NUP153 Phenylalanine-Glycine Motifs Engage a Common Binding Pocket within the HIV-1 Capsid Protein to Mediate Lentiviral Infectivity. PLoS Pathogens 9.

Matsubayashi, H., T. Koike, I. Mikata, H. Takei, and S. Hagiwara. 1959. A case of *Encephalitozoon*-like body infection in man. A.M.A. archives of pathology 67:181–7.

Mattila, H. R., and G. W. Otis. 2007. Dwindling pollen resources trigger the transition to broodless populations of long-lived honeybees each autumn. Ecological Entomology 32:496–505.

Méténier, G., and C. P. Vivarès. 2001. Molecular characteristics and physiology of microsporidia. Microbes and Infection 3:407–415.

Milbrath, M. O., T. van Tran, W.-F. Huang, L. F. Solter, D. R. Tarpy, F. Lawrence, and Z. Y. Huang. 2015. Comparative virulence and competition between *Nosema apis* and *Nosema ceranae* in honey bees (*Apis mellifera*). Journal of Invertebrate Pathology 125:9–15.

Miller, L. H., D. I. Baruch, K. Marsh, and O. K. Doumbo. 2002. The pathogenic basis of malaria. Nature 415:673–679.

de Miranda, J. R., G. Cordoni, and G. Budge. 2010. The Acute bee paralysis virus-Kashmir bee virus-Israeli acute paralysis virus complex. Journal of Invertebrate Pathology 103:S30–S47.

de Miranda, J. R., and I. Fries. 2008. Venereal and vertical transmission of deformed wing virus in honeybees (*Apis mellifera* L.). Journal of Invertebrate

Pathology 98:184–189.

Mironov, A. A., V. V Banin, I. S. Sesorova, V. V Dolgikh, A. Luini, and G. V Beznoussenko. 2007. Evolution of the endoplasmic reticulum and the Golgi complex. Advances in Experimental Medicine and Biology 607:61–72.

Miyagi, T., C. Y. S. Peng, R. Y. Chuang, E. C. Mussen, M. S. Spivak, and R. H. Doi. 2000. Verification of Oxytetracycline-Resistant American Foulbrood Pathogen *Paenibacillus larvae* in the United States. Journal of Invertebrate Pathology:95–96.

Mommaerts, V., S. Reynders, J. Boulet, L. Besard, G. Sterk, and G. Smagghe. 2010. Risk assessment for side-effects of neonicotinoids against bumblebees with and without impairing foraging behavior. Ecotoxicology 19:207–215.

Morales-Johansson, H., P. Jenoe, F. T. Cooke, and M. N. Hall. 2004. Negative regulation of phosphatidylinositol 4,5-bisphosphate levels by the INP51-associated proteins TAX4 and IRS4. The Journal of Biological Chemistry 279:39604–10.

Moretto, M. M., D. I. Harrow, and I. A. Khan. 2015. Effector CD8 T cell immunity in microsporidial infection: a lone defense mechanism. Seminars in Immunopathology 37:281–287.

Morgan, W., and S. Kamoun. 2007. RXLR effectors of plant pathogenic oomycetes. Current Opinion in Microbiology 10:332–338.

Mullen, J. R., V. Kaliraman, S. S. Ibrahim, and S. J. Brill. 2001. Requirement for three novel protein complexes in the absence of the Sgs1 DNA helicase in *Saccharomyces cerevisiae*. Genetics 157:103–18.

Mullin, C. A., M. Frazier, J. L. Frazier, S. Ashcraft, R. Simonds, D. vanEngelsdorp, and J. S. Pettis. 2010. High Levels of Miticides and Agrochemicals in North American Apiaries: Implications for Honey Bee Health. PLoS ONE 5.

Mussen, E. 2000. Antibiotic-resistant American foulbrood. American Bee Journal 140:300–301.

Nageli, K. 1857. Uber die neue Krankheit der Seidenraupe und verwandte Organismen. Bot Z.

Nakjang, S., T. A. Williams, E. Heinz, A. K. Watson, P. G. Foster, K. M. Sendra, S. E. Heaps, R. P. Hirt, and T. Martin Embley. 2013. Reduction and expansion in microsporidian genome evolution: new insights from comparative genomics. Genome Biology and Evolution 5:2285–303.

Nathan, C., and M. U. Shiloh. 2000. Reactive oxygen and nitrogen intermediates in the relationship between mammalian hosts and microbial pathogens. Proceedings of the National Academy of Sciences of the United States of America 97:8841–8848.

Naug, D. 2009. Nutritional stress due to habitat loss may explain recent honeybee colony collapses. Biological Conservation 142:2369–2372.

Nickel, W. 2003. The mystery of nonclassical protein secretion: A current view on cargo proteins and potential export routes. European Journal of Biochemistry 270:2109–2119.

Nothwehr, S. F., and J. I. Gordon. 1989. Eukaryotic signal peptide structure/function relationships. Journal of Biological Chemistry 264:3979–3987.

Nothwehr, S. F., and J. I. Gordon. 1990. Structural features in the NH2-terminal region of a model eukaryotic signal peptide influence the site of its cleavage by signal peptidase. Journal of Biological Chemistry 265:17202–17208.

Novick, P., B. C. Osmond, and D. Botstein. 1989. Suppressors of yeast actin mutations. Genetics 121:659–74.

Office International des Epizooties (OIE) 2008. Nosemosis of Honey Bees. Manual of Standards for Diagnostic Test and Vaccines, Chapter 2.2.4.

Oldroyd, B. P. 1999. Coevolution while you wait: *Varroa jacobsoni*, a new parasite of western honeybees. Trends in Ecology and Evolution 14:312–315.

Oldroyd, B. P. 2007. What's killing American honey bees? PLoS Biology 5:1195–1199.

Oskay, D. 2007. Plasticity in flight muscle development and honey bee division of labor. University of Puerto Rico.

Palacios, G., J. Hui, P. L. Quan, a Kalkstein, K. S. Honkavuori, A. V Bussetti, S. Conlan, J. Evans, Y. P. Chen, D. vanEngelsdorp, H. Efrat, J. Pettis, D. Cox-Foster, E. C. Holmes, T. Briese, and W. I. Lipkin. 2008. Genetic analysis of Israel acute paralysis virus: distinct clusters are circulating in the United States. Journal of virology 82:6209–6217.

Paldi, N., E. Glick, M. Oliva, Y. Zilberberg, L. Aubin, J. Pettis, Y. Chen, and J. D. Evans. 2010. Effective gene silencing in a microsporidian parasite associated with honeybee (*Apis mellifera*) colony declines. Applied and Environmental Microbiology 76:5960–5964.

Pan, G., J. Xu, T. Li, Q. Xia, S.-L. Liu, G. Zhang, S. Li, C. Li, H. Liu, L. Yang, T. Liu, X. Zhang, Z. Wu, W. Fan, X. Dang, H. Xiang, M. Tao, Y. Li, J. Hu, Z. Li, L. Lin, J. Luo, L. Geng, L. Wang, M. Long, Y. Wan, N. He, Z. Zhang, C. Lu, P. J. Keeling, J. Wang, Z. Xiang, and Z. Zhou. 2013. Comparative genomics of parasitic silkworm microsporidia reveal an association between genome expansion and host adaptation. BMC Genomics 14:1.

Park, C.-H., S. Chen, G. Shirsekar, B. Zhou, C. H. Khang, P. Songkumarn, A. J. Afzal, Y. Ning, R. Wang, M. Bellizzi, B. Valent, and G.-L. Wang. 2012. The *Magnaporthe oryzae* effector AvrPiz-t targets the RING E3 ubiquitin ligase

APIP6 to suppress pathogen-associated molecular pattern-triggered immunity in rice. The Plant cell 24:4748–62.

Pasteur, L. 1870. Etudes sur la Maladie des vers a soie. Gauthier-Villars, Imprimeur-Libraire, Paris.

Paxton, R. J., J. Klee, S. Korpela, and I. Fries. 2007. *Nosema ceranae* has infected *Apis mellifera* in Europe since at least 1998 and may be more virulent than *Nosema apis*. Apidologie 38:558–565.

van Pel, D. M., I. J. Barrett, Y. Shimizu, B. V Sajesh, B. J. Guppy, T. Pfeifer, K. J. McManus, and P. Hieter. 2013. An evolutionarily conserved synthetic lethal interaction network identifies FEN1 as a broad-spectrum target for anticancer therapeutic development. PLoS Genetics 9:e1003254.

Petersen, T. N., S. Brunak, G. von Heijne, and H. Nielsen. 2011. SignalP 4.0: discriminating signal peptides from transmembrane regions. Nature Methods 8:785–786.

Petri, W. A., R. Haque, and B. J. Mann. 2002. The bittersweet interface of parasite and host: lectin-carbohydrate interactions during human invasion by the parasite *Entamoeba histolytica*. Annual Review of Microbiology 56:39–64.

Pettis, J. S., A. M. Collins, R. Wilbanks, and M. F. Feldlaufer. 2004. Effects of coumaphos on queen rearing in the honey bee, *Apis mellifera*. Apidologie 35:605–610.

Pettis, J. S., D. Vanengelsdorp, J. Johnson, and G. Dively. 2012. Pesticide exposure in honey bees results in increased levels of the gut pathogen *Nosema*. Naturwissenschaften 99:153–158.

Peuvel, I., P. Peyret, G. Méténier, C. P. Vivarès, and F. Delbac. 2002. The microsporidian polar tube: Evidence for a third polar tube protein (PTP3) in *Encephalitozoon cuniculi*. Molecular and Biochemical Parasitology 122:69–80.

Peuvel-Fanget, I., V. Polonais, D. Brosson, C. Texier, L. Kuhn, P. Peyret, C. Vivarès, and F. Delbac. 2006. EnP1 and EnP2, two proteins associated with the *Encephalitozoon cuniculi* endospore, the chitin-rich inner layer of the microsporidian spore wall. International Journal for Parasitology 36:309–318.

Peyretaillade, E., C. Biderre, P. Peyret, F. Duffieux, G. Méténier, M. Gouy, B. Michot, and C. P. Vivarès. 1998. Microsporidian *Encephalitozoon cuniculi*, a unicellular eukaryote with an unusual chromosomal dispersion of ribosomal genes and a LSU rRNA reduced to the universal core. Nucleic Acids Research 26:3513–3520.

Pilling, E. D., and P. C. Jepson. 1993. Synergism between EBI fungicides and a pyrethroid insecticide in the honeybee (*Apis mellifera*). Pesticide Science 39:293–297.

Pisa, L. W., V. Amaral-Rogers, L. P. Belzunces, J. M. Bonmatin, C. A. Downs, D.

Goulson, D. P. Kreutzweiser, C. Krupke, M. Liess, M. McField, C. A. Morrissey, D. A. Noome, J. Settele, N. Simon-Delso, J. D. Stark, J. P. Van der Sluijs, H. Van Dyck, and M. Wiemers. 2014. Effects of neonicotinoids and fipronil on non-target invertebrates. Environmental Science and Pollution Research 22:68–102.

Plischuk, S., R. Martín-Hernández, L. Prieto, M. Lucía, C. Botías, A. Meana, A. H. Abrahamovich, C. Lange, and M. Higes. 2009. South American native bumblebees (Hymenoptera: Apidae) infected by *Nosema ceranae* (Microsporidia), an emerging pathogen of honeybees (*Apis mellifera*). Environmental Microbiology Reports 1:131–135.

Polonais, V., G. Prensier, G. Méténier, C. P. Vivarès, and F. Delbac. 2005. Microsporidian polar tube proteins: Highly divergent but closely linked genes encode PTP1 and PTP2 in members of the evolutionarily distant *Antonospora* and *Encephalitozoon* groups. Fungal Genetics and Biology 42:791–803.

Pombert, J.-F., M. Selman, F. Burki, F. T. Bardell, L. Farinelli, L. F. Solter, D. W. Whitman, L. M. Weiss, N. Corradi, and P. J. Keeling. 2012. Gain and loss of multiple functionally related, horizontally transferred genes in the reduced genomes of two microsporidian parasites. Proceedings of the National Academy of Sciences 109:12638–12643.

Di Prisco, G., V. Cavaliere, D. Annoscia, P. Varricchio, E. Caprio, F. Nazzi, G. Gargiulo, and F. Pennacchio. 2013. Neonicotinoid clothianidin adversely affects insect immunity and promotes replication of a viral pathogen in honey bees. Proceedings of the National Academy of Sciences of the United States of America 110:18466–71.

Di Prisco, G., F. Pennacchio, E. Caprio, H. F. Boncristiani, J. D. Evans, and Y. Chen. 2011. *Varroa destructor* is an effective vector of Israeli acute paralysis virus in the honeybee, *Apis mellifera*. Journal of General Virology 92:151–155.

R Core Team. 2013. R: A language and environment for statistical computing. R Foundation for Statistical Computing, Vienna, Austria.

Retschnig, G., P. Neumann, and G. R. Williams. 2014. Thiacloprid-*Nosema ceranae* interactions in honey bees: host survivorship but not parasite reproduction is dependent on pesticide dose. Journal of Invertebrate Pathology 118:18–9.

Richards, T. A, R. P. Hirt, B. A. P. Williams, and T. M. Embley. 2003. Horizontal gene transfer and the evolution of parasitic protozoa. Protist 154:17–32.

Ritter, W., and P. Akratanakul. 2006. Honey bee diseases and pests: a practical guide. Agricultural and Food Engineering Technical Report ISSN 1814-1137.

Rivero, A, P. Agnew, S. Bedhomme, C. Sidobre, and Y. Michalakis. 2007. Resource depletion in *Aedes aegypti* mosquitoes infected by the microsporidia *Vavraia culicis*. Parasitology 134:1355–1362.

Robinson, M. D., J. Grigull, N. Mohammad, and T. R. Hughes. 2002. FunSpec: a web-based cluster interpreter for yeast. BMC Bioinformatics 3:1–5.

Roetschi, A., H. Berthoud, R. Kuhn, and A. Imdorf. 2008. Infection rate based on quantitative real-time PCR of *Melissococcus plutonius*, the causal agent of European foulbrood, in honeybee colonies before and after apiary sanitation. Apidologie 39:362–371.

Rondeau, G., F. Sánchez-Bayo, H. A. Tennekes, A. Decourtye, R. Ramírez-Romero, and N. Desneux. 2014. Delayed and time-cumulative toxicity of imidacloprid in bees, ants and termites. Scientific Reports 4:5566.

Rosenkranz, P., P. Aumeier, and B. Ziegelmann. 2010. Biology and control of *Varroa destructor*. Journal of Invertebrate Pathology 103:S96–S119.

Rundlöf, M., G. K. S. Andersson, R. Bommarco, I. Fries, V. Hederström, L. Herbertsson, O. Jonsson, B. K. Klatt, T. R. Pedersen, J. Yourstone, and H. G. Smith. 2015. Seed coating with a neonicotinoid insecticide negatively affects wild bees. Nature 521, 77–80.

Saka, H. A., and R. Valdivia. 2012. Emerging Roles for Lipid Droplets in Immunity and Host-Pathogen Interactions. Annual Review of Cell and Developmental Biology 28:411–437.

Sam-Yellowe, T. Y. 1996. Rhoptry organelles of the apicomplexa: Their role in host cell invasion and intracellular survival. Parasitology Today 12:308–316.

Sambrook, J., E. F. Fritsch, and T. Maniatis. 1989. Molecular Cloning: A Laboratory Manual. Cold Spring Harbor Laboratory Press.

Sanchez-Bayo, F., and K. Goka. 2014. Pesticide residues and bees - A risk assessment. PLoS ONE 9.

Sandrock, C., M. Tanadini, L. G. Tanadini, A. Fauser-Misslin, S. G. Potts, and P. Neumann. 2014. Impact of chronic neonicotinoid exposure on honeybee colony performance and queen supersedure. PLoS ONE 9:1–13.

Scanlon, M., G. J. Leitch, G. S. Visvesvara, and A. P. Shaw. 2004. Relationship between the Host Cell Mitochondria and the Parasitophorous Vacuole in Cells Infected with *Encephalitozoon* Microsporidia. Journal of Eukaryotic Microbiology 51:81–87.

Scarborough-Bull, A., and E. Weidner. 1985. Some Properties of Discharged *Glugea hertwigi* (Microsporida) Sporoplasms. The Journal of Protozoology 32:284–289.

Schaafsma, A., V. Limay-Rios, T. Baute, J. Smith, and Y. Xue. 2015. Neonicotinoid Insecticide Residues in Surface Water and Soil Associated with Commercial Maize (Corn) Fields in Southwestern Ontario. PloS ONE 10:e0118139.

Schmidhempel, P., and T. Wolf. 1988. Foraging Effort and Life-Span of Workers in

a Social Insect. Journal of Animal Ecology 57:509–521.

Schmuck, R., T. Stadler, and H. W. Schmidt. 2003. Field relevance of a synergistic effect observed in the laboratory between an EBI fungicide and a chloronicotinyl insecticide in the honeybee (*Apis mellifera* L, Hymenoptera). Pest Management Science 59:279–286.

Schneider, C. W., J. Tautz, B. Grünewald, and S. Fuchs. 2012. RFID tracking of sublethal effects of two neonicotinoid insecticides on the foraging behavior of *Apis mellifera*. PLoS ONE 7:1–9.

Schornack, S., E. Huitema, L. M. Cano, T. O. Bozkurt, R. Oliva, M. Van Damme, S. Schwizer, S. Raffaele, A. Chaparro-Garcia, R. Farrer, M. E. Segretin, J. Bos, B. J. Haas, M. C. Zody, C. Nusbaum, J. Win, M. Thines, and S. Kamoun. 2009. Ten things to know about oomycete effectors. Molecular Plant Pathology 10:795–803.

Senderskiy, I. V., S. A. Timofeev, E. V Seliverstova, O. a Pavlova, and V. V Dolgikh. 2014. Secretion of *Antonospora (Paranosema) locustae* proteins into infected cells suggests an active role of microsporidia in the control of host programs and metabolic processes. PloS ONE 9:e93585.

Shannon, P., A. Markiel, O. Ozier, N. S. Baliga, J. T. Wang, D. Ramage, N. Amin, B. Schwikowski, and T. Ideker. 2003. Cytoscape : A Software Environment for Integrated Models of Biomolecular Interaction Networks. Genome Research 13:2498–2504.

Sharpe, R. J., and L. C. Heyden. 2009. Honey bee colony collapse disorder is possibly caused by a dietary pyrethrum deficiency. Bioscience Hypotheses 2:439–440.

Sherman, F. 1998. An Introduction to the Genetics and Molecular Biology of the Yeast *Saccharomyces cerevisiae*. The Encyclopedia of Molecular Biology and Molecular Medinicine 6:302–325.

Shimanuki, H., N. W. Calderone, and D. A. Knox. 1994. Parasitic mite syndrome: the symptoms. American Bee Journal (USA).

Shohdy, N., J. A. Efe, S. D. Emr, and H. a Shuman. 2005. Pathogen effector protein screening in yeast identifies *Legionella* factors that interfere with membrane trafficking. Proceedings of the National Academy of Sciences of the United States of America 102:4866–4871.

Shuel, R. 1992. The production of nectar and pollen. (J. M. Graham, Ed.) The hive and the honey bee. Revised ed. Bookcrafters, Hamilton IL.

Sin, N., L. Meng, M. Q. Wang, J. J. Wen, W. G. Bornmann, and C. M. Crews. 1997. The anti-angiogenic agent fumagillin covalently binds and inhibits the methionine aminopeptidase, MetAP-2. Proceedings of the National Academy of Sciences of the United States of America 94:6099–6103.

Snow, D. W., and C. Perrins. 1997. The Birds of the Western Palearctic. Oxford University Press.

Southern, T. R., C. E. Jolly, M. E. Lester, and J. R. Hayman. 2007. EnP1, a microsporidian spore wall protein that enables spores to adhere to and infect host cells in vitro. Eukaryotic Cell 6:1354–1362.

Sparks, J. L., H. Chon, S. M. Cerritelli, T. A. Kunkel, E. Johansson, R. J. Crouch, and P. M. Burgers. 2012. RNase H2-initiated ribonucleotide excision repair. Molecular Cell 47:980–6.

Sprague, V., and S. H. Vernick. 1968. The Golgi complex of Microsporida and its role in spore morphogenesis. Am Zool 8:824.

Stentiford, G. D., S. W. Feist, D. M. Stone, K. S. Bateman, and A. M. Dunn. 2013. Microsporidia: Diverse, dynamic, and emergent pathogens in aquatic systems. Trends in Parasitology 29:567–578.

Suwannapong, G., T. Yemor, C. Boonpakdee, and M. E. Benbow. 2011. *Nosema ceranae*, a new parasite in Thai honeybees. Journal of Invertebrate Pathology 106:236–241.

Takvorian, P. M., and A. Cali. 1981. The occurrence of *Glugea stephani* (Hagenmuller, 1899) in American winter flounder, *Pseudopleuronects americanus* (Walbaum) from the New York-New Jersey lower bay complex. Journal of Fish Biology 18:491–501.

Takvorian, P. M., and A. Cali. 1986. The ultrastructure of spores (Protozoa: Microsporida) from *Lophius americanus*, the angler fish. The Journal of Protozoology 33:570–5.

Takvorian, P. M., and A. Cali. 1996. Polar tube formation and nucleoside diphosphatase activity in the microsporidian, *Glugea stephani*. The Journal of Eukaryotic Microbiology 43:102S–103S.

Takvorian, P. M., L. M. Weiss, and A. Cali. 2005. The early events of *Brachiola algerae* (Microsporidia) infection: spore germination, sporoplasm structure, and development within host cells. Folia Parasitologica 52:118–29.

Tan, K.-C., H. T. T. Phan, K. Rybak, E. John, Y. H. Chooi, P. S. Solomon, and R. P. Oliver. 2015. Functional redundancy of necrotrophic effectors – consequences for exploitation for breeding. Frontiers in Plant Science 6:1–9.

Tanabe, Y., M. M. Watanabe, and J. Sugiyama. 2002. Are Microsporidia really related to Fungi?: a reappraisal based on additional gene sequences from basal fungi. Mycological Research 106:1380–1391.

Tatusova, T., S. Ciufo, B. Fedorov, K. O'Neill, and I. Tolstoy. 2014. RefSeq microbial genomes database: New representation and annotation strategy. Nucleic Acids Research 42:553–559.

Taupin, V., E. Garenaux, M. Mazet, E. Maes, H. Denise, G. Prensier, C. P. Vivarès, Y. Guérardel, and G. Méténier. 2007. Major O-glycans in the spores of two microsporidian parasites are represented by unbranched manno-oligosaccharides containing α-1,2 linkages. Glycobiology 17:56–67.

Tentcheva, D., L. Gauthier, L. Bagny, J. Fievet, B. Dainat, F. Cousserans, M. E. Colin, and M. Bergoin. 2006. Comparative analysis of deformed wing virus (DWV) RNA in *Apis mellifera* and *Varroa destructor*. Apidologie 37:41–50.

Tentcheva, D., L. Gauthier, N. Zappulla, B. Dainat, F. Cousserans, M. Edouard, M. Bergoin, and M. E. Colin. 2004. Prevalence and Seasonal Variations of Six Bee Viruses in *Apis mellifera* L . and *Varroa destructor* Mite Populations in France Prevalence and Seasonal Variations of Six Bee Viruses in *Apis mellifera* L . and *Varroa destructor* Mite Populations in France. Applied And Environmental Microbiology 70:7185–7191.

Tian, B., N. H. Fadhil, J. E. Powell, W. K. Kwong, and N. A. Moran. 2012. Long-term exposure to antibiotics has caused accumulation of resistance determinants in the gut microbiota of honeybees. mBio 3(6) e00377-12.

Timpel, C., S. Zink, S. Strahl-Bolsinger, K. Schröppel, and J. Ernst. 2000. Morphogenesis, adhesive properties, and antifungal resistance depend on the Pmt6 protein mannosyltransferase in the fungal pathogen *Candida albicans*. Journal of Bacteriology 182:3063–71.

Tkach, J. M., A. Yimit, A. Y. Lee, M. Riffle, M. Costanzo, D. Jaschob, J. A. Hendry, J. Ou, J. Moffat, C. Boone, T. N. Davis, C. Nislow, and G. W. Brown. 2012. Dissecting DNA damage response pathways by analysing protein localization and abundance changes during DNA replication stress. Nature Cell Biology 14:966–76.

van Tomé, H. V., G. F. Martins, M. A. P. Lima, L. A. O. Campos, and R. N. C. Guedes. 2012. Imidacloprid-induced impairment of mushroom bodies and behavior of the native stingless bee *Melipona quadrifasciata anthidioides*. PLoS ONE 7:1–9.

Tomizawa, M., and J. E. Casida. 2005. Neonicotinoid insecticide toxicology: mechanisms of selective action. Annual Review of Pharmacology and toxicology 45:247–268.

Tomkies, V., V. Tomkies, J. Flint, J. Flint, G. Johnson, R. Waite, G. Johnson, R. Waite, S. Wilkins, S. Wilkins, C. Danks, M. Watkin, C. Danks, a Cuthbertson, M. Watkin, E. Carpana, A. G. S. Cuthbertson, G. Marris, E. Carpana, G. Marris, G. Budge, G. Budge, M. Brown, and M. a. Brown. 2009. Development and validation of a novel field test kit for European foulbrood. Apidologie 40:63–72.

Tong, A. H. Y., and C. Boone. 2005. Synthetic Genetic Array Analysis in *Saccharomyces cerevisiae*. Methods in Molecular Biology 313:171–191.

Tong, A. H. Y., M. Evangelista, A. B. Parsons, H. Xu, G. D. Bader, N. Pagé, M. Robinson, S. Raghibizadeh, C. W. Hogue, H. Bussey, B. Andrews, M. Tyers, and C. Boone. 2001. Systematic genetic analysis with ordered arrays of yeast deletion mutants. Science (New York, N.Y.) 294:2364–2368.

Tong, A. H. Y., G. Lesage, G. D. Bader, H. Ding, H. Xu, X. Xin, J. Young, G. F. Berriz, R. L. Brost, M. Chang, Y. Chen, X. Cheng, G. Chua, H. Friesen, D. S. Goldberg, J. Haynes, C. Humphries, G. He, S. Hussein, L. Ke, N. Krogan, Z. Li, J. N. Levinson, H. Lu, P. Menard, C. Munyana, A. B. Parsons, O. Ryan, R. Tonikian, T. Roberts, A. M. Sdicu, J. Shapiro, B. Sheikh, B. Suter, S. L. Wong, L. V Zhang, H. Zhu, C. G. Burd, S. Munro, C. Sander, J. Rine, J. Greenblatt, M. Peter, A. Bretscher, G. Bell, F. P. Roth, G. W. Brown, B. Andrews, H. Bussey, and C. Boone. 2004. Global Mapping of the Yeast Genetic Interaction Network. Science 303:808–813.

Torto-Alalibo, T., C. W. Collmer, M. Gwinn-Giglio, M. Lindeberg, S. Meng, M. C. Chibucos, T.-T. Tseng, J. Lomax, B. Biehl, A. Ireland, D. Bird, R. A. Dean, J. D. Glasner, N. Perna, J. C. Setubal, A. Collmer, and B. M. Tyler. 2010. Unifying themes in microbial associations with animal and plant hosts described using the gene ontology. Microbiology and Molecular Biology reviews 74:479–503.

Tsaousis, A. D., E. R. S. Kunji, A. V Goldberg, J. M. Lucocq, R. P. Hirt, and T. M. Embley. 2008. A novel route for ATP acquisition by the remnant mitochondria of *Encephalitozoon cuniculi*. Nature 453:553–556.

Undeen, A. H., and R. K. Vander Meer. 1999. Microsporidian intrasporal sugars and their role in germination. Journal of Invertebrate Pathology 73:294–302.

Usher, J., G. Thomas, and K. Haynes. 2015. Utilising established SDL-screening methods as a tool for the functional genomic characterisation of model and non-model organisms. FEMS yeast research 15:1–8.

Valdivia, R. H. 2008. *Chlamydia* effector proteins and new insights into chlamydial cellular microbiology. Current Opinion in Microbiology 11:53–59.

Vanbergen, A. J., M. S. Heard, T. Breeze, S. G. Potts, and N. Hanley. 2014. Status and Value of Pollinators and Pollination Services. DEFRA Report.

VanEngelsdorp, D., and M. D. Meixner. 2010. A historical review of managed honey bee populations in Europe and the United States and the factors that may affect them. Journal of Invertebrate Pathology 103:S80–S95.

VanEngelsdorp, D., N. Speybroeck, J. D. Evans, B. K. Nguyen, C. Mullin, M. Frazier, J. Frazier, D. Cox-Foster, Y. Chen, D. R. Tarpy, E. Haubruge, J. S. Pettis, and C. Saegerman. 2010. Weighing risk factors associated with bee colony collapse disorder by classification and regression tree analysis. Journal of Economic Entomology 103:1517–1523.

Vanengelsdorp, D., R. Underwood, D. Caron, and J. Hayes. 2007. An estimate of

managed colony losses in the winter of 2006-2007: A report commissioned by the apiary inspectors of America. American Bee Journal 147:599–603.

Vavra, J. 1976. Structure of the microsporidia. Pages 1–85 *in* L. A. J. Bulla and T. C. Cheng, editors. Comparative Pathobiology. Plenum Press, New York.

Vávra, J., and J. I. R. Larsson. 1999. The Microsporidia and Microsporidiosis. (L. M. Weiss and M. Wittner, Eds.). American Society of Microbiology.

Vávra, J., and J. Lukeš. 2013. Microsporidia and "the art of living together". In: Rollinson, D. (Ed.), Advances in Parasitology, Academic Press, pp. 253–320.

Velthuis, H. H. W., and A. Van Doorn. 2006. A century of advances in bumblebee domestication and the economic and environmental aspects of its commercialization for pollination. Apidologie 37:421–451.

Visvesvara, G. S., G. J. Leitch, A. J. Da Silva, G. P. Croppo, H. Moura, S. Wallace, S. B. Slemenda, D. A. Schwartz, D. Moss, R. T. Bryan, and N. J. Pieniazek. 1994. Polyclonal and monoclonal antibody and PCR-amplified small-subunit rRNA identification of a microsporidian, *Encephalitozoon hellem*, isolated from an AIDS patient with disseminated infection. Journal of Clinical Microbiology 32:2760–2768.

Vivarès, C. P., and G. Méténier. 2000. Towards the minimal eukaryotic parasitic genome. Current Opinion in Microbiology 3:463–467.

Voorhies, E., F. Todd, and J. Galbraith. 1933. Economic aspects of the bee industry. University of California press.

Vossbrinck, C. R., J. V Maddox, S. Friedman, B. A. Debrunner-Vossbrinck, and C. R. Woese. 1987. Ribosomal RNA sequence suggests microsporidia are extremely ancient eukaryotes. Nature 326:411–4.

Wagih, O., M. Usaj, A. Baryshnikova, B. VanderSluis, E. Kuzmin, M. Costanzo, C. L. Myers, B. J. Andrews, C. M. Boone, and L. Parts. 2013. SGAtools: One-stop analysis and visualization of array-based genetic interaction screens. Nucleic Acids Research 41:591–596.

Wahl, O., and K. Ulm. 1983. Influence of pollen feeding and physiological condition on pesticide sensitivity of the honey bee *Apis mellifera carnica*. Oecologia 59:106–128.

Wang, D. I., and F. E. Moeller. 1970. Division Of Labor and Queen Attendance Behavior Of Nosema-Infected Worker Honey Bees Hymenotera-Apidae. Journal of Economic Entomology 63:1539–&.

Weber, R., and R. T. Bryan. 1994. Microsporidial infections in immunodeficient and immunocompetent patients. Clinical infectious diseases : an official publication of the Infectious Diseases Society of America 19:517–521.

Weber, R., R. T. Bryan, R. L. Owen, M. C. Wilcox, L. Gorelkin, and G. S.

Visvesvara. 1992. Improved Light-Microscopical Detection of Microsporidia Spores in Stool and Duodenal Aspirates. The New England Journal of Medicine 327:1135–40.

Webster, T. C. 1994. Fumagillin Affects *Nosema apis* and Honey Bees (Hymonopterai Apidae). Journal of Economic Entomology 87:601–604.

Weidner, E. 1972. Ultrastructural study of microsporidian invasion into cells. Zeitschrift fur Parasitenkunde 40:227–242.

Weidner, E. 1976. The microsporidian spore invasion tube. The ultrastructure, isolation, and characterization of the protein comprising the tube. Journal of Cell Biology 71:23–34.

Weidner, E. 2000. Cytoplasmic Proteins on the Surface of Discharged Microsporidian Sporoplasms. Biology Bullitin 199:208–209.

Weidner, E., and W. Byrd. 1982. The microsporidian spore invasion tube. II. Role of calcium in the activation of invasion tube discharge. Journal of Cell Biology 93:970–975.

Weidner, E., A. M. Findley, V. Dolgikh, and J. Sokolova. 1999. Microsporidian Biochemistry and Physiology. Pages 172–195 *in* L. M. Weiss and M. Wittner, editors. The Microsporidia and Microsporidiosis. American Society of Microbiology.

Weiss, L. M. 2001. Microsporidia: Emerging pathogenic protists. Acta Tropica 78:89–102.

Weiss, L. M., and J. J. Becnel. 2014. Microsporidia: Pathogens of Opportunity. (First Edition). John Wiley & Sons, Inc.

Weitzman, M. D., and J. B. Weitzman. 2014. What's the Damage? The Impact of Pathogens on Pathways that Maintain Host Genome Integrity. Cell Host Microbe 15:283–294.

Whitehorn, P. R., S. O'Connor, F. L. Wackers, and D. Goulson. 2012. Neonicotinoid Pesticide Reduces Bumble Bee Colony Growth and Queen Production. Science 336:351–352.

Whittington, R., and M. L. Winston. 2003. Effects of Nosema bombi and its treatment fumagillin on bumble bee (*Bombus occidentalis*) colonies. Journal of Invertebrate Pathology 84:54–58.

Wilkins, S., M. A. Brown, and A. G. S. Cuthbertson. 2007. The incidence of honey bee pests and diseases in England and Wales. Pest Management Science 63:1062–1068.

Williams, B. A. P. 2009. Unique physiology of host-parasite interactions in microsporidia infections. Cellular Microbiology 11:1551–1560.

Williams, B. A. P., V. V Dolgikh, and Y. Y. Sokolova. 2014. Microsporidian

Biochemistry and Physiology. Pages 245–260 *in* L. M. Weiss and J. J. Becnel, editors. Microsporidia: Pathogens of Opportunity. First edition. John Wiley & Sons, Inc., Chichester, UK.

Williams, B. A. P., C. Elliot, L. Burri, Y. Kido, K. Kita, A. L. Moore, and P. J. Keeling. 2010. A broad distribution of the alternative oxidase in microsporidian parasites. PLoS Pathogens 6:1–8.

Williams, B. A. P., R. P. Hirt, J. M. Lucocq, and T. M. Embley. 2002. A mitochondrial remnant in the microsporidian *Trachipleistophora hominis*. Nature 418:865–869.

Williams, G. R., M. A. Sampson, D. Shutler, and R. E. L. Rogers. 2008. Does fumagillin control the recently detected invasive parasite *Nosema ceranae* in western honey bees (*Apis mellifera*)? Journal of Invertebrate Pathology 99:342–344.

Williams, G. R., D. Shutler, C. M. Little, K. L. Burgher-Maclellan, and R. E. L. Rogers. 2011. The microsporidian *Nosema ceranae*, the antibiotic Fumagilin-B®, and western honey bee (*Apis mellifera*) colony strength. Apidologie 42:15–22.

Williams, P. H., and J. L. Osborne. 2009. Bumblebee vulnerability and conservation world-wide. Apidologie 40:367–387.

Williams, P. H., R. W. Thorp, L. L. Richardson, and S. R. Colla. 2014. Bumble Bees of North America: An Identification Guide. Princeton University Press.

Williamson, S. M., D. D. Baker, and G. A. Wright. 2013. Acute exposure to a sublethal dose of imidacloprid and coumaphos enhances olfactory learning and memory in the honeybee *Apis mellifera*. Invertebrate Neuroscience 13:63–70.

Winzeler, E. A., D. D. Shoemaker, A. Astromoff, H. Liang, K. Anderson, B. Andre, R. Bangham, R. Benito, J. D. Boeke, H. Bussey, A. M. Chu, C. Connelly, K. Davis, F. Dietrich, S. W. Dow, M. El Bakkoury, F. Foury, S. H. Friend, E. Gentalen, G. Giaever, J. H. Hegemann, T. Jones, M. Laub, H. Liao, N. Liebundguth, D. J. Lockhart, A. Lucau-Danila, M. Lussier, N. M'Rabet, P. Menard, M. Mittmann, C. Pai, C. Rebischung, J. L. Revuelta, L. Riles, C. J. Roberts, P. Ross-MacDonald, B. Scherens, M. Snyder, S. Sookhai-Mahadeo, R. K. Storms, S. Véronneau, M. Voet, G. Volckaert, T. R. Ward, R. Wysocki, G. S. Yen, K. Yu, K. Zimmermann, P. Philippsen, M. Johnston, and R. W. Davis. 1999. Functional characterization of the *S. cerevisiae* genome by gene deletion and parallel analysis. Science (New York, N.Y.) 285:901–6.

De Wit, P. J. G. M., R. Mehrabi, H. A. Van Den Burg, and I. Stergiopoulos. 2009. Fungal effector proteins: Past, present and future: Review. Molecular Plant Pathology 10:735–747.

Wittner, M., and L. M. Weiss. 1999. The Microsporidia and Microsporidiosis.

American Society of Microbiology. Washington (D. C.).

Wolf, T. J., and P. Schmid-Hempel. 1989. Extra Loads and Foraging Life Span in Honeybee Workers. Journal of Animal Ecology 58:943–954.

Wu, Z., Y. Li, G. Pan, X. Tan, J. Hu, Z. Zhou, and Z. Xiang. 2008. Proteomic analysis of spore wall proteins and identification of two spore wall proteins from *Nosema bombycis* (Microsporidia). Proteomics 8:2447–61.

Xu, Y., P. Takvorian, A. Cali, F. Wang, G. Orr, L. M. Weiss, and H. Zhang. 2006. Identification of a New Spore Wall Protein from *Encephalitozoon cuniculi*. Infection and Immunity 74:239–247.

Xu, Y., P. M. Takvorian, A. Cali, G. Orr, and L. M. Weiss. 2004. Glycosylation of the major polar tube protein of *Encephalitozoon hellem*, a microsporidian parasite that infects humans. Infection and Immunity 72:6341–6350.

Xu, Y., and L. M. Weiss. 2005. The microsporidian polar tube: A highly specialised invasion organelle. International Journal for Parasitology 35:941–953.

Yang, E. C., Y. C. Chuang, Y. L. Chen, and L. H. Chang. 2008. Abnormal Foraging Behavior Induced by Sublethal Dosage of Imidacloprid in the Honey Bee (Hymenoptera: Apidae). Journal of Economic Entomology 101:1743–1748.

Yang, X., and D. Cox-Foster. 2005. Impact of an ectoparasite on the immunity and pathology of an invertebrate: evidence for host immunosuppression and viral amplification. Proceedings of the National Academy of Sciences of the United States of America 102:7470–7475.

Yang, X., and D. Cox-Foster. 2007. Effects of parasitization by *Varroa destructor* on survivorship and physiological traits of *Apis mellifera* in correlation with viral incidence and microbial challenge. Parasitology 134:405–412.

Yue, C., and E. Genersch. 2005. RT-PCR analysis of Deformed wing virus in honeybees (*Apis mellifera*) and mites (*Varroa destructor*). Journal of General Virology 86:3419–3424.

Yue, C., M. Schröder, K. Bienefeld, and E. Genersch. 2006. Detection of viral sequences in semen of honeybees (*Apis mellifera*): evidence for vertical transmission of viruses through drones. Journal of Invertebrate Pathology 92:105–108.

Yue, C., M. Schröder, S. Gisder, and E. Genersch. 2007. Vertical-transmission routes for deformed wing virus of honeybees (*Apis mellifera*). Journal of General Virology 88:2329–2336.

Zaluski, R., S. M. Kadri, D. P. Alonso, P. E. Martins Ribolla, and R. De Oliveira Orsi. 2015. Fipronil promotes motor and behavioral changes in honey bees (*Apis mellifera*) and affects the development of colonies exposed to sublethal doses. Environmental Toxicology and Chemistry 34:1062–1069.

Zander, E. 1909. Tierische parasiten als krankenheitserreger bei der biene. Münchener Bienenzeitung.

Van der Zee, R., T. Gómez-Moracho, L. Pisa, S. Sagastume, P. García-Palencia, X. Maside, C. Bartolomé, R. Martín-Hernández, and M. Higes. 2014. Virulence and polar tube protein genetic diversity of *Nosema ceranae* (Microsporidia) field isolates from Northern and Southern Europe in honeybees (*Apis mellifera iberiensis*). Environmental Microbiology Reports 6:401–413.

Appendix I | *N. ceranae* gene-ID for secretome (NcS) ORFs.

GeneID	NcS-ID	GeneID	NcS-ID	GeneID	NcS-ID	GeneID	NcS-ID
NCER_101078	NcS-1	NCER_100426	NcS-26	NCER_101591	NcS-51	NCER_101469	NcS-76
NCER_101082	NcS-2	NCER_101526	NcS-27	NCER_100522	NcS-52	NCER_101600	NcS-77
NCER_100547	NcS-3	NCER_101416	NcS-28	NCER_100581	NcS-53	NCER_102300	NcS-78
NCER_100618	NcS-4	NCER_100828	NcS-29	NCER_101413	NcS-54	NCER_101061	NcS-79
NCER_101994	NcS-5	NCER_101239	NcS-30	NCER_101900	NcS-55	NCER_101528	NcS-80
NCER_100164	NcS-6	NCER_101463	NcS-31	NCER_101271	NcS-56	NCER_101940	NcS-81
NCER_101626	NcS-7	NCER_102345	NcS-32	NCER_100044	NcS-57	NCER_101691	NcS-82
NCER_101673	NcS-8	NCER_100802	NcS-33	NCER_100575	NcS-58	NCER_102495	NcS-83
NCER_100557	NcS-9	NCER_100703	NcS-34	NCER_102372	NcS-59	NCER_102060	NcS-84
NCER_100987	NcS-10	NCER_100960	NcS-35	NCER_102145	NcS-60	NCER_101884	NcS-85
NCER_100710	NcS-11	NCER_101165	NcS-36	NCER_100949	NcS-61	NCER_102146	NcS-86
NCER_101349	NcS-12	NCER_100064	NcS-37	NCER_102103	NcS-62	NCER_100295	NcS-87
NCER_100505	NcS-13	NCER_100048	NcS-38	NCER_101938	NcS-63	NCER_100914	NcS-88
NCER_100163	NcS-14	NCER_101999	NcS-39	NCER_100197	NcS-64	NCER_102068	NcS-89
NCER_101950	NcS-15	NCER_102151	NcS-40	NCER_100216	NcS-65	NCER_102348	NcS-90
NCER_101108	NcS-16	NCER_102328	NcS-41	NCER_100566	NcS-66	NCER_100899	NcS-91
NCER_100355	NcS-17	NCER_100177	NcS-42	NCER_101785	NcS-67	NCER_102158	NcS-92
NCER_101049	NcS-18	NCER_100070	NcS-43	NCER_101124	NcS-68	NCER_101985	NcS-93
NCER_100533	NcS-19	NCER_101687	NcS-44	NCER_101532	NcS-69	NCER_100813	NcS-94
NCER_100305	NcS-20	NCER_100301	NcS-45	NCER_100347	NcS-70	NCER_100308	NcS-95
NCER_100569	NcS-21	NCER_100838	NcS-46	NCER_100341	NcS-71	NCER_100327	NcS-96
NCER_101848	NcS-22	NCER_102053	NcS-47	NCER_100083	NcS-72	NCER_102617	NcS-97
NCER_101906	NcS-23	NCER_100302	NcS-48	NCER_100056	NcS-73	NCER_101403	NcS-98
NCER_102454	NcS-24	NCER_102217	NcS-49	NCER_102178	NcS-74	NCER_100135	NcS-99
NCER_100691	NcS-25	NCER_101663	NcS-50	NCER_101590	NcS-75	NCER_102083	NcS-100

Red text indicates ORFs from the originally inferred secretome that are no longer predicted to be secreted.

GeneID	NcS-ID	GeneID	NcS-ID	GeneID	NcS-ID	GeneID	NcS-ID
NCER_100165	NcS-101	NCER_101438	NcS-123	NCER_100716	NcS-145	NCER_101806	NcS-167
NCER_100856	NcS-102	NCER_101509	NcS-124	NCER_100816	NcS-146	NCER_101870	NcS-168
NCER_100279	NcS-103	NCER_101774	NcS-125	NCER_100961	NcS-147	NCER_101886	NcS-169
NCER_101367	NcS-104	NCER_102512	NcS-126	NCER_100977	NcS-148	NCER_101908	NcS-170
NCER_101263	NcS-105	NCER_102551	NcS-127	NCER_101076	NcS-149	NCER_101925	NcS-171
NCER_101972	NcS-106	NCER_100154	NcS-128	NCER_101079	NcS-150	NCER_101960	NcS-172
NCER_101475	NcS-107	NCER_100208	NcS-129	NCER_101141	NcS-151	NCER_102009	NcS-173
NCER_100526	NcS-108	NCER_100248	NcS-130	NCER_101267	NcS-152	NCER_102065	NcS-174
NCER_101617	NcS-109	NCER_100290	NcS-131	NCER_101426	NcS-153	NCER_102080	NcS-175
NCER_101917	NcS-110	NCER_100339	NcS-132	NCER_101457	NcS-154	NCER_102099	NcS-176
NCER_101721	NcS-111	NCER_100382	NcS-133	NCER_101458	NcS-155	NCER_102121	NcS-177
NCER_101889	NcS-112	NCER_100392	NcS-134	NCER_101551	NcS-156	NCER_102127	NcS-178
NCER_101662	NcS-113	NCER_100468	NcS-135	NCER_101605	NcS-157	NCER_102133	NcS-179
NCER_101276	NcS-114	NCER_100482	NcS-136	NCER_101608	NcS-158	NCER_102153	NcS-180
NCER_100694	NcS-115	NCER_100529	NcS-137	NCER_101610	NcS-159	NCER_102184	NcS-181
NCER_102152	NcS-116	NCER_100531	NcS-138	NCER_101612	NcS-160	NCER_102191	NcS-182
NCER_101075	NcS-117	NCER_100532	NcS-139	NCER_101625	NcS-161	NCER_102378	NcS-183
NCER_101121	NcS-118	NCER_100570	NcS-140	NCER_101657	NcS-162	NCER_102379	NcS-184
NCER_101477	NcS-119	NCER_100610	NcS-141	NCER_101701	NcS-163	NCER_102405	NcS-185
NCER_102066	NcS-120	NCER_100626	NcS-142	NCER_101735	NcS-164	NCER_102419	NcS-186
NCER_102326	NcS-121	NCER_100648	NcS-143	NCER_101777	NcS-165	NCER_102424	NcS-187
NCER_102520	NcS-122	NCER_100677	NcS-144	NCER_101786	NcS-166	NCER_102612	NcS-188

Appendix II | Yeast strains used during this study.

Strain	Genotype	Source
BY4741a	*MAT***a** *his3Δ1 leu2Δ0 met15Δ0 ura3Δ0*	Open Biosystems
Y7092	*can1Δ*::STE2pr-SP-*his5 lyp1Δ his3Δ1 leu2Δ0 ura3Δ0 met15Δ0* LYS2+	Tong et al. (2001)
ERG6-GFP	*MAT***a** *his3Δ1 leu2Δ0 met15Δ0 ura3Δ0 erg6Δ::erg6-GFP*	Thermo Fisher Scientific
GT001	*MAT***a**, *his3Δ1, leu2Δ0, met15Δ0, ura3Δ0;* pAG423GPD::NcS-49-EGFP	This study
GT002	*MAT***a**, *his3Δ1, leu2Δ0, met15Δ0, ura3Δ0;* pAG423GPD::NcS-50-EGFP	This study
GT003	*MAT***a**, *his3Δ1, leu2Δ0, met15Δ0, ura3Δ0;* pAG423GPD::NcS-51-EGFP	This study
GT004	*MAT***a**, *his3Δ1, leu2Δ0, met15Δ0, ura3Δ0;* pAG423GPD::NcS-65-EGFP	This study
GT005	*MAT***a**, *his3Δ1, leu2Δ0, met15Δ0, ura3Δ0;* pAG423GPD::NcS-67-EGFP	This study
GT006	*MAT***a**, *his3Δ1, leu2Δ0, met15Δ0, ura3Δ0;* pAG423GPD::NcS-68-EGFP	This study
GT007	*MAT***a**, *his3Δ1, leu2Δ0, met15Δ0, ura3Δ0;* pAG423GPD::NcS-75-EGFP	This study
GT008	*MAT***a**, *his3Δ1, leu2Δ0, met15Δ0, ura3Δ0;* pAG423GPD::NcS-76-EGFP	This study
GT009	*MAT***a**, *his3Δ1, leu2Δ0, met15Δ0, ura3Δ0;* pAG423GPD::NcS-77-EGFP	This study
GT010	*MAT***a**, *his3Δ1, leu2Δ0, met15Δ0, ura3Δ0;* pAG423GPD::NcS-79-EGFP	This study
GT011	*MAT***a**, *his3Δ1, leu2Δ0, met15Δ0, ura3Δ0;* pAG423GPD::NcS-83-EGFP	This study
GT012	*MAT***a**, *his3Δ1, leu2Δ0, met15Δ0, ura3Δ0;* pAG423GPD::NcS-85-EGFP	This study
GT013	*MAT***a**, *his3Δ1, leu2Δ0, met15Δ0, ura3Δ0;* pAG423GPD::NcS-86-EGFP	This study
GT014	*MAT***a** *his3Δ1 leu2Δ0 met15Δ0 ura3Δ0 erg6Δ::erg6-GFP;* pAG426GPD::NcS-50-DsRed	This study
GT015	*MAT***a** *his3Δ1 leu2Δ0 met15Δ0 ura3Δ0 erg6Δ::erg6-GFP;* pAG426GPD::NcS-85-DsRed	This study
GT016	*MAT***a**, *his3Δ1, leu2Δ0, met15Δ0, ura3Δ0;* pAG423GPD::NcS-75-EGFP; pAG426GPD::NcS-76-DsRed	This study
GT017	*can1Δ*::STE2pr-SP-*his5 lyp1Δ his3Δ1 leu2Δ0 ura3Δ0 met15Δ0* LYS2+; pAG426::NcS-50	This study
GT018	*can1Δ*::STE2pr-SP-*his5 lyp1Δ his3Δ1 leu2Δ0 ura3Δ0 met15Δ0* LYS2+; pAG426::NcS-65	This study
GT019	*can1Δ*::STE2pr-SP-*his5 lyp1Δ his3Δ1 leu2Δ0 ura3Δ0 met15Δ0* LYS2+; pAG426::NcS-68	This study
GT020	*can1Δ*::STE2pr-SP-*his5 lyp1Δ his3Δ1 leu2Δ0 ura3Δ0 met15Δ0* LYS2+; pAG426::NcS-79	This study
GT021	*can1Δ*::STE2pr-SP-*his5 lyp1Δ his3Δ1 leu2Δ0 ura3Δ0 met15Δ0* LYS2+; pAG426::NcS-85	This study

Appendix III | Oligonucleotides used in this study.

NcS-ORF	Oligo Name	Sequence 5' to 3'
47	NCER_102053 REVERSE	ACAAGAAAGCTGGGTCCTTCTTCTTCTGTAGGACGATTAGATACAC
47	NCER_102053 FORWARD without SP	ACAAAAAAGCAGGCTTCATGATCGATTACACATCTTTTGTCACTAAA
48	NCER_100302 REVERSE	ACAAGAAAGCTGGGTCAAATGGCTTGTCTTGCTCATTTTTTTCATT
48	NCER_100302 FORWARD without SP	ACAAAAAAGCAGGCTTCATGTGGAAGATCAGAGGAATATTCTCGTTA
49	NCER_102217 REVERSE	ACAAGAAAGCTGGGTCACAATTCAAACCCATCCCTGCCCAGTCTGC
49	NCER_102217 FORWARD without SP	ACAAAAAAGCAGGCTTCATGGGCCATTTAAGTCATCTTTATAAGATA
50	NCER_101663 REVERSE	ACAAGAAAGCTGGGTCCAAATCACTCTCTTCATTCTTTTTTTTAAG
50	NCER_101663 FORWARD without SP	ACAAAAAAGCAGGCTTCATGCTTCAAACACCAATTTTTAAAAAGAAA
51	NCER_101591 REVERSE	ACAAGAAAGCTGGGTCTTGTACGCATACATTCTGGTGTGCTTGTAA
51	NCER_101591 FORWARD without SP	ACAAAAAAGCAGGCTTCATGAACATATGTGCCCCTAATCAAGGAAAA
52	NCER_100522 REVERSE	ACAAGAAAGCTGGGTCAAACTGTTCTAACTCAGTATTTTTCCTATT
52	NCER_100522 FORWARD without SP	ACAAAAAAGCAGGCTTCATGTTAATTTTTCATAAAAATTCAGCTGAA
53	NCER_100581 REVERSE	ACAAGAAAGCTGGGTCCCTCTTCATTGGTCTGTAATGTCTATGTCC
53	NCER_100581 FORWARD without SP	ACAAAAAAGCAGGCTTCATGGAAGAATTACAATTTTTAGTTAAGGGA
54	NCER_101413 REVERSE	ACAAGAAAGCTGGGTCAGATTGTGTTGTTTCTTCTCCCCCCAATAC
54	NCER_101413 FORWARD without SP	ACAAAAAAGCAGGCTTCATGACGACGCCACCACCAGCATCAACAACA
55	NCER_101900 REVERSE	ACAAGAAAGCTGGGTCAGGACGGATTCTTTTCTTCGGGGCAAACAT
55	NCER_101900 FORWARD without SP	ACAAAAAAGCAGGCTTCATGGAGAAACCAGTACTTATTGACTATCCA
56	NCER_101271 REVERSE	ACAAGAAAGCTGGGTCTGTTGCTACAAAGATAAATACTGATAAAAA
56	NCER_101271 FORWARD without SP	ACAAAAAAGCAGGCTTCATGAAAATGTCTGCTCAAAATGCTCAAACA
57	NCER_100044 REVERSE	ACAAGAAAGCTGGGTCTAAAGATGCTAATATCGCATTTTCCATCTG
57	NCER_100044 FORWARD without SP	ACAAAAAAGCAGGCTTCATGACAAATATGTTACTACAAACTAATGAA
58	NCER_100575 REVERSE	ACAAGAAAGCTGGGTCTTCATTAAAATATACAAGTTTCAGCTTTTC
58	NCER_100575 FORWARD without SP	ACAAAAAAGCAGGCTTCATGCACCATCACTGTTTAGATAATCAGCCA
59	NCER_102372 REVERSE	ACAAGAAAGCTGGGTCCTCAACTTTAAATTTTAACTTCTGCTTCAT
59	NCER_102372 FORWARD without SP	ACAAAAAAGCAGGCTTCATGAGAAAAGTTTGGTTTTCATCAAAAAAA

60	NCER_102145 REVERSE	ACAAGAAAGCTGGGTCATGTAGATAGTGAATAAACCCAACATACTT
60	NCER_102145 FORWARD without SP	ACAAAAAAGCAGGCTTCATGGCTTTTTATTCTAATGAAATATCAAAA
61	NCER_100949 REVERSE	ACAAGAAAGCTGGGTCTTGCAATAAAGATAATATCTTTTTAGGATT
61	NCER_100949 FORWARD without SP	ACAAAAAAGCAGGCTTCATGTACCTATTTAAAAAGAAAATAAAATAC
62	NCER_102103 REVERSE	ACAAGAAAGCTGGGTCATATTTTTTAATGTAATGACTGCTTCGTTT
62	NCER_102103 FORWARD without SP	ACAAAAAAGCAGGCTTCATGGATGGATCACAGAATATTTGTCAACAA
63	NCER_101938 REVERSE	ACAAGAAAGCTGGGTCGTACTTCCTTTTATTTCTAAAGCAGTATGA
63	NCER_101938 FORWARD without SP	ACAAAAAAGCAGGCTTCATGGAATATCTAAACATGACGATGACGCAT
64	NCER_100197 REVERSE	ACAAGAAAGCTGGGTCATTTAATAAGTGCTCAAACGCTTTTTTAAA
64	NCER_100197 FORWARD without SP	ACAAAAAAGCAGGCTTCATGAATTGCGATGTTGATGAAATGTTTACG
65	NCER_100216 REVERSE	ACAAGAAAGCTGGGTCTCTCGCCATTGGTTCAATTAATCGATCTGC
65	NCER_100216 FORWARD without SP	ACAAAAAAGCAGGCTTCATGACTGAAACTATGGAAATTAGTGAGCCA
66	NCER_100566 REVERSE	ACAAGAAAGCTGGGTCTTTTTCAAAACATCCAAAAGTCAATATACA
66	NCER_100566 FORWARD without SP	ACAAAAAAGCAGGCTTCATGAAATTTTGTGAAAGAGAAAATGTTGAT
67	NCER_101785 REVERSE	ACAAGAAAGCTGGGTCATCTAAATCAGAAGAATCGAGAGGAAGATC
67	NCER_101785 FORWARD without SP	ACAAAAAAGCAGGCTTCATGGCTTTATGGGTTACAGGAACGTGGCCA
68	NCER_101124 REVERSE	ACAAGAAAGCTGGGTCGTCTTTTTTTATAAATTTCCAAATTGTTGT
68	NCER_101124 FORWARD without SP	ACAAAAAAGCAGGCTTCATGGTCCCTTTAGATGCTGAAACTACCACC
69	NCER_101532 REVERSE	ACAAGAAAGCTGGGTCAAAGAAACTTCCTAATTCCTCAACGTAATT
69	NCER_101532 FORWARD without SP	ACAAAAAAGCAGGCTTCATGGTATATAACAATTTATTAGATAGTGTC
70	NCER_100347 REVERSE	ACAAGAAAGCTGGGTCACTTTGGTAAAATATTGAAATAAGATTTTC
70	NCER_100347 FORWARD without SP	ACAAAAAAGCAGGCTTCATGAACATTAACTCCCTAGATAGTAAAGTT
71	NCER_100341 REVERSE	ACAAGAAAGCTGGGTCCTTCTTGTACAAATATCTAAAGAATAATAT
71	NCER_100341 FORWARD without SP	ACAAAAAAGCAGGCTTCATGTTTAATACTATCTATAAAAAACAAACA
72	NCER_100083 REVERSE	ACAAGAAAGCTGGGTCCCTTTGAGGAGATGAAGCGATACCTAATCT
72	NCER_100083 FORWARD without SP	ACAAAAAAGCAGGCTTCATGAGAATATTAAAATCAAATAGACGGGGG
73	NCER_100056 REVERSE	ACAAGAAAGCTGGGTCTAAGTGTCTAAAAATCTGTATACCTTCAGT
73	NCER_100056 FORWARD without SP	ACAAAAAAGCAGGCTTCATGATATTTTGTAGTGAAGATATAAATGAA
74	NCER_102178 REVERSE	ACAAGAAAGCTGGGTCATTTGTCCTAAATTTCATAAAAAAATTGTT

74	NCER_102178 FORWARD without SP	ACAAAAAAGCAGGCTTCATGTCAAATATTAATACATATGAAGGCCTA
75	NCER_101590 REVERSE	ACAAGAAAGCTGGGTCTTTAGCGGGTTCTGCATCCTTGTCTTTATT
75	NCER_101590 FORWARD without SP	ACAAAAAAGCAGGCTTCATGTTTGTAGGATCTGTTCCCGGCAATAAT
76	NCER_101469 REVERSE	ACAAGAAAGCTGGGTCAGCTAAATCTCCATCATTTTCTTCATCGGA
76	NCER_101469 FORWARD without SP	ACAAAAAAGCAGGCTTCATGGAAGATGTTGATGAACAGGCATTAGAAA
77	NCER_101600 REVERSE	ACAAGAAAGCTGGGTCGACAGGATTTTTTTTCTTGTTTTCTGTCTC
77	NCER_101600 FORWARD without SP	ACAAAAAAGCAGGCTTCATGGATAACTCTCAAGAGACATGTGAAAAT
78	NCER_102300 REVERSE	ACAAGAAAGCTGGGTCTTTTAAATATTCAATAAAGAAAACGTAATT
78	NCER_102300 FORWARD without SP	ACAAAAAAGCAGGCTTCATGTTTTACTCCATTAGAATAGATGAATCT
79	NCER_101061 REVERSE	ACAAGAAAGCTGGGTCGTTAAAAGATAATTCATCTTCTTTACATGG
79	NCER_101061 FORWARD without SP	ACAAAAAAGCAGGCTTCATGACGGAACAACAGCATTTATTAGATGAT
80	NCER_101528 REVERSE	ACAAGAAAGCTGGGTCTTTTTTAAATTTTATGTAAAATTCATTGAG
80	NCER_101528 FORWARD without SP	ACAAAAAAGCAGGCTTCATGCATTTTAATACACATGAACGAATTTAT
81	NCER_101940 REVERSE	ACAAGAAAGCTGGGTCCTTTTTTGGAAATGCAATGTTAAAAAAATT
81	NCER_101940 FORWARD without SP	ACAAAAAAGCAGGCTTCATGATTTATGAGGAATTAAAAGAAGCTGTT
82	NCER_101691 REVERSE	ACAAGAAAGCTGGGTCATTATACGTCATTTTTCCTATTAAAATCTT
82	NCER_101691 FORWARD without SP	ACAAAAAAGCAGGCTTCATGAATGATATGCAAGATACAGACAGCTCA
83	NCER_102495 REVERSE	ACAAGAAAGCTGGGTCGCAAAAAAATACGGGTTCAACCCTATTATA
83	NCER_102495 FORWARD without SP	ACAAAAAAGCAGGCTTCATGATTTATGAAGATTTATTGAGCATTGTT
84	NCER_102060 REVERSE	ACAAGAAAGCTGGGTCTCTTTTTTTACTATATACTTTTTCTACAAC
84	NCER_102060 FORWARD without SP	ACAAAAAAGCAGGCTTCATGTTTGCAATCCATATATATAGGAATGAA
85	NCER_101884 REVERSE	ACAAGAAAGCTGGGTCATGTAGATAGTGAATAAACCCAACATACTT
85	NCER_101884 FORWARD without SP	ACAAAAAAGCAGGCTTCATGTTTTATTCTGATGTATTCTTAAAATAC
86	NCER_102146 REVERSE	ACAAGAAAGCTGGGTCAAATTTATTTAAATCAAAAAACTCTTTCAA
86	NCER_102146 FORWARD without SP	ACAAAAAAGCAGGCTTCATGCATATAAATTACTTCAATAATCAATTT
87	NCER_100295 REVERSE	ACAAGAAAGCTGGGTCTATGCTTAATACAATTTTGCTAAAAACGGC
87	NCER_100295 FORWARD without SP	ACAAAAAAGCAGGCTTCATGTACAATCTATTTGATGAAGAACATAAA
88	NCER_100914 REVERSE	ACAAGAAAGCTGGGTCTTCTTTTCTAAATTTCATTAAAAAATTGAT
88	NCER_100914 FORWARD without SP	ACAAAAAAGCAGGCTTCATGGACGTTAATACACACGGGGACTTTTGT

M13 Forward	GTAAAACGACGGCCAG
M13 Reverse	CAGGAAACAGCTATGAC
ATTP Forward	GGGACAAGTTTGTACAAAAAAGCAGGCTTC
ATTP Reverse	GGGGACCACTTTGTACAAGAAAGCTGGGTC
pAG423 Forward	TTCTAGAACTAGTGGATCCC
pAG423 Reverse	ACTTTGTACAAGAAAGCTGA
S. cerevisiae HIS3_Forward	ATAAGAACACCTTTGGTGGAGGGAACATCG
S. cerevisiae HIS3_Reverse	ATGACAGAGCAGAAAGCCCTAGTAAAGCGT
N. ceranae F I (Chen, 2008)	CGGATAAAAGAGTCCGTTACC
N. ceranae R I (Chen, 2008)	TGAGCAGGGTTCTAGGGAT
N. apis F I (Chen, 2008)	CCATTGCCGGATAAGAGAGT
N. apis R I (Chen, 2008)	CACGCATTGCTGCATCATTGAC
N. apis F II (M-H, 2007)	GGGGGCATGTCTTTGACGTACTATGTA
N. apis R II (M-H, 2007)	GGGGGGCGTTTAAAATGTGAAACAACTATG
N. ceranae F II (M-H, 2007)	CGGCGACGATGTGATATGAAAATATTAA
N. ceranae R II (M-H, 2007)	CCCGGTCATTCTCAAACAAAAAACCG

Appendix IV | Cellular compartment markers used from the yeast GFP collection.

Compartment/structure	Marker
Actin cytoskeleton	*Sac6*
Early Golgi/COPI	*Cop1*
Endoplasmic reticulum to Golgi	*Sec13*
Endosome	*Snf7*
Golgi apparatus	*Anp1*
Histone4	*Hhf1*
Late Golgi/clathrin	*Chc1*
Lipid particle	*Erg6*
Nuclear periphery	*Nic96*
Nucleolus	*Sik1*
Peroxisome	*Pex3*
Spindle pole	*Spc42*
Vacuoles	*Prc1*

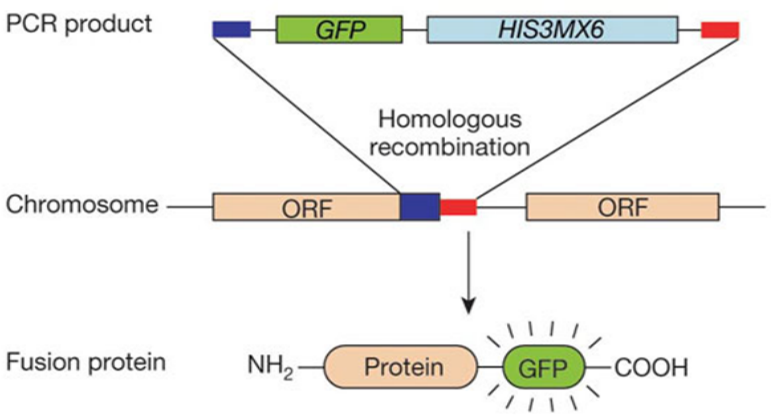

Figure IV.1 | Strategy for library construction. PCR products containing the GFP tag and a selectable marker gene were inserted at the C terminus of each ORF through homologous recombination, yielding a C-terminally GFP-tagged protein (Huh et al., 2003).

Appendix V | *N. ceranae* secretome ORFs with homologs in *N. apis.*

N. ceranae GeneID	*N. apis* GeneID	*N. apis* Protein description	BLASTP e-value
NCER_100987	EQB60498.1	3-ketodihydrosphingosine reductase	2.00E-109
NCER_100710	EQB60790.1	acid phosphatase precursor	8.00E-122
NCER_102617	EQB59843.1	chromosome segregation protein	3.00E-15
NCER_100694	EQB61299.1	coatomer subunit delta-like protein	5.00E-115
NCER_100802	EQB61315.1	dnaj-class molecular chaperone	3.00E-17
NCER_100899	EQB62005.1	e3 ubiquitin-protein ligase rfwd3	5.00E-109
NCER_102158	EQB60054.1	eukaryotic translation initiation factor 1a	2.00E-48
NCER_100135	EQB61941.1	glutamyl aminopeptidase	5.00E-53
NCER_100165	EQB60835.1	glutaredoxin 3	2.00E-17
NCER_101994	EQB59878.1	heat shock protein 70	0
NCER_101108	EQB60724.1	hexokinase	5.00E-64
NCER_101617	EQB60871.1	hydrolase of the alpha beta-hydrolase	3.00E-103
NCER_100856	EQB60817.1	n-acetylglucosaminylphosphatidylinositol de-n-acetylase family protein	3.00E-53
NCER_101263	EQB61781.1	peptidyl-prolyl cis-trans isomerase	1.00E-52
NCER_101590	EQB61988.1	polar tube protein 2	2.00E-39
NCER_101403	EQB60675.1	polysaccharide deacetylase	4.00E-67
NCER_100305	EQB60148.1	prosalpha6	9.00E-110
NCER_100813	EQB61305.1	protein disulfide isomerase	6.00E-25
NCER_101950	EQB61305.1	protein disulfide isomerase	0
NCER_101985	EQB61305.1	protein disulfide isomerase	8.00E-22
NCER_101889	EQB59936.1	protein sel-1-like protein	6.00E-117
NCER_100618	EQB61877.1	pup1p	3.00E-16
NCER_101626	EQB61529.1	putative translocation protein sec66	2.00E-29
NCER_102068	EQB60867.1	ring-box protein 1	2.00E-10
NCER_100557	EQB60379.1	serine threonine-protein kinase	5.00E-121

NCER_101082	EQB62243.1	spore wall and anchoring disk complex protein 1	7.00E-21
NCER_100295	EQB62210.1	spore wall protein 26, precursor	4.00E-51
NCER_100327	EQB61712.1	t-complex protein 1 subunit epsilon	4.00E-142
NCER_100308	EQB60312.1	t-complex protein eta subunit	2.00E-132
NCER_101900	EQB60243.1	vesicle transport v-snare protein	2.00E-42
NCER_101141	EQB62203.1	vip36-like vesicular integral membrane protein	5.00E-25
NCER_101475	EQB62198.1	hypothetical protein NAPIS_ORF00225	3.00E-37
NCER_100570	EQB62169.1	hypothetical protein NAPIS_ORF00249	3.00E-07
NCER_100566	EQB62174.1	hypothetical protein NAPIS_ORF00254	4.00E-18
NCER_100716	EQB61970.1	hypothetical protein NAPIS_ORF00455	4.00E-13
NCER_100064	EQB61910.1	hypothetical protein NAPIS_ORF00514	1.00E-13
NCER_100070	EQB61741.1	hypothetical protein NAPIS_ORF00688	2.00E-10
NCER_100382	EQB61606.1	hypothetical protein NAPIS_ORF00800	1.00E-18
NCER_100392	EQB61617.1	hypothetical protein NAPIS_ORF00811	8.00E-49
NCER_101662	EQB61564.1	hypothetical protein NAPIS_ORF00861	1.00E-77
NCER_100522	EQB61565.1	hypothetical protein NAPIS_ORF00862	4.00E-12
NCER_101663	EQB61565.1	hypothetical protein NAPIS_ORF00862	5.00E-19
NCER_102053	EQB61547.1	hypothetical protein NAPIS_ORF00869	4.00E-14
NCER_100529	EQB61483.1	hypothetical protein NAPIS_ORF00940	5.00E-47
NCER_100531	EQB61487.1	hypothetical protein NAPIS_ORF00944	9.00E-29
NCER_100532	EQB61488.1	hypothetical protein NAPIS_ORF00945	2.00E-15
NCER_100290	EQB61332.1	hypothetical protein NAPIS_ORF01100	3.00E-47
NCER_101367	EQB61193.1	hypothetical protein NAPIS_ORF01246	5.00E-74
NCER_101721	EQB61159.1	hypothetical protein NAPIS_ORF01260	5.00E-14
NCER_101416	EQB61121.1	hypothetical protein NAPIS_ORF01303	3.00E-24
NCER_101413	EQB61123.1	hypothetical protein NAPIS_ORF01305	8.00E-26
NCER_101886	EQB61101.1	hypothetical protein NAPIS_ORF01330	4.00E-15
NCER_101906	EQB60960.1	hypothetical protein NAPIS_ORF01470	9.00E-14
NCER_101271	EQB60910.1	hypothetical protein NAPIS_ORF01524	1.00E-67

NCER_100164	EQB60837.1	hypothetical protein NAPIS_ORF01589	9.00E-21
NCER_100163	EQB60838.1	hypothetical protein NAPIS_ORF01590	2.00E-26
NCER_102348	EQB60801.1	hypothetical protein NAPIS_ORF01644	3.00E-11
NCER_101591	EQB60694.1	hypothetical protein NAPIS_ORF01737	2.00E-09
NCER_100828	EQB60621.1	hypothetical protein NAPIS_ORF01820	1.00E-29
NCER_101917	EQB60583.1	hypothetical protein NAPIS_ORF01849	2.00E-54
NCER_100083	EQB60507.1	hypothetical protein NAPIS_ORF01922	6.00E-88
NCER_100626	EQB60463.1	hypothetical protein NAPIS_ORF01972	2.00E-78
NCER_100279	EQB59946.1	hypothetical protein NAPIS_ORF02469	5.00E-45
NCER_102328	EQB59872.1	hypothetical protein NAPIS_ORF02569	3.00E-60
NCER_101972	EQB59873.1	hypothetical protein NAPIS_ORF02570	3.00E-65
NCER_100526	EQB59824.1	hypothetical protein NAPIS_ORF02610	4.00E-16
NCER_101673	EQB59798.1	hypothetical protein NAPIS_ORF02626	1.00E-12
NCER_100581	EQB59805.1	hypothetical protein NAPIS_ORF02633	6.00E-11
NCER_100482	EQB59766.1	hypothetical protein NAPIS_ORF02660	3.00E-17

Appendix VI | Features of the *N. ceranae* secretome.

NcS	SignalP 4.1	TMHMM	Species specific	Pfam	BLASTP
1	Y	PredHel=0	Y	.	.
2	Y	PredHel=0	N	.	spore wall and anchoring disk complex protein [Nosema ceranae]
3	Y	PredHel=10	N	UAA transporter family	uaa transporter protein [Nosema ceranae]
4	Y	PredHel=0	N	Proteasome subunit	proteasome subunit beta type-6 [Nosema bombycis CQ1]
5	Y	PredHel=0	N	Hsp70 protein	heat shock protein 70 [Nosema apis BRL 01]
6	Y	PredHel=0	N	Glutaredoxin	hypothetical protein NAPIS_ORF01588 [Nosema apis BRL 01]
7	Y	PredHel=0	N	.	translocation protein sec66 [Nosema ceranae]
8	Y	PredHel=0	N	.	Ricin B lectin [Nosema bombycis CQ1]
9	Y	PredHel=0	N	Ribonuclease 2-5A	serine threonine-protein kinase [Nosema apis BRL 01]
10	Y	PredHel=1	N	short chain dehydrogenase	3-ketodihydrosphingosine reductase [Nosema apis BRL 01]
11	Y	PredHel=0	N	Histidine phosphatase superfamily	acid phosphatase precursor [Nosema ceranae]
12	**N**				
13	Y	PredHel=7	N	Dolichyl-phosphate-mannose-protein mannosyltransferase	dolichyl-phosphate-mannose-protein mannosyltransferase [Nosema ceranae]
14	Y	PredHel=0	N	Putative acetyl-transferase	hypothetical protein NBO_100gi002 [Nosema bombycis CQ1]
15	Y	PredHel=1	N	Thioredoxin	protein disulfide isomerase [Nosema apis BRL 01]
16	Y	PredHel=0	N	Hexokinase	hexokinase [Nosema ceranae]
17	**N**				
18	**N**				
19	Y	PredHel=0	Y	.	.
20	Y	PredHel=0	N	Proteasome subunit	proteasome alpha subunit c6 [Nosema ceranae]
21	Y	PredHel=0	Y	.	.
22	Y	PredHel=0	Y	.	.
23	Y	PredHel=1	N	.	hypothetical protein NAPIS_ORF01470 [Nosema apis BRL 01]
24	Y	PredHel=0	Y	.	.

25	Y	PredHel=0	Y	.	.
26	Y	PredHel=3	Y	.	.
27	Y	PredHel=0	Y	.	hypothetical protein CPAR2_403180 [Candida parapsilosis]
28	Y	PredHel=7	N	.	.
29	Y	PredHel=1	N	.	.
30	Y	PredHel=0	Y	.	.
31	Y	PredHel=0	Y	.	.
32	Y	PredHel=0	Y	.	.
33	Y	PredHel=1	N	.	hypothetical protein ECU06_1340 [Encephalitozoon cuniculi GB-M1]
34	Y	PredHel=0	Y	.	.
35	Y	PredHel=0	Y	.	.
36	Y	PredHel=0	Y	.	.
37	Y	PredHel=0	N	.	.
38	**N**				
39	Y	PredHel=2	Y	.	.
40	Y	PredHel=2	Y	.	.
41	Y	PredHel=1	N	Spore wall protein	hypothetical protein NAPIS_ORF02569 [Nosema apis BRL 01]
42	**N**				
43	Y	PredHel=0	N	.	.
44	**N**				
45	Y	PredHel=1	Y	.	.
46	Y	PredHel=0	Y	.	.
47	Y	PredHel=0	N	.	hypothetical protein NAPIS_ORF00869 [Nosema apis BRL 01]
48	**N**				
49	Y	PredHel=0	Y	.	alpha-l-fucosidase [Nosema ceranae]
50	Y	PredHel=1	N	.	.
51	Y	PredHel=0	N	.	polar tube protein 1, partial [Nosema ceranae]
52	Y	PredHel=1	N	.	.

53	Y	PredHel=0	N	.	hypothetical protein NBO_1136g0001 [Nosema bombycis CQ1]
54	Y	PredHel=8	N	.	.
55	Y	PredHel=1	N	.	vesicle transport v-snare protein [Nosema apis BRL 01]
56	Y	PredHel=0	N	.	hypothetical protein NAPIS_ORF01524 [Nosema apis BRL 01]
57	Y	PredHel=1	Y	.	.
58	**N**				
59	Y	PredHel=0	Y	.	.
60	Y	PredHel=0	Y	.	.
61	**N**				
62	Y	PredHel=0	Y	.	.
63	Y	PredHel=0	Y	.	.
64	Y	PredHel=0	Y	.	.
65	Y	PredHel=0	Y	.	.
66	Y	PredHel=0	N	.	.
67	**N**				
68	Y	PredHel=2	Y	.	.
69	Y	PredHel=0	Y	.	.
70	Y	PredHel=0	Y	.	.
71	**N**				
72	Y	PredHel=0	N	.	Polar tube protein 3 [Nosema bombycis CQ1]
73	Y	PredHel=1	Y	.	.
74	Y	PredHel=0	Y	.	.
75	Y	PredHel=0	N	Polar tube protein 2 from Microsporidia	polar tube protein 2, partial [Nosema ceranae]
76	Y	PredHel=0	Y	.	.
77	Y	PredHel=0	Y	Nucleoporin FG repeat region	.
78	Y	PredHel=0	Y	.	.
79	Y	PredHel=0	Y	.	.
80	**N**				

81	Y	PredHel=0	Y	.	.
82	Y	PredHel=2	Y	.	.
83	Y	PredHel=0	Y	.	.
84	Y	PredHel=1	Y	.	.
85	Y	PredHel=0	Y	.	.
86	**N**				
87	Y	PredHel=0	N	.	hypothetical protein NAPIS_ORF00269 [Nosema apis BRL 01]
88	Y	PredHel=0	Y	.	.
89	Y	PredHel=0	N	RING-H2 zinc finger	anaphase promoting complex subunit [Nosema ceranae]
90	Y	PredHel=1	N	Ring finger domain	ring finger protein 148 [Nosema ceranae]
91	Y	PredHel=0	N	Ring finger domain	e3 ubiquitin-protein ligase rfwd3 [Nosema ceranae]
92	Y	PredHel=0	N	Translation initiation factor 1A / IF-1	eukaryotic translation initiation factor 1a [Nosema ceranae]
93	Y	PredHel=0	N	Thioredoxin	protein disulfide isomerase [Nosema ceranae]
94	Y	PredHel=0	N	Thioredoxin	protein disulfide isomerase [Nosema ceranae]
95	Y	PredHel=0	N	TCP-1/cpn60 chaperonin family	t-complex protein 1 subunit eta [Nosema ceranae]
96	Y	PredHel=0	N	TCP-1/cpn60 chaperonin family	chaperonin-containing t-complex epsilon subunit cct5 [Nosema ceranae]
97	Y	PredHel=0	N	RecF/RecN/SMC N terminal domain	nuclear condensin complex subunit [Nosema ceranae]
98	Y	PredHel=0	N	Polysaccharide deacetylase	polysaccharide deacetylase [Nosema apis BRL 01]
99	Y	PredHel=0	N	Peptidase family M1	M1 family aminopeptidase 1 [Nosema bombycis CQ1]
100	Y	PredHel=0	N	Peptidase C13 family	PREDICTED: GPI-anchor transamidase-like [Papilio xuthus]
101	Y	PredHel=0	N	Glutaredoxin	glutaredoxin 3 [Nosema ceranae]
102	Y	PredHel=0	N	GlcNAc-PI de-N-acetylase	n-acetylglucosaminyl-phosphatidylinositol de-n-acetylase [Nosema ceranae]
103	Y	PredHel=1	N	.	hypothetical protein NBO_655g0001, partial [Nosema bombycis CQ1]
104	Y	PredHel=0	N	DnaJ domain	chaperone protein dnaj [Nosema ceranae] | hypothetical spore wall protein [Nosema bombycis]
105	Y	PredHel=0	N	Cyclophilin type peptidyl-prolyl cis-trans isomerase/CLD	peptidyl-prolyl cis-trans isomerase [Nosema apis BRL 01]
106	Y	PredHel=5	N	.	dolichyl-phosphate mannose protein mannosyltransferase [Nosema bombycis CQ1]

107	Y	PredHel=0	N	.	hypothetical protein NBO_12g0016 [Nosema bombycis CQ1]
108	Y	PredHel=0	N	.	PREDICTED: uncharacterized protein ECU07_1090-like [Papilio xuthus]
109	Y	PredHel=0	N	.	hydrolase of the alpha beta-hydrolase [Nosema apis BRL 01]
110	Y	PredHel=2	N	.	hypothetical protein NAPIS_ORF01849 [Nosema apis BRL 01]
111	Y	PredHel=0	N	.	hypothetical protein NBO_499gi001, partial [Nosema bombycis CQ1]
112	Y	PredHel=1	N	Sel1 repeat	hcp-like protein [Nosema ceranae]
113	Y	PredHel=0	N	.	hypothetical protein NAPIS_ORF00861 [Nosema apis BRL 01]
114	Y	PredHel=0	N	dUTPase	deoxyuridine 5 triphosphate nucleotidohydrolase [Nosema ceranae]
115	Y	PredHel=1	N	.	coatomer complex delta subunit [Nosema ceranae]
116	Y	PredHel=4	Y	.	.
117	Y	PredHel=2	Y	.	.
118	Y	PredHel=2	Y	.	.
119	Y	PredHel=2	Y	.	.
120	Y	PredHel=2	Y	.	.
121	Y	PredHel=2	Y	.	.
122	Y	PredHel=2	Y	.	.
123	Y	PredHel=1	Y	.	.
124	Y	PredHel=1	Y	.	.
125	Y	PredHel=1	Y	.	.
126	Y	PredHel=1	Y	.	.
127	Y	PredHel=1	Y	.	.
128	Y	PredHel=0	Y	.	.
129	Y	PredHel=0	Y	.	.
130	Y	PredHel=0	Y	.	.
131	Y	PredHel=0	N	.	hypothetical protein NAPIS_ORF01100 [Nosema apis BRL 01]
132	Y	PredHel=0	Y	.	.
133	Y	PredHel=0	N	.	hypothetical protein [Encephalitozoon cuniculi GB-M1]

134	Y	PredHel=0	N	.	hypothetical protein NAPIS_ORF00811 [Nosema apis BRL 01]
135	Y	PredHel=0	Y	.	.
136	Y	PredHel=0	N	.	hypothetical protein ECU09_1880 [Encephalitozoon cuniculi GB-M1]
137	Y	PredHel=0	N	.	hypothetical protein NAPIS_ORF00940 [Nosema apis BRL 01]
138	Y	PredHel=0	N	.	hypothetical protein NAPIS_ORF00944 [Nosema apis BRL 01]
139	Y	PredHel=0	N	.	hypothetical protein NAPIS_ORF00945 [Nosema apis BRL 01]
140	Y	PredHel=0	N	.	.
141	Y	PredHel=0	Y	.	.
142	Y	PredHel=0	N	.	hypothetical protein NAPIS_ORF01972 [Nosema apis BRL 01]
143	Y	PredHel=0	Y	.	.
144	Y	PredHel=0	Y	.	.
145	Y	PredHel=0	N	.	hypothetical protein NAPIS_ORF00455 [Nosema apis BRL 01]
146	Y	PredHel=0	Y	.	.
147	Y	PredHel=0	Y	.	.
148	Y	PredHel=0	Y	.	.
149	Y	PredHel=0	Y	.	.
150	Y	PredHel=0	Y	.	.
151	Y	PredHel=0	N	.	vip36-like vesicular integral membrane protein [Nosema ceranae]
152	Y	PredHel=0	Y	.	.
153	Y	PredHel=0	Y	.	.
154	Y	PredHel=0	Y	.	.
155	Y	PredHel=0	Y	.	.
156	Y	PredHel=0	Y	.	.
157	Y	PredHel=0	Y	.	.
158	Y	PredHel=0	Y	.	.
159	Y	PredHel=0	Y	.	.
160	Y	PredHel=0	Y	.	.
161	Y	PredHel=0	Y	.	.

162	Y	PredHel=0	Y	.	.
163	Y	PredHel=0	Y	.	.
164	Y	PredHel=0	Y	.	.
165	Y	PredHel=0	Y	.	.
166	Y	PredHel=0	Y	.	.
167	Y	PredHel=0	Y	.	.
168	Y	PredHel=0	Y	.	.
169	Y	PredHel=0	N	.	hypothetical protein NAPIS_ORF01330 [Nosema apis BRL 01]
170	Y	PredHel=0	Y	.	.
171	Y	PredHel=0	Y	.	.
172	Y	PredHel=0	Y	.	.
173	Y	PredHel=0	Y	.	.
174	Y	PredHel=0	Y	.	PREDICTED: transcriptional regulatory protein AlgP-like [Biomphalaria glabrata]
175	Y	PredHel=0	Y	.	.
176	Y	PredHel=0	Y	.	.
177	Y	PredHel=0	Y	.	.
178	Y	PredHel=0	Y	.	.
179	Y	PredHel=0	Y	.	.
180	Y	PredHel=0	Y	.	.
181	Y	PredHel=0	Y	.	.
182	Y	PredHel=0	Y	.	.
183	Y	PredHel=0	Y	.	.
184	Y	PredHel=0	Y	.	.
185	Y	PredHel=0	Y	.	.
186	Y	PredHel=0	Y	.	.
187	Y	PredHel=0	Y	.	.
188	Y	PredHel=0	Y	.	.

Appendix VII | *N. ceranae* secretome ORFs with homologs in *E. romaleae* as an indication of minimal secretome components.

N. ceranae **GeneID**	***E. romalaeae*** **GeneID**	***E. romalaeae*** **Protein description**	**BLASTP e-value**
NCER_100710	XP_009264759.1	acid phosphatase precursor	8E-65
NCER_100135	XP_009263970.1	aminopeptidase N	6E-34
NCER_101403	XP_009265516.1	chitooligosaccharide deacetylase-like protein	4E-46
NCER_102617	XP_009264811.1	chromosome segregation ATPase	7E-28
NCER_101276	XP_009264455.1	deoxyuridine 5'triphosphate nucleotidohydrolase	3E-19
NCER_101994	XP_009263973.1	DnaK-like protein	3E-142
NCER_101972	XP_009264679.1	dolichyl-phosphate-mannose protein O-mannosyltransferase-like protein	2E-24
NCER_100505	XP_009264093.1	dolichyl-phosphate-mannose-protein O-mannosyl transferase	0
NCER_101626	XP_009264354.1	endoplasmic reticulum translocation complex subunit Sec66	2E-13
NCER_102158	XP_009264379.1	eukaryotic translation initiation factor IF1A	7E-35
NCER_100165	XP_009265190.1	glutaredoxin	9E-07
NCER_102083	XP_009265262.1	glycosylphosphatidylinositol transamidasesubunit Gpi8	8E-48
NCER_101108	XP_009265621.1	hexokinase	2E-19
NCER_101263	XP_009265478.1	peptidyl-prolyl cis-trans isomerase	5E-39
NCER_100083	XP_009265611.1	polar tube protein 3	1E-87
NCER_100305	XP_009265355.1	proteasome alpha subunit C6	6E-76
NCER_100618	XP_009265446.1	proteasome subunit beta type-6	2E-91
NCER_100813	XP_009264048.1	protein disulfide isomerase	1E-11
NCER_101950	XP_009264048.1	protein disulfide isomerase	3E-143
NCER_101985	XP_009264048.1	protein disulfide isomerase	1E-09
NCER_100694	XP_009264945.1	putative coatomer complex subunit delta	4E-87
NCER_100987	XP_009265574.1	putative short chain dehydrogenase	3E-67
NCER_101900	XP_009264339.1	putative vesicle transport V-snare protein	2E-26
NCER_102068	XP_009263931.1	SCF ubiquitin ligase and anaphase-promoting	2E-08

NCER_101082	XP_009263902.1	spore wall and anchoring disk complex protein EnP1	9E-11
NCER_100327	XP_009264683.1	T complex protein 1 subunit epsilon	2E-115
NCER_100308	XP_009265363.1	T complex protein 1 subunit eta	0
NCER_100547	XP_009264315.1	UAA transporter protein	2E-77
NCER_101662	XP_009263869.1	hypothetical protein EROM_010270	5E-24
NCER_100279	XP_009263899.1	hypothetical protein EROM_010580	9E-38
NCER_102328	XP_009263978.1	hypothetical protein EROM_020060	2E-26
NCER_101889	XP_009264066.1	hypothetical protein EROM_020940	9E-78
NCER_101367	XP_009264274.1	hypothetical protein EROM_040060	3E-54
NCER_101721	XP_009264405.1	hypothetical protein EROM_041430	4E-17
NCER_101917	XP_009264418.1	hypothetical protein EROM_041570	1E-33
NCER_100626	XP_009264439.1	hypothetical protein EROM_050080	5E-06
NCER_100064	XP_009264535.1	hypothetical protein EROM_051070	8E-09
NCER_100899	XP_009264595.1	hypothetical protein EROM_060030	9E-59
NCER_101413	XP_009264643.1	hypothetical protein EROM_060520	1E-12
NCER_100802	XP_009264720.1	hypothetical protein EROM_061330	2E-17
NCER_101617	XP_009264835.1	hypothetical protein EROM_070870	1E-35
NCER_100531	XP_009264843.1	hypothetical protein EROM_070950	2E-11
NCER_100526	XP_009264853.1	hypothetical protein EROM_071050	2E-37
NCER_101886	XP_009264888.1	hypothetical protein EROM_071400	2E-07
NCER_101271	XP_009264932.1	hypothetical protein EROM_080120	3E-15
NCER_100856	XP_009264941.1	hypothetical protein EROM_080220	6E-55
NCER_100163	XP_009265050.1	hypothetical protein EROM_081370	1E-35
NCER_100164	XP_009265052.1	hypothetical protein EROM_081390	3E-12
NCER_102348	XP_009265054.1	hypothetical protein EROM_081410	6E-12
NCER_101475	XP_009265061.1	hypothetical protein EROM_081480	3E-17
NCER_101673	XP_009265084.1	hypothetical protein EROM_081710	4E-06
NCER_100392	XP_009265124.1	hypothetical protein EROM_090090	2E-07
NCER_101141	XP_009265206.1	hypothetical protein EROM_090930	3E-06

NCER_100382	XP_009265218.1	hypothetical protein EROM_091050	4E-21
NCER_100482	XP_009265303.1	hypothetical protein EROM_091920	1E-15

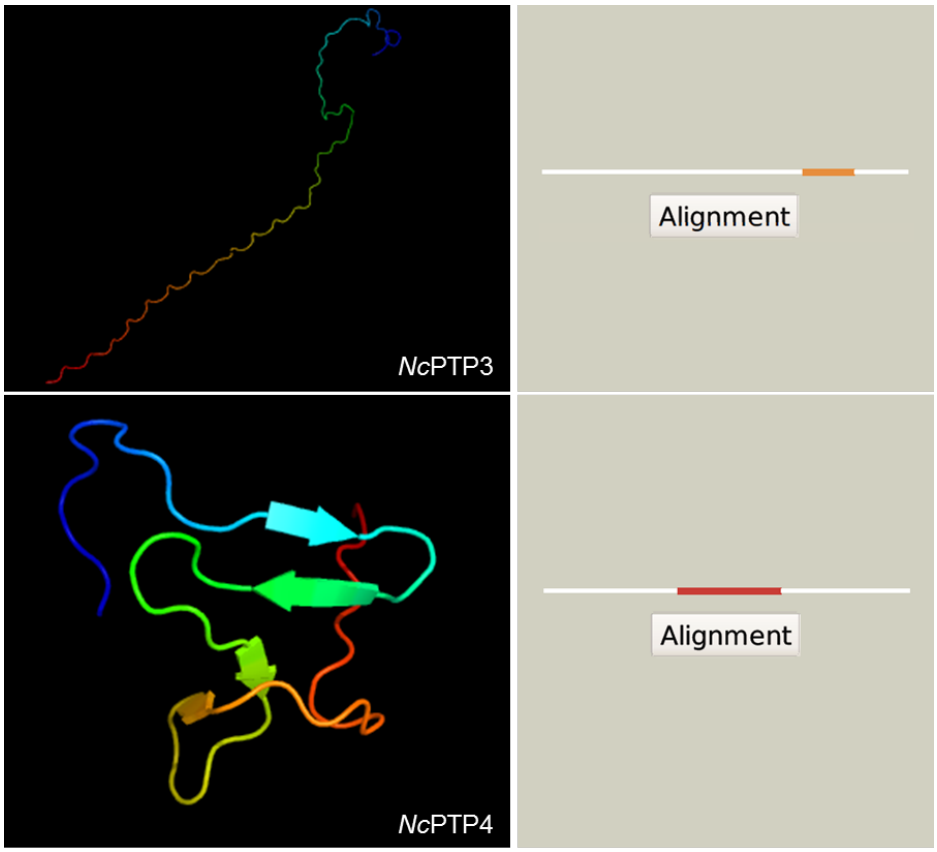

Appendix VIII | Predicted structure of *Nc*PTP3 and *Nc*PTP4.

Amino acid sequences for *Nc*PTP3 and *Nc*PTP4 were submitted to the Phyre2 server version 2.0 (http://www.sbg.bio.ic.ac.uk/phyre2/html/page.cgi?id=index) (Kelley et al., 2015). The top two panels are the results for *Nc*PTP3 showing model based on protein data bank (PDB) template c3ipkA. PDB header: cell adhesion; PDB molecule: agi/ii; PDB title: crystal structure of a3vp1 of agi/ii of *Streptococcus mutans*. 81 residues (6% of sequence) have been modelled with 89.9% confidence by the single highest scoring template. The alignment diagram on the right shows this structure occurs towards the C-terminus. Bottom two panels are the results for *Nc*PTP4 showing model based on PDB template c1xhbA. PDB header: transferase; PDB molecule: polypeptide n-acetylgalactosaminyltransferase 1; PDB title: the crystal structure of UDP-GAL-N-Ac: polypeptide α-N-2 acetylgalactosamin-yltransferase-t1. 55 residues (29% of sequence) have been modelled with 90.6% confidence by the single highest scoring template. The alignment diagram shows this structure occurs in the center of the amino acid chain.

Appendix IX | *S. cerevisiae* deletion mutants that have synthetic genetic interactions with *N. ceranae* secretome ORF-50.

Systematic name	Gene name	Full name	Gene function summary
YAL029C	MYO4	MYOsin	-
YAR003W	SWD1	Set1c, WD40 repeat protein	-
YBL091C	MAP2	Methionine AminoPeptidase	-
YBL098W	BNA4	Biosynthesis of Nicotinic Acid	Kynurenine 3-monooxygenase involved in de novo NAD biosynthesis from tryptophan; localizes to the mitochondrial outer membrane
YBR031W	RPL4A	Ribosomal Protein of the Large subunit	Subunit of the cytosolic large ribosomal subunit; involved in translation
YBR107C	IML3	Increased Minichromosome Loss	-
YBR274W	CHK1	CHeckpoint Kinase	-
YBR286W	APE3	AminoPEptidase	-
YCR009C	RVS161	Reduced Viability on Starvation	Cytoskeletal protein; forms a complex with Rvs167p and is involved in actin cytoskeleton reorganization and endocytosis; localizes to the actin cortical patch
YCR028C	FEN2	FENpropimorph resistance	-
YCR043C	-	-	Protein whose biological role is unknown; localizes to the Golgi apparatus and the mating projection tip in large-scale studies
YDL002C	NHP10	Non-Histone Protein	-
YDL115C	IWR1	Interacts With RNA polymerase II	-
YDL157C	-	-	Protein whose biological role is unknown; localizes to the mitochondrion in a large-scale study
YDL179W	PCL9	Pho85 CycLin	Component of the cyclin-dependent protein kinase holoenzyme complex; regulator of the Pho85p kinase; involved in regulation of transcription during G1/S transition of mitotic cell cycle and establishment or maintenance of cell polarity; localizes to the bud neck and incipient bud site
YDR028C	REG1	REsistance to Glucose repression	-
YDR034C	LYS14	LYSine requiring	Sequence-specific DNA-binding RNA polymerase II transcription factor that regulates expression of genes involved in lysine biosynthesis
YDR217C	RAD9	RADiation sensitive	-

YDR219C	MFB1	Mitochondria-associated F-Box protein	-
YDR272W	GLO2	GLyOxalase	-
YDR352W	YPQ2	Yeast PQ-loop protein	-
YDR363W	ESC2	Establishment of Silent Chromatin	-
YDR389W	SAC7	Suppressor of ACtin	-
YEL046C	GLY1	GLYcine requiring	-
YEL052W	AFG1	ATPase Family Gene	-
YEL060C	PRB1	PRoteinase B	-
YEL064C	AVT2	Amino acid Vacuolar Transport	Protein of unknown biological role; localizes to the endoplasmic reticulum
YER095W	RAD51	RADiation sensitive	Recombinase enzyme with DNA-dependent ATPase activity; due to its role in DNA recombination, it is involved telomere maintenance, meiotic recombination and double strand break repair; localized to nuclear chromosomes
YFR001W	LOC1	LOCalization of mRNA	-
YGL057C	GEP7	GEnetic interactors of Prohibitins	Protein whose biological role is unknown; localizes to the mitochondrion in a large-scale study
YGL205W	POX1	-	-
YGR038W	ORM1	-	-
YGR086C	PIL1	Phosphorylation Inhibited by Long chain bases	-
YGR104C	SRB5	Suppressor of RNA polymerase B	Core RNA polymerase II binding transcription factor component of the mediator complex involved in the initiation of basal RNA polymerase II transcription; binds TATA-binding protein and is involved in assembly of the RNA polymerase II transcriptional preinitiation complex; also involved in transcription termination
YGR133W	PEX4	PEroXin	Peroxisomal ubiquitin-protein ligase involved in peroxisome organization and the recycling of peroxisome targeting sequence receptors from cargo proteins back to the cytosol
YGR141W	VPS62	Vacuolar Protein Sorting	-
YGR146C	ECL1	Extends Chronological Lifespan	-
YGR159C	NSR1	-	-
YGR225W	AMA1	Activator of Meiotic APC/C	-
YGR282C	BGL2	Beta-GLucanase	-
YHR048W	YHK8	-	-

YHR100C	GEP4	GEnetic interactors of Prohibitins	-
YHR139C	SPS100	SPorulation Specific	-
YHR185C	PFS1	Prospore Formation at Spindles	-
YIL038C	NOT3	-	-
YIL128W	MET18	METhionine requiring	-
YIL138C	TPM2	TroPoMyosin	-
YIL140W	AXL2	AXiaL budding pattern	-
YIR016W	-	-	-
YJL030W	MAD2	Mitotic Arrest-Deficient	A subunit of the mitotic checkpoint complex; involved in mitotic spindle assembly checkpoint and chromosome decondensation; localizes to the condensed nuclear kinetochore and nuclear pore
YJL043W	-	-	Protein whose biological role is unknown; localizes to the mitochondrion and cytoplasm in different large-scale studies
YJL106W	IME2	Inducer of MEiosis	-
YJL116C	NCA3	Nuclear Control of ATPase	-
YJL136C	RPS21B	Ribosomal Protein of the Small subunit	Subunit of the cytosolic small ribosomal subunit; involved in rRNA processing, and translation
YJL153C	INO1	INOsitol requiring	Inositol-3-phosphate synthase involved in myo-inositol biosynthesis; localized in cytoplasm
YJL208C	NUC1	NUClease	-
YJR055W	HIT1	HIgh Temperature growth	Protein involved in C/D snoRNP assembly; localized to nucleus and cytoplasm in high-throughput studies
YJR124C	-	-	Predicted integral membrane protein whose biological role is unknown; localizes to the vacuolar membrane in a large-scale study
YKL198C	PTK1	Putative serine/Threonine protein Kinase	-
YKR017C	HEL1	Histone E3 Ligase	-
YKR019C	IRS4	Increased rDNA Silencing	-
YKR048C	NAP1	Nucleosome Assembly Protein	-
YKR057W	RPS21A	Ribosomal Protein of the Small subunit	Subunit of the cytosolic small ribosomal subunit; involved in rRNA processing, and translation
YLR025W	SNF7	Sucrose NonFermenting	-
YLR074C	BUD20	BUD site selection	-

YLR102C	APC9	Anaphase Promoting Complex	Ubiquitin transferase that is a component of the anaphase-promoting complex involved in degradation of mitotic cyclins and transition from metaphase to anaphase during mitotic cell cycle
YLR118C	-	-	-
YLR214W	FRE1	Ferric REductase	-
YLR221C	RSA3	RiboSome Assembly	-
YLR308W	CDA2	Chitin DeAcetylase	-
YLR415C	-	-	-
YLR426W	TDA5	Topoisomerase I Damage Affected	-
YLR452C	SST2	SuperSensiTive	-
YLR461W	PAU4	seriPAUperin family	-
YML022W	APT1	Adenine PhosphoribosylTransferase	-
YML032C	RAD52	RADiation sensitive	Recombinase involved in the repair of DNA double-strand breaks and single-strand postreplication gaps, as well as the formation of meiotic four-stranded branched intermediates
YML037C	-	-	Protein whose biological role is unknown; localizes to clathrin-coated vesicle
YML059C	NTE1	Neuropathy Target Esterase	-
YML097C	VPS9	Vacuolar Protein Sorting	-
YML108W	-	-	Protein whose biological role is unknown; localizes to the cytoplasm and nucleus in different large-scale studies
YML123C	PHO84	PHOsphate metabolism	-
YMR030W	RSF1	ReSpiration Factor	-
YMR139W	RIM11	Regulator of IME2	-
YMR145C	NDE1	NADH Dehydrogenase, External	-
YMR166C	MME1	Mitochondrial Magnesium Exporter	Magnesium ion exporter of the mitochondrial inner membrane; involved in magnesium ion homeostasis
YMR167W	MLH1	MutL Homolog	-
YMR171C	EAR1	Endosomal Adaptor of Rsp5p	-
YMR283C	RIT1	Ribosylation of Initiator tRNA	-
YMR310C	-	-	-

YNL031C	HHT2	Histone H Three	-
YNL071W	LAT1	-	-
YNL165W	-	-	-
YNL204C	SPS18	SPorulation-Specific	-
YNL215W	IES2	Ino Eighty Subunit	Subunit of the Ino80 complex whose biological role is unknown; localizes to the nucleus in a large-scale study
YNL271C	BNI1	Bud Neck Involved	-
YNL280C	ERG24	ERGosterol biosynthesis	-
YNL299W	TRF5	Topoisomerase one-Related Function	-
YNL305C	BXI1	BaX Inhibitor	-
YNL321W	VNX1	Vacuolar Na+/H+ eXchanger	-
YNR010W	CSE2	Chromosome SEgregation	-
YOL081W	IRA2	Inhibitory Regulator of the RAS-cAMP pathway	-
YOL119C	MCH4	MonoCarboxylate transporter Homologue	-
YOL132W	GAS4	Glycophospholipid-Anchored Surface protein	-
YOL137W	BSC6	Bypass of Stop Codon	Protein whose biological role; localizes to clathrin coated vesicles in high-throughput studies
YOR035C	SHE4	Swi5p-dependent HO Expression	-
YOR042W	CUE5	Coupling of Ubiquitin conjugation to ER degradation	Ubiquitin binding protein involved in ubiquitin-dependent protein catabolic processes; acts as an Atg8p-ubiquitin adaptor during nitrogen starvation response
YOR073W	SGO1	ShuGOshin (Japanese for "guardian spirit")	-
YOR140W	SFL1	Suppressor gene for FLocculation	-
YOR141C	ARP8	Actin-Related Protein	-
YOR165W	SEY1	Synthetic Enhancement of YOP1	-
YOR184W	SER1	SERine requiring	-
YOR293W	RPS10A	Ribosomal Protein of the Small subunit	Subunit of the cytosolic small ribosomal subunit; involved in nuclear export of rRNA and translation
YOR302W	-	-	-

YOR304C-A	BIL1	Bud6-Interacting Ligand	-
YOR305W	RRG7	Required for Respiratory Growth	Protein whose biological role is unknown; localizes to the mitochondrion in a large-scale study
YOR355W	GDS1	-	-
YOR368W	RAD17	RADiation sensitive	-
YPL002C	SNF8	Sucrose NonFermenting	-
YPL013C	MRPS16	Mitochondrial Ribosomal Protein, Small subunit	Component of the small subunit of the mitochondrial ribosome, which mediates translation in the mitochondrion
YPL057C	SUR1	SUppressor of Rvs161 and rvs167 mutations	-
YPL256C	CLN2	CycLiN	Cyclin-dependent protein kinase (CDK) regulatory subunit involved in regulating passage through the cell cycle, as well as cell cycle re-entry after pheromone-induced arrest; localizes to both the cytoplasm and nucleus
YPR020W	ATP20	ATP synthase	Subunit of the F0 coupling factor of mitochondrial F1F0 ATP synthase; also has a role in formation of dimers and oligomers of the complex; ATP synthase complex is localized to the mitochondrial inner membrane
YPR071W	-	-	Predicted integral membrane protein whose biological role is unknown
YPR073C	LTP1	-	-
YPR122W	AXL1	AXiaL budding	-
YPR128C	ANT1	Adenine Nucleotide Transporter	-
YPR179C	HDA3	Histone DeAcetylase	-

Appendix X | *S. cerevisiae* deletion mutants that have synthetic genetic interactions with *N. ceranae* secretome ORF-65.

Systematic name	Gene name	Full name	Gene function summary
YNL089C	-	-	-
YNL155W	CUZ1	Cdc48-associated UBL/Zn-finger protein	Protein that binds to proteasomes and has roles in ubiquitin-dependent protein catabolism and the response to arsenic; localizes to both the nucleus and cytoplasm
YNL242W	ATG2	AuTophaGy related	Protein involved in macroautophagy, cytoplasm-to-vacuole targeting (CVT) pathway, mitochondrial, peroxisomal degradation, autophagic vacuole assembly, late nucleophagy, piecemeal microautophagy of nucleus; localizes to the cytoplasm and the pre-autophagosomal structure (PAS)
YNL278W	CAF120	CCR4 Associated Factor	-
YNL324W	-	-	-
YNR045W	PET494	PETite colonies	-
YOL018C	TLG2	T-snare affecting a Late Golgi compartment	-
YOL046C	-	-	-
YOL071W	SDH5	Succinate DeHydrogenase	-
YOL075C	-	-	-
YOL108C	INO4	INOsitol requiring	Component of sequence specific DNA-binding heteromeric transcription factor Ino2/Ino4p that activates transcription of genes involved in phospholipid metabolism
YOR030W	DFG16	Defective for Filamentous Growth	-
YOR059C	LPL1	LD phospholipase	-
YOR112W	CEX1	Cytoplasmic EXport protein	-
YOR124C	UBP2	UBiquitin-specific Protease	-
YOR129C	AFI1	ArF3-Interacting protein	-
YOR251C	TUM1	ThioUridine Modification	-
YOR277C	-	-	-
YOR343C	-	-	-
YOR344C	TYE7	Ty1-mediated Expression	-

YOR378W	AMF1	AMmonium Facilitator	-
YPL038W	MET31	METhionine requiring	-
YPL040C	ISM1	Isoleucyl tRNA Synthetase of Mitochondria	-
YPL041C	MRX11	Mitochondrial organization of gene expression	-
YPL101W	ELP4	ELongator Protein	-
YPL193W	RSA1	RiboSome Assembly	-
YPL194W	DDC1	DNA Damage Checkpoint	-
YPL223C	GRE1	Genes de Respuesta a Estres (spanish for stress responsive genes)	Protein whose biological role is unknown; localizes to the cytoplasm in different large-scale studies
YPL227C	ALG5	Asparagine-Linked Glycosylation	-
YPL272C	PBI1	PSTB2 Interacting protein 1	-
YPL273W	SAM4	S-AdenosylMethionine metabolism	-
YPR014C	-	-	-
YPR018W	RLF2	Rap1 protein Localization Factor	-
YPR039W	-	-	-
YNL089C	-	-	-
YNL155W	CUZ1	Cdc48-associated UBL/Zn-finger protein	Protein that binds to proteasomes and has roles in ubiquitin-dependent protein catabolism and the response to arsenic; localizes to both the nucleus and cytoplasm
YNL242W	ATG2	AuTophaGy related	Protein involved in macroautophagy, cytoplasm-to-vacuole targeting (CVT) pathway, mitochondrial, peroxisomal degradation, autophagic vacuole assembly, late nucleophagy, piecemeal microautophagy of nucleus; localizes to the cytoplasm and the pre-autophagosomal structure (PAS)
YNL278W	CAF120	CCR4 Associated Factor	-
YNL324W	-	-	-
YNR045W	PET494	PETite colonies	-
YOL018C	TLG2	T-snare affecting a Late Golgi compartment	-
YOL046C	-	-	-
YOL071W	SDH5	Succinate DeHydrogenase	-

YOL075C	-	-	-
YOL108C	INO4	INOsitol requiring	Component of sequence specific DNA-binding heteromeric transcription factor Ino2/Ino4p that activates transcription of genes involved in phospholipid metabolism
YOR030W	DFG16	Defective for Filamentous Growth	-
YOR059C	LPL1	LD phospholipase	-
YOR112W	CEX1	Cytoplasmic EXport protein	-
YOR124C	UBP2	UBiquitin-specific Protease	-
YOR129C	AFI1	ArF3-Interacting protein	-
YOR251C	TUM1	ThioUridine Modification	-
YOR277C	-	-	-
YOR343C	-	-	-
YOR344C	TYE7	Ty1-mediated Expression	-
YOR378W	AMF1	AMmonium Facilitator	-
YPL038W	MET31	METhionine requiring	-
YPL040C	ISM1	Isoleucyl tRNA Synthetase of Mitochondria	-
YPL041C	MRX11	Mitochondrial organization of gene expression	-
YPL101W	ELP4	ELongator Protein	-
YPL193W	RSA1	RiboSome Assembly	-
YPL194W	DDC1	DNA Damage Checkpoint	-
YPL223C	GRE1	Genes de Respuesta a Estres (spanish for stress responsive genes)	Protein whose biological role is unknown; localizes to the cytoplasm in different large-scale studies
YPL227C	ALG5	Asparagine-Linked Glycosylation	-
YPL272C	PBI1	PSTB2 Interacting protein 1	-
YPL273W	SAM4	S-AdenosylMethionine metabolism	-
YPR014C	-	-	-
YPR018W	RLF2	Rap1 protein Localization Factor	-
YPR039W	-	-	-

YNL089C	-	-	-
YNL155W	CUZ1	Cdc48-associated UBL/Zn-finger protein	Protein that binds to proteasomes and has roles in ubiquitin-dependent protein catabolism and the response to arsenic; localizes to both the nucleus and cytoplasm
YNL242W	ATG2	AuTophaGy related	Protein involved in macroautophagy, cytoplasm-to-vacuole targeting (CVT) pathway, mitochondrial, peroxisomal degradation, autophagic vacuole assembly, late nucleophagy, piecemeal microautophagy of nucleus; localizes to the cytoplasm and the pre-autophagosomal structure (PAS)
YNL278W	CAF120	CCR4 Associated Factor	-
YNL324W	-	-	-
YNR045W	PET494	PETite colonies	-
YOL018C	TLG2	T-snare affecting a Late Golgi compartment	-
YOL046C	-	-	-
YOL071W	SDH5	Succinate DeHydrogenase	-
YOL075C	-	-	-
YOL108C	INO4	INOsitol requiring	Component of sequence specific DNA-binding heteromeric transcription factor Ino2/Ino4p that activates transcription of genes involved in phospholipid metabolism
YOR030W	DFG16	Defective for Filamentous Growth	-
YOR059C	LPL1	LD phospholipase	-
YOR112W	CEX1	Cytoplasmic EXport protein	-
YOR124C	UBP2	UBiquitin-specific Protease	-
YOR129C	AFI1	ArF3-Interacting protein	-
YOR251C	TUM1	ThioUridine Modification	-
YOR277C	-	-	-
YOR343C	-	-	-
YOR344C	TYE7	Ty1-mediated Expression	-
YOR378W	AMF1	AMmonium Facilitator	-
YPL038W	MET31	METhionine requiring	-
YPL040C	ISM1	Isoleucyl tRNA Synthetase of Mitochondria	-
YPL041C	MRX11	Mitochondrial organization of gene expression	-

YPL101W	ELP4	ELongator Protein	-
YPL193W	RSA1	RiboSome Assembly	-
YPL194W	DDC1	DNA Damage Checkpoint	-
YPL223C	GRE1	Genes de Respuesta a Estres (spanish for stress responsive genes)	Protein whose biological role is unknown; localizes to the cytoplasm in different large-scale studies
YPL227C	ALG5	Asparagine-Linked Glycosylation	-
YPL272C	PBI1	PSTB2 Interacting protein 1	-
YPL273W	SAM4	S-AdenosylMethionine metabolism	-
YPR014C	-	-	-
YPR018W	RLF2	Rap1 protein Localization Factor	-
YPR039W	-	-	-
YNL089C	-	-	-
YNL155W	CUZ1	Cdc48-associated UBL/Zn-finger protein	Protein that binds to proteasomes and has roles in ubiquitin-dependent protein catabolism and the response to arsenic; localizes to both the nucleus and cytoplasm
YNL242W	ATG2	AuTophaGy related	Protein involved in macroautophagy, cytoplasm-to-vacuole targeting (CVT) pathway, mitochondrial, peroxisomal degradation, autophagic vacuole assembly, late nucleophagy, piecemeal microautophagy of nucleus; localizes to the cytoplasm and the pre-autophagosomal structure (PAS)
YNL278W	CAF120	CCR4 Associated Factor	-
YNL324W	-	-	-
YNR045W	PET494	PETite colonies	-
YOL018C	TLG2	T-snare affecting a Late Golgi compartment	-
YOL046C	-	-	-
YOL071W	SDH5	Succinate DeHydrogenase	-
YOL075C	-	-	-
YOL108C	INO4	INOsitol requiring	Component of sequence specific DNA-binding heteromeric transcription factor Ino2/Ino4p that activates transcription of genes involved in phospholipid metabolism
YOR030W	DFG16	Defective for Filamentous Growth	-
YOR059C	LPL1	LD phospholipase	-

YOR112W	CEX1	Cytoplasmic EXport protein	-
YOR124C	UBP2	UBiquitin-specific Protease	-
YOR129C	AFI1	ArF3-Interacting protein	-
YOR251C	TUM1	ThioUridine Modification	-
YOR277C	-	-	-
YOR343C	-	-	-
YOR344C	TYE7	Ty1-mediated Expression	-
YOR378W	AMF1	AMmonium Facilitator	-
YPL038W	MET31	METhionine requiring	-
YPL040C	ISM1	Isoleucyl tRNA Synthetase of Mitochondria	-
YPL041C	MRX11	Mitochondrial organization of gene expression	-
YPL101W	ELP4	ELongator Protein	-
YPL193W	RSA1	RiboSome Assembly	-
YPL194W	DDC1	DNA Damage Checkpoint	-
YPL223C	GRE1	Genes de Respuesta a Estres (spanish for stress responsive genes)	Protein whose biological role is unknown; localizes to the cytoplasm in different large-scale studies
YPL227C	ALG5	Asparagine-Linked Glycosylation	-
YPL272C	PBI1	PSTB2 Interacting protein 1	-
YPL273W	SAM4	S-AdenosylMethionine metabolism	-
YPR014C	-	-	-
YPR018W	RLF2	Rap1 protein Localization Factor	-
YPR039W	-	-	-
YNL089C	-	-	-
YNL155W	CUZ1	Cdc48-associated UBL/Zn-finger protein	Protein that binds to proteasomes and has roles in ubiquitin-dependent protein catabolism and the response to arsenic; localizes to both the nucleus and cytoplasm
YNL242W	ATG2	AuTophaGy related	Protein involved in macroautophagy, cytoplasm-to-vacuole targeting (CVT) pathway, mitochondrial, peroxisomal degradation, autophagic vacuole assembly, late nucleophagy, piecemeal microautophagy of nucleus; localizes to the cytoplasm and

			the pre-autophagosomal structure (PAS)
YNL278W	CAF120	CCR4 Associated Factor	-
YNL324W	-	-	-
YNR045W	PET494	PETite colonies	-
YOL018C	TLG2	T-snare affecting a Late Golgi compartment	-
YOL046C	-	-	-
YOL071W	SDH5	Succinate DeHydrogenase	-
YOL075C	-	-	-

Appendix XI | *S. cerevisiae* deletion mutants that have synthetic genetic interactions with *N. ceranae* secretome ORF-68.

Systematic name	Gene name	Full name	Gene function summary
YAR018C	KIN3	protein KINase	-
YBL007C	SLA1	Synthetic Lethal with ABP1	-
YBL012C	-	-	-
YBL016W	FUS3	cell FUSion	MAP kinase involved in pheromone-dependent signal transduction during mating; has a role in invasive growth in response to glucose limitation and negative regulation of MAPK cascade; localized to both the nucleus and mating projection tip
YBR007C	DSF2	Deletion Suppressor of mptFive/pufFive mutation	Protein whose biological role is unknown; localizes to the bud tip in large scale studies
YBR008C	FLR1	FLuconazole Resistance	-
YBR012C	-	-	-
YBR028C	YPK3	-	-
YBR098W	MMS4	Methyl MethaneSulfonate sensitivity	Subunit of Holliday junction resolvase complex that contributes to crossover junction endodeoxyribonuclease activity; involved in cellular response to DNA damage stimulus, reciprocal meiotic recombination, DNA toplogical changes and repair
YBR100W	-	-	-

YCL001W	RER1	Retention in the Endoplasmic Reticulum	-
YDL069C	CBS1	Cytochrome B Synthesis	-
YDL071C	-	-	-
YDR069C	DOA4	Degradation Of Alpha	-
YDR098C	GRX3	GlutaRedoXin	-
YDR181C	SAS4	Something About Silencing	-
YDR263C	DIN7	DNA Damage INducible	-
YEL007W	MIT1	Muc1 expressed Independent of TEC1	Protein whose biological role is unknown; localizes to the nucleus and cytoplasm in a large scale study
YEL033W	MTC7	Maintenance of Telomere Capping	-
YER010C	-	-	-
YGL101W	-	-	Protein whose biological role is unknown; localizes to the nucleus and cytoplasm in a large-scale study
YGL104C	VPS73	Vacuolar Protein Sorting	-
YGR217W	CCH1	-	-
YGR233C	PHO81	PHOsphate metabolism	-
YGR247W	CPD1	Cyclic nucleotide PhosphoDiesterase	-
YHR160C	PEX18	PEroXin	Peroxisomal protein involved in the import of proteins into the peroxisomal matrix
YIL108W	-	-	Protein whose biological role is unknown; localizes to the cytoplasm in large scale studies
YJL142C	IRC9	Increased Recombination Centers	-
YJR003C	MRX12	Mitochondrial organization of gene expression	Protein whose biological role is unknown; localizes to the mitochondrion in different large-scale studies
YKL048C	ELM1	ELongated Morphology	Serine/threonine kinase; involved in cytokinesis, septin ring assembly, cell morphogenesis and bud growth; localizes to the bud neck
YKL072W	STB6	Sin Three Binding protein	-
YKL081W	TEF4	Translation Elongation Factor	-
YKR023W	-	-	Protein whose biological role is unknown; localizes to the cytoplasm and mitochondrion in large-scale studies
YKR106W	GEX2	Glutathione EXchanger	-

YLL051C	FRE6	Ferric REductase	-
YLR012C	-	-	-
YLR173W	-	-	Protein whose biological role is unknown; localizes to the vacuolar membrane in a large-scale study
YLR203C	MSS51	Mitochondrial Splicing Suppressor	-
YLR401C	DUS3	DihydroUridine Synthase	-
YLR404W	SEI1	SEIpin	Protein of the endoplasmic reticulum involved in lipid droplet biogenesis
YMR024W	MRPL3	Mitochondrial Ribosomal Protein, Large subunit	Component of the large subunit of the mitochondrial ribosome, which mediates translation in the mitochondrion
YNL063W	MTQ1	Methyltransferase	-
YNL090W	RHO2	Ras HOmolog	-
YNL092W	-	-	Protein methyltransferase of unknown localization
YNL095C	-	-	Predicted integral membrane protein whose biological role is unknown
YNL125C	ESBP6	-	-
YNL183C	NPR1	Nitrogen Permease Reactivator	-
YNL190W	-	-	-
YOL031C	SIL1	Suppressor of the Ire1/Lhs1 double mutant	-
YOL151W	GRE2	Genes de Respuesta a Estres (stress responsive genes)	-
YOR043W	WHI2	WHIskey	-
YOR078W	BUD21	BUD site selection	-
YOR079C	ATX2	AnTioXidant	Manganese ion transmembrane transporter involved in manganese ion homeostasis; localizes to the Golgi membrane
YOR267C	HRK1	Hygromycin Resistance Kinase	-
YOR271C	FSF1	Fungal SideroFlexin 1	Predicted integral membrane protein whose biological role is unknown; localizes to the mitochondrion in different large-scale studies
YPL101W	ELP4	ELongator Protein	-
YPR160W	GPH1	Glycogen PHosphorylase	-

Appendix XII | *S. cerevisiae* deletion mutants that have synthetic genetic interactions with *N. ceranae* secretome ORF-79.

Systematic name	Gene name	Full name	Gene function summary
YAL039C	CYC3	CYtochrome C	-
YBL075C	SSA3	Stress-Seventy subfamily A	ATPase involved in protein folding
YBR026C	ETR1	2-Enoyl Thioester Reductase	-
YBR032W	-	-	-
YBR040W	FIG1	Factor-Induced Gene	-
YBR069C	TAT1	Tyrosine and tryptophan Amino acid Transporter	-
YBR106W	PHO88	PHOsphate metabolism	-
YBR125C	PTC4	Phosphatase Two C	-
YBR132C	AGP2	high-Affinity Glutamine Permease	Polyamine transmembrane protein that positively regulates the traport of (R)-carnitine and polyamines across membranes; localizes to plasma, vacuole, and endoplasmic reticulum membranes
YBR184W	-	-	-
YBR189W	RPS9B	Ribosomal Protein of the Small subunit	Subunit of the cytosolic small ribosomal subunit; involved in maturation of the small subunit rRNA, and the regulation of translational fidelity
YBR231C	SWC5	SWr Complex	-
YBR239C	ERT1	Ethanol Regulated Transcription factor	-
YBR282W	MRPL27	Mitochondrial Ribosomal Protein, Large subunit	Component of the large subunit of the mitochondrial ribosome, which mediates translation in the mitochondrion
YBR286W	APE3	AminoPEptidase	-
YCL033C	MXR2	peptide Methionine sulfoXide Reductase	-
YCR033W	SNT1	SaNT domains	-
YCR085W	-	-	-
YCR106W	RDS1	Regulator of Drug Sensitivity	-
YDL009C	-	-	-

YDL057W	-	-	-
YDL091C	UBX3	UBiquitin regulatory X	-
YDL117W	CYK3	CYtoKinesis	-
YDL191W	RPL35A	Ribosomal Protein of the Large subunit	Subunit of the cytosolic large ribosomal subunit; involved in maturation of the large subunit rRNA, and translation
YDR225W	HTA1	Histone h Two A	-
YDR289C	RTT103	Regulator of Ty1 Transposition	-
YDR306C	-	-	-
YDR371W	CTS2	ChiTinaSe	-
YDR386W	MUS81	MMS and UV Sensitive	-
YEL062W	NPR2	Nitrogen Permease Regulator	Subunit of SEACIT, a subcomplex of the SEA complex that acts as a GTPase-activating protein (GAP) to negatively regulates signaling through the heterodimeric Gtr1p-Gtr2p GTPase; negative regulator of TORC1 signaling in response to amino acid deprivation; positive regulator of autophagy and autophagosome formation; loosely associated with the vacuolar membrane
YER056C	FCY2	FluoroCYtosine resistance	-
YER060W	FCY21	FluoroCYtosine resistance	-
YFL011W	HXT10	HeXose Transporter	-
YFR021W	ATG18	AuTophaGy related	Subunit of the phosphatidylinositol 3-kinase complex that binds phosphatidylinositol-3,5-bisphosphate and ubiquitin; involved in macroautophagy, cytoplasm-to-vacuole targeting (CVT) pathway late nucleophagy, peroxisomal degradation, piecemeal microautophagy of nucleus, vacuolar protein processing and late endosome to vacuole transport; localizes to the pre-autophagosomal structure (PAS)
YGL010W	MPO1	Metabolism of PHS to Odd-numbered fatty acids	Protein required for degradation of sphingoid bases; localized in the endoplasmic reticulum
YGL037C	PNC1	Pyrazinamidase and NiCotinamidase	-
YGL079W	KXD1	KxDL homologue	-
YGL244W	RTF1	Restores TBP Function	Non-DNA binding transcription factor; subunit of the CDc73/Paf1 transcription elongation complex; involved in regulation of transcription from RNA Pol I and II promoters, snoRNA 3'-end processing, regulation of histone H2B ubiquitination and H3 methylation and other cellular processes
YGR096W	TPC1	Thiamine Pyrophosphate Carrier	-

YGR203W	YCH1	Yeast Cdc25 Homologue	-
YGR230W	BNS1	Bypasses Need for Spo12p	-
YGR270W	YTA7	Yeast Tat-binding Analog	-
YHR039C	MSC7	Meiotic Sister-Chromatid recombination	-
YHR075C	PPE1	Phosphoprotein Phosphatase methylEsterase	Putative protein C-terminal demethylase that acts on protein phosphatase 2A; also identified as a component of the small subunit of the mitochondrial ribosome
YHR097C	-	-	Protein whose biological role is unknown; localizes to the nuclear periphery in a classical study and to nucleus and cytoplasm in a large scale study
YHR200W	RPN10	Regulatory Particle Non-ATPase	-
YHR210C	-	-	-
YIL055C	-	-	Protein whose biological role is unknown; localizes to the mitochondrion in a large scale study
YIL059C	-	-	-
YIL092W	-	-	Protein whose biological role is unknown; localizes to the nucleus and cytoplasm in a large-scale study
YIL097W	FYV10	Function required for Yeast Viability	-
YIL123W	SIM1	Start Independent of Mitosis	-
YJL062W	LAS21	Local Anestheticum Sensitive	-
YJL119C	-	-	-
YJL131C	AIM23	Altered Inheritance rate of Mitochondria	Initiation factor for mitochondrial translation
YJL206C	-	-	-
YJL208C	NUC1	NUClease	-
YJR117W	STE24	STErile	Metalloendopeptidase involved in the CAAX-box dependent processing and maturation of a-factor mating pheromone; localizes to both the inner nuclear membrane, and integral to the endoplasmic reticulum membrane
YJR124C	-	-	Predicted integral membrane protein whose biological role is unknown; localizes to the vacuolar membrane in a large-scale study
YJR144W	MGM101	Mitochondrial Genome Maintenance	A single-strand DNA binding protein involved in recombinatorial mitochondrial DNA repair process to maintain mitochondrial genome; localized to the mitochondrial nucleoid
YKL029C	MAE1	MAlic Enzyme	-

YKL079W	SMY1	Suppressor of MYo2-66	-
YKL086W	SRX1	SulfiRedoXin	-
YKR104W	-	-	-
YLL056C	-	-	-
YLR044C	PDC1	Pyruvate DeCarboxylase	Pyruvate decarboxylase involved in amino acid catabolism and the fermentation of glucose to ethanol; localizes to both the nucleus and the cytosol
YLR067C	PET309	PETite colonies	-
YLR182W	SWI6	SWItching deficient	Transcription cofactor that activates transcription by RNA polymerase II during heat stress and during the G1/S mitotic transition; also regulates meiotic recombination; component of both the MBF and SBF complexes
YLR303W	MET17	METhionine requiring	Bifunctional enzyme with O-acetylserine and O-acetylhomoserine sulfhydrylase activities involved in methionine and cysteine metabolism; catalyses the reaction between acetylated serine or homoserine with thiol to produce the corresponding amino acids; localized to the cytoplasm and plasma membrane
YLR443W	ECM7	ExtraCellular Mutant	-
YML084W	-	-	-
YML086C	ALO1	D-Arabinono-1,4-Lactone Oxidase	-
YML095C	RAD10	RADiation sensitive	-
YML121W	GTR1	GTp binding protein Resemblance	-
YMR024W	MRPL3	Mitochondrial Ribosomal Protein, Large subunit	Component of the large subunit of the mitochondrial ribosome, which mediates translation in the mitochondrion
YMR070W	MOT3	Modifier of Transcription	-
YMR136W	GAT2	-	-
YMR141C	-	-	-
YMR182C	RGM1	-	-
YMR195W	ICY1	Interacting with the CYtoskeleton	Protein whose biological role is unknown; localizes to the vacuolar membrane in a large-scale study
YMR230W	RPS10B	Ribosomal Protein of the Small subunit	Subunit of the cytosolic small ribosomal subunit; involved in nuclear export of rRNA and translation
YNL015W	PBI2	Proteinase B Inhibitor	-
YNL116W	DMA2	Defective in Mitotic Arrest	Ubiquitin protein ligase involved in septin ring assembly and organization, and the mitotic spindle orientation checkpoint
YNL166C	BNI5	Bud Neck Involved	Protein that binds to the septin ring at the bud neck; recruits myosin to the bud neck

YNL170W	-	-	-
YNL184C	-	-	-
YNL275W	BOR1	BORon transporter	Transmembrane, plasma membrane localized boron efflux transporter; involved in vacuolar protein trafficking
YNL280C	ERG24	ERGosterol biosynthesis	-
YNL288W	CAF40	CCR4 Associated Factor	-
YNL329C	PEX6	PEroXin	Peroxisomal ATPase involved in replicative cell aging and the recycling of peroxisome targeting sequence receptors from cargo proteins back to the cytosol
YNL335W	DDI3	DNA Damage Inducible	Cyanamide hydratase involved in detoxification of cyanamide
YOL003C	PFA4	Protein Fatty Acyltransferase	-
YOL020W	TAT2	Tryptophan Amino acid Transporter	-
YOL029C	-	-	-
YOL063C	CRT10	Constitutive RNR Transcription regulators	-
YOL067C	RTG1	ReTroGrade regulation	-
YOL118C	-	-	-
YOL153C	-	-	-
YOR041C	-	-	-
YOR079C	ATX2	AnTioXidant	Manganese ion transmembrane transporter involved in manganese ion homeostasis; localizes to the Golgi membrane
YOR084W	LPX1	Lipase of PeroXisomes	-
YOR139C	-	-	-
YOR154W	SLP1	SUN-Like Protein	-
YOR166C	SWT1	Synthetically lethal With Trex	-
YOR167C	RPS28A	Ribosomal Protein of the Small subunit	Subunit of the cytosolic small ribosomal subunit; involved in nuclear rRNA export, implicated in mRNA decay
YOR255W	OSW1	Outer Spore Wall	-
YOR317W	FAA1	Fatty Acid Activation	-
YPL055C	LGE1	LarGE cells	-
YPL107W	-	-	Protein whose biological role is unknown; localizes to the mitochondrion in a large-scale study

YPL193W	RSA1	RiboSome Assembly	-
YPL249C	GYP5	Gtpase-activating protein for Ypt Proteins	-
YPL271W	ATP15	ATP synthase	Subunit of the central stalk of the F1 catalytic core of mitochondrial F1F0 ATP synthase; ATP synthase complex is localized to the mitochondrial inner membrane
YPR047W	MSF1	Mitochondrial aminoacyl-tRNA Synthetase, Phenylalanine (F)	-
YPR079W	MRL1	Mannose 6-phosphate Receptor Like	-
YPR118W	MRI1	MethylthioRibose-1-phosphate Isomerase	A S-methyl-5-thioribose-1-phosphate isomerase involved in the generation of L-methionine from methylthioadenosine; cellular process unknown
YPR120C	CLB5	CycLin B	Cyclin-dependent kinase regulatory subunit involved in the regulation of both G1/S and G2/M phase transitions of the mitotic cell cycle; regulates mitotic and premeiotic DNA replication, as well as mitotic spindle assembly; localizes to the nucleus
YPR200C	ARR2	ARsenicals Resistance	-

Appendix XIII | *S. cerevisiae* deletion mutants that have synthetic genetic interactions with *N. ceranae* secretome ORF-85.

Systematic name	Gene name	Full name	Gene function summary
YAL015C	NTG1	eNdonuclease Three-like Glycosylase	-
YAL056W	GPB2	-	-
YAL067C	SEO1	Suppressor of sulfoxyde EthiOnine resistance	Putative transporter based on sequence similarity to membrane transporter gene families
YAR003W	SWD1	Set1c, WD40 repeat protein	-
YAR014C	BUD14	BUD site selection	-
YBL017C	PEP1	carboxyPEPtidase Y-deficient	-
YBL044W	-	-	-
YBR031W	RPL4A	Ribosomal Protein of the Large subunit	Subunit of the cytosolic large ribosomal subunit; involved in translation

YBR145W	ADH5	Alcohol DeHydrogenase	NAD-dependent alcohol dehydrogenase that converts ethanol to acetylaldehyde
YBR215W	HPC2	Histone Periodic Control	DNA- and nucleosome-binding subunit of the HIR complex; involved in nucleosome assembly and transcription regulation involved in the G1/S transition of the mitotic cell cycle
YBR229C	ROT2	Reversal Of Tor2 lethality	-
YBR244W	GPX2	Glutathione PeroXidase	-
YBR274W	CHK1	CHeckpoint Kinase	-
YBR286W	APE3	AminoPEptidase	-
YBR291C	CTP1	Citrate Transport Protein	-
YCL030C	HIS4	HIStidine requiring	-
YCL033C	MXR2	peptide Methionine sulfoXide Reductase	-
YCL044C	MGR1	Mitochondrial Genome Required	-
YCR043C	-	-	Protein whose biological role is unknown; localizes to the Golgi apparatus and the mating projection tip in large-scale studies
YCR076C	FUB1	FUnction of Boundary	Proteasome-binding protein whose biological role is unknown
YDL093W	PMT5	Protein O-MannosylTransferase	-
YDL197C	ASF2	Anti-Silencing Function	-
YDL198C	GGC1	GDP/GTP Carrier	-
YDR030C	RAD28	RADiation sensitive	-
YDR032C	PST2	Protoplasts-SecreTed	Protein whose biological role is unknown; colocalizes with membrane rafts; localizes to cytoplasm, mitochondrion and plasma membranes in a large-scale study
YDR108W	TRS85	TRapp Subunit	-
YDR155C	CPR1	Cyclosporin A-sensitive Proline Rotamase	-
YDR222W	-	-	Protein whose biological role is unknown; localizes to the cytoplasm in a large-scale study
YDR293C	SSD1	Suppressor of SIT4 Deletion	-
YDR333C	RQC1	Ribosome Quality Control	Subunit of the ribosome quality control (RQC) complex, which is a ribosome bound complex involved in the ubiquitin-dependent degradation of aberrant translation products
YDR421W	ARO80	AROmatic amino acid requiring	Sequence specific DNA-binding transcriptional activator of genes involved in aromatic amino acid catabolism; localized to nucleus

YDR436W	PPZ2	Protein Phosphatase Z	-
YDR511W	SDH7	Succinate DeHydrogenase	Protein involved in gluconeogenisis regulation and carbon utilization; localized to mitochondrial intermembrane space
YEL013W	VAC8	VACuole related	-
YER039C	HVG1	Homologous to VRG4	Predicted integral membrane protein whose biological role is unknown
YER092W	IES5	Ino Eighty Subunit	-
YER095W	RAD51	RADiation sensitive	Recombinase enzyme with DNA-dependent ATPase activity; due to its role in DNA recombination, it is involved telomere maintenance, meiotic recombination and double strand break repair; localized to nuclear chromosomes
YFR026C	ULI1	Upr-L-Inducible gene	-
YGL058W	RAD6	RADiation sensitive	-
YGL205W	POX1	-	-
YGL255W	ZRT1	Zinc-Regulated Transporter	High-affinity zinc uptake transmembrane transporter of the plasma membrane involved in zinc ion transport
YGR020C	VMA7	-	-
YGR085C	RPL11B	Ribosomal Protein of the Large subunit	Subunit of the cytosolic large ribosomal subunit; involved in ribosomal large subunit assembly and translation
YGR111W	-	-	-
YGR173W	RBG2	RiBosome interacting Gtpase	-
YGR209C	TRX2	ThioRedoXin	-
YGR214W	RPS0A	Ribosomal Protein of the Small subunit	Subunit of the cytosolic small ribosomal subunit; involved in rRNA processing and export from the nucleus, assembly of the small ribosomal subunit, and translation
YHL028W	WSC4	cell Wall integrity and Stress response Component	-
YHL031C	GOS1	GOlgi Snare	-
YHR103W	SBE22	similar to SBE2	-
YHR104W	GRE3	Genes de Respuesta a Estres (stress responsive genes)	-
YHR117W	TOM71	Translocase of the Outer Mitochondrial membrane	-
YIL042C	PKP1	Protein Kinase of PDH	-
YIL053W	GPP1	Glycerol-3-Phosphate Phosphatase	-

YIL065C	FIS1	mitochondrial FISsion	Protein that positively regulates mitochondrial fission; also involved in peroxisome fission and cell aging; localized to mitochondrial outer membrane and peroxisome
YIL092W	-	-	Protein whose biological role is unknown; localizes to the nucleus and cytoplasm in a large-scale study
YIL145C	PAN6	PANtothenate biosynthesis	-
YIR016W	-	-	-
YJL024C	APS3	clathrin Associated Protein complex Small subunit	-
YJL084C	ALY2	Arrestin-Like Yeast protein	-
YJL098W	SAP185	Sit4 Associated Protein	-
YJL136C	RPS21B	Ribosomal Protein of the Small subunit	Subunit of the cytosolic small ribosomal subunit; involved in rRNA processing, and translation
YJL148W	RPA34	RNA Polymerase A	-
YJL168C	SET2	SET domain-containing	-
YJL206C	-	-	-
YJR056C	-	-	Protein whose biological role is unknown; localizes to the nucleus and cytoplasm in large-scale studies
YJR105W	ADO1	ADenOsine kinase	-
YJR144W	MGM101	Mitochondrial Genome Maintenance	A single-strand DNA binding protein involved in recombinatorial mitochondrial DNA repair process to maintain mitochondrial genome; localized to the mitochondrial nucleoid
YKL002W	DID4	Doa4-Independent Degradation	-
YKL041W	VPS24	Vacuolar Protein Sorting	-
YKL092C	BUD2	BUD site selection	-
YKL114C	APN1	APurinic/apyrimidinic eNdonuclease	-
YKL129C	MYO3	MYOsin	-
YKL132C	RMA1	Reduced Mating A	-
YKL175W	ZRT3	-	Zinc ion transmembrane transporter of the vacuolar membrane involved in zinc ion transport and cellular zinc ion homeostasis
YKR003W	OSH6	OxySterol binding protein Homolog	Phosphatidylinositol- and phosphatidic acid-binding protein involved in endocytosis, exocytosis, sterol metabolism, and maintenance of cell polarity; localizes to the cortical endoplasmic reticulum

YKR019C	IRS4	Increased rDNA Silencing	-
YKR024C	DBP7	Dead Box Protein	-
YLL010C	PSR1	Plasma membrane Sodium Response	-
YLL013C	PUF3	PUmilio-homology domain Family	-
YLL024C	SSA2	Stress-Seventy subfamily A	Subunit of the chaperonin-containing T-complex (CCT particle, TriC) that is predicted to be an ATPase; involved in protein folding and tRNA import into nucleus under starvation conditions
YLL033W	IRC19	Increased Recombination Centers	-
YLR042C	-	-	Protein whose biological role is unknown; localizes to the cell wall
YLR056W	ERG3	ERGosterol biosynthesis	-
YLR065C	ENV10	late ENdosome and Vacuole interface function	-
YLR072W	LAM6	Lipid transfer protein Anchored at Membrane contact site	Sterol transfer protein with a role in intracellular sterol transport; localizes to intracellular membrane contact sites between ER and other organelles
YLR107W	REX3	Rna EXonuclease	-
YLR201C	COQ9	COenzyme Q	-
YLR251W	SYM1	Stress-inducible Yeast Mpv17	-
YLR303W	MET17	METhionine requiring	Bifunctional enzyme with O-acetylserine and O-acetylhomoserine sulfhydrylase activities involved in methionine and cysteine metabolism; catalyses the reaction between acetylated serine or homoserine with thiol to produce the corresponding amino acids; localized to the cytoplasm and plasma membrane
YLR343W	GAS2	Glycophospholipid-Anchored Surface protein	-
YLR368W	MDM30	Mitochondrial Distribution and Morphology	Subunit of SCF ubiquitin ligase complex that contributes to ubiquitin-protein transferase activity; involved in mitochondrion organization, fusion, chronological cell aging, as well as ubiquitin-dependent protein catabolic processes
YLR372W	ELO3	fatty acid ELOngation	-
YLR376C	PSY3	Platinum SensitivitY	-
YLR390W	ECM19	ExtraCellular Mutant	Protein whose biological role is unknown; localizes to the mitochondrion
YLR414C	PUN1	Plasma membrane protein Upregulated during Nitrogen stress	-
YLR449W	FPR4	FKBP Proline Rotamase	Peptidyl-prolyl cis-trans isomerase (PPIase); involved in histone proline isomerization,

		(isomerase)	regulation of histone methylation and nucleosome assembly; localizes to the chromatin
YML002W	-	-	-
YML021C	UNG1	Uracil DNA N-Glycosylase	-
YML022W	APT1	Adenine PhosphoribosylTransferase	-
YML028W	TSA1	Thiol-Specific Antioxidant	-
YML029W	USA1	U1-Snp1 Associating	-
YML035C	AMD1	AMP Deaminase	-
YML055W	SPC2	Signal Peptidase Complex	-
YML097C	VPS9	Vacuolar Protein Sorting	-
YML108W	-	-	Protein whose biological role is unknown; localizes to the cytoplasm and nucleus in different large-scale studies
YMR002W	MIX17	Mitochondrial Intermembrane space CX(n)C motif protein	Protein localized to the mitochondrial intermembrane space; involved in aerobic respiration
YMR030W	RSF1	ReSpiration Factor	-
YMR060C	SAM37	Sorting and Assembly Machinery	-
YMR091C	NPL6	Nuclear Protein Localization	-
YMR152W	YIM1	-	-
YMR154C	RIM13	Regulator of IME2	-
YMR167W	MLH1	MutL Homolog	-
YMR175W	SIP18	Salt Induced Protein	-
YMR178W	-	-	Protein whose biological role is unknown; localizes to the nucleus and cytoplasm in a large-scale study
YMR180C	CTL1	Capping enzyme mRNA Triphosphatase-Like	-
YMR186W	HSC82	-	-
YMR190C	SGS1	Slow Growth Suppressor	Nucleolar ATP-dependent DNA helicase that is a subunit of the RecQ helicase-Topoisomerase III complex; melts and unwinds double-stranded DNA; involved in the formation of telomeric 3' overhangs, maintenance of telomeres by recombination, processing of DNA double-strand breaks, segregation of chromatids during mitosis, and segregation of chromosomes during meiosis; has a role in gene conversion at the mating-type loci, and also regulates meiotic recombination and the conversion of

			paired broken DNA and homologous duplex DNA into four-stranded branched intermediate joint molecules
YMR191W	SPG5	Stationary Phase Gene	-
YMR216C	SKY1	SRPK1-like Kinase in Yeast	-
YMR232W	FUS2	cell FUSion	Protein involved in regulating the termination of mating projection growth as well as karyogamy during mating; localizes to nucleus and mating projection tip
YMR289W	ABZ2	para-AminoBenZoic acid (PABA) biosynthesis	-
YMR299C	DYN3	DYNein	-
YNL037C	IDH1	Isocitrate DeHydrogenase	-
YNL067W	RPL9B	Ribosomal Protein of the Large subunit	Subunit of the cytosolic large ribosomal subunit; involved in translation
YNL098C	RAS2	homologous to RAS proto-oncogene	GTPase involved in the regulation of filamentous growth and regulation of transcription in response to nutrient changes; primarily localized in the plasma membrane but has been detected in the ER membrane and mitochondria
YNL190W	-	-	-
YNL248C	RPA49	RNA Polymerase A	-
YNL249C	MPA43	Multicopy PDC1 Activator	Protein whose biological role is unknown; localizes to the mitochondrion in different large-scale studies
YNL250W	RAD50	RADiation sensitive	Adenylate kinase and ATPase, component of the nuclear Mre11 complex that is involved in double-stranded break repair, telomere maintenance and initiating DSBs in meiosis
YNL297C	MON2	MONensin sensitivity	-
YNL320W	-	-	Protein whose biological role is unknown; localizes to the mitochondrion in a large-scale study
YNL328C	MDJ2	-	-
YNL332W	THI12	THIamine metabolism	-
YOL017W	ESC8	Establishes Silent Chromatin	-
YOL025W	LAG2	Longevity Assurance Gene	-
YOL052C-A	DDR2	DNA Damage Responsive	-
YOL065C	INP54	INositol polyphosphate 5-Phosphatase	-
YOL068C	HST1	Homolog of SIR Two (SIR2)	-

YOL083W	ATG34	AuTophaGy related	Component of the cytoplasm-to-vacuole targeting, CVT complex; involved in transport of alpha-mannosidase (Ams1p) to the vacuole during autophagy
YOL105C	WSC3	cell Wall integrity and Stress response Component	-
YOL152W	FRE7	Ferric REductase	-
YOR010C	TIR2	TIp1-Related	-
YOR025W	HST3	Homolog of SIR Two (SIR2)	-
YOR026W	BUB3	Budding Uninhibited by Benzimidazole	Ubiquitin binding subunit of the mitotic checkpoint complex; involved in mitotic spindle assembly checkpoint and mitotic DNA integrity checkpoint; localized to condensed nuclear chromosome kinetochore
YOR044W	IRC23	Increased Recombination Centers	Protein whose biological role is unknown; localizes to the endoplasmic reticulum in a large-scale study
YOR054C	VHS3	Viable in a Hal3 Sit4 background	-
YOR058C	ASE1	Anaphase Spindle Elongation	-
YOR092W	ECM3	ExtraCellular Mutant	-
YOR118W	RTC5	Restriction of Telomere Capping	Protein whose biological role is unknown; localizes to the cytoplasm in a large-scale study
YOR298C-A	MBF1	Multiprotein Bridging Factor	RNA polymerase II transcription coactivator
YOR298W	MUM3	MUddled Meiosis	-
YOR312C	RPL20B	Ribosomal Protein of the Large subunit	Subunit of the cytosolic large ribosomal subunit; involved in translation
YOR328W	PDR10	Pleiotropic Drug Resistance	-
YOR337W	TEA1	Ty Enhancer Activator	-
YOR348C	PUT4	Proline UTilization	-
YOR349W	CIN1	Chromosome INstability	-
YOR351C	MEK1	MEiotic Kinase	-
YOR371C	GPB1	-	-
YPL026C	SKS1	Suppressor Kinase of SNF3	-
YPL088W	-	-	-
YPL198W	RPL7B	Ribosomal Protein of the Large subunit	Subunit of the cytosolic large ribosomal subunit; involved in maturation of the large subunit rRNA, biogenesis of the ribosomal large subunit, and translation
YPL203W	TPK2	Takashi's Protein Kinase	cAMP-dependent protein kinase involved in signaling and invasive growth in response to glucose limitation; localizes to both nucleus and cytosol

YPL248C	GAL4	GALactose metabolism	Sequence-specific DNA-binding RNA polymerase II transcription factor involved positive regulation of transcription in response to galactose; also binds and recruits other transcription factors
YPL249C	GYP5	Gtpase-activating protein for Ypt Proteins	-
YPL253C	VIK1	Vegetative Interaction with Kar3p	-
YPL254W	HFI1	Histone H2A Functional Interactor	-
YPL260W	-	-	Protein whose biological role is unknown; localizes to the nucleus and cytoplasm in a large-scale study
YPR004C	AIM45	Altered Inheritance rate of Mitochondria	Protein whose biological role is unknown; localized to mitochondria
YPR005C	HAL1	HALotolerance	-
YPR120C	CLB5	CycLin B	Cyclin-dependent kinase regulatory subunit involved in the regulation of both G1/S and G2/M phase transitions of the mitotic cell cycle; regulates mitotic and premeiotic DNA replication, as well as mitotic spindle assembly; localizes to the nucleus
YPR173C	VPS4	Vacuolar Protein Sorting	-